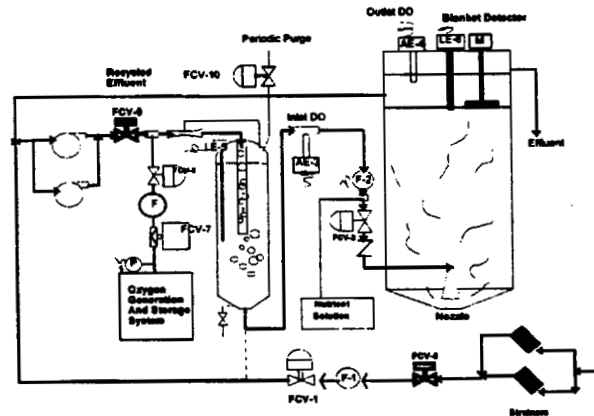


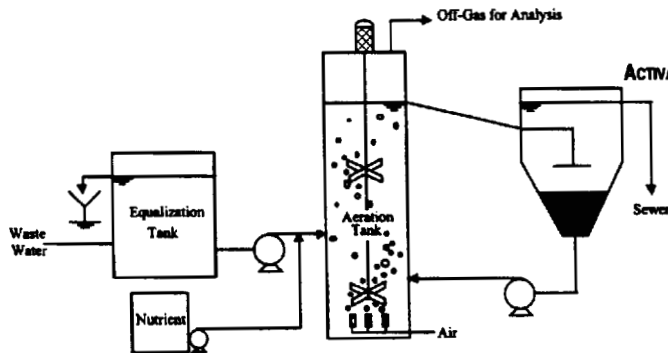
# FIELD EVALUATION OF BIOLOGICAL AND NON-BIOLOGICAL TREATMENT TECHNOLOGIES TO REMOVE MTBE/OXYGENATES FROM PETROLEUM PRODUCT TERMINAL WASTEWATERS

Health and Environmental Sciences Department  
 Publication Number 4655  
 August 1997

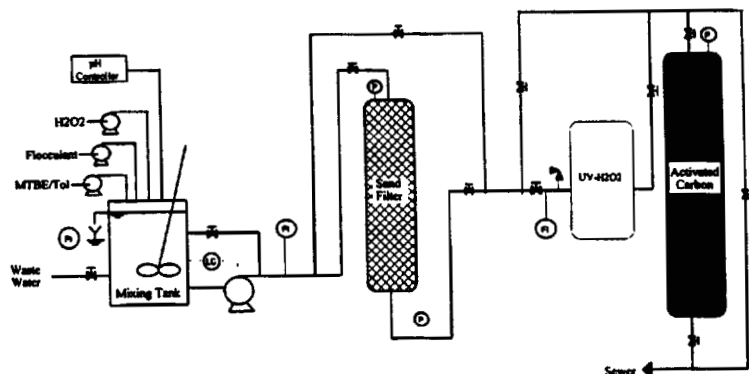
FLUIDIZED BED BIOLOGICAL REACTOR



ACTIVATED SLUDGE SYSTEM FOR THE TREATMENT OF MTBE CONTAMINATED WASTEWATER



UV-H<sub>2</sub>O<sub>2</sub> GROUNDWATER TREATMENT PROCESS





One of the most significant long-term trends affecting the future vitality of the petroleum industry is the public's concerns about the environment, health and safety. Recognizing this trend, API member companies have developed a positive, forward-looking strategy called STEP: Strategies for Today's Environmental Partnership. This initiative aims to build understanding and credibility with stakeholders by continually improving our industry's environmental, health and safety performance; documenting performance; and communicating with the public.

### **API ENVIRONMENTAL MISSION AND GUIDING ENVIRONMENTAL PRINCIPLES**

The members of the American Petroleum Institute are dedicated to continuous efforts to improve the compatibility of our operations with the environment while economically developing energy resources and supplying high quality products and services to consumers. We recognize our responsibility to work with the public, the government, and others to develop and to use natural resources in an environmentally sound manner while protecting the health and safety of our employees and the public. To meet these responsibilities, API members pledge to manage our businesses according to the following principles using sound science to prioritize risks and to implement cost-effective management practices:

- ❖ To recognize and to respond to community concerns about our raw materials, products and operations.
- ❖ To operate our plants and facilities, and to handle our raw materials and products in a manner that protects the environment, and the safety and health of our employees and the public.
- ❖ To make safety, health and environmental considerations a priority in our planning, and our development of new products and processes.
- ❖ To advise promptly, appropriate officials, employees, customers and the public of information on significant industry-related safety, health and environmental hazards, and to recommend protective measures.
- ❖ To counsel customers, transporters and others in the safe use, transportation and disposal of our raw materials, products and waste materials.
- ❖ To economically develop and produce natural resources and to conserve those resources by using energy efficiently.
- ❖ To extend knowledge by conducting or supporting research on the safety, health and environmental effects of our raw materials, products, processes and waste materials.
- ❖ To commit to reduce overall emission and waste generation.
- ❖ To work with others to resolve problems created by handling and disposal of hazardous substances from our operations.
- ❖ To participate with government and others in creating responsible laws, regulations and standards to safeguard the community, workplace and environment.
- ❖ To promote these principles and practices by sharing experiences and offering assistance to others who produce, handle, use, transport or dispose of similar raw materials, petroleum products and wastes.

# **Field Evaluation of Biological and Non-Biological Treatment Technologies to Remove MTBE/Oxygenates from Petroleum Product Terminal Wastewaters**

**Health and Environmental Sciences Department**

API PUBLICATION NUMBER 4655

PREPARED UNDER CONTRACT BY:

W.T. TANG AND P.T. SUN  
SHELL DEVELOPMENT COMPANY  
ENVIRONMENTAL DIRECTORATE  
HOUSTON, TEXAS

AUGUST 1997



## FOREWORD

API PUBLICATIONS NECESSARILY ADDRESS PROBLEMS OF A GENERAL NATURE. WITH RESPECT TO PARTICULAR CIRCUMSTANCES, LOCAL, STATE, AND FEDERAL LAWS AND REGULATIONS SHOULD BE REVIEWED.

API IS NOT UNDERTAKING TO MEET THE DUTIES OF EMPLOYERS, MANUFACTURERS, OR SUPPLIERS TO WARN AND PROPERLY TRAIN AND EQUIP THEIR EMPLOYEES, AND OTHERS EXPOSED, CONCERNING HEALTH AND SAFETY RISKS AND PRECAUTIONS, NOR UNDERTAKING THEIR OBLIGATIONS UNDER LOCAL, STATE, OR FEDERAL LAWS.

NOTHING CONTAINED IN ANY API PUBLICATION IS TO BE CONSTRUED AS GRANTING ANY RIGHT, BY IMPLICATION OR OTHERWISE, FOR THE MANUFACTURE, SALE, OR USE OF ANY METHOD, APPARATUS, OR PRODUCT COVERED BY LETTERS PATENT. NEITHER SHOULD ANYTHING CONTAINED IN THE PUBLICATION BE CONSTRUED AS INSURING ANYONE AGAINST LIABILITY FOR INFRINGEMENT OF LETTERS PATENT.

*All rights reserved. No part of this work may be reproduced, stored in a retrieval system, or transmitted by any means, electronic, mechanical, photocopying, recording, or otherwise, without prior written permission from the publisher. Contact the publisher, API Publishing Services, 1220 L Street, N.W., Washington, D.C. 20005.*

Copyright © 1997 American Petroleum Institute

## ACKNOWLEDGMENTS

THE FOLLOWING PEOPLE ARE RECOGNIZED FOR THEIR CONTRIBUTIONS OF TIME AND EXPERTISE DURING THIS STUDY AND IN THE PREPARATION OF THIS REPORT:

### API STAFF CONTACTS

Larry Magni, Manufacturing, Distribution & Marketing Department  
 Roger E. Claff, Health & Environmental Sciences Department

### MEMBERS OF TERMINAL EFFLUENT TASK FORCE

Robert R. Goodrich, Chairman, Exxon Research and Engineering Company  
 Dave Pierce, Vice-Chairman, Chevron Research and Technology  
 Jeff Baker, Conoco Inc.  
 Terrie Blackburn, Williams Pipeline  
 Don Hitchcock, Texaco Refining and Marketing  
 LeAnne Kunce, BP Oil  
 Al Schoen, Mobil Research & Development  
 Marilyn Shup, Sun Refining and Marketing  
 Carl Venzke, Citgo Petroleum

The authors would like to thank the following people for their assistance in this project: Mr. Steve L. Walker conducted all the field experimental work for this study. Dr. Manuel L. Cano participated in part of the experimental study and technical discussion of this project. Mrs. Mark E. Wilcox and Raymond J. Lesoon conducted the experimental work for the laboratory fluidized bed biological reactor study. Mr. Bill Perpich and Mr. Robert Hines of Envirex Ltd. contributed their expertise in setting up and operation of the field fluidized bed biological reactor. The contributions from all these people are very significant to this project and are greatly appreciated. The authors also would like to thank the Envirex Ltd. for donating the use of the fluidized bed biological reactor for this project duration.

## PREFACE

The American Petroleum Institute (API), through its Marketing Terminal Effluent Task Force, has been conducting a multi-year research program to evaluate and identify practical and environmentally sound technology options for handling and treating waters generated at petroleum product distribution terminals. The results of this program are intended to provide industry and regulatory agencies with technical information to make informed decisions on appropriate alternatives for individual terminal facilities.

The Task Force has sponsored and published a significant amount of work in prior years on handling and treating terminal waters. The work contained in this report focuses on higher volume, low contamination waters, including those containing an oxygenated compound used in motor gasoline, namely methyl tert-butyl ether (MTBE). In this study, low contamination terminal waters, mostly groundwater, containing benzene, toluene, ethylbenzene and xylene (BTEX) and MTBE were tested in three pilot sized units—two biological systems and one chemical oxidation system—at a terminal. The results of the pilot test work showed that all systems were able to remove at least 95% of the MTBE and BTEX in the feed waters at the few ppm level (0.5-10 mg/L) to low effluent concentrations, less than 100 ppb.

The study concluded that any of the three systems could be applied to a terminal, if needed. The choice of a particular type of technology, a fluidized bed biological reactor (FBBR), an activated sludge type biological treatment system, or a combined ultraviolet light (UV) and hydrogen peroxide ( $H_2O_2$ ) chemical oxidation system would depend on a life-cycle economics evaluation, expected time span needed for treatment (temporary vs. permanent treatment or remediation project), specific wastewater contamination, and operating staff capabilities at the individual terminal.

Prior studies sponsored by the Task Force have shown that operations and water characteristics at distribution terminals can vary significantly, as do regulatory

requirements in different geographical jurisdictions. Hence, it is recommended that terminal operators or engineers carefully review the terminal water characteristics and regulatory requirements for each facility before designing or installing treatment equipment. Also, other options such as pretreatment and discharge of waters to Publically Owned Treatment Works (POTWs), use of packaged, mobile units for temporary treatment needs, and integration of treatment with other existing petroleum or chemical facilities should be considered versus installation of equipment at the terminals. Other technologies, such as activated carbon adsorption and heated water/air stripping, should also be considered in addition to the treatment technologies tested in this research program.

The Task Force greatly acknowledges and appreciates the fine work performed by Shell Development Company, Houston, Texas in conducting this comprehensive and challenging technical study. In particular, we appreciate the dedication and expertise of Drs. W.T. Tang and P.T. Sun in completing this work.

## ABSTRACT

A pilot/demonstration study was conducted on three treatment technologies—the fluidized bed biological reactor (FBBR) process, the activated sludge process incorporated with iron flocculation, and the ultraviolet light-hydrogen peroxide (UV-H<sub>2</sub>O<sub>2</sub>) process—to evaluate their effectiveness in the treatment of petroleum marketing terminal wastewater contaminated with methyl tert-butyl ether (MTBE). Contaminated groundwater was the primary constituent of the wastewater, which contained 3 to 4 mg/L of benzene, toluene, xylenes, and ethylbenzene (BTEX). MTBE in the wastewater varied from 0.5 to 10 mg/L.

All three technologies were shown to consistently remove BTEX (>99%) from this wastewater. Consequently, the study focused on the MTBE degradation kinetics. For the FBBR process, a start-up period of 3 to 4 weeks was necessary to build up sufficient MTBE degraders to exhibit effective MTBE biodegradation. Removal of MTBE to less than 100 µg/L was demonstrated in the FBBR for a MTBE volumetric loading rate of up to 40 mg per liter of reactor volume per day.

For the activated sludge process, incorporation of iron flocculation in the process enhanced the retention of biomass and allowed the system to sustain excellent MTBE biodegradation at a hydraulic detention time of three (3) hours. An effluent of less than 100 µg/L MTBE was achieved in the activated sludge system at a MTBE loading rate of 10 mg per liter of reactor volume per day.

The UV-H<sub>2</sub>O<sub>2</sub> process was capable of degrading MTBE under high MTBE loading rates: using a photoreactor equipped with three 10-kW UV lamps, less than 100 µg/L MTBE in the effluent was achieved for a MTBE loading rate of 4800 mg/L/day. There was only a small reduction in the total organic carbon through the UV-H<sub>2</sub>O<sub>2</sub> process, indicating that the organics were not completely oxidized to CO<sub>2</sub>. In the presence of ferrous iron in the wastewater, lowering the pH to 3.5 enhanced the degradation efficiency of the UV-H<sub>2</sub>O<sub>2</sub>

process by increasing the hydroxyl radical generation through Fenton's reaction, and eliminated hydroxyl radical scavengers (carbonate/bicarbonate ions).

In summary, this study demonstrated that all three technologies can be applied at petroleum marketing terminals for the treatment of MTBE contaminated wastewater. Process selection depends on various factors, such as the wastewater flow, MTBE concentration in-and-out of the process, the concentrations of other relevant compounds in the wastewater, the estimated life span of the treatment required and the availability of competent operating man-power at the site.

In general, for the feed conditions evaluated, none of the technologies, when applied alone, will consistently and reliably meet effluent limits below about 100  $\mu\text{g/L}$ . Some of the technologies exhibit significant operability concerns, especially slow response to upsets. In addition, development of cost data was not included in the scope of this study, thus no conclusions were drawn about the practicality of these technologies. Future application of these technologies for MTBE removal will have to take these factors into consideration.

**TABLE OF CONTENTS**

<u>Section</u>	<u>Page</u>
EXECUTIVE SUMMARY .....	ES-1
1. INTRODUCTION.....	1-1
2. FLUIDIZED BED BIOLOGICAL PROCESSES.....	2-1
A. Introduction .....	2-1
B. Review of the Results of MTBE Biodegradation From Previous Studies .....	2-2
C. Experimental Setup .....	2-5
D. Results and Discussion.....	2-8
E. Conclusions.....	2-21
3. ACTIVATED SLUDGE SYSTEM.....	3-1
A. Introduction .....	3-1
B. Experimental Setup .....	3-2
C. Experimental Plan .....	3-2
D. Results and Discussion.....	3-3
E. Conclusions.....	3-9
4. MTBE DEGRADATION IN THE UV-H <sub>2</sub> O <sub>2</sub> PROCESS .....	4-1
A. Introduction .....	4-1
B. Literature Review .....	4-2
C. Experimental Setup .....	4-7
D. Results and Discussion.....	4-9
E. Conclusions.....	4-24
REFERENCES.....	R-1
APPENDICES .....	A-1

**LIST OF FIGURES**

<u>Figure</u>	<u>Page</u>
ES-1. Technology Application Range for MTBE Treatment .....	ES-5
2-1. Flow diagram of the pilot scale treatment system .....	2-28
2-2. Schematic diagram of the fluidized bed biological reactor .....	2-29
2-3. The performance of benzene degradation in the FBBR during the initial startup .....	2-30
2-4. The performance of MTBE degradation in the FBBR during the initial startup .....	2-31
2-5. The performance of DIPE degradation in the FBBR during the initial startup .....	2-32
2-6. The performance of MTBE degradation in the FBBR during the 2nd startup .....	2-33
2-7. The performance of DIPE degradation in the FBBR during the 2nd startup .....	2-34
2-8. The performance of benzene degradation in the FBBR during the 2nd startup .....	2-35
2-9. The performance of toluene degradation in the FBBR during the 2nd startup .....	2-36
2-10. Performance of MTBE biodegradation in the FBBR under different feed flow rate conditions - No MTBE was injected to the feed .....	2-37
2-11. Performance of benzene biodegradation in the FBBR under different feed flow rate conditions - No MTBE was injected to the feed .....	2-38
2-12. Performance of DIPE biodegradation in the FBBR under different feed flow rate conditions - No MTBE was injected to the feed ...	2-39
2-13. Performance of MTBE biodegradation in the FBBR under different feed flow rate conditions - Influent MTBE was increased to 1 mg/L and feed flow rate was maintained at 3.5 gpm .....	2-40

**LIST OF FIGURES (Continued)**

<u>Figure</u>	<u>Page</u>
2-14. Performance of DIPE biodegradation in the FBBR under different feed flow rate conditions - Influent MTBE was increased to 1 mg/L and feed flow rate was maintained at 3.5 gpm .....	2-41
2-15. Performance of benzene biodegradation in the FBBR under different feed flow rate conditions - Influent MTBE was increased to 1 mg/L and feed flow rate was maintained at 3.5 gpm .....	2-42
2-16. Effects of carbon particle properties, temperature, and iron on the MTBE biodegradation in laboratory FBBRs .....	2-43
2-17. Summary of the MTBE biodegradation data in a 30 gallon FBBR pilot unit - Influent MTBE loading vs. effluent MTBE concentration .....	2-44
3-1. Schematic diagram of the pilot scale activated sludge system for the treatment of MTBE contaminated wastewater .....	3-12
3-2. Performance of MTBE and DIPE biodegradation in the activated sludge system with iron-enhanced flocculation - HRT=17.3 hr .....	3-13
3-3. Performance of benzene and toluene biodegradation in the activated sludge system with iron-enhanced flocculation - HRT=17.3 hr .....	3-14
3-4. Performance of benzene, total xylenes, and ethylbenzene biodegradation in the activated sludge system with iron-enhanced flocculation - HRT=17.3 hr .....	3-15
3-5. Performance of MTBE and DIPE biodegradation in the activated sludge system with iron-enhanced flocculation - HRT=8.1 hr .....	3-16
3-6. Performance of benzene and toluene biodegradation in the activated sludge system with iron-enhanced flocculation - HRT=8.1 hr .....	3-17
3-7. Performance of total xylenes and ethylbenzene biodegradation in the activated sludge system with iron-enhanced flocculation - HRT=8.1 hr .....	3-18
3-8. Performance of MTBE and DIPE biodegradation in the activated sludge system with iron-enhanced flocculation - HRT=5.8 hr .....	3-19

**LIST OF FIGURES (Continued)**

<u>Figure</u>	<u>Page</u>
3-9. Performance of benzene and toluene biodegradation in the activated sludge system with iron-enhanced flocculation - HRT=5.8 hr . . . . .	3-20
3-10. Performance of total xylenes and ethylbenzene biodegradation in the activated sludge system with iron-enhanced flocculation - HRT=5.8 hr . . . . .	3-21
3-11. Performance of MTBE biodegradation in the activated sludge system with iron-enhanced flocculation - HRT=2.9 hr . . . . .	3-22
3-12. Performance of DIPE biodegradation in the activated sludge system with iron-enhanced flocculation - HRT=2.9 hr . . . . .	3-23
3-13. Performance of benzene and toluene biodegradation in the activated sludge system with iron-enhanced flocculation - HRT=2.9 hr . . . . .	3-24
3-14. Performance of total xylenes and ethylbenzene biodegradation in the activated sludge system with iron-enhanced flocculation - HRT=2.9 hr . . . . .	3-25
3-15. The sludge volume index of activated sludge system with iron enhanced flocculation . . . . .	3-26
3-16. The iron content in the biosludge in the activated sludge process . . . . .	3-27
3-17. Comparison of the off-gas MTBE concentration with the calculated value in equilibrium with effluent liquid . . . . .	3-28
3-18. Relative removal of MTBE by stripping and biodegradation in the four different test conditions . . . . .	3-29
3-19. Comparison of the effluent MTBE concentration of the experimental data with that calculated by Equation (3-3) using the fitted $K_1$ value for Run 1 . . . . .	3-30
3-20. Comparison of the effluent MTBE concentration of the experimental data with that calculated by Equation. (3-3) using the fitted $K_1$ value for Run 2 . . . . .	3-31
3-21. Relationship between the effluent MTBE concentration and its loading based on all the data obtained from this study . . . . .	3-32

## LIST OF FIGURES (Continued)

<u>Figure</u>	<u>Page</u>
4-1. Hypothetical pathways of MTBE degradation by hydroxyl free radical chain reactions .....	4-37
4-2. Hypothetical pathways of toluene degradation by hydroxyl free radical .....	4-38
4-3. Flow diagram for the UV-H <sub>2</sub> O <sub>2</sub> groundwater treatment process ..	4-39
4-4. Flow diagram for the UV-H <sub>2</sub> O <sub>2</sub> equipment .....	4-40
4-5. Photolysis of H <sub>2</sub> O <sub>2</sub> by UV in the test photoreactor .....	4-41
4-6. Rate constant of H <sub>2</sub> O <sub>2</sub> photodegradation by UV irradiation in the presence of organic contaminants .....	4-42
4-7. Degradation of MTBE by the UV-H <sub>2</sub> O <sub>2</sub> process under different pH conditions .....	4-43
4-8. Degradation of MTBE by the UV-H <sub>2</sub> O <sub>2</sub> process under different pH conditions .....	4-44
4-9. Effects of pH and soluble iron concentration on MTBE degradation in the UV-H <sub>2</sub> O <sub>2</sub> process .....	4-45
4-10. Summary of the effluent MTBE concentration in the pilot UV-H <sub>2</sub> O <sub>2</sub> unit under different MTBE loading conditions .....	4-46
4-11. Summary of the effects of total VOC concentration in the feed on the E <sub>90</sub> for MTBE .....	4-47
4-12. The effects of molar ratio of total VOC to MTBE in the feed on the E <sub>90</sub> of MTBE .....	4-48
4-13. The effects of total VOC concentration in the feed on the E <sub>90</sub> of toluene .....	4-49
4-14. The effects of molar ratio of total VOC to toluene in the feed on the E <sub>90</sub> of toluene .....	4-50
4-15. The effects of total VOC concentration in the feed on the E <sub>90</sub> for DIPE .....	4-51

**LIST OF FIGURES (Continued)**

<u>Figure</u>	<u>Page</u>
4-16. The effects of molar ratio of total VOC to DIPE in the feed on the E <sub>90</sub> of DIPE .....	4-52
4-17. Effluent MTBE concentration and the molar ratio of H <sub>2</sub> O <sub>2</sub> to total VOC .....	4-53
4-18. Effluent benzene concentration and the molar ratio of H <sub>2</sub> O <sub>2</sub> to total VOC .....	4-54
4-19. Effluent toluene concentration and the molar ratio of H <sub>2</sub> O <sub>2</sub> to total VOC .....	4-55

**LIST OF TABLES**

<u>Table</u>	<u>Page</u>
2-1. Chemical Characteristics of the Feed Wastewater .....	2-22
2-2. Contents of Polynuclear Aromatic Hydrocarbons in the Wastewater ...	2-23
2-3. Monitoring Parameters for the Characterization of the Feed and the Treated Effluent .....	2-24
2-4. Comparison of the TSS and the VSS in the Effluent of the LFBFRs After the Injection of Fe(SO <sub>4</sub> ) into LFBFR-2 .....	2-25
2-5. Sand Filter Operation Data - Test Run #1 .....	2-26
2-6. Sand Filter Operation Data - Test Run #2 .....	2-27
3-1. Operating Plan for the Activated Sludge System with the Iron-Enhanced Flocculation for the Treatment of MTBE Contaminated Wastewater .....	3-11
3-2. First Order Biodegradation Rate Constants for MTBE and DIPE .....	3-11
4-1. The Kinetic Constants for the Reactions of Hydroxyl Radical with Organic and Inorganic Solutes in Aqueous Solutions (From: F. Rose and A. Rose, 1977) .....	4-25
4-2. Reaction Rate Constants of MTBE, Toluene, and m-Xylene Determined by the Relative Rate Constant Method (Tang and Wilcox, 1990) .....	4-27
4-3. Photodegradation of Organic Compounds by UV Irradiation in the Test Photoreactor .....	4-28
4-4. Effects of H <sub>2</sub> O <sub>2</sub> Concentration on the Degradation of Organic Compounds in the UV-H <sub>2</sub> O <sub>2</sub> Process - Low Influent MTBE Concentration .....	4-29
4-5. Effects of H <sub>2</sub> O <sub>2</sub> Concentration on the Degradation of Organic Compounds in the UV-H <sub>2</sub> O <sub>2</sub> Process - Higher Influent MTBE Concentration .....	4-30

**LIST OF TABLES (Continued)**

<u>Table</u>	<u>Page</u>
4-6. Effects of Influent Toluene Concentration on the Degradation of MTBE and Other Volatile Organic Compounds in the UV-H <sub>2</sub> O <sub>2</sub> Process - Test #1 .....	4-31
4-7. Effects of Influent Toluene Concentration on the Degradation of MTBE and Other Volatile Organic Compounds in the UV-H <sub>2</sub> O <sub>2</sub> Process - Test #2 .....	4-32
4-8. Effects of pH on the Degradation of Organic Compounds in the UV-H <sub>2</sub> O <sub>2</sub> Process .....	4-33
4-9. Effects of pH and Soluble Iron Concentrations on the Degradation of Organic Compounds in the UV-H <sub>2</sub> O <sub>2</sub> Process .....	4-34
4-10. Effects of Iron Hydroxide Floccs on the Degradation of Organic Compounds in the UV-H <sub>2</sub> O <sub>2</sub> Process .....	4-35
4-11. Total Organic Carbon Reduction in the UV-H <sub>2</sub> O <sub>2</sub> Process .....	4-36
4-12. The Range and Average of E <sub>90</sub> for MTBE, DIPE, and BTEX .....	4-36

## EXECUTIVE SUMMARY

The wastewater generated in a petroleum marketing terminal can generally be divided into two categories: the high-concentration-low-flow tank water bottoms and the low-concentration-high-flow contaminated groundwater and runoff. These wastewaters are contaminated with different levels of gasoline components including benzene, toluene, ethylbenzene, and xylenes (BTEX); gasoline additives such as methyl tert-butyl ether (MTBE); and inorganics. MTBE is added to gasoline as an oxygenate to reduce automobile tailpipe emission of carbon monoxide and hydrocarbons. MTBE has been shown to be more soluble in water, less strippable, less adsorbable, and more difficult to biodegrade than BTEX, and presents a significant challenge from a wastewater treatment standpoint.

This project investigates the feasibility of different treatment technologies for removal of BTEX and MTBE in low-concentration-high-flow marketing terminal wastewaters. Treatment technologies for MTBE removal include activated carbon adsorption, steam stripping, air stripping with and without off-gas control, air stripping at elevated temperature, biological processes, and advanced oxidation processes. Among these treatment technologies, much information has been available for the activated carbon adsorption and air stripping processes. This current study focuses on evaluating the effectiveness of MTBE removal in two biological processes—the fluidized bed biological reactor (FBBR) process and the activated sludge process, and a chemical process—the UV-H<sub>2</sub>O<sub>2</sub> process.

The study was conducted at a petroleum product marketing terminal. Contaminated groundwater for that terminal made up the primary component of the wastewater used in the study. The wastewater contained about 3-4 mg/L BTEX and 0.5 mg/L MTBE. Additional MTBE was in some cases injected into the feed to vary the influent feed MTBE concentration.

In the FBBR study a 190-gallon reactor was used. It was filled with fluidized granular carbon particles on which bacteria could grow. The FBBR required a long startup time to build up a sufficient population of the MTBE degraders to exhibit effective MTBE biodegradation even

with an initial inoculation of a large quantity of the MTBE degrading mixed culture. The very slow buildup of the MTBE degrading bacteria in the FBBR was believed to result from the iron interference and the low temperature of the groundwater. Iron hydroxide deposited on carbon particles tended to flocculate the biomass. As the iron flocs sloughed off of carbon particles and elutriated out of the FBBR, loss of biomass from the FBBR resulted, thus slowing down the attachment of the culture. However, once the MTBE degraders were retained in the FBBR, the FBBR exhibited consistent MTBE removal and excellent stability against process upset. In lieu of the long startup time under field conditions, pre-immobilization of a large population of MTBE degraders onto the carbon particles before startup could be a viable alternative to ensure the success of the FBBR process for MTBE treatment.

This study demonstrated that removal of MTBE to less than 100  $\mu\text{g/L}$  in the FBBR effluent could be achieved with a MTBE loading rate of approximately 40 mg MTBE/L-reactor/day. It is likely that the FBBR can handle higher MTBE loadings if sufficient time is allowed for the FBBR to accumulate enough of an MTBE degrader population.

In the activated sludge process, incorporation of iron flocculation in the activated sludge operation helped retain the MTBE degraders in the system. As a result, very good MTBE degradation and effluent quality can be achieved in the activated sludge system even at an influent biochemical oxygen demand (BOD) concentration as low as 11 mg/L. The removal of MTBE in the activated sludge system was largely due to biodegradation. Loss of MTBE through volatilization was determined to be only 0.5 to 9% of the influent MTBE loading. Based on the test data, an effluent of less than 100  $\mu\text{g/L}$  MTBE could be achieved with a MTBE loading rate of less than 10 mg/day/L-reactor. This loading rate was considered a conservative value for sizing the MTBE biodegradation capacity in an activated sludge system. Overall, the activated sludge system does not possess as high a biomass concentration as the FBBR, and therefore requires a larger reactor to handle the same MTBE loading. The activated sludge system was also more prone to process upset than the attached film process used in the FBBR, and recovered at a slower pace. However, the activated sludge process could be started up (or re-started) rather

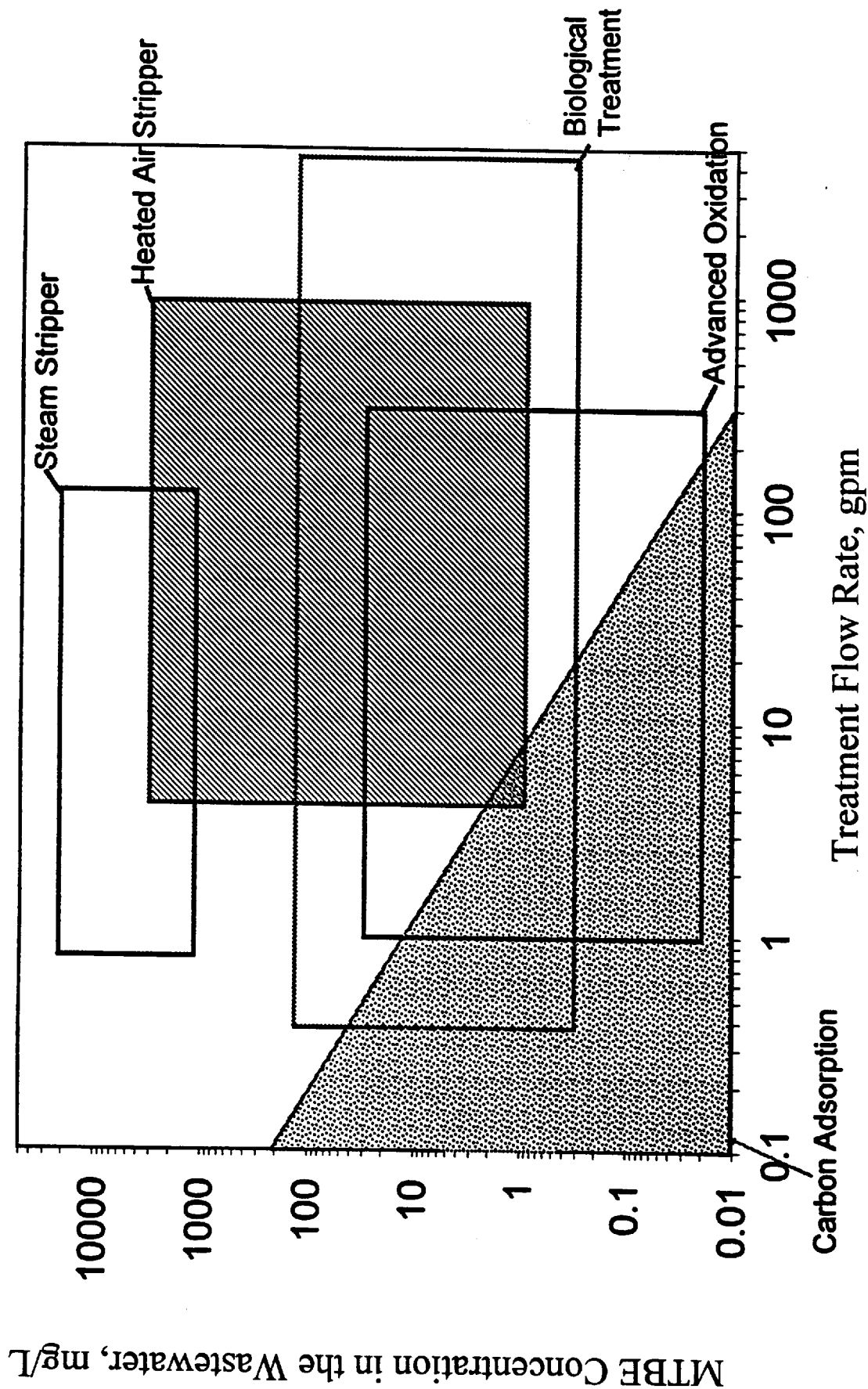
easily as compared to the FBBR, which was shown to be delayed by low temperature and iron interference.

The UV-H<sub>2</sub>O<sub>2</sub> process was capable of effectively degrading MTBE and other gasoline hydrocarbons under high MTBE and organic loading rates. Using a photoreactor equipped with three 10-kW UV lamps, less than 100 µg/L MTBE in the effluent could be achieved for a MTBE loading rate of up to 4800 mg/L-reactor/day. The hydraulic retention time used in the study ranged from 3 to 8 minutes. Despite its high degradation rate, there was only a small reduction in the total organic carbon through the UV-H<sub>2</sub>O<sub>2</sub> process, indicating that most of the organic contaminants were not oxidized to CO<sub>2</sub>. The by-products were likely to be alcohols, aldehydes and ketones. The aquatic toxicity of the treated effluent from the UV-H<sub>2</sub>O<sub>2</sub> process was not addressed in this study, but should be carefully examined when choosing this technology.

The contaminated groundwater contained naturally occurring soluble iron. The soluble iron would compete with the target organic compounds for hydroxyl radicals rendering the process less effective. In addition, once iron was oxidized, it formed iron hydroxide flocs which adsorbed and scattered the UV light. Fouling of the UV lamp quartz sheath by iron deposition could also occur. Therefore, presence of iron in the feed water would significantly reduce the degradation efficiency of the UV-H<sub>2</sub>O<sub>2</sub> process under neutral pH condition, and the UV-H<sub>2</sub>O<sub>2</sub> process should incorporate an iron removal pretreatment step. However, if the pH of the feed water was lowered to 3.5 or less, the generation of hydroxyl radicals through Fenton's reaction was increased and the hydroxyl radical scavengers such as bicarbonate and carbonate were eliminated. As a result, the overall degradation efficiency of the UV-H<sub>2</sub>O<sub>2</sub> process was significantly increased. The degradation of organic contaminants in the UV-H<sub>2</sub>O<sub>2</sub> process involves complex chain reactions, of which most of the kinetic information is not known. Prediction of the reaction results will be difficult, and laboratory and/or pilot testing is strongly recommended before selecting the process and sizing of the equipment.

This study provided some engineering design data, such as  $E_{90}$  (energy consumed for 90% reduction of a targeted compound) and  $H_2O_2$  consumption under different operating conditions, which may be used in the first-pass screening process for process selection.

In addition to the technologies considered in this study, several groundwater treatment techniques have been used to remove MTBE. They are carbon adsorption, steam stripping, and air stripping with and without heating the water (off gas control may or may not be required). Which technique to use for a specific wastewater treatment case depends on the following factors: water flow, MTBE concentration, MTBE discharge limit, off gas clean up requirement, other components in the wastewater (such as total organic concentration and/or iron content), the estimated duration of the treatment project, the variation of MTBE concentration during the pump-and-treat process, the available time for startup, and the availability of man power on-site. The treatment technology selection is a very complicated process and should be dealt with on a case-by-case basis. Nevertheless, general guidance can be provided based on knowledge gained from the study and from past experience. The following figure provides a screening guide for treatment technology selection based on cost and limitations of each process. The information provided in this figure is from general working knowledge and experience, and should not be used as a design tool.



ES-1. Technology Application Range for MTBE Treatment

## Section 1

### INTRODUCTION

The wastewater generated in a petroleum marketing terminal can generally be divided into two categories: the high-concentration-low-flow tank water bottoms and the low-concentration-high-flow contaminated groundwater and runoff. These wastewaters are contaminated with different levels of gasoline components including benzene, toluene, and xylenes; gasoline additives such as methyl tert-butyl ether (MTBE); and inorganics. MTBE is added to gasoline as an oxygenate to help reduce automobile tailpipe emission of carbon monoxide and hydrocarbons. Among the organic contaminants, MTBE presents the greatest technical challenge from a treatment standpoint.

The use of MTBE in gasoline blending has increased significantly because of the recent mandate by the Clean Air Act Amendments of 1993 to increase the oxygenate content in gasoline products. MTBE has a moderately high solubility in water, approximately 50,000 mg/L at 25 °C. Consequently, high levels of MTBE are often detected in wastewater or runoff water that has been in contact with gasoline products. For example, the MTBE concentration in tank bottoms is in the range of several thousand mg/L. In groundwater or runoff water contaminated with gasoline, MTBE at the level of several hundred mg/L has been detected.

Current regulation on MTBE concentration in gasoline contaminated wastewater from marketing terminals varies with location. The Office of Water of the Environmental Protection Agency is currently developing a drinking water health advisory for MTBE in drinking water. Several states have set guidelines to regulate MTBE concentration in the groundwater discharge permit, ranging from 50 to 1000 µg/L. In some states, even though MTBE may not be regulated in the discharge permit for treated terminal wastewater, a discharge limit on the total volatile organic concentration (VOC) is usually specified at 100 µg/L. Since MTBE is detected in the VOC measurement, and since it is

more difficult to remove than the other components from gasoline contaminated water, MTBE is essentially the governing factor regulated under this blanket VOC limit.

API's Marketing Terminal Effluent Task Force has sponsored extensive research on the treatment of low-volume-high-concentration tank water bottoms (Voung *et al.*, 1993). Although the treatment processes evaluated have been successful in meeting certain treatment goals, these treatment processes cannot be readily adapted to the treatment of the high-volume-low-strength wastewaters, particularly when the wastewater contains MTBE. In 1991, API conducted another study to evaluate cost-effective, alternative treatment technologies for reducing the concentrations of MTBE and methanol in groundwater (API, 1991). The study evaluated five technologies: air stripping (with off-gas carbon adsorption or off-gas incineration), steam stripping, diffused aeration, biological treatment, and UV-catalyzed oxidation. Cost estimates showed that UV-catalyzed oxidation, air stripping with off-gas incineration, and air stripping with off-gas carbon adsorption were the most cost-effective of the MTBE treatment technologies considered. Most of the data used in this report were derived using some laboratory evaluations and theoretical calculation. Although a biological treatment option was evaluated, it was judged to be one of the most expensive options, in part because conservative design parameters were used.

Biodegradation of MTBE has since been demonstrated to be feasible, and hence, the API Marketing Terminal Effluent Task Force sponsored this current project to conduct field demonstration research to evaluate both biological and non-biological MTBE treatment processes for high-volume-low-concentration marketing terminal wastewaters. The biological treatment processes evaluated in this study included the fluidized bed biological process and the activated sludge process. The UV-hydrogen peroxide process was the non-biological process tested in this study. This study focuses primarily on assessing the capacity and the effectiveness of the biological and UV-peroxide processes on MTBE removal under different processing and operating conditions. The data obtained from this

study would provide guidelines on the selection and design of an appropriate MTBE treatment system.

This report documents, in separate sections, the experience and data acquired from the field tests of both the biological and non-biological treatment processes. Extensive literature review on various treatment technologies applicable to MTBE degradation has been provided in previously published API reports and will not be repeated here.

However, relevant new literature information is included for discussion when appropriate.

## SECTION 2

### FLUIDIZED BED BIOLOGICAL PROCESSES

#### A. Introduction

Salanitro *et al.* (1994) first isolated a mixed culture that could degrade MTBE as sole carbon source. In their experiments, biodegradation of MTBE was clearly observed in an activated sludge process employing a mixed culture and receiving multiple organic substrates, including MTBE. They observed a few interesting characteristics of the mixed culture: (1) The MTBE degraders had a slow growth rate, and the MTBE biodegradation activity in the activated sludge system deteriorated if the sludge age was less than 30 days. (2) The MTBE biodegradation in an activated sludge system appeared to be susceptible to external disturbances, occasionally, the biodegradation efficiency of MTBE partially deteriorated for reasons not identified. (3) A pure culture of MTBE degrader could not be isolated. Since the MTBE biodegradation in this study was carried out using a mixed culture and multiple organic substrates, it was speculated that MTBE biodegradation might result from co-metabolism.

For the biological treatment of MTBE to be a viable process, the vulnerability of the MTBE degraders to the external disturbances needs to be further diminished. An attached film biological process appears to be a potentially superior alternative to the activated sludge process. An attached film biological process fixes the microbial cells onto solid carriers in a biological reactor. This process is capable of retaining a stable microbial population at a significantly higher cell concentration than the activated sludge process. The attached film process can thus improve both the operating stability and the biodegradation efficiency of the process on the basis of unit reactor volume. The configurations of an attached film biological process can be a packed bed biological reactor (including trickling filter), a fluidized bed biological reactor (FBBR), and a completely mixed reactor with solid carriers submerged and mixed in the reactor.

Tang and Wilcox (1993) used a laboratory-scale FBBR to address the operating stability and co-metabolism question encountered previously. In their study, the MTBE degraders were immobilized onto carbon particles in the FBBR to stabilize the MTBE degrader population in the reactor, and MTBE was used as the sole carbon source. MTBE biodegradation was clearly demonstrated without the presence of other organic compounds. This study also showed that MTBE could be consistently biodegraded to very low levels under well-controlled laboratory conditions (less than 20 µg/L). The study by Tang and Wilcox (1993) demonstrated some promising features of using the attached film biological processes for the practical treatment of MTBE contaminated wastewater. This current project intends to investigate the feasibility and performance of the attached film biological processes to the treatment of MTBE contaminated wastewater in petroleum product distribution terminals.

#### **B. Review of the Results of MTBE Biodegradation From Previous Studies**

Salanitro *et al.* (1994) first isolated a mixed bacterial consortium capable of degrading MTBE. The consortium was developed from seed microorganisms originating in a chemical plant biotreater sludge. It consisted of several bacterial species including coryneform-like species and species of *Pseudomonas* and *Achromobacter*. Through the study of the degradation of radiolabeled MTBE,  $(\text{CH}_3)_3\text{-O-C}^{14}\text{H}_3$ , they demonstrated that 40% of the MTBE biodegraded and was released as  $\text{CO}_2$ , 40% was incorporated in cell mass, and the remaining 20% was present in solution as unbiodegraded MTBE or intermediate metabolites. The mixed culture was capable of degrading ethyl tertiary butyl ether, tertiary butyl formate, and tertiary butyl alcohol, in addition to MTBE. Very high nitrification activity was observed in the culture. However, addition of ammonium salt did not enhance MTBE biodegradation, suggesting that the initial cleavage of MTBE was not related to the ammonium-oxygenase system. The culture was maintained at a sludge age of 70 days during the study. When the sludge age was less than 50 days, loss of partial MTBE degradation activity was observed.

Sun *et al.* (1994) studied the kinetics of MTBE biodegradation in an activated sludge system. They observed the susceptibility of the mixed culture to external stresses such as anaerobic condition and sudden change in feed concentration, and its recovery was very slow after these upsets. A Monod type of kinetics was fitted to the data:

$$r_{su} = \frac{\mu_m X S}{Y_g (K_s + S)} \quad (2-1)$$

where:

- $r_{su}$  = substrate utilization rate, mg MTBE/L day
- $\mu_m$  = maximum microorganism growth rate, day<sup>-1</sup>
- $X$  = microorganism concentration, mg mixed liquor volatile suspended solids (MLVSS)/L
- $S$  = substrate concentration, mg MTBE/L
- $Y_g$  = true biomass yield, mg MLVSS/mg MTBE
- $K_s$  = half saturation constant, mg MTBE/L

The biokinetic and stoichiometric parameters were determined:  $\mu_m = 0.2 \text{ day}^{-1}$  (maximum growth rate);  $K_s = 0.05 \text{ to } 0.45 \text{ mg/L}$  (the half saturation constant); and  $Y_g = 1.76 \text{ mg MLVSS/mg MTBE}$  (true biomass yield due to substrate removal). Based on these parameters and taking into account a design safety factor of 2, a minimum sludge age in the range of 20 to 30 days was suggested. The actual experimental data showed that a minimum sludge age of 25 days was required to achieve greater than 95% MTBE biodegradation. As the sludge age was reduced to less than 25 days, MTBE biodegradation deteriorated very rapidly. Biodegradation of MTBE was totally lost when the sludge age was reduced to 5 days.

Tang and Wilcox (1993) conducted an extensive study on MTBE biodegradation in a laboratory scale FBBR seeded with the mixed culture isolated by Salanitro *et al.* (1994). They investigated the effects of the following process and operating variables on MTBE biodegradation in a FBBR: carbon particle size, presence of other carbon sources in addition to MTBE in the feed, recycle ratio, oxygen requirements, and temperature. Their study showed that MTBE could be biodegraded consistently to less than 100  $\mu\text{g/L}$  under the conditions of a loading of 100 mg MTBE/day/L-FBBR and a hydraulic retention time of 50 minutes (both the loading and hydraulic retention time, HRT, were based on the

total FBBR reactor volume). The MTBE biodegradation effectiveness was the same for the FBBR with MTBE as the sole carbon source or with the presence of either methanol or benzene in the feed at a weight ratio to MTBE of 4:1. The MTBE biodegradation appeared to be very sensitive to oxygen supply. As the dissolved oxygen concentration was reduced to less than 1.5 mg/L due to either the reduced oxygenation or increased competition for oxygen by ammonia nitrification, deterioration in the MTBE biodegradation was observed. If the depletion of oxygen lasted for only a short time, the MTBE biodegradation activity could be rapidly restored as soon as the dissolved oxygen at the exit was raised above 1.5 mg/L. The average ratio of oxygen consumption to MTBE biodegradation was about 2-3 mg O<sub>2</sub>/mg MTBE.

The FBBR using a smaller carbon particle (300 μm) as carrier size did exhibit consistently lower effluent MTBE concentration than did the one with a large carbon particle size (600 μm) under the same feed and operating conditions. The difference, however, was not significant. Thus, the overall MTBE removal in FBBRs using different sizes of carbon particles was essentially the same. The MTBE degraders required a long adaptation time when the FBBR was switched from room temperature (23 °C) to a colder condition (17 °C). The effluent MTBE concentration increased immediately after the temperature shock. It took the FBBR about 2 weeks to return to the same MTBE biodegradation efficiency that existed prior to the temperature shock.

Based on these laboratory MTBE biodegradation results, the fluidized bed biological process appears to be a promising treatment technology for MTBE contaminated wastewater. This project was sponsored to further investigate the feasibility of this process under field conditions. The following sections describe the experimental setup and the results of the field-scale FBBR study.

### C. Experimental Setup

**Description of the Field FBBR Setup** The simplified flow diagram of the pilot scale treatment system is shown in Figure 2-1. It consisted of a feed preparation skid, a skid-mounted fluidized bed biological reactor system, an effluent surge tank, a sand filter and a carbon bed adsorber. The feed preparation skid was simply a pump and a piping network designed to provide the flexibility to direct the feed flow to different treatment units and to allow the injection of additional organics into the feed. Since the groundwater well pump produced enough discharge pressure to push the feed through the influent skid to the FBBR, the pump in the influent skid was not used. Two sections of the pipes on the influent skid were installed with an in-line mixer to provide necessary mixing when concentrated MTBE solution was dosed into the feed.

The effluent surge tank had a volume of 80 gallons. The water in the effluent surge tank was pumped to the sand filter and the carbon adsorber before it was discharged to the sewer. The carbon adsorber was installed to remove any residual organic compounds that were not degraded in the FBBR so that the treatment system at the marketing terminal would not be impacted by the pilot test. The sand filter protected the carbon adsorber from plugging with biomass and iron flocs. It was also used to obtain field data for sand filter sizing in similar applications. The sand filter was 12 inches in diameter and 54 inches in height. The filter media included sand and anthracite.

A wastewater treatment laboratory trailer was installed on site next to the pilot scale test unit to provide analytical support. The trailer was equipped with Photovac portable gas chromatography for analysis of volatile organic compounds, CEM LabWave Moisture/Solids Analyzer and Muffle Furnace for measurements of total and volatile suspended solids, and other general water quality analytical equipment such as pH meter, balance, etc.

The pilot scale fluidized bed biological reactor system consisted of an air separation unit for oxygen production, an oxygen saturation unit, and the fluidized bed reactor column (Figure 2-2). The air separation unit was comprised of a compressor and a pressure swing adsorber (PSA). The pressure swing adsorber utilized two molecular sieve columns operated alternatively under about 100 psig to separate air into oxygen and nitrogen. The nitrogen gas was bled off to the ambient, while the oxygen (approximately 95% purity) was stored in an oxygen storage tank.

The release of oxygen to the wastewater was controlled by an adaptive controller that manipulated the oxygen feed rate through a control valve according to the deviation of the dissolved oxygen concentration in the FBBR effluent from the set point. When the oxygen control valve was open, oxygen was mixed with the incoming wastewater through an eductor that effectively dispersed and dissolved oxygen in the wastewater. The oxygen-water mixture entered the oxygen saturation tank through a draft tube. Any gas not dissolved in the wastewater would rise to the top of the saturation tank and form a gaseous space (i.e., a big gaseous bubble). The residual oxygen in the gaseous space was continuously recycled back to the eductor to mix with the wastewater for further dissolution.

The 95% purity oxygen gas contained nitrogen and argon. These gases would slowly accumulate in the gaseous bubble on top of the oxygen saturation tank. When the gaseous bubble grew over a certain size such that the liquid level in the tank was suppressed to a preset level, the level probe installed in the tank sent out a signal to the controller which opened up a control valve to vent off the gases accumulated in the saturation tank. The amount of gas thus released was very small and so was the emission of the organic compounds from the vent gas. This oxygen saturation system, therefore, very effectively utilized the oxygen. A dissolved oxygen concentration of 35 mg/L in the saturation tank could be obtained at its maximum design flow rate, 30 gpm. The oxygen saturation tank was grounded to eliminate the source of electrostatic ignition in case there was free product accumulated on the liquid surface in the saturation tank.

The fluidized bed column was 20 inches in diameter and 15 feet in height. The exit of the column was located at 14 feet from the column base. The working volume of the FBBR was thus approximately 200 gallons. The recycle port was located at 1 foot below the column exit. Both the feed and recycle merged before the intake of the reactor pump which delivered a constant 30 gpm flow. The recycle rate was therefore automatically adjusted according to the feed rate. Both the recycle and feed first passed through the oxygen saturation tank to saturate the water with oxygen before they entered the FBBR column. The feed could also bypass the oxygen saturation tank to merge with the recycle right before the FBBR column. This option was implemented in case of free product accumulation in the saturation tank.

**Wastewater Characteristics** The chemical composition of the feed, a contaminated groundwater, is shown in Tables 2-1 and 2-2. It was high in hardness and alkalinity, approximately 600 and 400 mg/L, respectively. The iron concentration in the feed water was about 10 mg/L. The wastewater was relatively low in organics: toluene was the highest in concentration among the typical hydrocarbon contaminants from gasoline. The polynuclear aromatic hydrocarbons were mostly below the detection limit (1 µg/L). During the field test, concentrated MTBE solution was dosed into the feed to evaluate the biodegradation efficiency of the biological system at different influent MTBE concentrations. Therefore, the concentration of MTBE in the feed varied with experimental conditions. This water also contained some level of di-isopropyl ether which was specific to this location.

Because the feed wastewater was deficient in nitrogen and phosphorus, a mixture of urea and diammonium phosphate was added to the feed to supplement the nitrogen and phosphorus requirements for biological growth. The nitrogen and phosphorus nutrients were dosed at a rate to give the nitrogen and phosphorus concentrations in the feed the relationship of COD:N:P=100:5:1.

***Analytical Procedures*** During the field experiments, several parameters were monitored at a predetermined interval. Table 2-3 summarizes the monitoring parameters and frequency. The volatile organic compounds were analyzed using purge-and-trap gas chromatography. The quantification limits for the volatile components benzene, toluene, xylenes, ethyl benzene, MTBE and DIPE were 1 µg/L. The general water quality parameters such as Biological Oxygen Demand (BOD), Chemical Oxygen Demand (COD), cations, anions, nitrogen, etc. were analyzed according to the *Standard Methods* (1985). The heavy metals were analyzed using graphite furnace atomic absorption spectrometry (GFAA). The polynuclear aromatic hydrocarbons were analyzed based on EPA Method 625 (EPA 1982).

## **D. Results and Discussion**

### ***FBBR Start-Up***

The key to the success of the fluidized bed biological reactor process is to immobilize a high concentration of MTBE degraders onto carbon particles. The following startup procedure was therefore intended to provide a favorable environment to maximize the retention of the MTBE degrading mixture on the carbon particles. Before the startup, the adsorption isotherm of the carbon particles for MTBE was determined. At the startup, 360 lbs of carbon particles were loaded into the FBBR. Feed wastewater was then pumped through the FBBR to wash out the carbon fines. After the fines were removed, the feed wastewater was stopped, and the FBBR was converted to batch recycle mode. MTBE was then dosed into the FBBR to allow the carbon particles to adsorb MTBE. The amount of MTBE dosed was determined based on the MTBE adsorption isotherm data, the total carbon weight, and the MTBE concentration in the feed wastewater. The intent was to make the equilibrium MTBE concentration in the recycling water approximately the same as that in the feed wastewater. The reasons to pre-equilibrate carbon particles with MTBE are two fold: (1) create, through adsorption, an MTBE rich microenvironment on the carbon surface, encouraging the attachment of MTBE

degraders; and (2) exhaust the carbon so that once the FBBR was converted to continuous operation, any reduction of MTBE in the FBBR would indicate the biodegradation of MTBE.

After MTBE was dosed to the FBBR in recycling mode and the MTBE concentration in the water reached about 250 µg/L, 10 gallons of the MTBE degrading mixed culture with a mixed liquor volatile suspended solids (MLVSS) of 3000 mg/L were inoculated to the FBBR. This MTBE degrading mixed culture was maintained in the laboratory with MTBE as the sole carbon source. The FBBR was again left in recycle mode overnight to allow ample time for the bacterial species to attach to carbon surface. Due to the severe winter condition, the temperature of the water dropped to about 4 °C in the morning. The FBBR was then converted to continuous operation and started to receive 6 gpm of feed wastewater. The reactor temperature was about 15 °C under the continuous operation condition. The degradation data of benzene, MTBE, and DIPE during the startup period are shown in Figures 2-3 to 2-5.

As shown in Figure 2-3, benzene started to break through after 3 days of operation. However, the biodegradation of benzene started to take off in the same period, and the effluent benzene concentration was rapidly reduced to below the detection limit thereafter. The biodegradation of toluene, xylenes and ethyl benzene was very similar to that of benzene and is not shown here.

Despite the effort to pre-equilibrate the carbon with about 200 µg/L MTBE, adsorption of feed MTBE occurred after the continuous operation of the FBBR commenced. This adsorption was due to the fluctuation of the influent MTBE concentration between 200 and 450 µg/L. The difference between the influent and effluent MTBE concentrations during the first 20 days was believed to be mainly attributable to adsorption. The influent and effluent MTBE concentrations from the 20th to 30th days were essentially the same, indicating minimal biodegradation activity. Additional MTBE degraders were inoculated to the FBBR on Day-34 and Day-40. The feed rate was also reduced from 6 gpm to

2 gpm on Day-33. There was evidence of MTBE reduction immediately after the seeding of the MTBE degraders in both cases. The effluent MTBE concentration, however, slowly increased afterwards, suggesting that some MTBE degraders were not retained in the system. Two weeks after the last re-seeding, the FBBR started to display a more consistent removal of MTBE. The MTBE removal, however, was in the range of 25-50%. The effluent MTBE concentration appeared to level off at about 200 µg/L. The performance of DIPE biodegradation in the FBBR during the startup paralleled that of MTBE. The removal of DIPE during the first 25 days was attributed primarily to adsorption. After approximately 30 days of operation, the effluent DIPE concentration was slowly reduced to about 300 µg/L, and stabilized around that level without further improvement.

The removal of both MTBE and DIPE during the startup phase at best was only 50 to 60%. After biodegradation activity started, both the effluent MTBE and DIPE concentrations stayed at the 200-300 µg/L level without further declination. This is unusual, compared with the previous laboratory study which showed that greater than 95% of removal could be easily achieved once the MTBE biodegradation activity started to take off in the FBBR.

The results of the first two months of field study showed that an expedient startup and establishment of the FBBR to effectively remove MTBE under low initial MTBE concentration conditions was not satisfactory, especially during the cold weather. This run was thus terminated, and another startup with modification in the immobilization procedure was attempted.

### ***Second Start-Up***

Two factors might be related to the very low MTBE biodegradation activity in the first startup: (1) the carbon was equilibrated with only 200 µg/L MTBE concentration in the solution, which may not have created a sufficiently enriched micro-environment to

encourage effective attachment of most MTBE degraders on the carbon surface; and (2) the temperature of the water dropped to 4 °C during the batch recycle operating right after inoculation. It is not known whether this low temperature has a significantly adverse impact on the attachment of MTBE degraders.

Since the startup occurred during winter and the FBBR was not equipped to heat the water, the problem associated with low temperature during the attachment phase could not be resolved. During the second startup, MTBE was dosed so that at equilibrium the carbon was equilibrated with approximately 5 mg/L MTBE in the recycle water. The FBBR was subsequently inoculated with 10 gallons of the same MTBE degrading mixed culture with a MLVSS of 2000 mg/L. The lower MLVSS of the mixed culture was due to depletion of the culture stock. After inoculation, the FBBR was operated again in batch recycle mode. The temperature again dropped to approximately 2 °C after which the FBBR was fed with 1 gpm of feed wastewater.

Figure 2-6 shows the influent and effluent MTBE concentrations after the inoculation. Since the carbon was pre-equilibrated with 5 mg/L MTBE and since the influent MTBE concentration was less than 1 mg/L, desorption of MTBE from carbon occurred once the wastewater was fed through the FBBR. The desorption lasted for about 50 days after which the effluent MTBE concentration continued to drop until it stabilized at 100 to 150 µg/L. The difference between the influent and effluent MTBE concentration was definitely due to biodegradation. However, as also observed in the first startup, the effluent MTBE concentration was not further reduced to a very low level as did other easily biodegradable organic substrates (benzene, for example), suggesting that the MTBE biodegradation in the FBBR might be limited by either kinetics or other unknown factors. These questions will be addressed later in this report.

DIPE biodegradation data during the second startup are shown in Figure 2-7. As a result of carbon adsorption, DIPE was not detected in the effluent initially. Breakthrough of DIPE occurred after approximately 15 days of FBBR operation. The effluent DIPE

concentration did not rise significantly after breakthrough due to the concomitant removal of DIPE by biodegradation. The effluent DIPE concentration was eventually stabilized at approximately 50-70  $\mu\text{g/L}$ . The DIPE removal across the FBBR was greater than 80% as compared with 30-50% in the first startup.

Figures 2-8 and 2-9 show the biodegradation of benzene and toluene in the FBBR. Both the effluent benzene and toluene concentrations were below the detection limit (1  $\mu\text{g/L}$ ) most of the time. The influent toluene concentration fluctuated significantly between the 30th and 50th days of operation due to the variability of groundwater characteristics. The effluent toluene concentration, however, was not impacted, showing the stability to the FBBR against feed concentration variation. The biodegradation behavior of xylenes and ethyl benzene was similar to those of toluene, and was not shown here. The raw data for the second startup were tabulated in the Appendix.

### ***Effects of Loading on the Performance of FBBR Biodegradation***

Once the biodegradation of MTBE was established in the FBBR, the focus of the test program was to establish the MTBE biodegradation capacity of the FBBR by gradually increasing the MTBE loading (i.e., by varying feed flow rate and MTBE concentration). The loading to the FBBR was changed according to the following sequence: The feed rate was first raised stepwise from 1 gpm to 2 gpm and finally to 3.5 gpm without dosing MTBE in the feed. Each of these test conditions lasted for 3 to 5 weeks. The hydraulic retention times corresponding to the feed rates of 1, 2, and 3.5 gpm were 3.17, 1.58, and 0.9 hours, respectively.

Subsequently, the influent MTBE concentration was increased from 400  $\mu\text{g/L}$  to 1.1 mg/L while maintaining the feed rate at 3.5 gpm. Later, the influent MTBE concentration was further raised to 10 mg/L. During the last period, the field study of MTBE degradation in the UV- $\text{H}_2\text{O}_2$  process was carried out. Frequent shut down of the groundwater well was encountered due to overproduction of groundwater. The frequent shut down did not

adversely impact the UV-H<sub>2</sub>O<sub>2</sub> test since it was not operated 24 hours continuously. However, it did introduce significant perturbation to the FBBR and it is doubtful that there was sufficient time to allow the FBBR to stabilize at a pseudo-steady state for the last loading condition. The data gathered in this period (i.e., 3 gpm and 10 mg/L influent MTBE concentration) are included in this report since they shed some light on the response of the FBBR to frequent perturbation in concentration shocks. However, the data are not interpreted due to the entangled effects of adsorption and biodegradation in transient states. The following sections present the results gathered under different loading conditions.

Figure 2-10 shows the chronological data of MTBE biodegradation in the FBBR under 3 different flow rate conditions. After one month's operation under 1 gpm, MTBE was reduced from 400 to about 100 µg/L. The average MTBE removal was 64%. As the flow rate was increased to 2 gpm, the effluent MTBE concentration was slightly increased and the average MTBE removal dropped marginally to 63%. At 3.5 gpm, the effluent MTBE concentration increased to about 200 µg/L, and the decrease of MTBE removal was more obvious, from 63% to 52%.

The net MTBE removal rate, however, increased with increasing MTBE loading (or feed flow rate) despite the deterioration of effluent quality (i.e., higher effluent MTBE concentration). Theoretically, as the net MTBE removal rate increases, the rate of the MTBE degrader population growth should also increase, leading to accelerated MTBE biodegradation. However, within the 3-4 weeks of operation for each flow condition, the improvement in the effluent MTBE concentration with time was not obvious. The results suggest that the growth or the retention of the newly proliferated MTBE degraders might be impeded in the FBBR by some factors yet to be identified; it is also possible that the growth rate of the MTBE degrading culture was so low that these short period runs might be too short to allow the FBBR to display its full capacity.

The biodegradation of benzene, on the other hand, was not affected at all by the increase in the benzene loading. In all three flow conditions, essentially all the benzene was removed: the effluent benzene concentration was below the detection limits (Figure 2-11). The biodegradation of DIPE in the FBBR was very similar to that of MTBE (Figure 2-12), and the effluent DIPE concentration increased and the overall DIPE removal decreased with increasing feed flow rate. The removal of DIPE was averaged at 90%, 77%, and 57% for the 1, 2 and 3.5 gpm conditions, respectively. The influent concentrations of MTBE and DIPE were about the same under these test conditions. The DIPE removal in the FBBR was significantly higher than MTBE, indicating that DIPE was more biodegradable than MTBE.

Starting June 2, 1994, concentrated MTBE solution was injected into the feed to raise the influent MTBE concentration to about 1 mg/L, representing an MTBE loading increase of 125%. There was no deterioration of effluent MTBE concentration immediately after the increase in the loading, due mainly to carbon adsorption. By the end of June, 1994, the effluent MTBE concentration slightly decreased with time. The increase in biodegradation rate suggests that there might be an increase, though at a very slow pace, in the population of MTBE degraders in the system.

As mentioned previously, well overproduction problems were encountered in mid-July. The well water flow rate fluctuated significantly with time. Figure 2-13 shows that there were significant fluctuations in the influent MTBE concentration due to erratic feed flow rate. It is difficult to segregate the effects of adsorption from biodegradation under such circumstances. Therefore, MTBE removal after mid-July might not be completely attributed to biodegradation. However, the plot of MTBE removal with time from June to mid-July (the middle plot in Figure 2-13) revealed a clear trend of continuous improvement in MTBE biodegradation with time.

During July 2 to July 8, the MTBE injection pump failed. The influent MTBE concentration dropped to the original 400-500  $\mu\text{g/L}$  level. The effluent MTBE

concentration during that period was reduced to less than 30  $\mu\text{g/L}$  as compared with the greater than 100  $\mu\text{g/L}$  level previously measured. Similar phenomena were observed again on July 23 and August 3. These data strongly indicate that the growth and retention of the MTBE degraders in the FBBR did occur. However, the growth proceeded at a significantly slower rate than that expected from the MTBE biodegradation kinetics information obtained in the laboratory.

Figure 2-14 shows the biodegradation of DIPE in the FBBR after MTBE injection to the feed. Note that this set of data was the continuation of those of the last condition in Figure 2-11 (i.e., 3.5 gpm) since the influent DIPE concentration was maintained at the same level. The effluent DIPE concentration remained constant for a month after the feed flow rate was changed to 3.5 gpm, and slowly declined with time afterwards. The decline in the effluent DIPE concentration accelerated at the beginning of July with the effluent DIPE concentration reduced to less than 10  $\mu\text{g/L}$ .

Figure 2-15 shows the benzene biodegradation data in the FBBR during June 2 to August 10. Biodegradation of toluene, xylenes, and ethyl benzene was similar to benzene in that they were consistently degraded to less than 1  $\mu\text{g/L}$  under all test conditions.

### ***Effects of Low Temperature and Iron on MTBE Biodegradation in the FBBR***

As previously discussed, it was a surprise that it took the field FBBR a significantly longer time than the laboratory units to achieve the desirable MTBE removal. The major differences between the laboratory and the field unit include the following: (1) The laboratory unit used 300 to 600  $\mu\text{m}$  carbon particles as compared with the field FBBR which used 1.2 mm carbon particles. The particles in the field and the laboratory units obviously experienced different fluid shear, which might affect the attachment and retention of MTBE degraders on particle surface. (2) The laboratory unit was operated at 22  $^{\circ}\text{C}$ , while the water temperature in the field unit was between 14  $^{\circ}\text{C}$  in the winter and 17  $^{\circ}\text{C}$  in the summer. (3) The existing field FBBR data showed no effects of iron on

the biodegradation of the aromatic hydrocarbons. The potential impact of iron was therefore not investigated in the previous laboratory FBBR study on MTBE biodegradation. However, MTBE degraders had exhibited some unusual behavior such as susceptibility to environmental stresses. The potential iron interference with the attachment and retention of MTBE degraders should not be arbitrarily ruled out without further investigation.

A laboratory FBBR study was therefore initiated to evaluate the three factors described above. The study used three FBBR columns. Each column was 1 inch in diameter and 5 feet in height. Column 1 (designated as LFBBR-1) was loaded with 160 grams of carbon particles with an average size of 1.2 mm. Columns 2 and 3 (LFBBR-2 and 3) each used 100 grams of carbon particles with an average size of 0.75 mm. All three LFBBRs therefore had the same total external surface area onto which the microbial cells could attach. The carbon particles in LFBBR-1 and those in LFBBR-2 and 3 were from different carbon vendors: LFBBR-1 used the same carbon particles as the field unit, while the carbon particles used in LFBBR-2 and 3 were the same as those used in the previous laboratory study (Tang and Wilcox, 1993). LFBBR-1 and LFBBR-2 were operated at 22 °C, while LFBBR-3 was operated at 15 °C.

The initial phase of this study was to investigate the effects of particle size and operating temperature. Later, ferrous sulfate was injected in the feed to study the effects of iron. To simulate the fluid-particle shear condition in the field FBBR unit, the recycle rate for all three LFBBRs was 300 ml/min, which gave the same superficial upward liquid velocity as that in the field FBBR unit. All the carbon particles had been equilibrated with the intended influent MTBE concentration, approximately 400 µg/L, before the MTBE degrading mixed culture was seeded. Two hundred milliliters of MTBE degrading mixed culture with a MLVSS of 1950 mg/L was seeded to each of the LFBBRs.

The results of the laboratory study are summarized in Figure 2-16. MTBE biodegradation started almost immediately after seeding in LFBBR-1 and 2. The effluent MTBE

concentration was reduced consistently to below 20  $\mu\text{g/L}$  and 10  $\mu\text{g/L}$  for LFBBR-1 and 2, respectively. Since LFBBR-1 and 2 were operated under the same conditions except for the particle size and source, it is clear that those differences were not the cause for the significantly slower MTBE biodegradation in the field FBBR. However, it is interesting to note that the effluent quality of LFBBR-2 was consistently better than that of LFBBR-1, indicating effects of particle property could not be totally discounted.

The MTBE degraders seemed to require a long adaptation phase when subjected to low temperature shock as occurred in LFBBR-3. Very little MTBE biodegradation was observed within the first 20 days after the culture was seeded at 15 °C. MTBE biodegradation eventually took off after that, and achieved an even better effluent quality than LFBBR-1 after 2 months of operation. In comparison, for a FBBR which had an already established stable population of the MTBE degraders, the MTBE degradation deteriorated slightly when subjected to the same magnitude of temperature shock, but regained complete adaptation after 2 weeks (Tang and Wilcox, 1993). Therefore, it appears that the low temperature shock affected strongly the immobilization of the MTBE degraders onto carbon particles and their subsequent growth and development. This result also implies that if the carbon can be pre-immobilized with sufficient population of MTBE degraders, the startup of the FBBR for MTBE treatment can be greatly accelerated over what has been experienced in this field study.

Ferrous sulfate was injected at a concentration of 10 mg/L at the entrance of the LFBBR-2 column, to evaluate the effects of iron on MTBE biodegradation in the FBBR. After approximately 1 week of ferrous sulfate injection, the majority of the carbon particles were covered with reddish iron flocs. As shown in Figure 2-16, the effluent quality of LFBBR-2 was not impacted after continuous injection of ferrous sulfate for 1 month. It appears that once the MTBE degraders have been established on the carbon surface, the presence of iron and coverage of iron flocs on the carbon surface do not adversely affect the MTBE biodegradation in the FBBR.

On about Day-90, the influent MTBE concentration was increased from 500 µg/L to 4 mg/L for two purposes: (1) Additional growth and retention of the MTBE degraders would be needed to handle the extra MTBE loading. Therefore, this test allowed the effects of iron to be evaluated under conditions similar to the startup period. (2) The test would also provide a better controlled condition for observation of the effect of concentration shock on the MTBE biodegradation under a lower temperature, 15 °C.

Figure 2-16 shows that all three LFBBRs were adversely impacted by the concentration shock. Shortly after the shock, the effluent MTBE concentration in LFBBR-1 increased sharply to about 1 mg/L. It then stabilized at the 1 mg/L level for about 1 month, and improved slowly with time afterwards. At the time this test was terminated, the effluent MTBE concentration in LFBBR-1 had been reduced to less than 400 µg/L.

The effluent MTBE concentration in LFBBR-2, which was dosed with ferrous sulfate, increased drastically to 2 mg/L, and started to decrease at a very slow pace thereafter. The effluent MTBE concentration in LFBBR-2, which was consistently lower than that of LFBBR-1 before concentration shock, was significantly higher than LFBBR-1 throughout the concentration shock test.

For LFBBR-3 operated at 15 °C, the effluent MTBE concentration increased immediately after the concentration shock and maintained at a level very close to the influent concentration. The difference between the influent and effluent concentrations after the concentration shock was only slightly greater than that maintained before the shock, indicating that the magnitude of MTBE biodegradation remained about the same. Judging from the previous data that showed LFBBR-3 required three times longer than LFBBR-1 and 2 to achieve desirable MTBE biodegradation during the startup phase and that it took LFBBR-1 about 1.5 months after this concentration shock to display effective MTBE biodegradation, significant improvement in MTBE biodegradation in LFBBR-3 was not anticipated within 4 to 6 months. The laboratory tests were terminated at the conclusion of the field project.

Table 2-4 shows the total suspended solids (TSS) and volatile suspended solids (VSS) in the effluents of the three LFBBRs. The TSS in the effluent of LFBBR-2, which was dosed with 10 mg/L ferrous sulfate, was significantly higher than that in the effluent of LFBBR-1 and 3, primarily due to the iron flocs elutriated out of the unit. The VSS in the effluent of LFBBR-2 was also higher than LFBBR-1 and 3, suggesting that some biomass might be lost together with iron flocs from the system. It is possible that the biomass enmeshed with iron flocs on the carbon particle surface. Upon particle-particle collision or fluid shear, iron flocs were sloughed off of the particle surface, and were elutriated out of this LFBBR. It is possible that the loss of MTBE degraders with iron flocs might also occur in the field unit such that the increase in the MTBE degrader population in the FBBR was significantly delayed and hence partially contributed to the slow progress of MTBE biodegradation observed in the field unit.

### *Polishing of the Field FBBR Effluent*

After a prolonged operation of the field FBBR, sloughing of biofilm from the carbon particles can occur particularly if the organic loading is high. Occasionally high total suspended solids (TSS) resulting from the dislodging of the biomass from the FBBR thus can occur in the effluent. In some cases, carbon adsorbers may be used downstream of the FBBR to ensure complete compliance of the discharge. Both of these two conditions require a polishing step following the FBBR to remove TSS and to prolong the operation of carbon adsorbers. During this study, two test runs of a sand filter were conducted to evaluate its performance as a polishing process for the FBBR effluent. The results are tabulated in Tables 2-5 and 2-6.

In the sand filter tests, the FBBR effluent was gravity-drained to a surge tank before it was pumped to the sand filter. The first test run was operated at a flow rate of 2 gpm and the second run at about 3.2 gpm. The sand filter had a cross-sectional area of 0.785 ft<sup>2</sup>. Therefore, the filtration flux was 2.55 and 4 gpm/ft<sup>2</sup>, respectively for Runs #1 and 2.

In Run #1, the TSS coming out of the FBBR were in the range of 8 to 10 mg/L. The constituents of the suspended solids were about 2 mg/L of biomass measured in terms of VSS and about 2-3 mg/L of iron (equivalent to 4-6 mg/L iron hydroxide). Approximately half of the iron in the FBBR effluent was in the soluble or non-filterable form. The filter was operated continuously for the 34-day period without backwash. The loading of solids increased dramatically at the end of the run, primarily due to the dislodging of solids adhered to the wall of the surge tank. The pressure of the sand filter increased to 20 psi around Day-34, the sand filter was shutdown for backwash. Throughout Run #1, the effluent TSS concentration had been maintained close to zero.

The TSS in the FBBR effluent in Run #2 were approximately 20 mg/L, significantly higher than that in Run #1. This is primarily due to higher organic loading into the FBBR as evidenced from the VSS data in Run #2. Interestingly, the iron in the FBBR effluent was primarily non-filterable iron since the concentration of the total iron was about the same as that of soluble iron. The pressure in the sand filter increased rapidly after 11 days of operation at 4 gpm/ft<sup>2</sup>. The sand filter was shut down for backwash after 2 weeks of operation.

The total suspended solids loading to the sand filter before back wash were 10-11 lbs for both runs. The results of the sand filter test runs show that excellent effluent quality can be achieved with a sand filter operated under a solid loading of 10 to 20 mg/L and a filtration rate of 2 to 4 gpm/ft<sup>2</sup>. The backwash frequency under such operating conditions is from 10 to 30 days.

### ***The MTBE Biodegradation Capacity of the FBBR***

Figure 2-17 summarizes the relationship between the influent MTBE loading and effluent MTBE concentration for all the MTBE biodegradation data obtained in the pilot FBBR study. It appears that the FBBR could achieve the desirable < 100 µg/L effluent MTBE concentration under a loading of up to 40 mg/day/L FBBR. This loading is substantially

lower than the 100 mg/day/L demonstrated in the laboratory study by Tang and Wilcox (1993). The difference in the maximum MTBE loading rate between the laboratory and the field unit could be attributed to the slow growth of the MTBE degraders at low temperature and the iron interference encountered in the field unit. Given sufficient time for the field unit to fully adapt to the low temperature and iron condition, there is no obvious reason why the field unit would not deliver the desirable effluent MTBE quality at a loading rate similar to that of the laboratory units.

### **E. Conclusions**

1. Iron interference with the retention and accumulation of the MTBE degrader biomass on carbon particles should be further investigated. Iron interference together with low temperature of groundwater may have delayed the growth of the MTBE degrader population in the FBBR.
2. In lieu of the long startup time under the field conditions, pre-immobilization of a large population of MTBE degraders onto the carbon particles before startup could be a viable alternative to ensure the success of the FBBR process for MTBE treatment.
3. Once the MTBE degraders are retained in the FBBR, the FBBR exhibited consistent MTBE removal and excellent stability against process upset.
4. In this pilot study, an effluent of less than 100  $\mu\text{g/L}$  MTBE could be achieved with a MTBE loading rate of approximately 40 mg MTBE/L/day. It is likely that the FBBR can handle even higher MTBE loading if sufficient time is allowed for the FBBR to accumulate enough MTBE degrader population.

Table 2-1. Chemical Characteristics of the Feed Wastewater  
Single Sample Taken During Planing Phase

<b>ANALYTIC PARAMETERS</b>	<b>Concentration (mg/L)</b>
<b>GENERAL</b>	
BOD	9
COD	29.5
TOC	6
O&G (Gravimetric)	BDL (< 5 mg/L)
TSS	18
TDS	1758
Conductivity (µmho/cm)	3100
Sulfide	BDL (< 1 mg/L)
Cyanide	BDL (< 5 µg/L)
Ammonia N	BDL (< 1 mg/L)
Nitrate N	BDL (< 1 mg/L)
TKN	0.3
Total Iron	9
Soluble Iron	7
Alkalinity (as CaCO <sub>3</sub> )	430
Hardness (as CaCO <sub>3</sub> )	635
pH	7.2
<b>VOLATILES</b>	
Benzene	0.68
Toluene	1.396
Xylenes	0.307
MTBE	0.302
DIPE	0.483
<b>METALS</b>	
Arsenic	0.018
Beryllium	BDL (< 2 µg/L)
Cadmium	BDL (< 1 µg/L)
Chromium	0.005
Copper	0.011
Lead	BDL (< 1 µg/L)
Mercury	BDL (< 1 µg/L)
Silver	BDL (< 2 µg/L)
Zinc	0.02
<b>OTHER CATIONS &amp; ANIONS</b>	
Chloride	270
Phosphate	< 1

Note: BDL - below detection limit

Table 2-2. Contents of Polynuclear Aromatic Hydrocarbons in the Wastewater

Polynuclear Aromatic Hydrocarbons	Influent ( $\mu\text{g/L}$ )
Naphthalene	4
Acenaphthylene	< 1
Acenaphthene	< 1
Fluorene	< 1
Phenanthrene	< 1
Anthracene	< 1
Fluoranthene	< 1
Pyrene	< 1
Benzo(a)Anthracene	< 1
Chrysene	< 1
Benzo(b)Fluoranthene	< 1
Benzo(k)Fluoranthene	< 1
Benzo(a)pyrene	< 1
Benzo(g,h,i)pyrene	< 1
Indeno(1,2,3-c,d)pyrene	< 1
Dibenzo(a,h)anthracene	< 1

Table 2-3. Monitoring Parameters for the Characterization of the Feed and the Treated Effluent

ANALYTIC PARAMETERS	Influent (mg/L)	Effluent (mg/L)
<b>GENERAL</b>		
BOD	1/week	1/week
COD	2/week	2/week
TOC	2/week	2/week
O&G (Gravimetric)	2/test conditions	2/test conditions
TSS	2/week	2/week
TDS	Initial sample	
Conductivity	1/week	1/week
Sulfide	initial sample	
Cyanide	initial sample	
Ammonia N	2/week	2/week
Nitrate N	2/week	2/week
Total Kjehdel Nitrogen (TKN)	initial sample	initial sample
Total Iron	daily	daily
Soluble Iron	daily	daily
Alkalinity (as CaCO <sub>3</sub> )	2/month	2/month
Hardness (as CaCO <sub>3</sub> )	2/month	2/month
pH	daily	daily
<b>VOLATILES</b>		
Benzene	daily	daily
Toluene	daily	daily
Xylenes	daily	daily
MTBE	daily	daily
DIPE	daily	daily
<b>OTHERS</b>		
Carbon Bed Height	2/week	2/week
Dissolved Oxygen (DO)	daily	daily

Note: This single sample was collected during the planning phase.

Table 2-4. Comparison of the TSS and the VSS in the Effluent of the LFBBRs After the Injection of Fe<sub>2</sub>(SO<sub>4</sub>)<sub>3</sub> into LFBBR-2

Run Days	LFBBR-1 Effluent		LFBBR-2 Effluent		LFBBR-3 Effluent	
	TSS (mg/L)	VSS (mg/L)	TSS (mg/L)	VSS (mg/L)	TSS (mg/L)	VSS (mg/L)
60	2	1	11	3	4	~0
87	3	2	17	5	3	1
106	2	1	6	2	4	~0
114	0	1	17	3	2	~0
126	1	1	10	2	2	~0
140	2	~0	12	3	3	1
143	3	~0	8	1	5	2
158	3	1	11	3	0	2
172	4	2	14	3	4	1

Table 2-5. Sand Filter Operation Data - Test Run #1

Run (Days)	Flow (gpm)	Press. (psi)	TSS (mg/L)		VSS (mg/L)		Total Fe (mg/L)		Soluble Fe (mg/L)	
			Inlet	Outlet	Inlet	Outlet	Inlet	Outlet	Inlet	Outlet
0	2	0	8	0	2	0	2.1	0	1	0
1	2	2	8	0	2	0	1.7	0	0.5	0
2	2	2	8	0	2	0	2.1	0	1	0
3	2	2	8	0	2	0	2	0	1	0
7	1	2	10	0	1	0	2	0	1	0
8	2	2	8	0	2	0	2.1	0	1	0
9	2	2	7	0	2	0	1.8	0	0.6	0
10	2	2	8	0	2	0	1.8	0	1	0
11	2	2	8	0	2	0	1.8	0	1	0
12	2	2	7	0	2	0	1.6	0	1	0
13	2	2	6	0	2	0	2.2	0	1	0
14	2	2	6	0	2	0	2.3	0	1	0
15	2	2	6	0	2	0	2.6	0	1	0
16	2	2	7	0	2	0	2.2	0	1	0
17	2	2	6	0	2	0	2.3	0	1	0
18	2	2	8	0	2	0	2.6	0	1	0
19	2	2	8	0	2	0	3.1	0	1	0
20	2	6	8	0	2	0	2.2	0	1	0
21	2	2	6	0	2	0	2	0	1.2	0
22	2	6	6	0	2	0	1.3	0	1.2	0
23	2	6	6	0	2	0	1.5	0	1.2	0
24	2	8	7	0	2	0	1.5	0	1.2	0
25	2	7	7	0	2	0	1.5	0	1	0
26	2	8	8	0	2	0	1.4	0	1.2	0
27	2	8	8	0	2	0	1.2	0	1.3	0
28	2	8	8	0	2	0	1.5	0	1.2	0
29	2	10	8	0	2	0	1.5	0	1	0
30	2	12	11	0	8	0	2	0	1.2	0
31	2	16	22	0	16	0	8	0	1.2	0
32	2	20	22	0	16	0	8	0	1.2	0
33	2	20	35	0	22	0	8	0.1	1.4	0
34	2	20	154	0	100	0	15	0.2	1.4	0

Table 2-6. Sand Filter Operation Data - Test Run #2

Run (Days)	Flow (gpm)	Press. (psi)	TSS (mg/L)		VSS (mg/L)		Total Fe (mg/L)		Soluble Fe (mg/L)	
			Inlet	Outlet	Inlet	Outlet	Inlet	Outlet	Inlet	Outlet
0	3.2	6	11	0	6	0	3.4	6.8	2.5	5.4
1	3.1	6	15	0	6	0	3.5	0	2.6	2.1
2	3.2	6	21	0	10	0	3.5	1	3	0.5
3	3.2	6	21	0	11	0	3	0	3	0
4	3.2	6	21	0	12	0	4	0	3	0
5	3.2	10	22	0	11	0	3.5	1.2	3	0
6	3.4	15	21	0	11	0	3.6	1	3.5	0
7	3.15	15	23	0	11	0	3.6	1	3.2	0.3
8	3.1	20	13	0	2	0	3.5	1	3.1	0
9	3.16	20	15	0	4	0	5	1	4.6	0
10	3.15	20	12	0	6	0	3.4	1	3.4	0
11	3.2	20	21	0	9	0	3.7	1	3.2	0
12	3.21	26	32	0	8	0	3.4	1	3.2	0
13	3.08	35	24	0	9	0	3.6	1	3	0
14	3.11	35	23	0	11	0	3.6	1	3	0.2

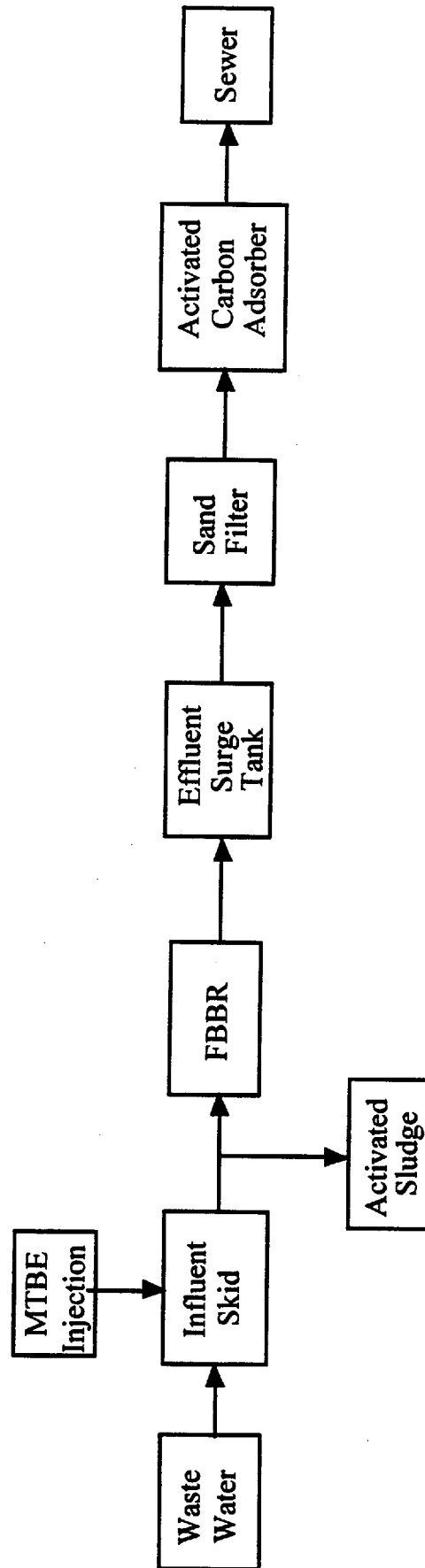


Figure 2-1. Flow diagram of the pilot scale treatment system

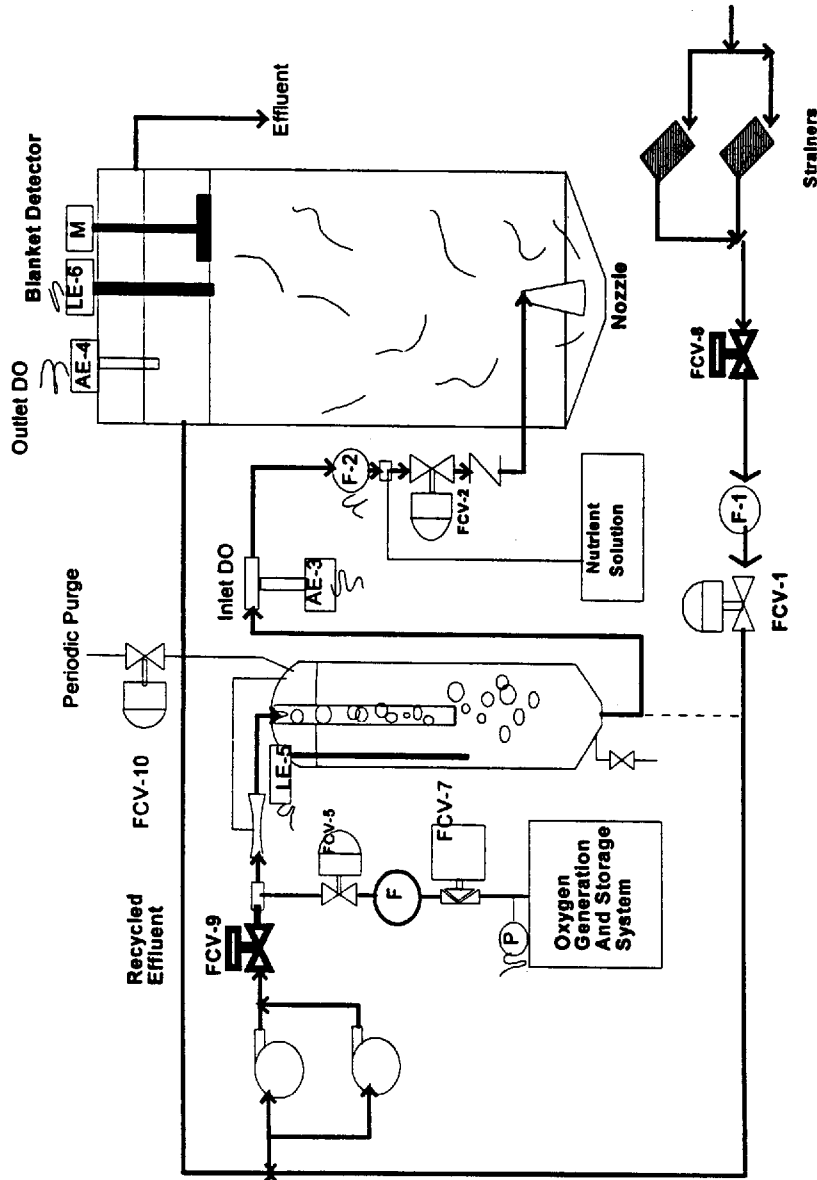


Figure 2-2. Schematic diagram of the fluidized bed biological reactor

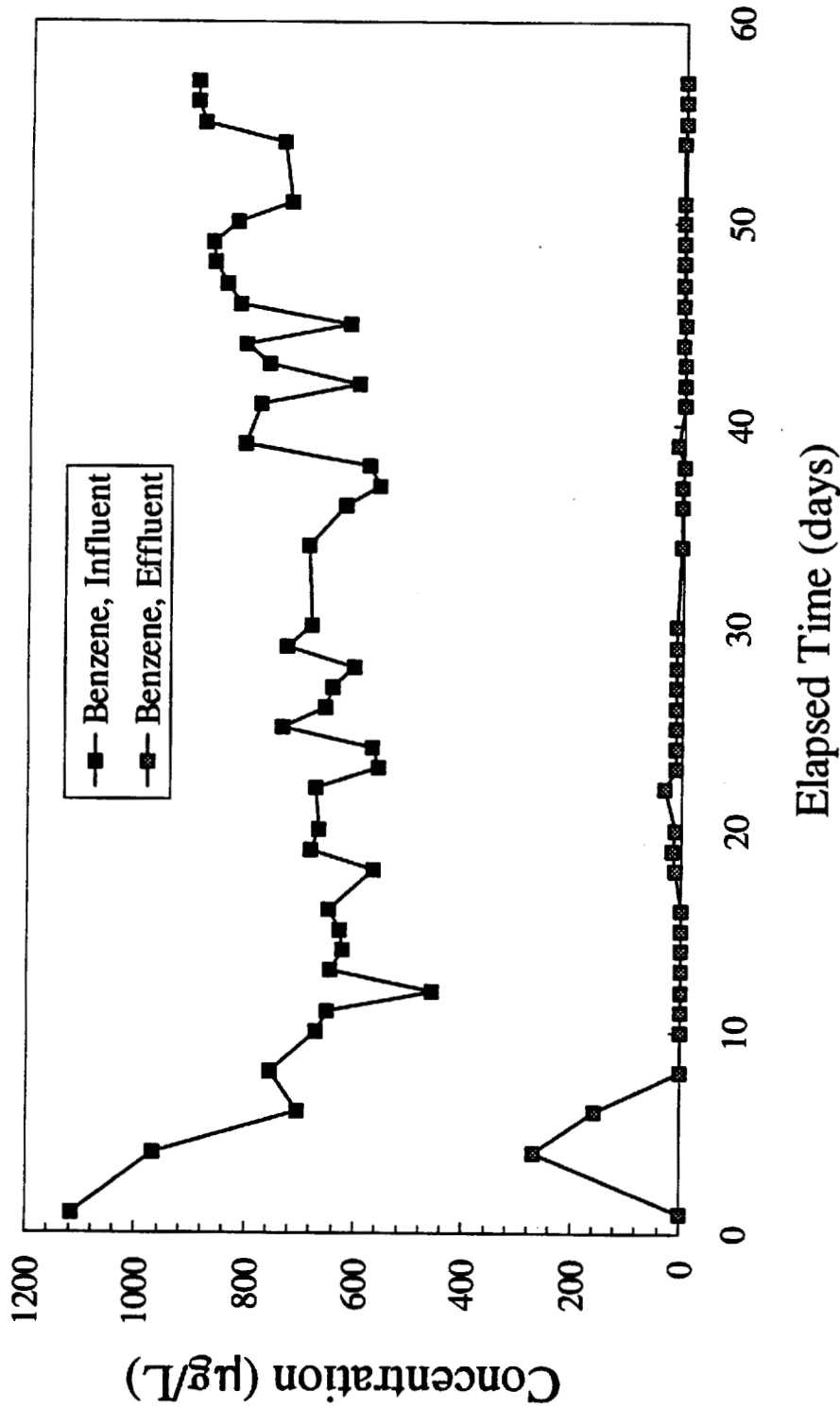


Figure 2-3. The performance of benzene degradation in the FBBR during the initial startup

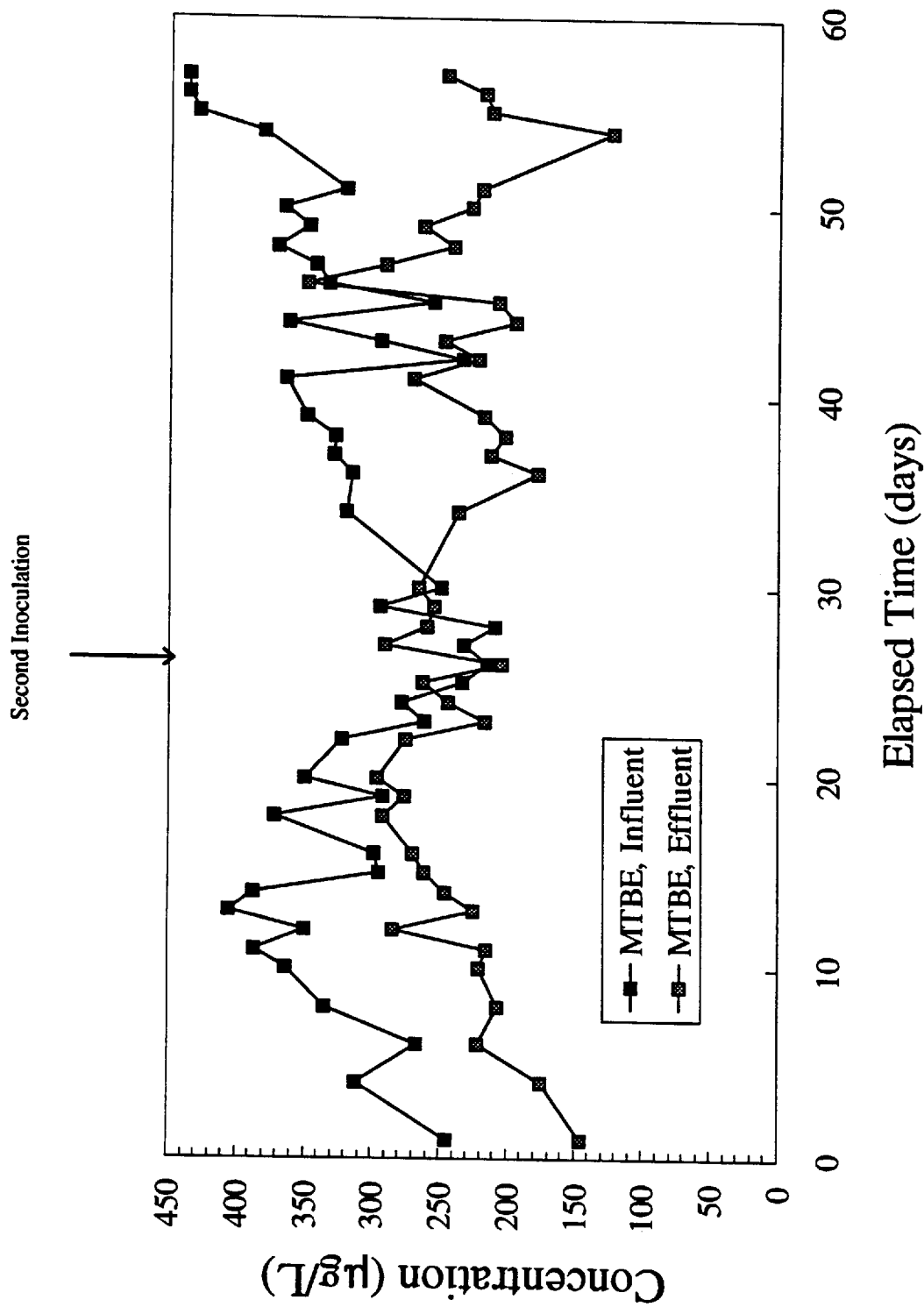


Figure 2-4. The performance of MTBE degradation in the FBR during the initial startup

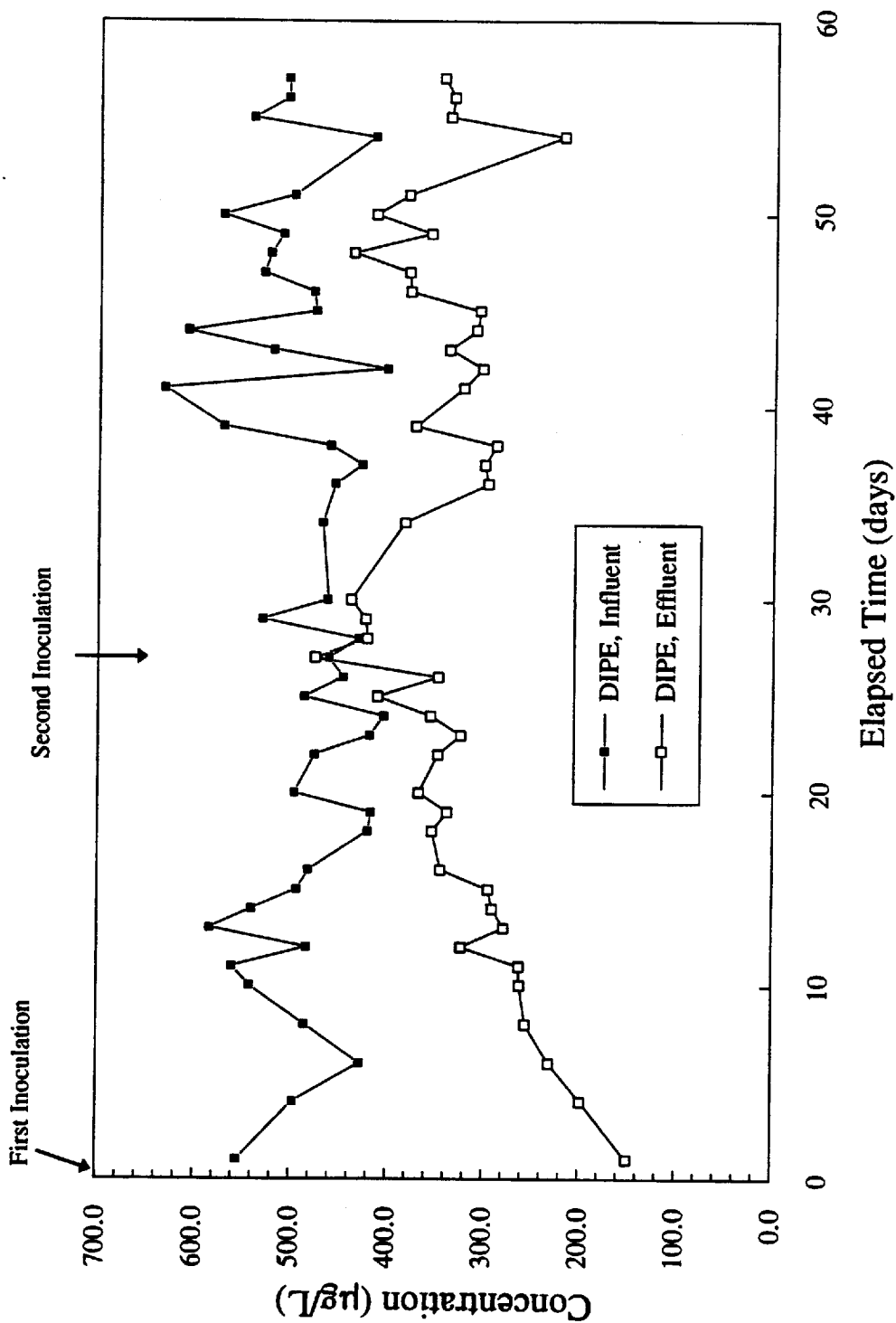


Figure 2-5. The performance of DIPE degradation in the FBBR during the initial startup

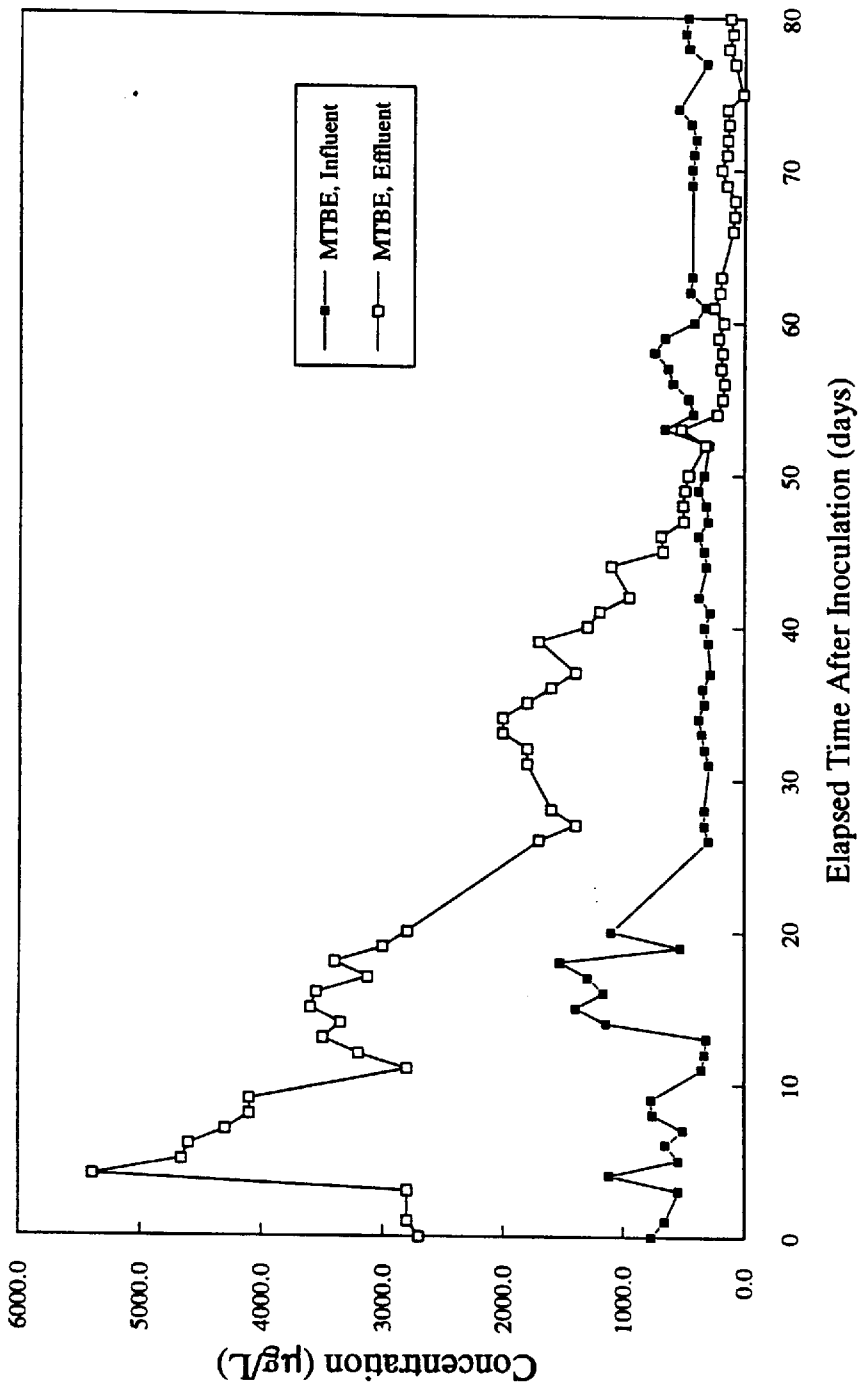


Figure 2-6. The performance of MTBE degradation in the FBRR during the 2nd startup

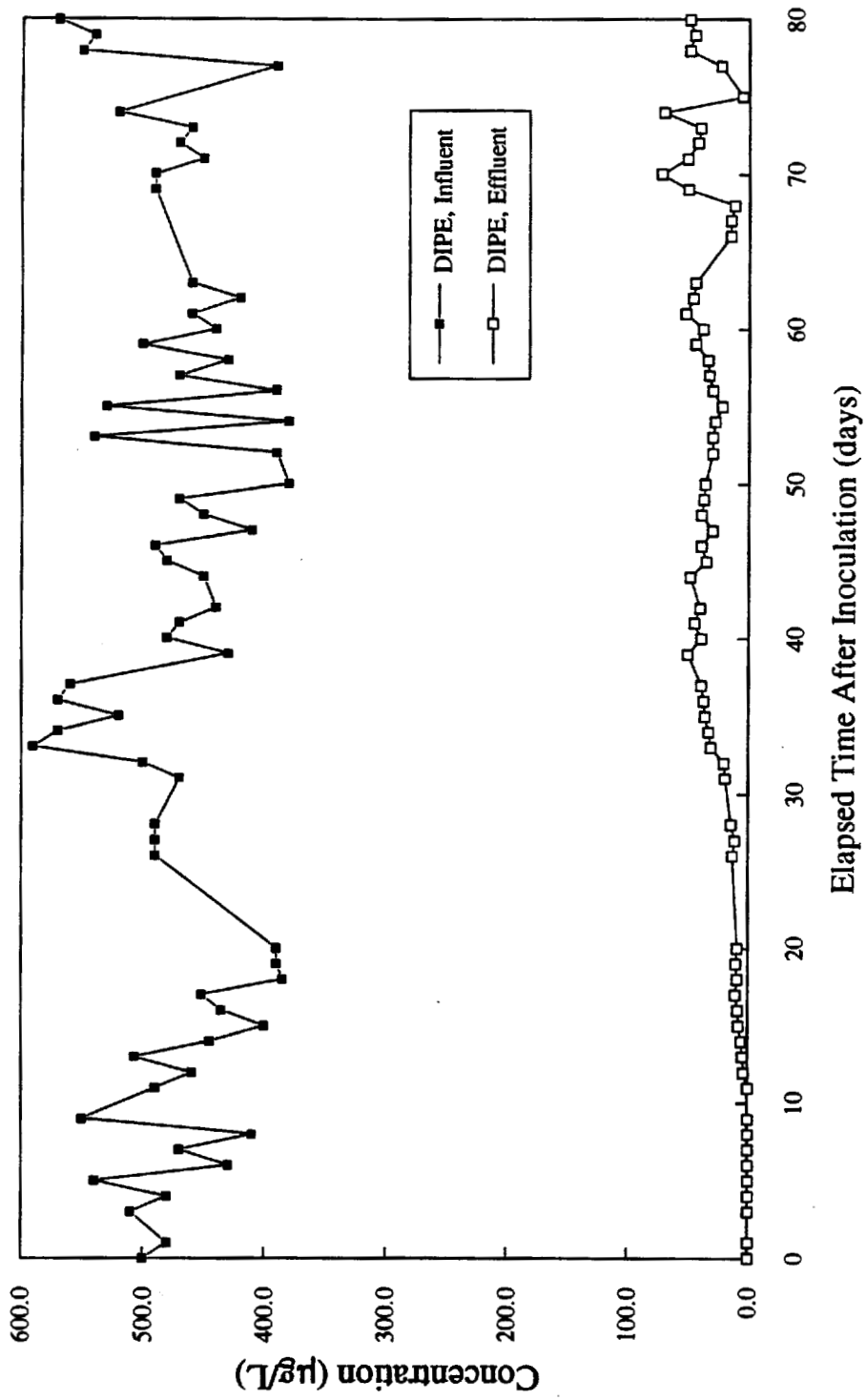


Figure 2-7. The performance of DIPE degradation in the FBRR during the 2nd startup

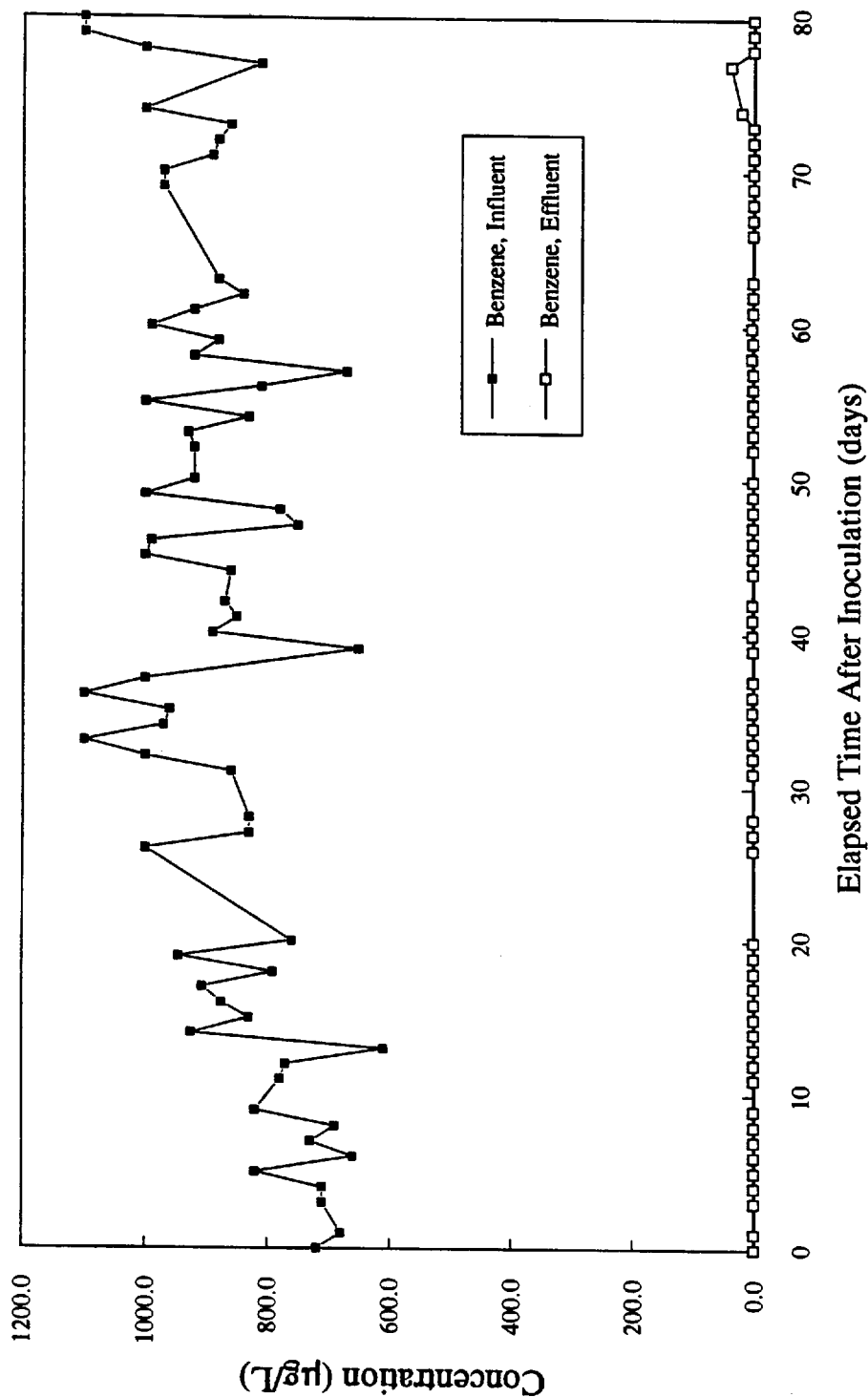


Figure 2-8. The performance of benzene degradation in the FBBR during the 2nd startup

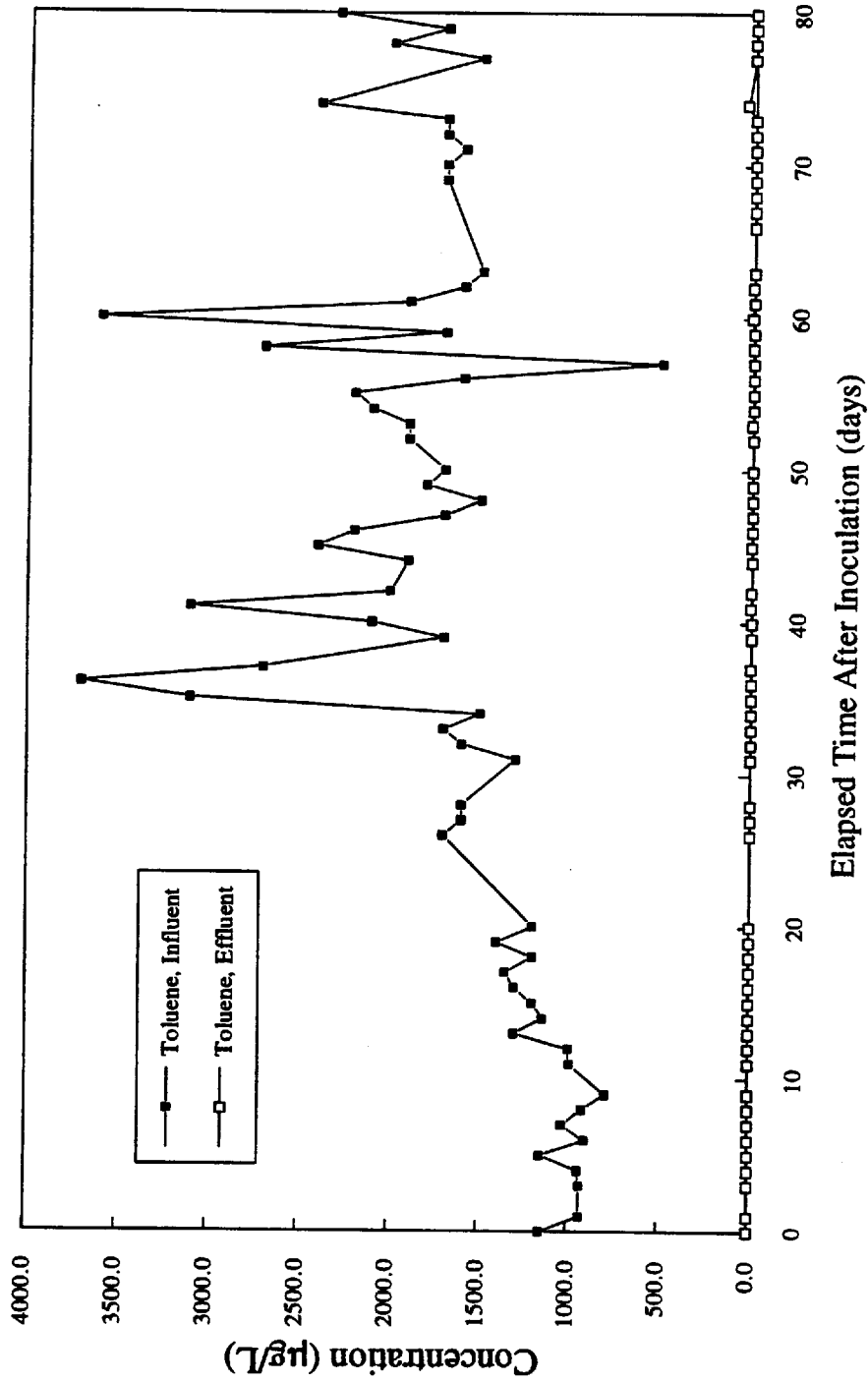


Figure 2-9. The performance of toluene degradation in the FBBR during the 2nd startup

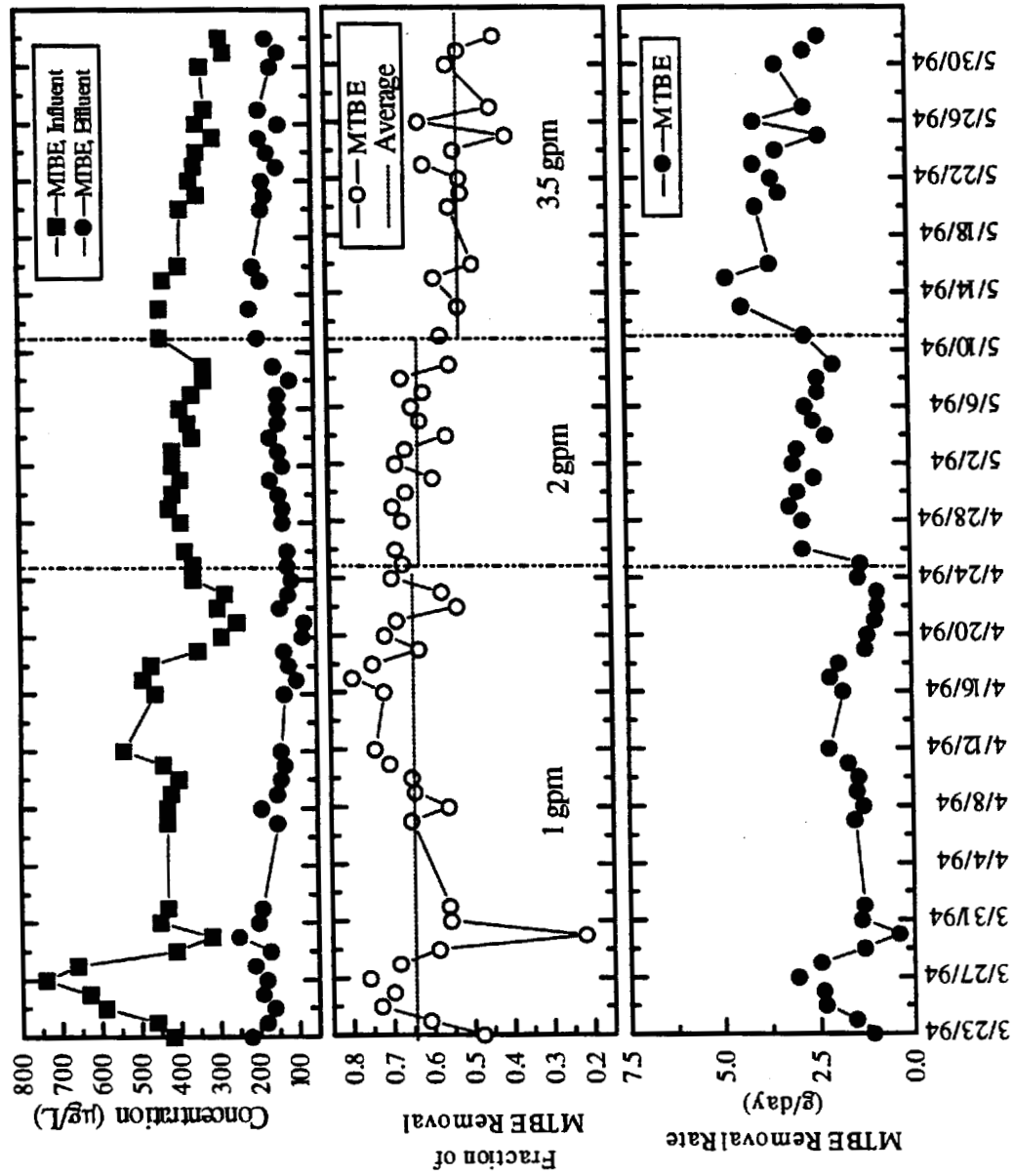


Figure 2-10. Performance of MTBE biodegradation in the FBFR under different feed flow rate conditions - No MTBE was injected in the feed

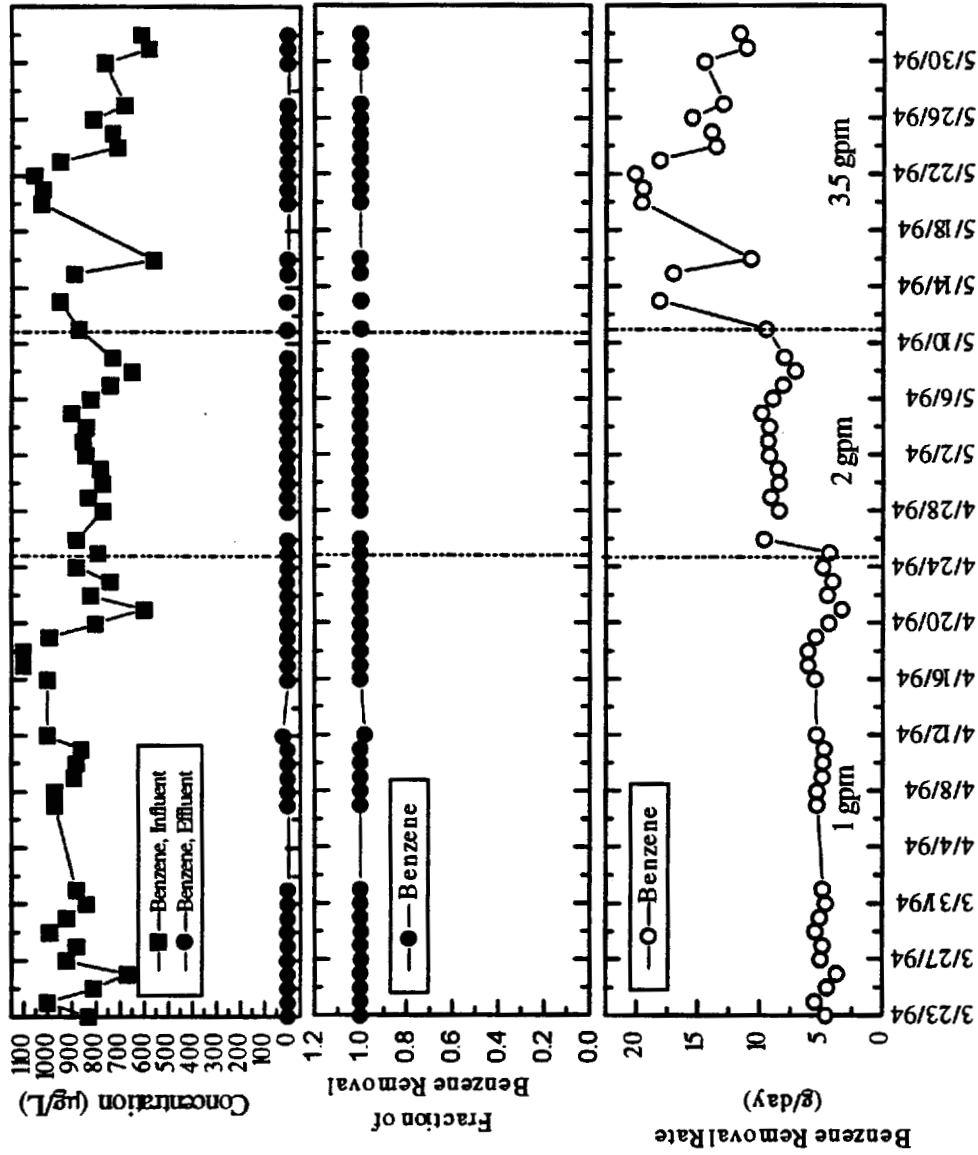


Figure 2-11. Performance of benzene biodegradation in the FBRR under different feed flow rate conditions  
 - No MTBE was injected to the feed

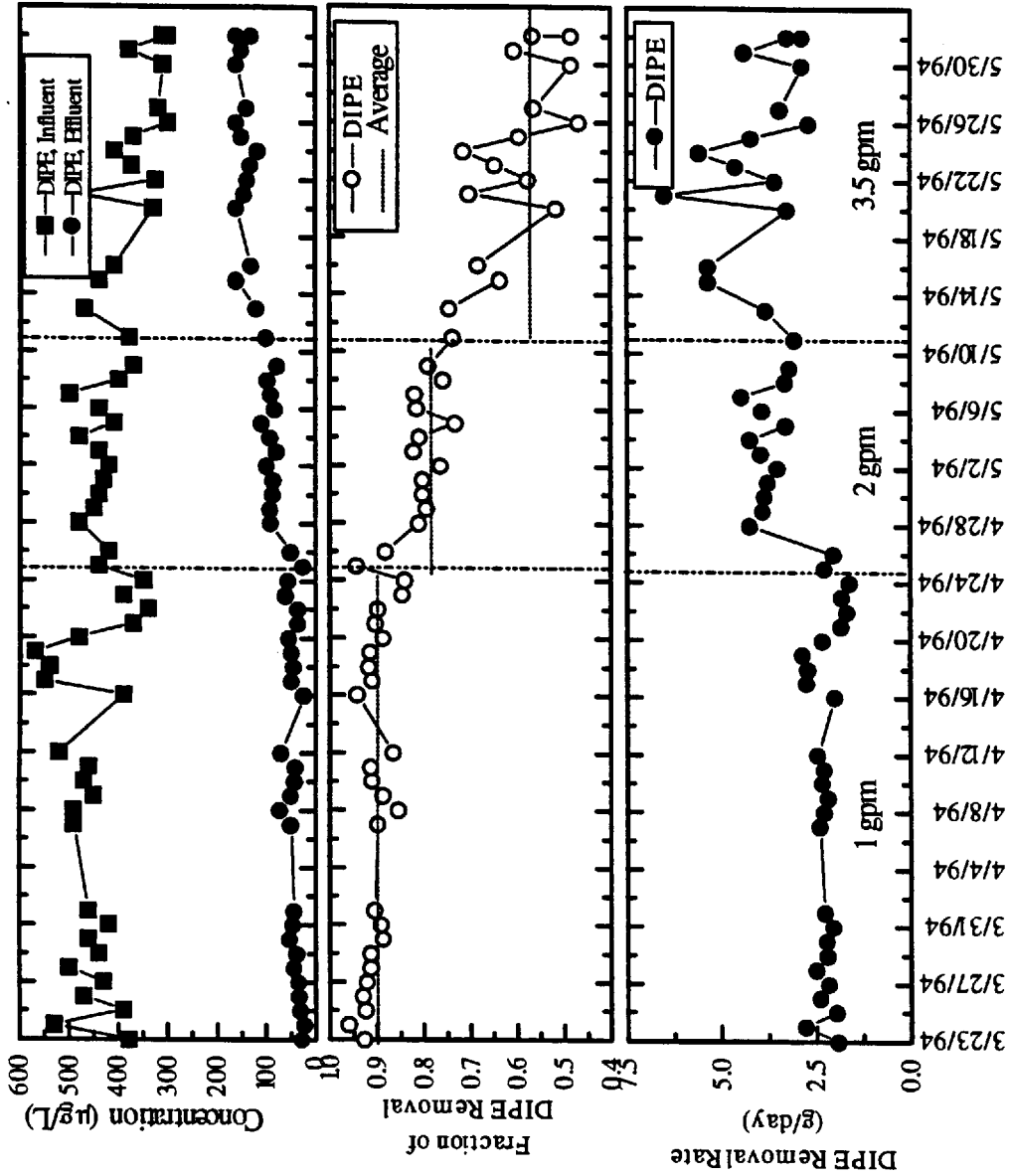


Figure 2-12. Performance of DIPE biodegradation in the FBBR under different feed flow rate conditions - No MTBE was injected to the feed

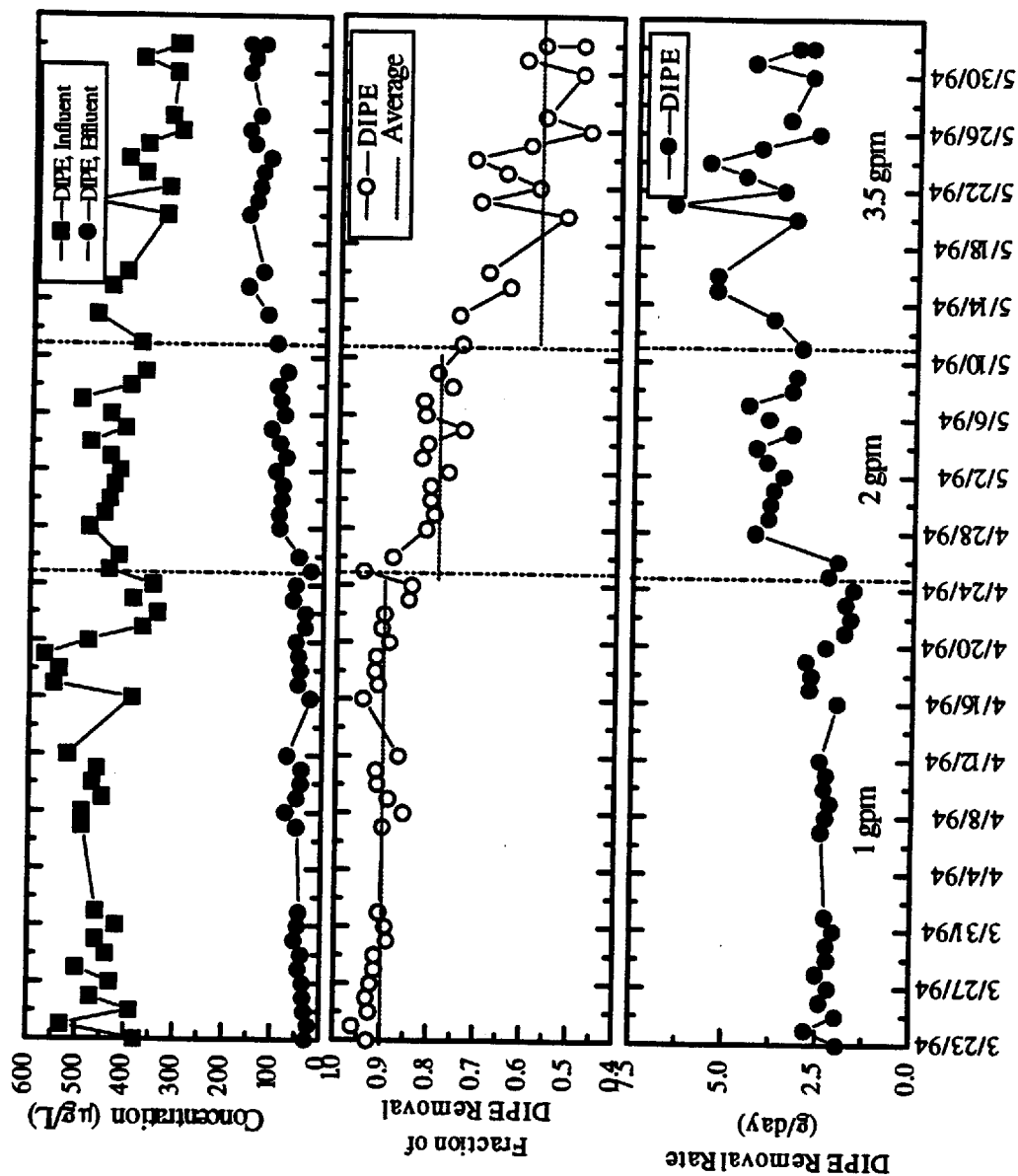


Figure 2-12. Performance of DIPE biodegradation in the FBRR under different feed flow rate conditions - No MTBE was injected to the feed

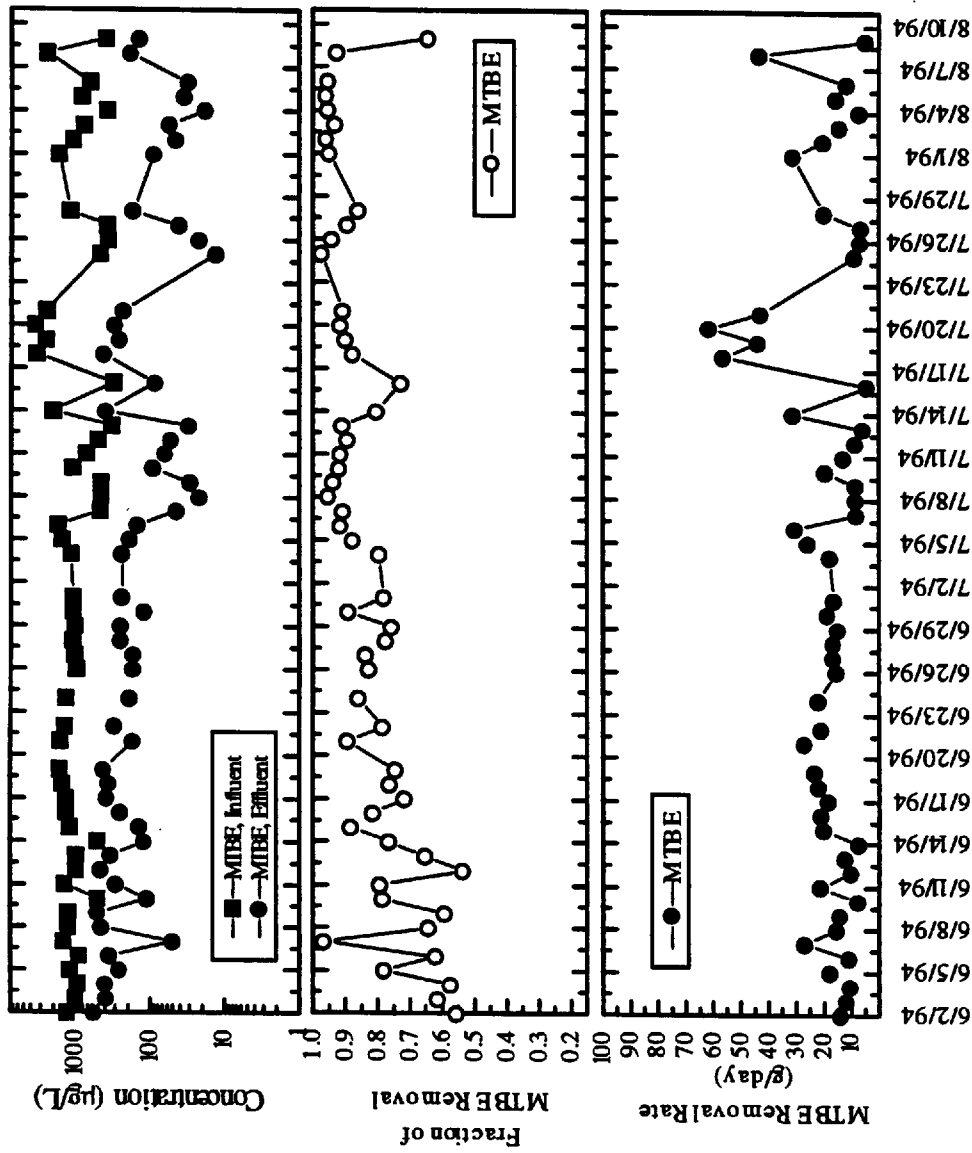


Figure 2-13. Performance of MTBE biodegradation in the FBFR under different feed flow rate conditions - Influent MTBE was increased to 1 mg/L and feed flow rate was maintained at 3.5 gpm

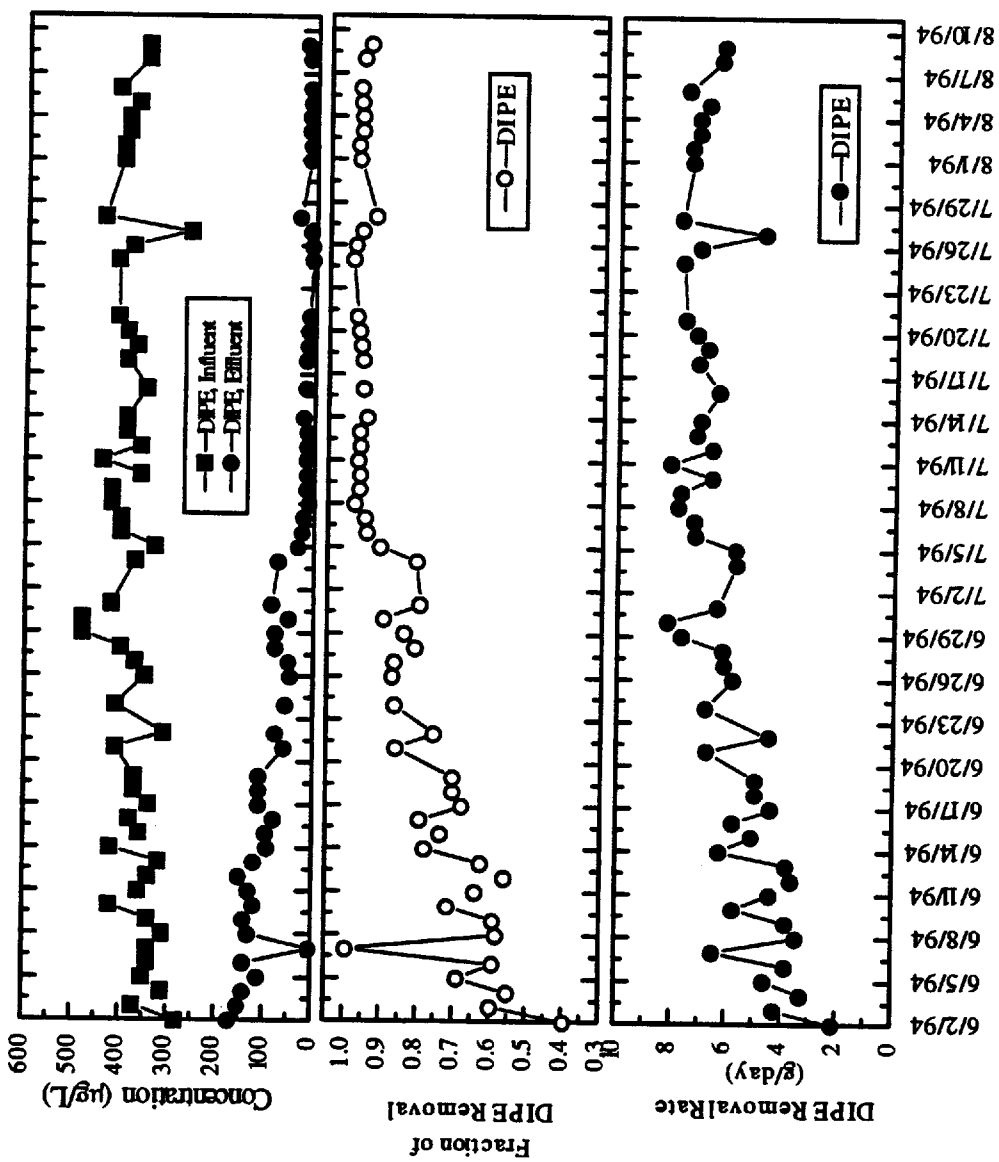


Figure 2-14. Performance of DIPE biodegradation in the FBFR under different feed flow rate conditions - Influent MTBE was increased to 1 mg/L and feed flow rate was maintained at 3.5 gpm

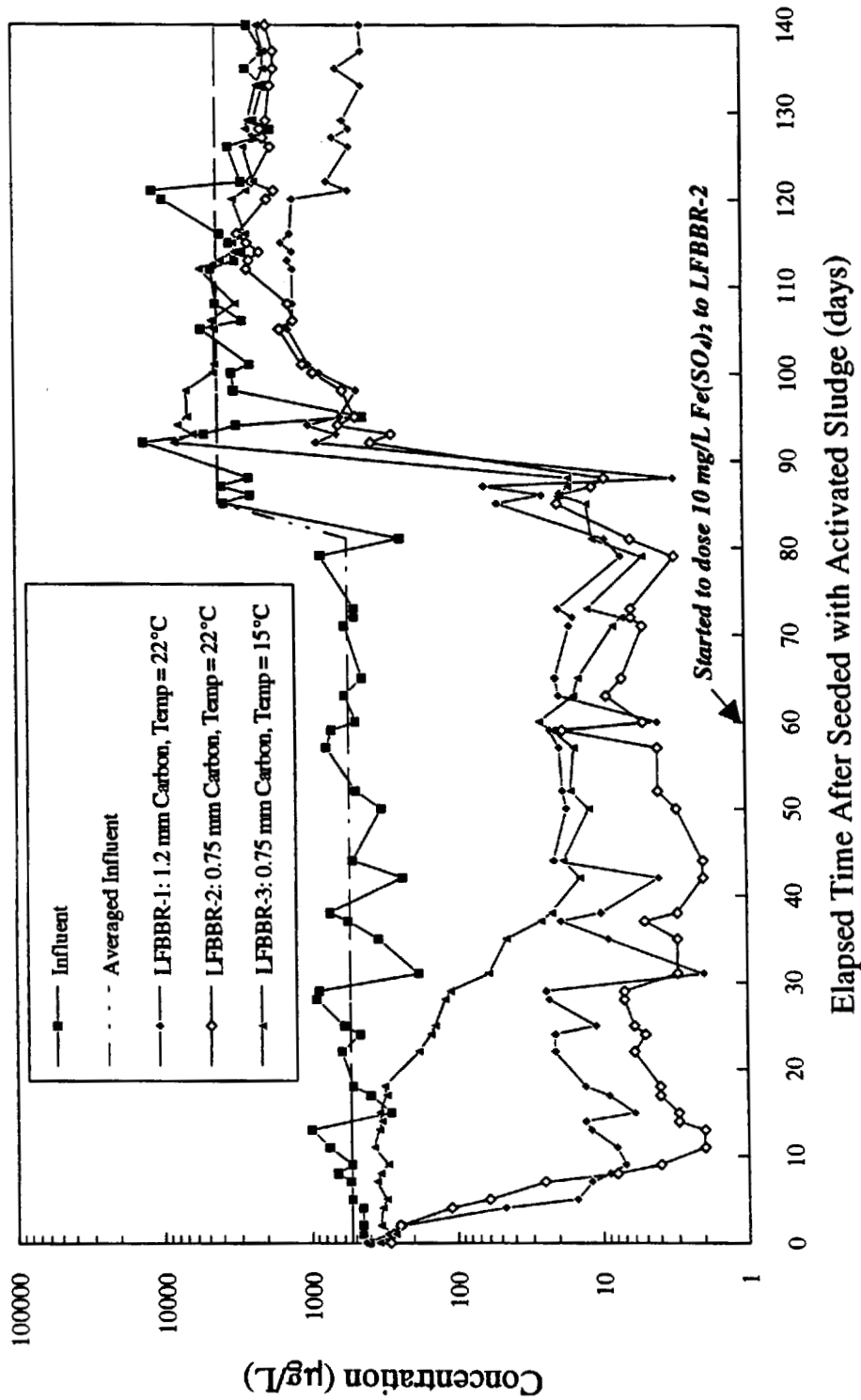
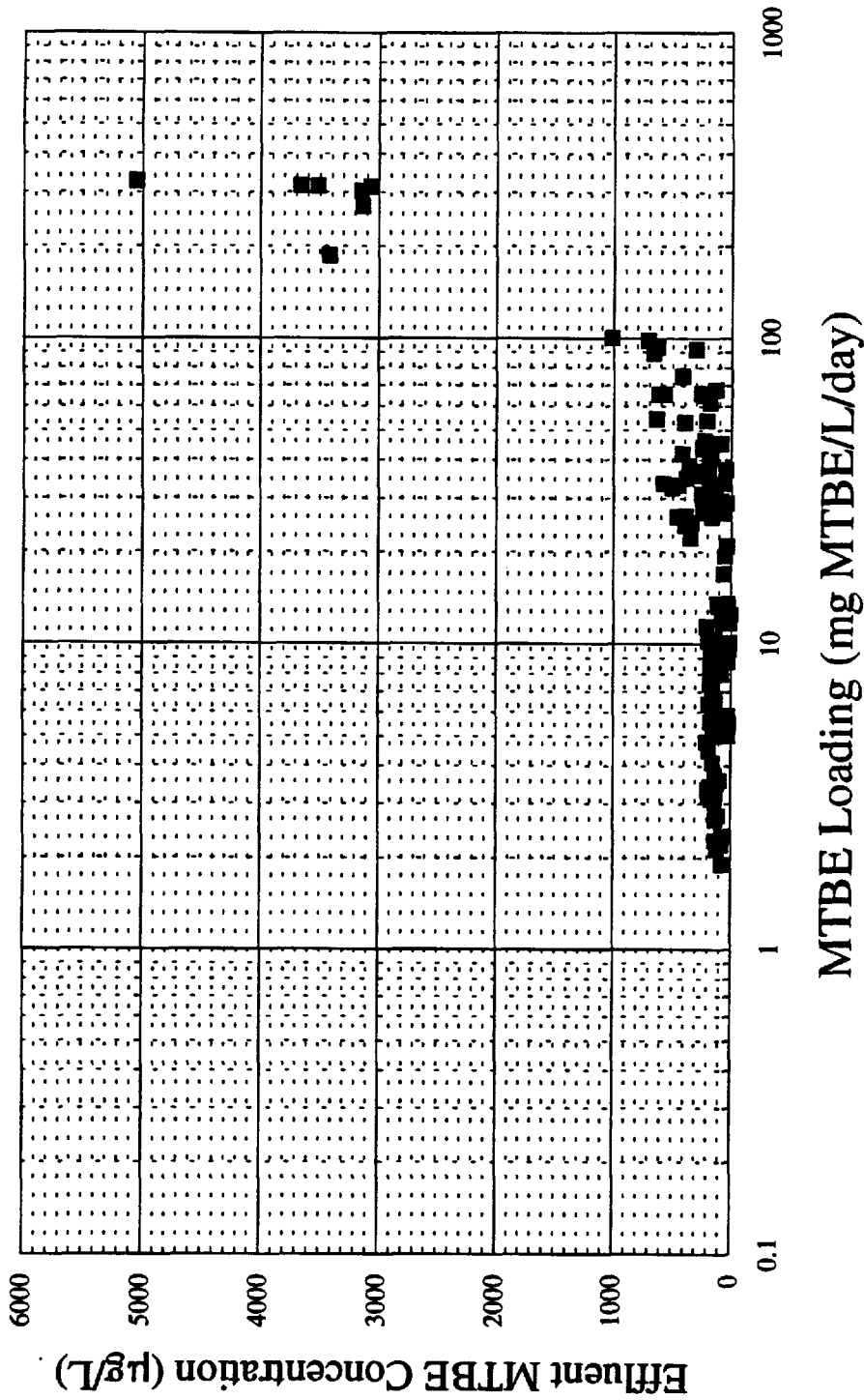


Figure 2-16. Effects of carbon particle properties, temperature, and iron on the MTBE biodegradation in laboratory FBRRs



**Total Reactor volume is 190 gallons**

**Figure 2-17. Summary of the MTBE biodegradation data in a 30 gallon FBBR pilot unit**  
 - Influent MTBE loading vs. effluent MTBE concentration

### Section 3

## ACTIVATED SLUDGE SYSTEM

### A. Introduction

The activated sludge process is the most widely used biological wastewater treatment process. It is a relatively straightforward and cost-effective process in both operation and maintenance. These features are important for a treatment system to be deployed at marketing distribution terminals which normally are not staffed with skilled wastewater treatment personnel. The conventional activated sludge system, however, does not work well for wastewater containing very low organic concentrations such as those in this study because the biomass loss from the clarifier can exceed the biomass generated from the process.

The operating range of the activated sludge system, however, can be extended to the lower organic concentration conditions by some modifications. Two examples are the recently developed membrane biological process and the activated sludge with iron-assisted flocculation. The former replaces the conventional clarifier with a membrane filtration system to control the effluent clarity and to concentrate and recycle biomass back to the aeration process. The latter uses naturally occurring iron or involves the addition of ferric chloride to enhance the settlability and retention of biomass through the formation of denser iron-biomass flocs.

The membrane biological reactor system has a wider operating range than the iron-flocculated activated sludge process because the effluent quality can be easily controlled by selecting the membrane with a desirable pore size. However, it also requires significantly more maintenance due to loss in filtration capacity with operating time. In this project, the iron flocculated activated sludge was selected because it is relatively simple and the feed water contained adequate levels of naturally occurring iron for this application.

## B. Experimental Setup

The activate sludge pilot plant system consisted of an equalization tank, a biotreater (an aeration vessel), a clarifier, and a return sludge pumping system (Figure 3-1). The equalization tank had a volume of 80 gallons which served partially as an oil-water separator. The biotreater was 12 inches in diameter and 6 feet in height. The actual working volume was about 27.5 gallons. The biotreater was equipped with a motor-driven agitator with two propellers located at 1 ft and 3 ft intervals from the bottom of the reactor. The agitator provided the required mixing to avoid excess aeration. Air was sparged through four stone-diffusers into the biotreater. The aeration rate was from 4 to 8 standard cubic feet per hour (CFH). The liquid flow rate used in this study ranged from 100 ml/min to 600 ml/min. The hydraulic retention times operated in this study therefore ranged from 3 to 18 hours. The clarifier had a diameter of 12 inches and a total height of 40 inches. It had an 18-inch high conical bottom. The thickened sludge was recycled back to the biotreater at about 1 gpm. Urea and diammonium phosphate were used as the N and P nutrients, and were fed into the biotreater feed at a predetermined ratio of: COD:N:P=100:5:1 for all test conditions.

## C. Experimental Plan

The objectives of this study are: (1) to verify that the activated sludge system, with the enhanced flocculation by iron hydroxide, can be used for the treatment of MTBE-contaminated wastewater under very low organic concentration conditions; (2) to evaluate the performance and the limitations of the activated sludge system for removal of MTBE and other organic contaminants; and (3) to gain practical operating experience of such a system and to understand its operation/maintenance requirements. The experimental plan was therefore arranged to start the system with wastewater containing a very low level of organic contaminants (including MTBE), and increase the loading by either raising the feed rate or concentration once the steady state was achieved. Table 3-1 describes the experimental conditions of this study. The operating temperatures were different for different runs due to the change in ambient temperature with the seasons.

## D. Results and Discussion

### *Operating Data*

**Run 1** The activated sludge system was seeded with 10 gallons of MTBE-degrading mixed culture (MLVSS about 1000 mg/L) isolated by Salanitro *et al.* (1994). The mixed culture had been acclimated to MTBE prior to the seeding. Therefore, MTBE biodegradation began almost immediately after seeding. It should be emphasized based on past experience that without the acclimated MTBE degrading mixed culture, very little MTBE biodegradation activity could be realized.

Run 1 was intended to evaluate the performance of the activated sludge system under very low organic loading conditions—6 mg of total degradable organics per liter of aeration volume per day. The biodegradation of ethers, MTBE and DIPE, and BTEX is plotted in Figures 3-2 to 3-4. The performance data and other ancillary monitoring and operating data are included in the Appendix. Except for an upset on Day-29 and Day-30 due to plugging in the return sludge line, the effluent concentrations of benzene, toluene, xylenes, and ethyl benzene were mostly below the detection limit. Discounting the data during the upset period, the effluent MTBE and DIPE concentrations were 15 and 8  $\mu\text{g/L}$  in average, respectively. The effluent MTBE concentration did exhibit more fluctuation than other VOC compounds. This is consistent with the previous observation that MTBE degradation in an activated sludge tended to be more vulnerable to operational upset. When subjected to an operational upset, the pace of recovery for MTBE biodegradation was also the slowest among the volatile organic compounds monitored.

Regarding MTBE removal by volatilization due to long hydraulic retention time (HRT) and slow biodegradation rate, the off-gas measurement from the reactor showed that the average MTBE concentration in the off gas was 0.25 ppmv. The removal of MTBE by stripping based on this off gas MTBE concentration amounted to approximately 4% of the

total mass of MTBE input to the treatment system. Therefore, it is clear that the majority of MTBE removal in the activated sludge system resulted from biodegradation.

Overall, this test run demonstrated that the activated sludge system could consistently and effectively remove MTBE under extremely low organic loading conditions (F/M ratio of 0.005 g VOC/g MLVSS-day and an influent BOD concentration as low as 11 mg/L).

**Run 2** In Run-2, the feed flow rate was doubled from 100 ml/min to 200 ml/min. The average total VOC loading to the system was increased to 1.45 g/day. The effluent MTBE and DIPE concentrations were elevated due to this hydraulic shock loading for about 2 weeks. The activated sludge system gained complete adaptation thereafter: The effluent MTBE and DIPE concentrations were in a majority of cases less than 20 and 10  $\mu\text{g/L}$ , respectively (Figure 3-5).

The increase in the feed flow rate by twofold, however, did not impact the biodegradation of benzene, toluene, xylenes, and ethyl benzene (Figures 3-6 and 3-7). On Day-14, there was a change in groundwater characteristics. Toluene and xylenes concentrations started to increase significantly. Trace oil sheen was present in the groundwater to the feed tank. The effluent benzene and toluene concentrations on that day were more than 10  $\mu\text{g/L}$  due to the change in the feed characteristics. The effluent benzene and toluene concentrations returned to less than 1  $\mu\text{g/L}$  immediately even though the influent concentration of toluene increased by 3 to 5 fold. The influent total xylene concentration also increased from 340  $\mu\text{g/L}$  to 920  $\mu\text{g/L}$  on average. No deterioration of xylene biodegradation was observed.

**Run 3** In Run-3, the feed flow rate was again increased from 200 to 300 ml/min. In the meantime, the influent MTBE concentration was also raised from 360 to 1260  $\mu\text{g/L}$  by spiking the groundwater with pure MTBE. The results are shown in Figures 3-8 to 3-10. The activated sludge system appeared to adapt to the shock loading at a faster pace than in Run-2, probably due to increase in MTBE degrader population and warmer temperature. Within a week, the effluent MTBE concentration was reduced from 150

µg/L to less than 15 µg/L. Twice during this run the effluent MTBE concentration increased above the 190 µg/L level. No abnormality in operation had been observed during these two occasions, and these unexpected fluctuations in MTBE biodegradation could not be explained. During the run, the effluent DIPE concentration remained less than 10 µg/L, even immediately after the feed rate increase.

**Run 4** In Run-4, the feed flow rate was further raised from 300 to 600 ml/min. Starting at Day 8, the response of the FBBR to high influent MTBE concentration (approximately 10 mg/L) was tested. Since the activated sludge system shared the same feed as the FBBR, the influent MTBE concentration to the activated sludge system was increased to the same level. The periods before and after the increase in the influent MTBE concentration were designated as Run 4A and Run 4B, respectively, to distinguish the drastic difference in the total MTBE loading between these two conditions.

In Run 4A, immediately following the increase in the influent flow rate and reducing the hydraulic retention time (HRT) from 5.8 to 2.9 hours, the effluent MTBE concentration was only slight elevated from less than 10 µg/L to about 35 µg/L, indicating that the activated sludge system had accumulated considerable quantity of MTBE degraders to rapidly respond to shock loading.

In Run 4B, the influent MTBE concentration was increased by about 10 fold. The MTBE removal in the activated sludge system dropped from more than 93% to about 70%. The total mass of MTBE removed by biodegradation, however, increased by approximately a factor of 10, from about 600 mg/day to 6000 mg/day after the shock loading.

Interestingly, the DIPE removal was affected by the sharp increase in the influent MTBE concentration and net MTBE removal, implying possible competition between the biodegradation of MTBE and DIPE for the same resources.

The biodegradation of benzene, toluene, xylenes, and ethyl benzene remained unaffected by the increase in feed flow rate and influent MTBE loading. The project was terminated

before the system had sufficient time to increase the number of MTBE and DIPE degraders. The effluent MTBE and DIPE concentrations and removals should improve with time, and the data in Run 4B should not be used to draw any conclusions on the limitation of the system's MTBE degradation capacity.

Sludge Characteristics As mentioned in the introduction section, one unique feature of the current process was the use of iron hydroxide flocculation to enhance the settlability and therefore the retention of the biosludge at very low organic loading conditions. The enhanced settlability of the biosludge by the iron hydroxide in this study was evidenced from Figure 3-15 which shows that sludge volume index (SVI) rapidly dropped from about 200 at the beginning of the test to less than 30.

Iron readily flocculated the biosludge as soon as the biotreater was started up. Iron accounted for about 8% of the total suspended solids within 2 days of operation. The iron content in the biosludge then increased slowly with operation, and leveled off at about 25% of the total suspended solids due to sludge wasting (Figure 3-16).

### *Loss of MTBE via Stripping*

Since MTBE was not completely degraded to a non-detectable level, some portion of the MTBE in the feed was expected to be lost through stripping. The biotreater used in this study had a liquid height of 57 inches, which allowed a good contact time between the gas bubbles and the liquid phase. Equilibration of organic compounds between the gas phase and the liquid phase was thus possible.

During the pilot study, the off-gas from the biotreater was monitored occasionally with a portable GC. The measured off-gas MTBE data were thus plotted in Figure 3-17 against the calculated gaseous MTBE concentrations in equilibrium with the effluent liquid. From the plot, it is evidenced that MTBE in the off-gas of the biotreater closely approached

equilibrium relation might be unique to the current biotreater configuration and operation. For other biotreaters, such emissions can be predicted knowing the overall mass transfer coefficient of the system.

Since MTBE in the off-gas was approximately in equilibrium with the effluent liquid MTBE concentration, the emission of MTBE from the biotreater could be calculated knowing the aeration rate, MTBE's Henry's constant at the operating temperature, and the effluent MTBE concentration. Figure 3-18 shows the relative quantity of MTBE removal via stripping and biodegradation expressed as averaged values for each run. As described in the previous sections, the effluent MTBE concentrations in these four runs were at similar levels, i.e., 20 to 80 µg/L. Consequently, the percentage of MTBE removed by biodegradation was higher for the runs with a higher MTBE feed concentration, and conversely, the percentage of MTBE removal due to stripping became greater for the runs with a lower MTBE loading.

In general, stripping accounted for less than 9% of the total MTBE removal, and greater than 87% of MTBE removal was achieved through biodegradation in this activated sludge pilot system. Significant lower stripping can be achieved for a full-scale groundwater activated sludge system with better oxygen transfer characteristics.

### ***First Order MTBE Biodegradation Rate Constants***

Under steady state condition, the mass balance of MTBE across the biotreater is given as:

$$C^{\text{in}} - C - \frac{Q_g}{Q_L} \left( \frac{H}{RT} \right) C - \theta X K_1 C = 0 \quad (3-1)$$

where

- $Q_L$  = liquid flow rate
- $Q_g$  = aeration rate
- $C^{\text{in}}$  = influent MTBE concentration
- $C$  = effluent MTBE concentration
- $H$  = Henry's law constant of MTBE

R = universal gas constant  
 T = temperature  
 V<sub>R</sub> = biotreater volume  
 X = mixed liquor suspended solids (MLSS)  
 K<sub>1</sub> = first order biodegradation rate constant  
 θ = V<sub>R</sub>/Q<sub>L</sub> = hydraulic retention time

Since the effluent concentration was low in the pilot test, the biodegradation could be approximated as a first order reaction as depicted in the last term of the above equation. The first order biodegradation rate constant for a specific substrate in an activated sludge system treating multiple organic substrates, however, is not an intrinsic kinetic parameter. It varies with the population of the degraders for that specific substrate in the mixed culture and the composition of the wastewater. Based on Equation (3-1), given the biomass concentration, Henry's law constant, the influent and the effluent MTBE concentration, the first order biodegradation rate constant for MTBE, K<sub>1</sub>, can be readily obtained by least square fitting of the experimental data obtained under steady state operation:

$$\text{Minimize } (C_{\text{cal}} - C_{\text{exp}})^2 \quad \text{subject to } K_1 \geq 0 \quad (3-2)$$

where C<sub>exp</sub> is the steady state effluent MTBE concentration data and C<sub>cal</sub> is given as:

$$C_{\text{cal}} = \frac{C^{\text{in}}}{1 + \frac{Q_g}{Q_L} \frac{H}{RT} + \theta X K_1} \quad (3-3)$$

Figures 3-19 and 3-20 are given as examples for comparison of the effluent MTBE concentration of the experimental data with those calculated by Equation (3-3) using the fitted K<sub>1</sub> value. In general, there is good agreement between the experimental and the calculated effluent MTBE concentration.

A similar approach was used to obtain the first order biodegradation rate constant for DIPE. Table 3- 2 summarizes the K<sub>1</sub> values for both MTBE and DIPE under the operating conditions conducted in this pilot study. The K<sub>1</sub> value varied from 1 to 6 L/g-

VSS-hr for MTBE, and from 2.3 to 4.3 L/g-VSS-hr for DIPE. The  $K_1$  values for both MTBE and DIPE appeared to increase as the pilot study progressed because of the slow increase in the degrader population for these two compounds as a result of the increase in their loading. However, no definite correlation could be established between the  $K_1$  values and the loading of MTBE and DIPE or their concentration relative to the total feed organic level.

### ***MTBE Biodegradation Capacity of the Activated Sludge System***

Figure 3-19 plots the effluent concentration against the MTBE loading per unit volume of the reactor from all the data collected from this study. Based on this figure, the effluent MTBE concentration of less than 100  $\mu\text{g/L}$  can be consistently achieved in the activated sludge process for a MTBE loading of less than 10 mg/day/L reactor. This information, together with the range of HRT, sludge concentration and sludge age used in this study, can be used to roughly size the activated sludge system for treating MTBE contaminated wastewater with contaminant compositions similar to that encountered in this study. However, as discussed previously, the poorer MTBE biodegradation performance under the high loading conditions in this study was primarily due to insufficient time for the activated sludge system to fully adapt to the high loading conditions. Therefore, using the maximum loading of 10 mg/day/L to determine the MTBE biodegradation capacity presents a conservative approach. Alternatively, the size of the biotreater can be designed based on simulation of a biotreater model using the first order MTBE biodegradation rate constant obtained from this study.

## **E. Conclusions**

1. Iron flocculation helps retain the biomass in the activated sludge system. As a result, very good MTBE degradation and effluent quality can be achieved in the activated sludge system even at an influent BOD concentration as low as 11 mg/L and a F/M ratio of 0.005 g VOC/g MLVSS-day.

2. In this pilot study, an effluent of less than 100  $\mu\text{g/L}$  MTBE could be achieved with a MTBE loading rate of less than 10 mg/day/L reactor. This loading rate is considered a conservative number to determine the MTBE biodegradation capacity in an activated sludge system. Overall, the activated sludge system does not possess as high a biomass concentration as the FBBR, and therefore requires a larger reactor to handle the same MTBE loading.
3. Loss of MTBE through volatilization ranged from less than 0.5% to 9% of the total influent MTBE loading. Under higher MTBE loading conditions, the MTBE biodegradation rate was higher, and thus the contribution of volatilization to MTBE removal was reduced.
4. The activated sludge system was more prone to process upset than the attached film process such as the FBBR, and recovered at a slower pace. However, the activated sludge process could be started up (or re-startup) rather easily as compared to the FBBR.

Table 3-1. Operating Plan For the Activated Sludge System With the Iron-Enhanced Flocculation For the Treatment Of MTBE Contaminated Wastewater

<i>Operating Conditions</i>	Run-1	Run-2	Run-3	Run-4A	Run-4B
Flow Rate (ml/min)	100	200	300	600	600
Hydraulic Retention Time (hrs)	17.2	8.1	5.8	2.9	2.9
Sludge Retention Time (days)	64	40	40	40	40
Air Flow Rate (SCFH)	6	4	4	4	4
F/M (g VOC/g MLVSS-day)	0.005	0.011	0.012	0.020	0.057
MLSS (mg/L)	1524	2579	2972	3310	3310
MLVSS (mg/L)	1192	1309	1592	1742	1742
pH	7.3	7.3	7.2	7.3	7.3
Dissolved Oxygen (mg/L)	8	8	8	8	8
Temperature (C)	17	17	20	21	21
Avg. Influent MTBE ( $\mu\text{g/L}$ )	427	357	1263	748	9605
Avg. Influent BTEX ( $\mu\text{g/L}$ )	3479	4303	2828	3132	2880
Avg. Influent VOC ( $\mu\text{g/L}$ )*	4347	5035	4469	4270	12875
Avg. Influent COD (mg/L)	34	41	38	35	51
Influent BOD (mg/L)	11	18	10	13	13
Influent Alkalinity	450	430	420	420	420

\* The average VOC is the sum of BTEX, DIPE and MTBE.

Table 3-2. First Order Biodegradation Rate Constants for MTBE and DIPE

Test	MTBE Load (mg/day/L)	MTBE/VOC (g/g)	$K_1$ (MTBE) (L/g-VSS-hr)	DIPE Load (g/day/L)	DIPE/VOC (g/g)	$K_1$ (DIPE) (L/g-VSS-hr)
Run-1	0.59	0.098	1.04	0.63	0.104	2.28
Run-2	0.99	0.071	1.1	1.08	0.078	2.27
Run-3	5.25	0.283	5.88	1.57	0.084	4.28
Run-4A	6.21	0.189	3.65	3.24	0.098	3.57

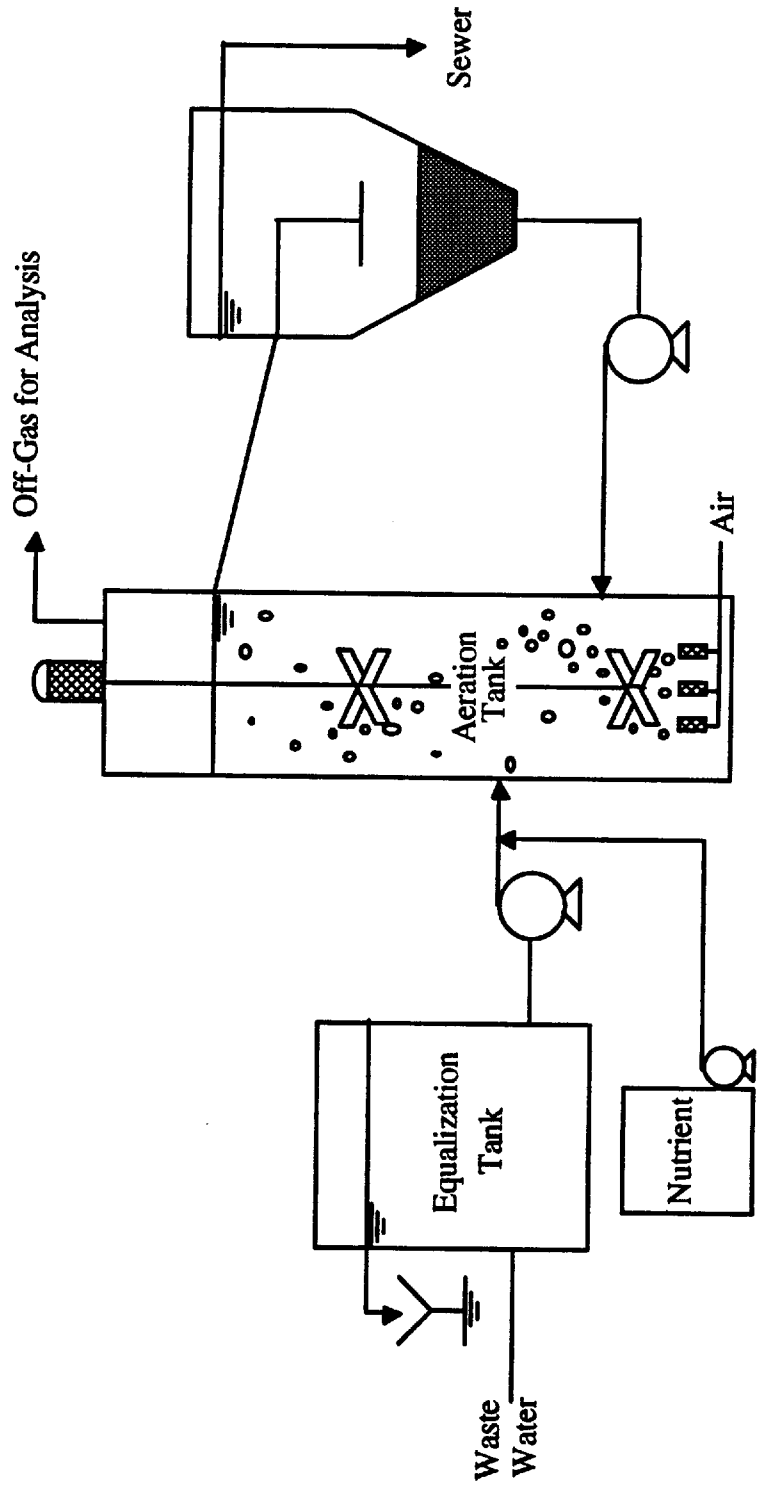


Figure 3-1. Schematic diagram of the pilot scale activated sludge system for the treatment of MTBE contaminated wastewater

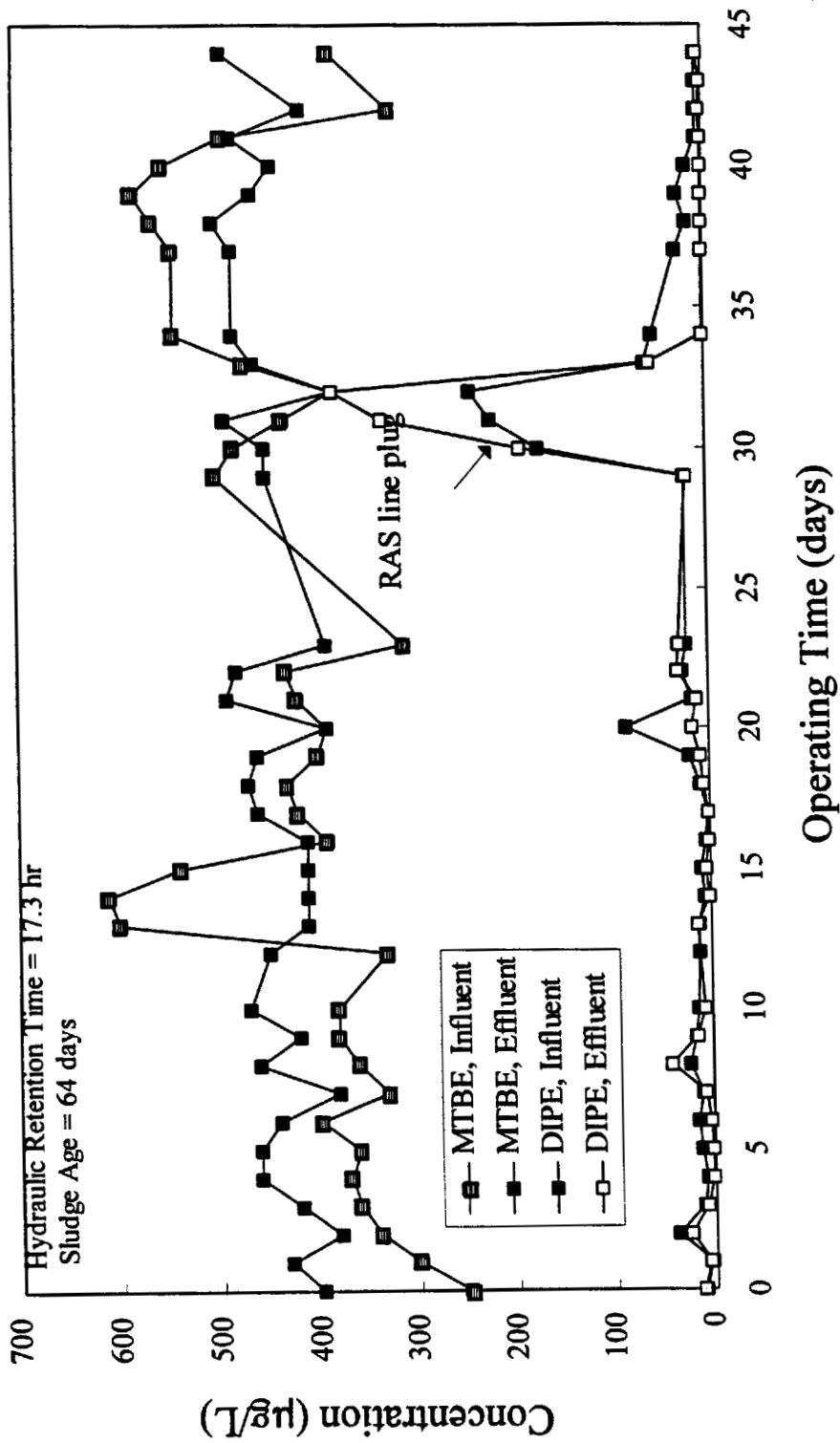


Figure 3-2. Performance of MTBE and DIPE biodegradation in the activated sludge system with iron-enhanced flocculation - HRT=17.3 hr

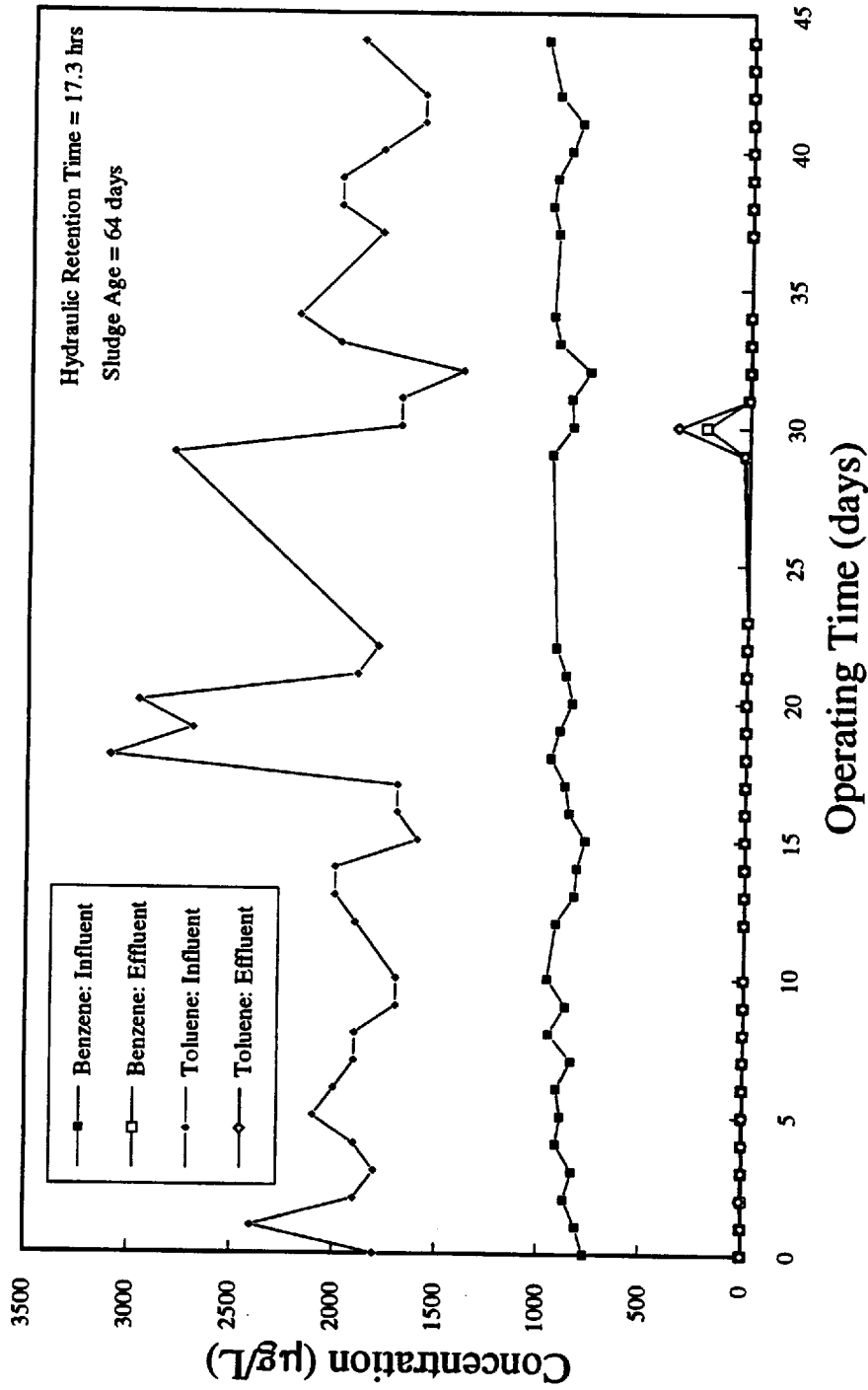


Figure 3-3. Performance of benzene and toluene biodegradation in the activated sludge system with iron-enhanced flocculation - HRT=17.3 hr

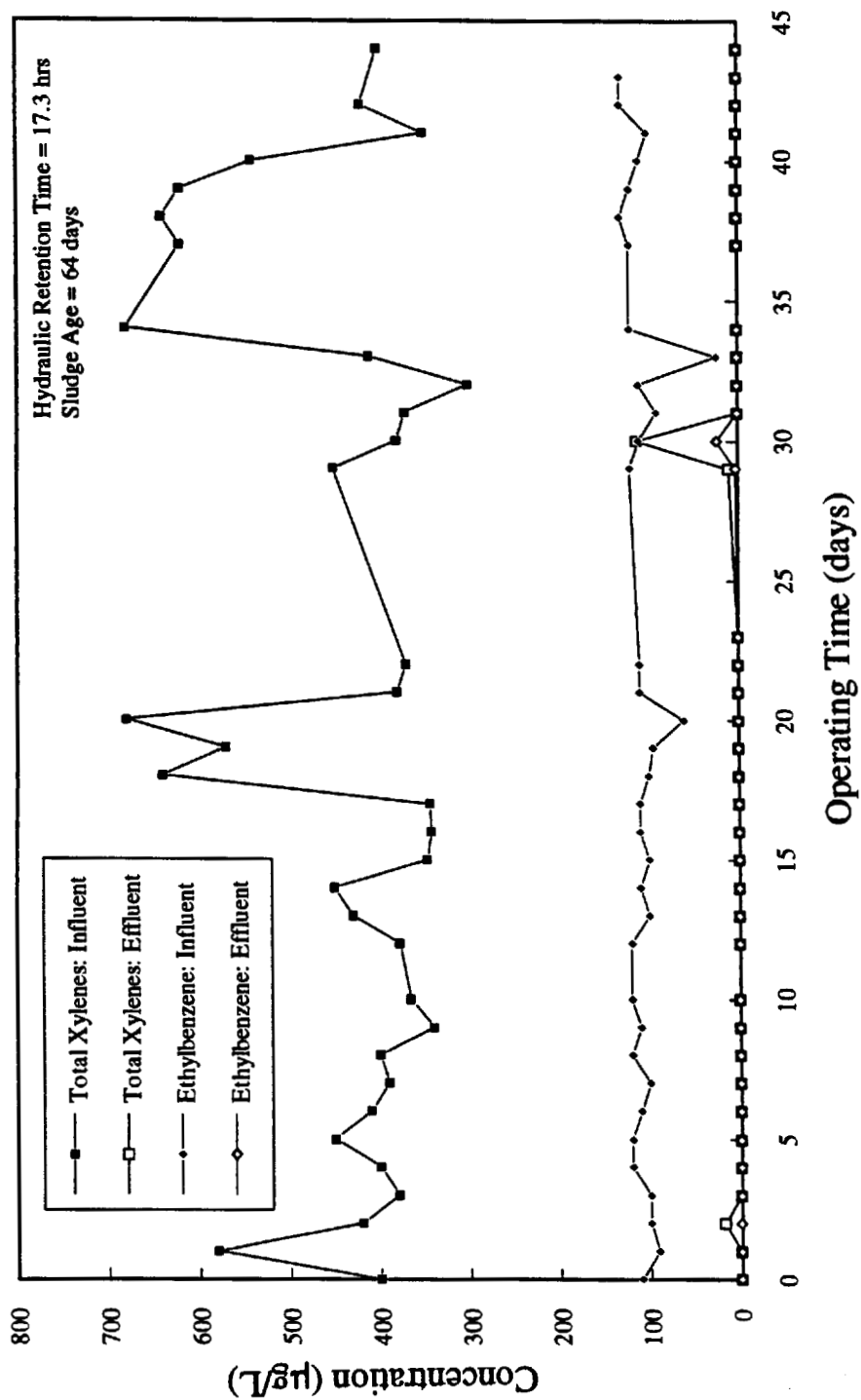


Figure 3-4. Performance of benzene, total xylenes, and ethylbenzene biodegradation in the activated sludge system with iron-enhanced flocculation - HRT=17.3 hr

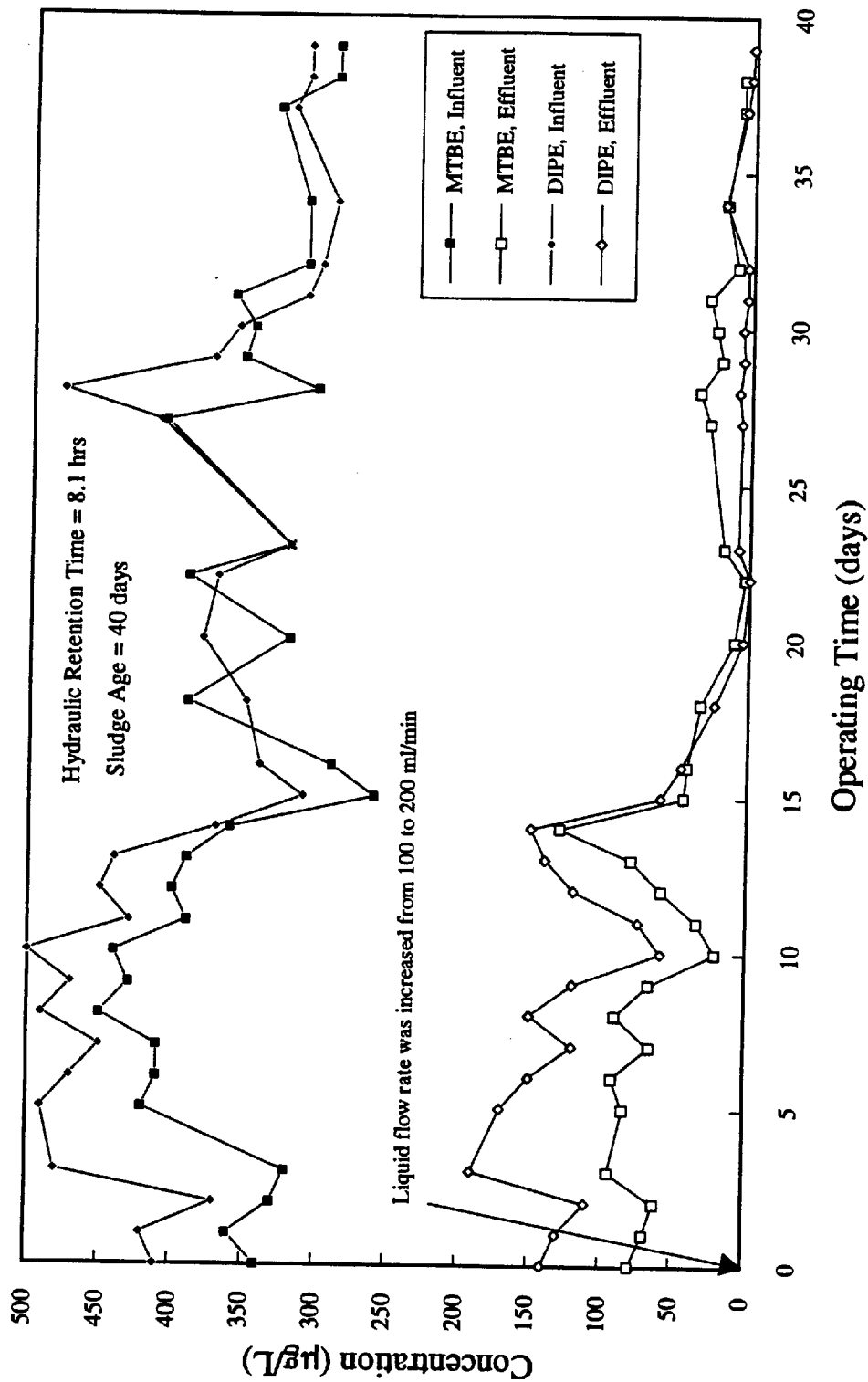


Figure 3-5. Performance of MTBE and DIPE biodegradation in the activated sludge system with iron-enhanced flocculation - HRT=8.1 hr

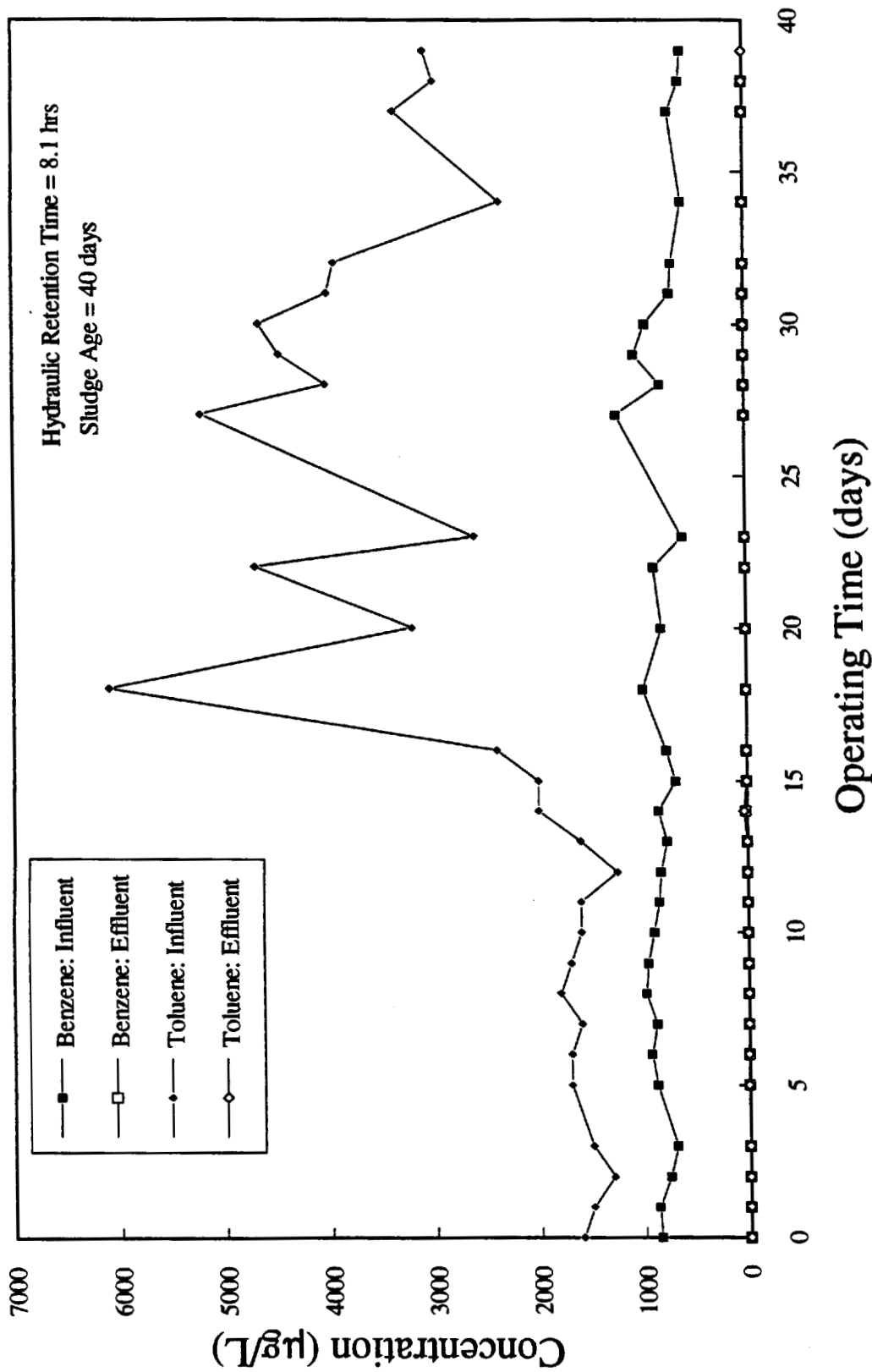


Figure 3-6. Performance of benzene and toluene biodegradation in the activated sludge system with iron-enhanced flocculation - HRT=8.1 hr

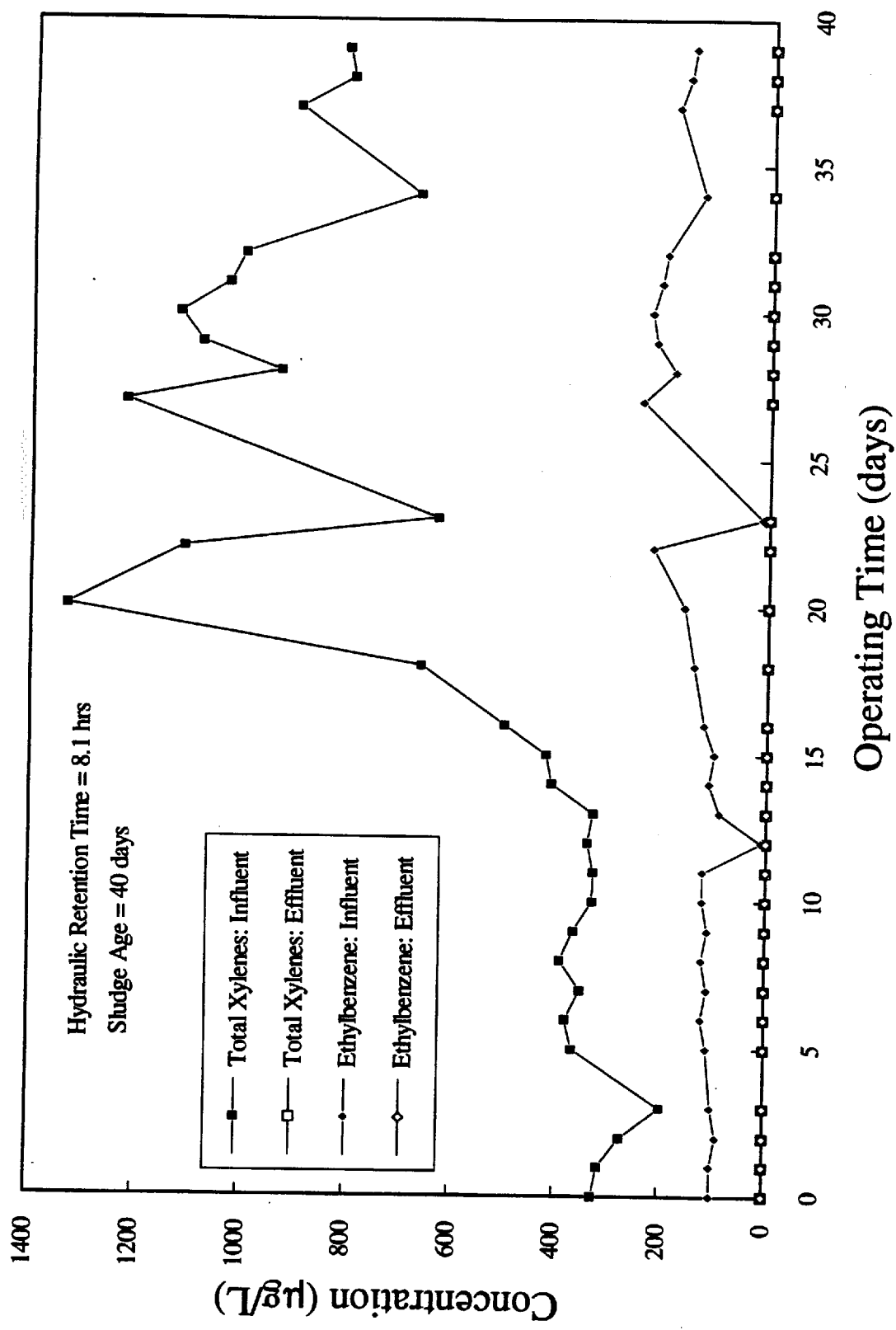


Figure 3-7. Performance of total xylenes and ethylbenzene biodegradation in the activated sludge system with iron-enhanced flocculation - HRT=8.1 hr

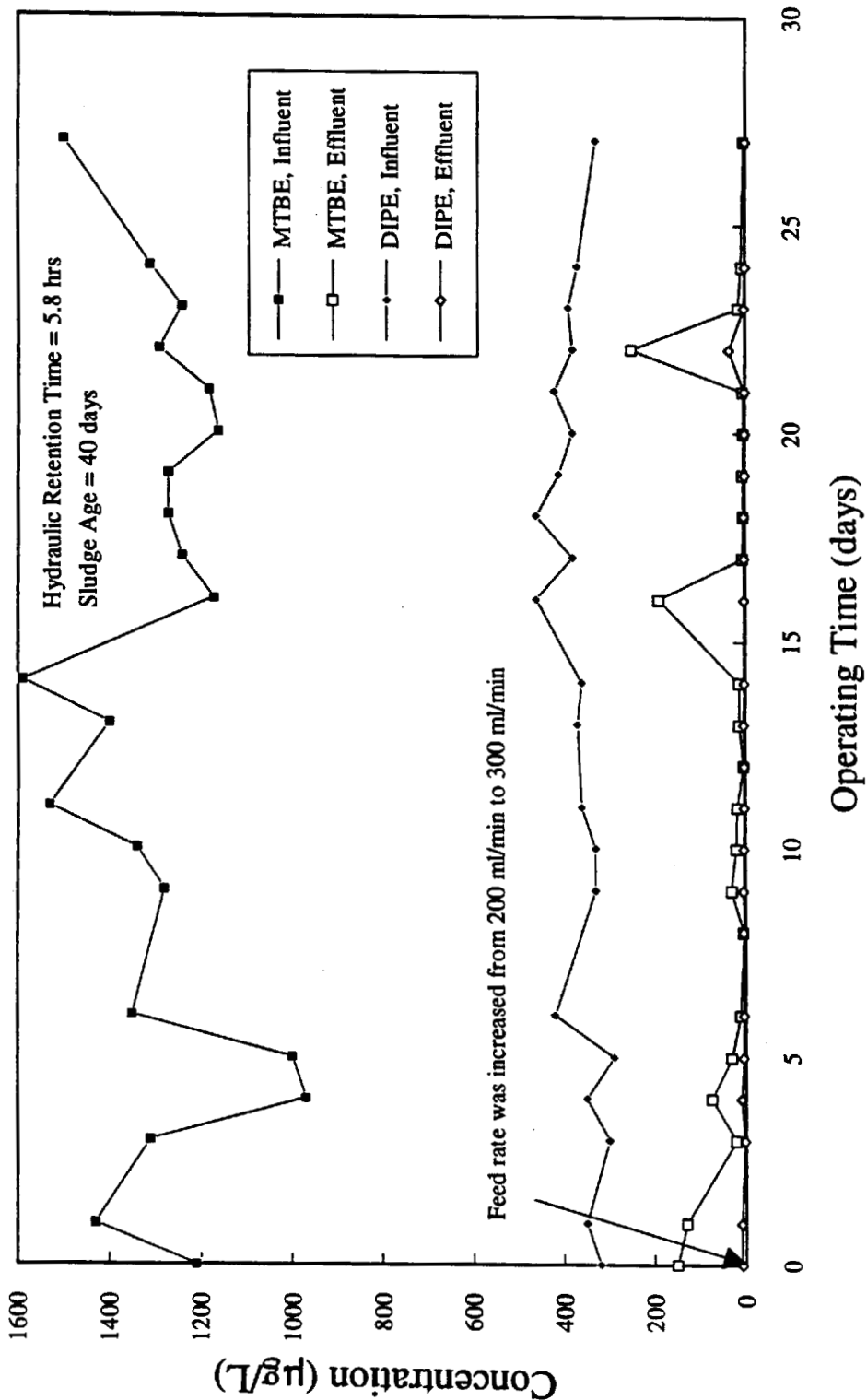


Figure 3-8. Performance of MTBE and DIPE biodegradation in the activated sludge system with iron-enhanced flocculation - HRT=5.8 hr

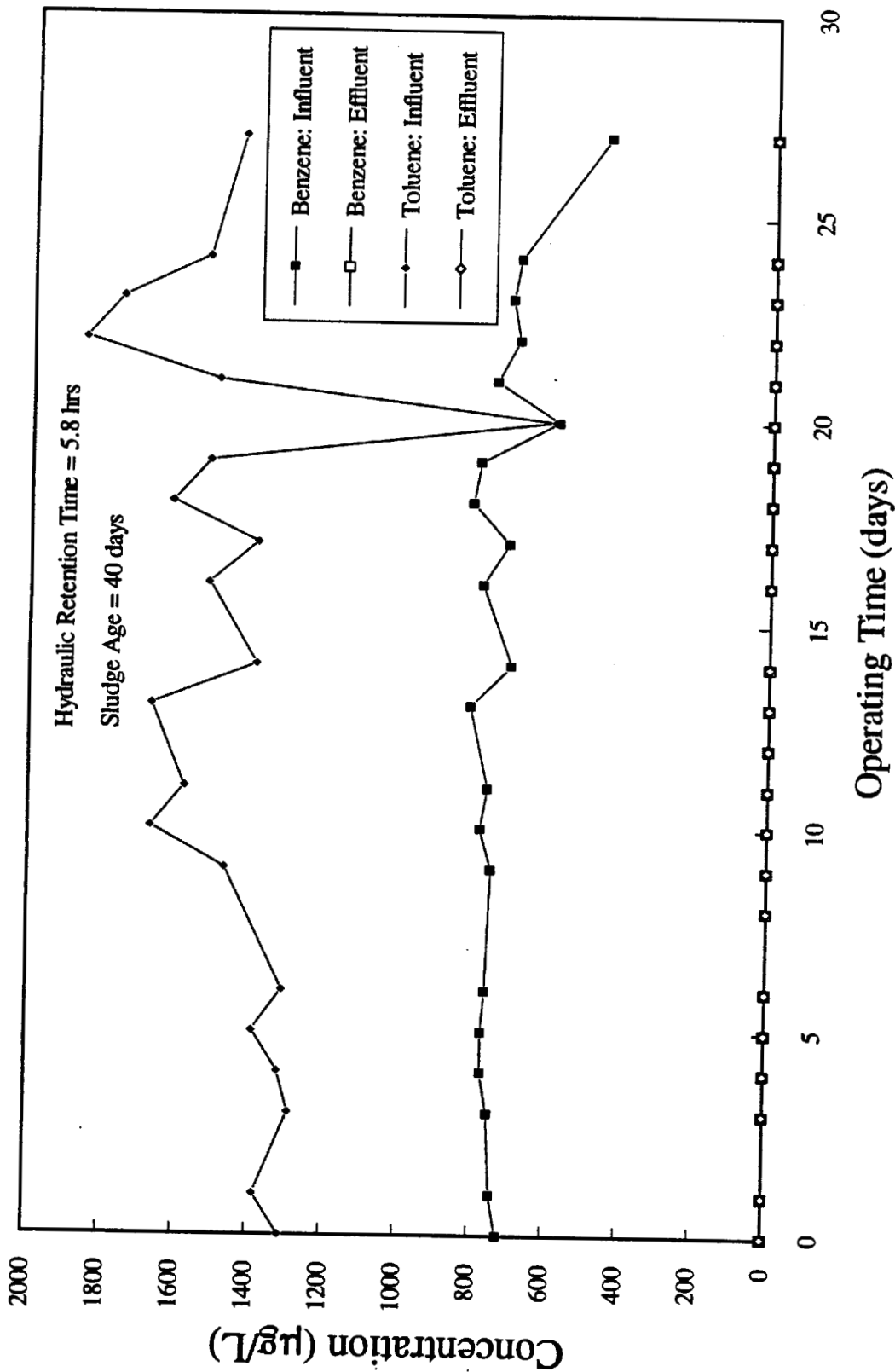


Figure 3-9. Performance of benzene and toluene biodegradation in the activated sludge system with iron-enhanced flocculation - HRT=5.8 hr

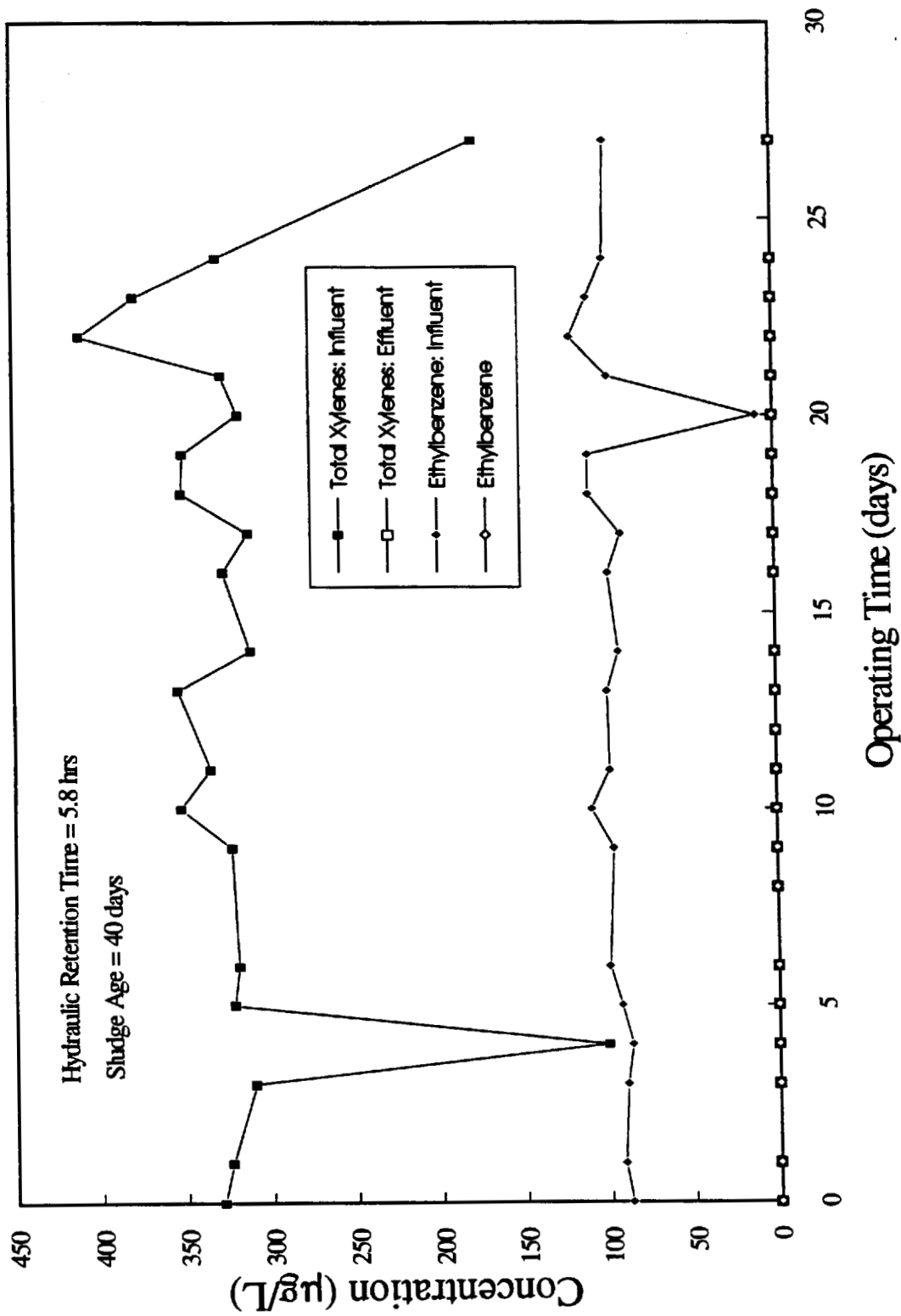


Figure 3-10. Performance of total xylenes and ethylbenzene biodegradation in the activated sludge system with iron-enhanced flocculation - HRT=5.8 hr

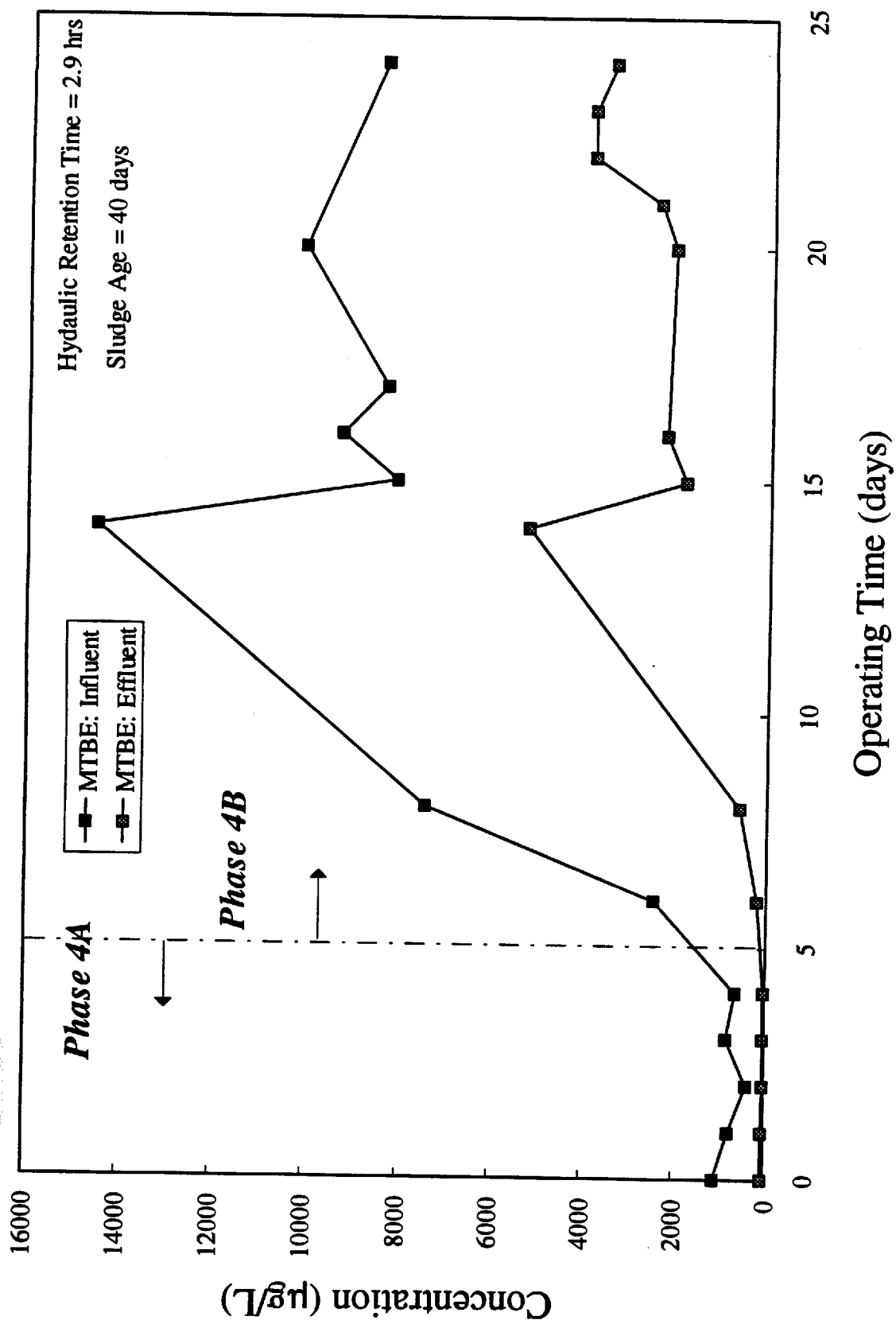


Figure 3-11. Performance of MTBE biodegradation in the activated sludge system with iron-enhanced flocculation - HRT=2.9 hr

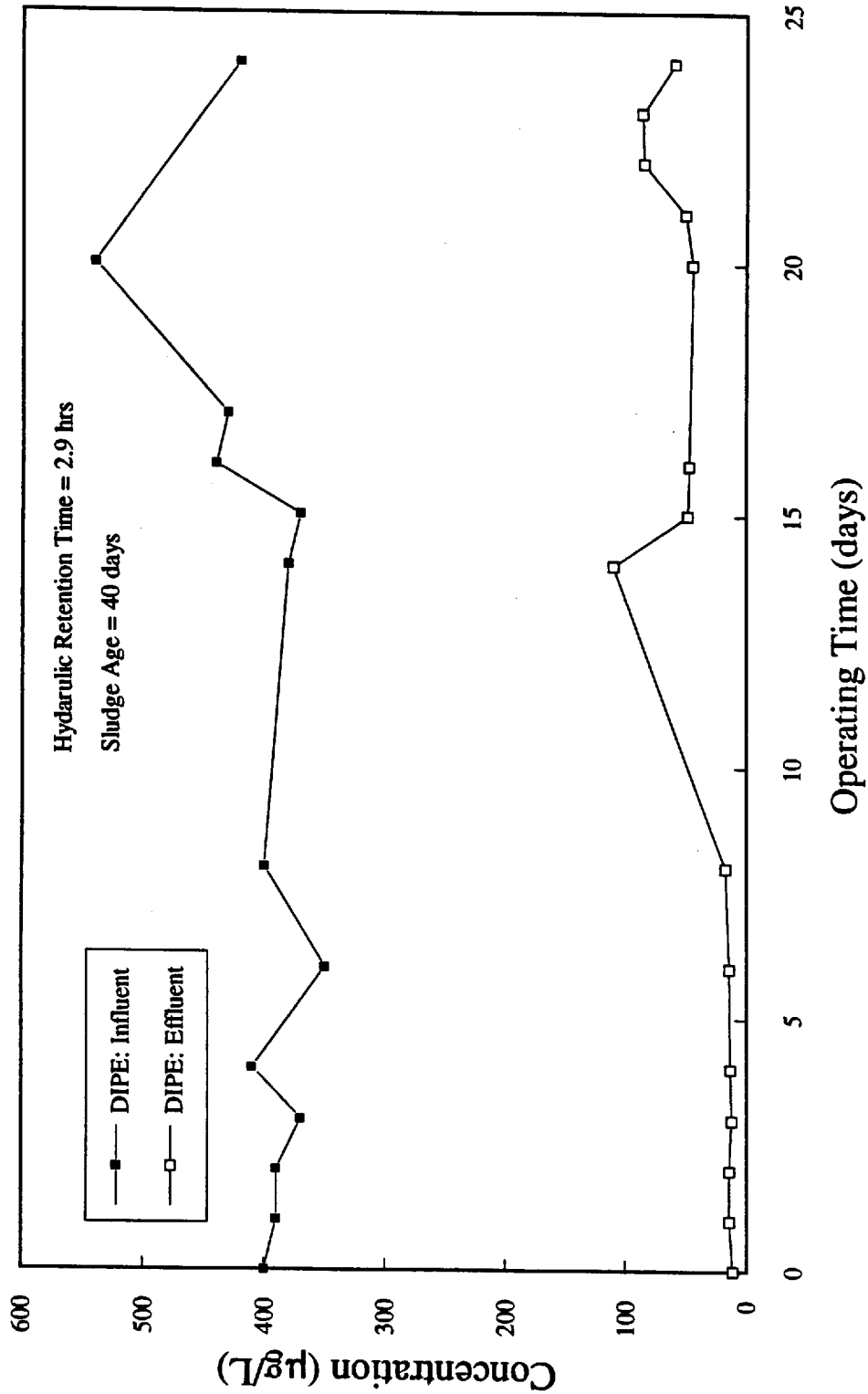


Figure 3-12. Performance of DIPE biodegradation in the activated sludge system with iron-enhanced flocculation - HRT=2.9 hr

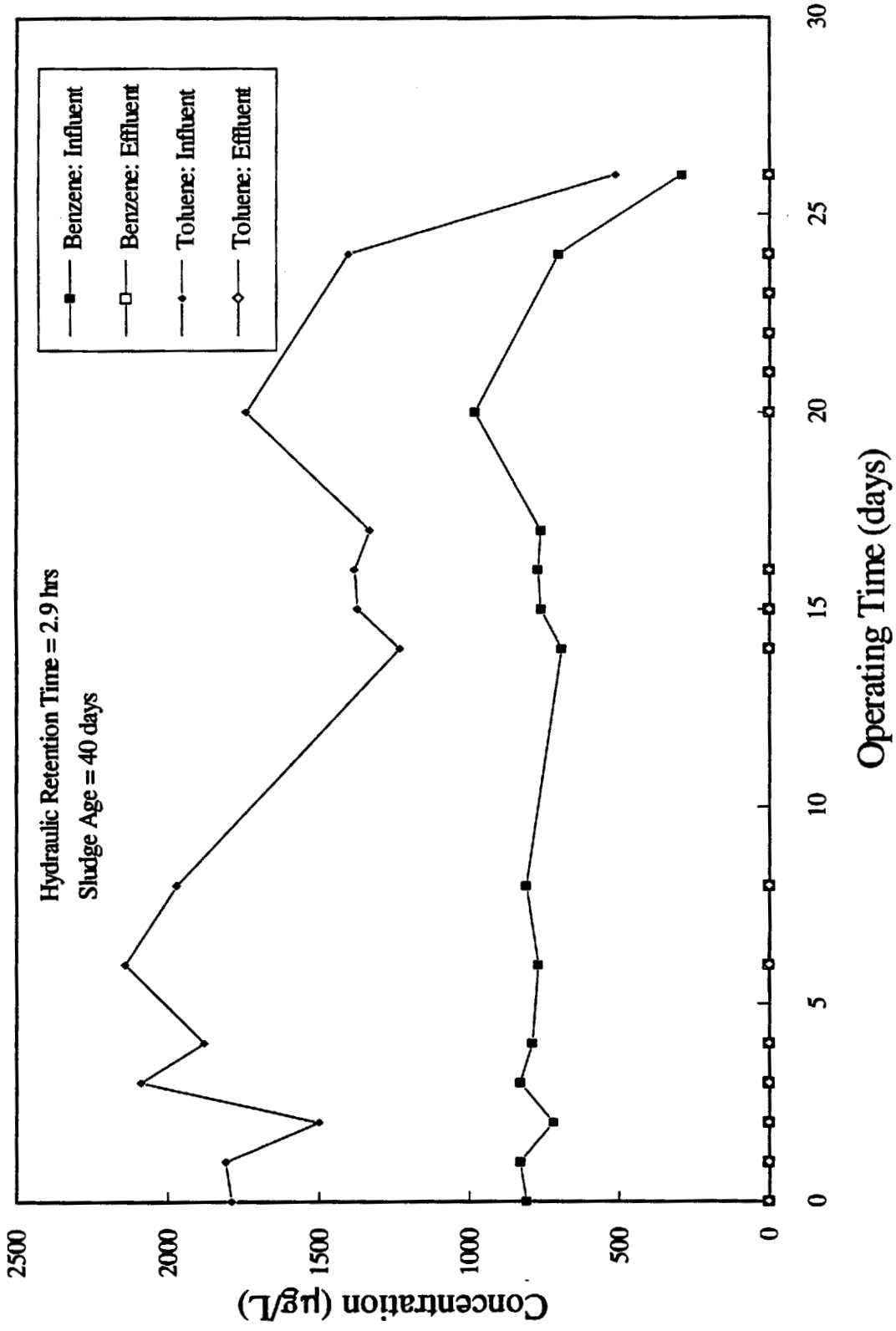


Figure 3-13. Performance of benzene and toluene biodegradation in the activated sludge system with iron-enhanced flocculation - HRT=2.9 hr

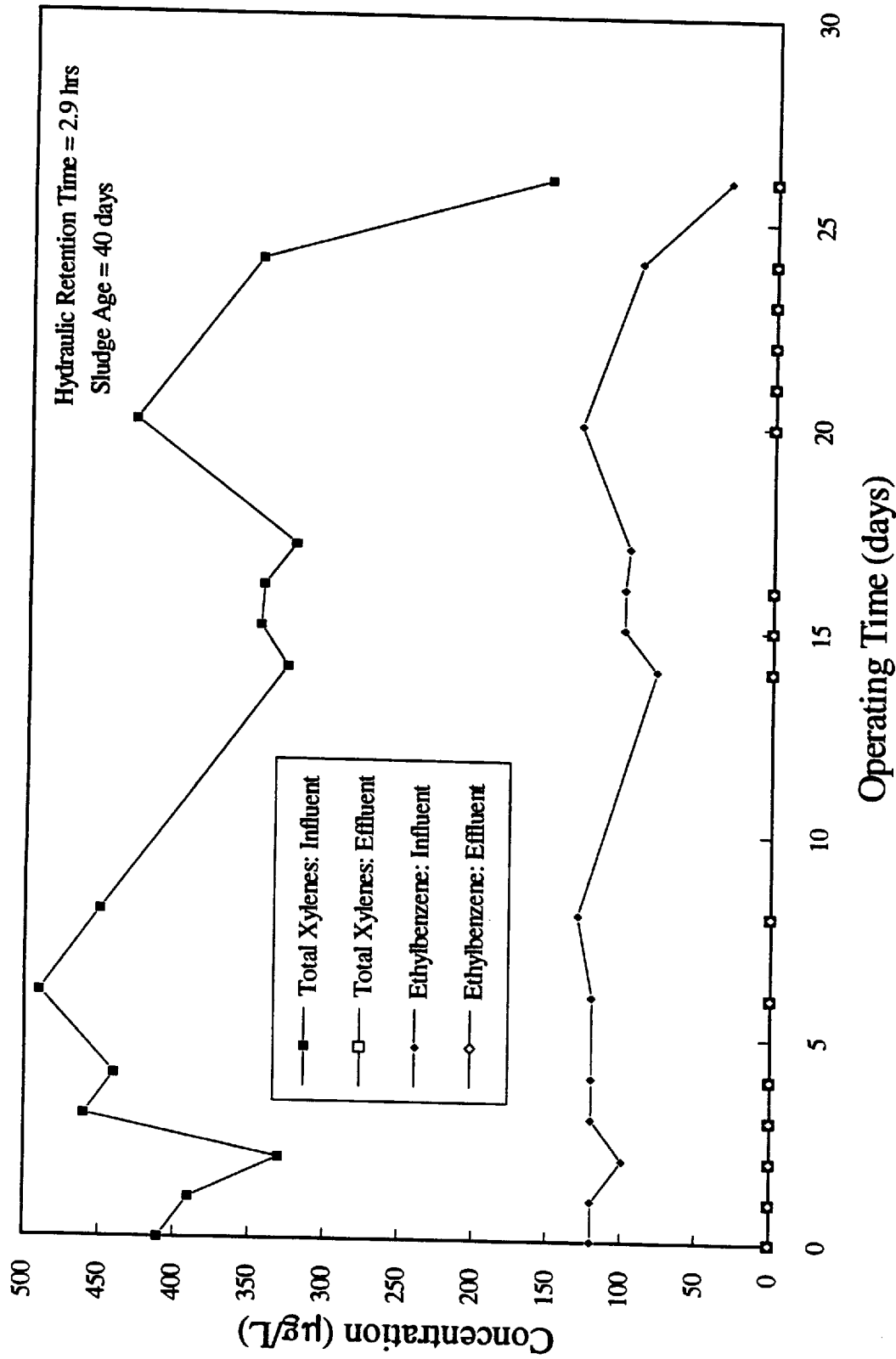


Figure 3-14. Performance of total xylenes and ethylbenzene biodegradation in the activated sludge system with iron-enhanced flocculation - HRT=2.9 hr

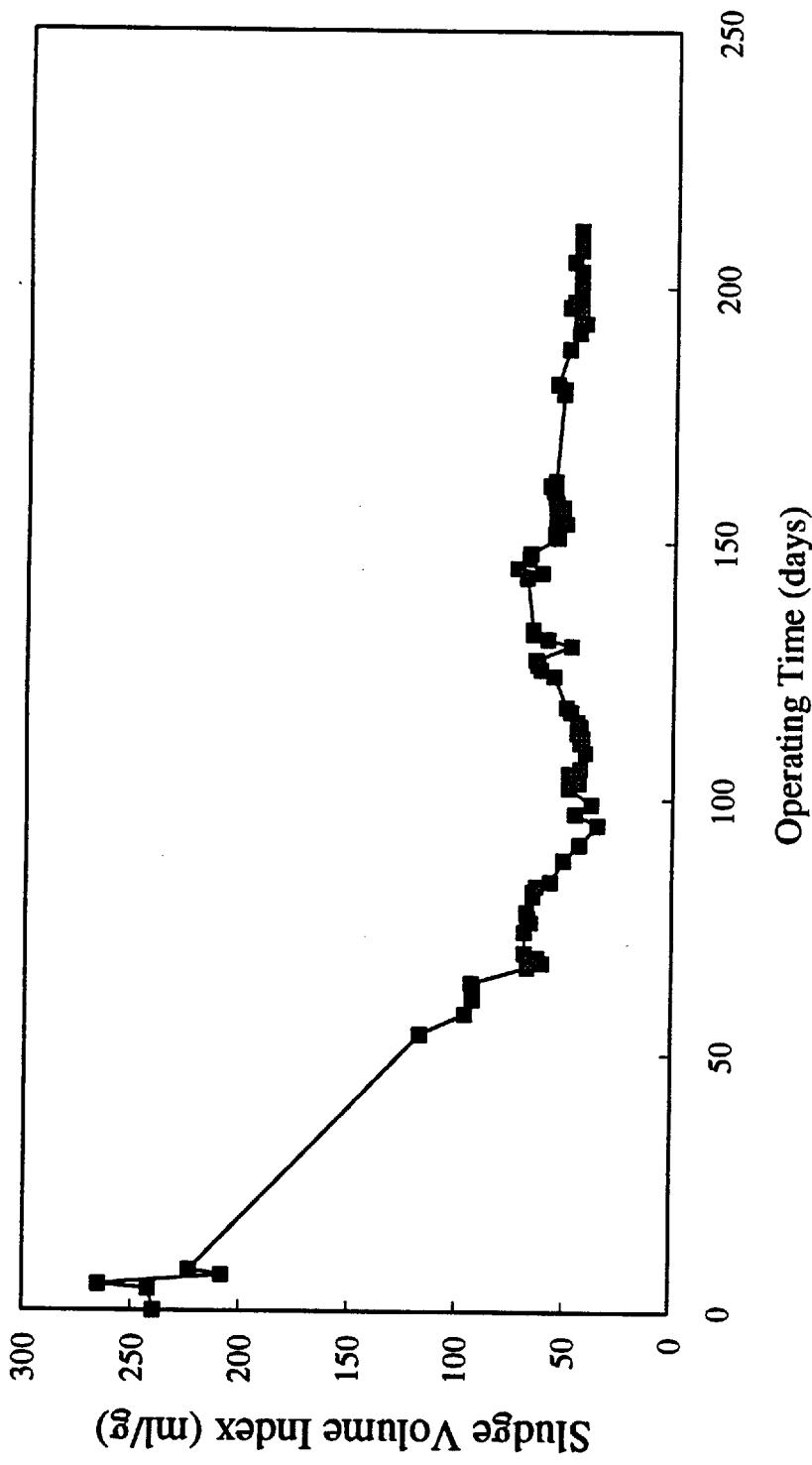


Figure 3-15. The sludge volume index of activated sludge system with iron enhanced flocculation

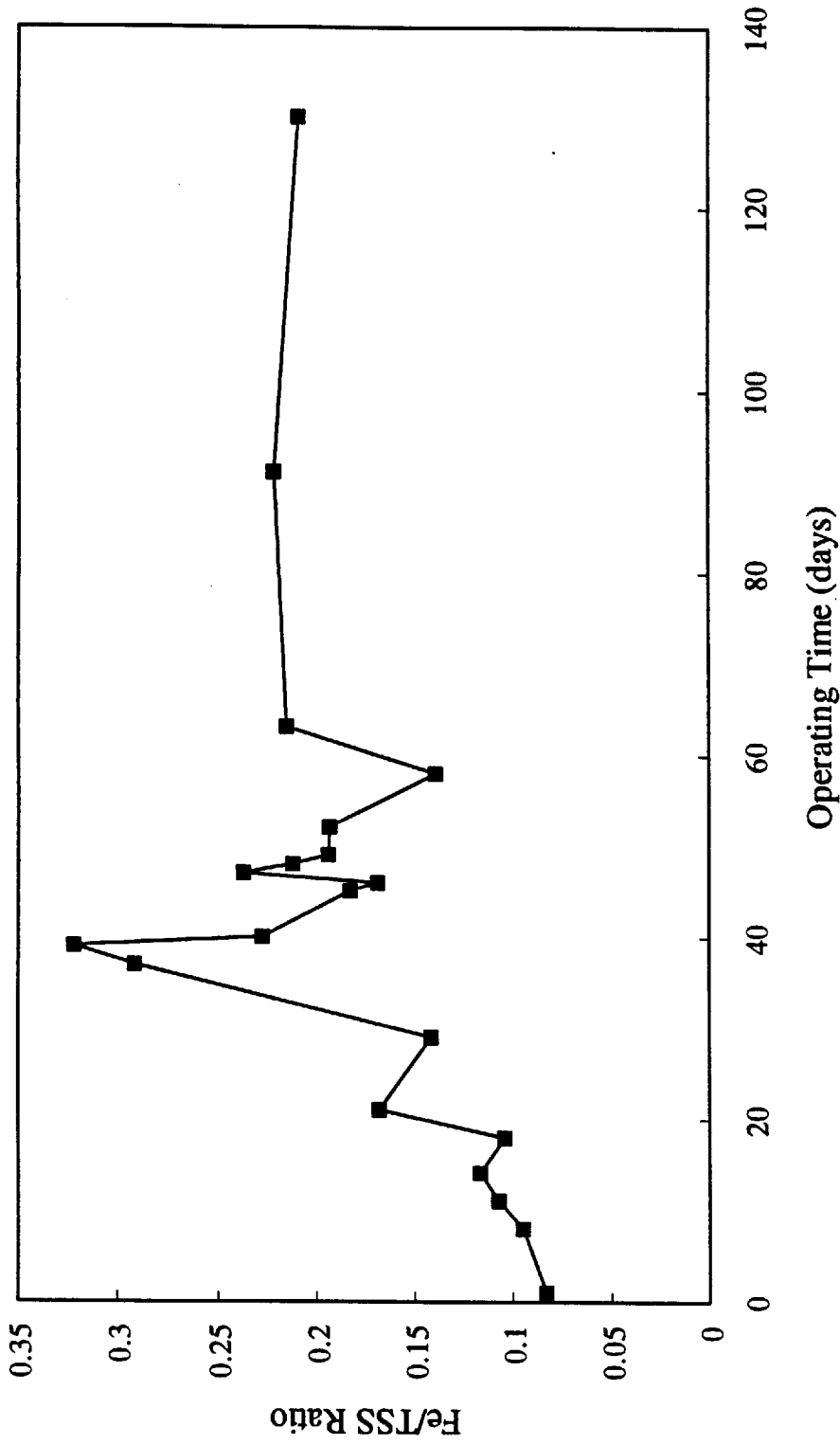


Figure 3-16. The iron content in the biosludge in the activated sludge process

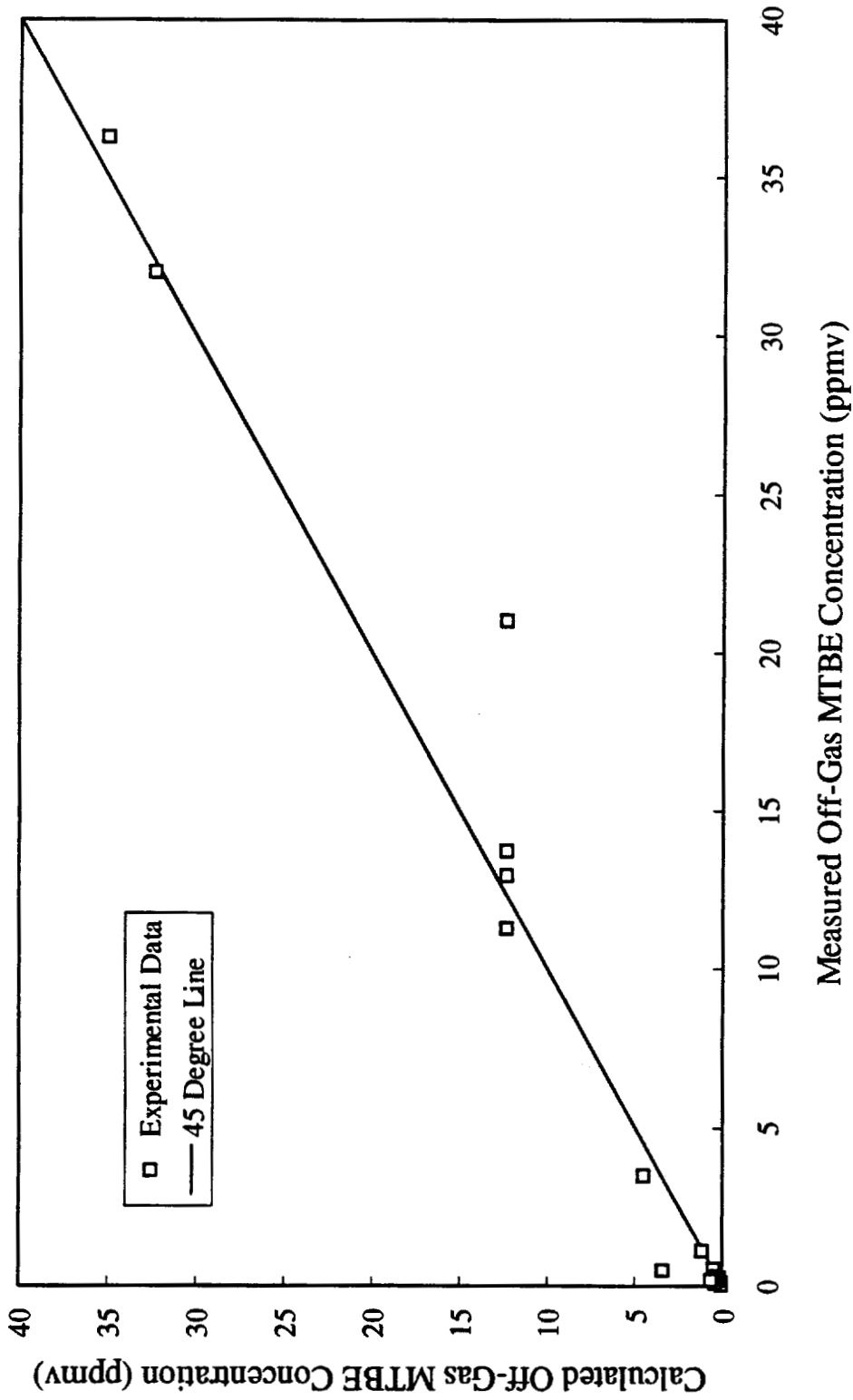


Figure 3-17. Comparison of the off-gas MTBE concentration with the calculated value in equilibrium with effluent liquid

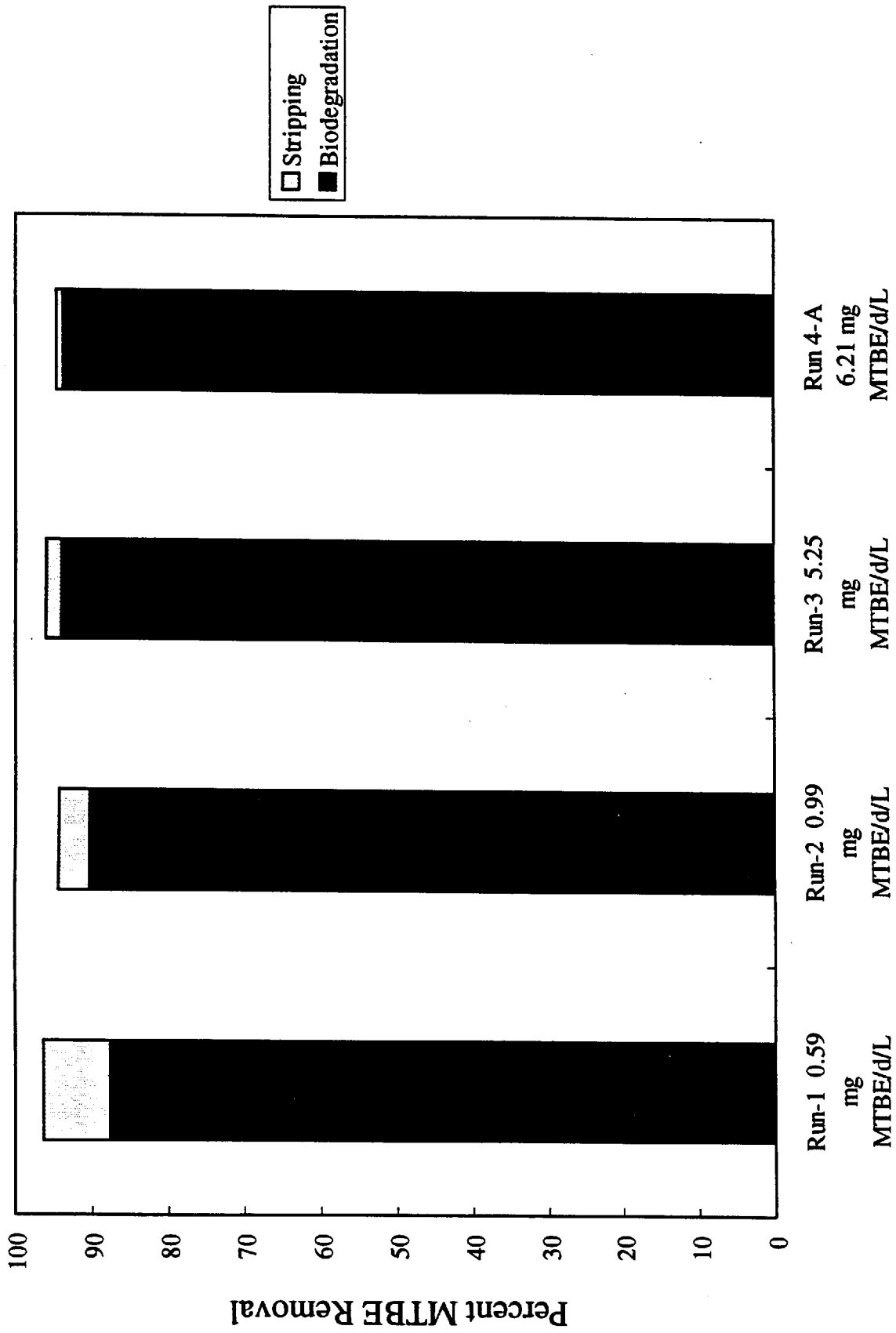


Figure 3-18. Relative removal of MTBE by stripping and biodegradation in the four different test conditions

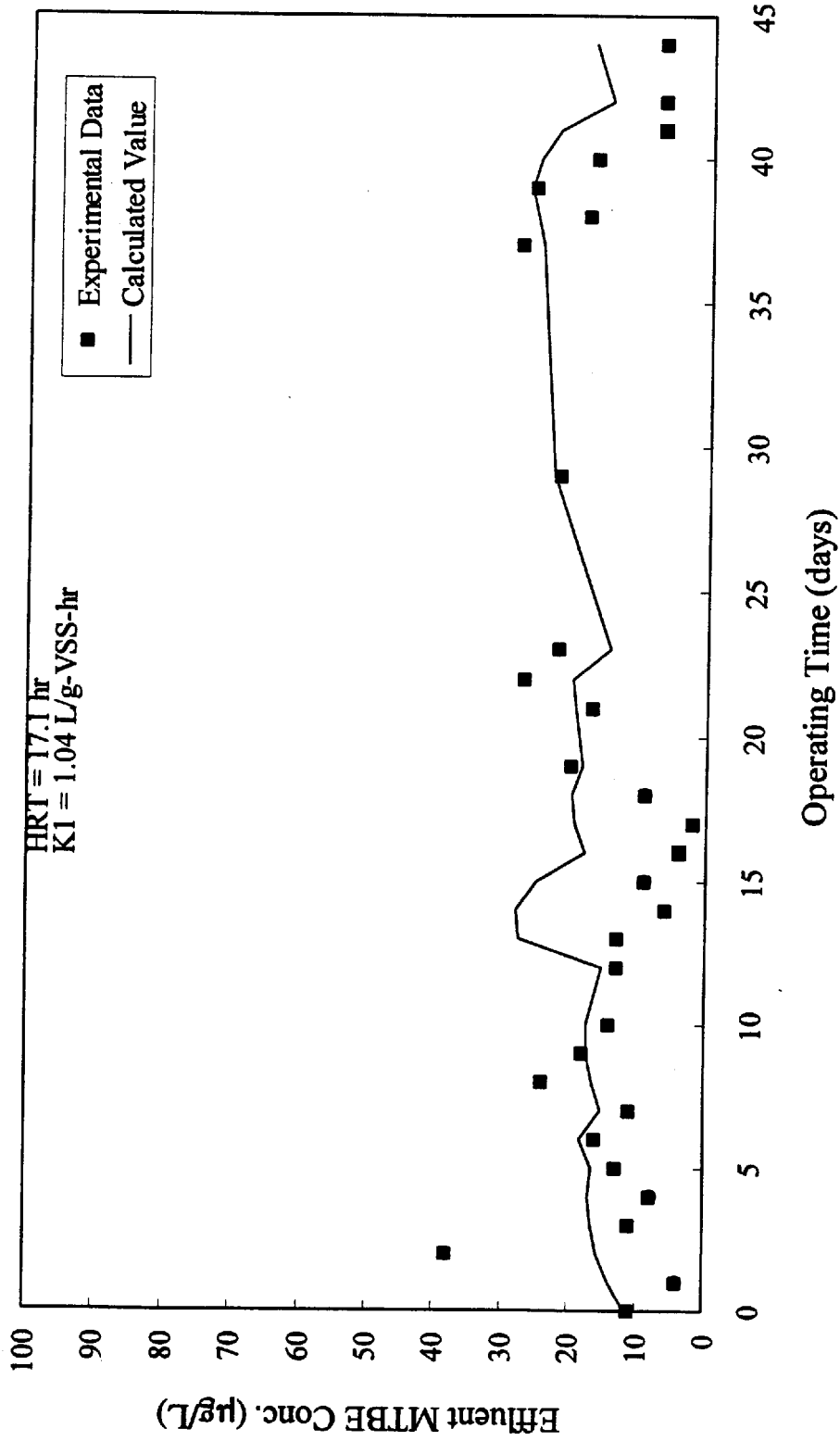


Figure 3-19. Comparison of the effluent MTBE concentration of the experimental data with that calculated by Equation (3-3) using the fitted  $K_1$  value for Run 1

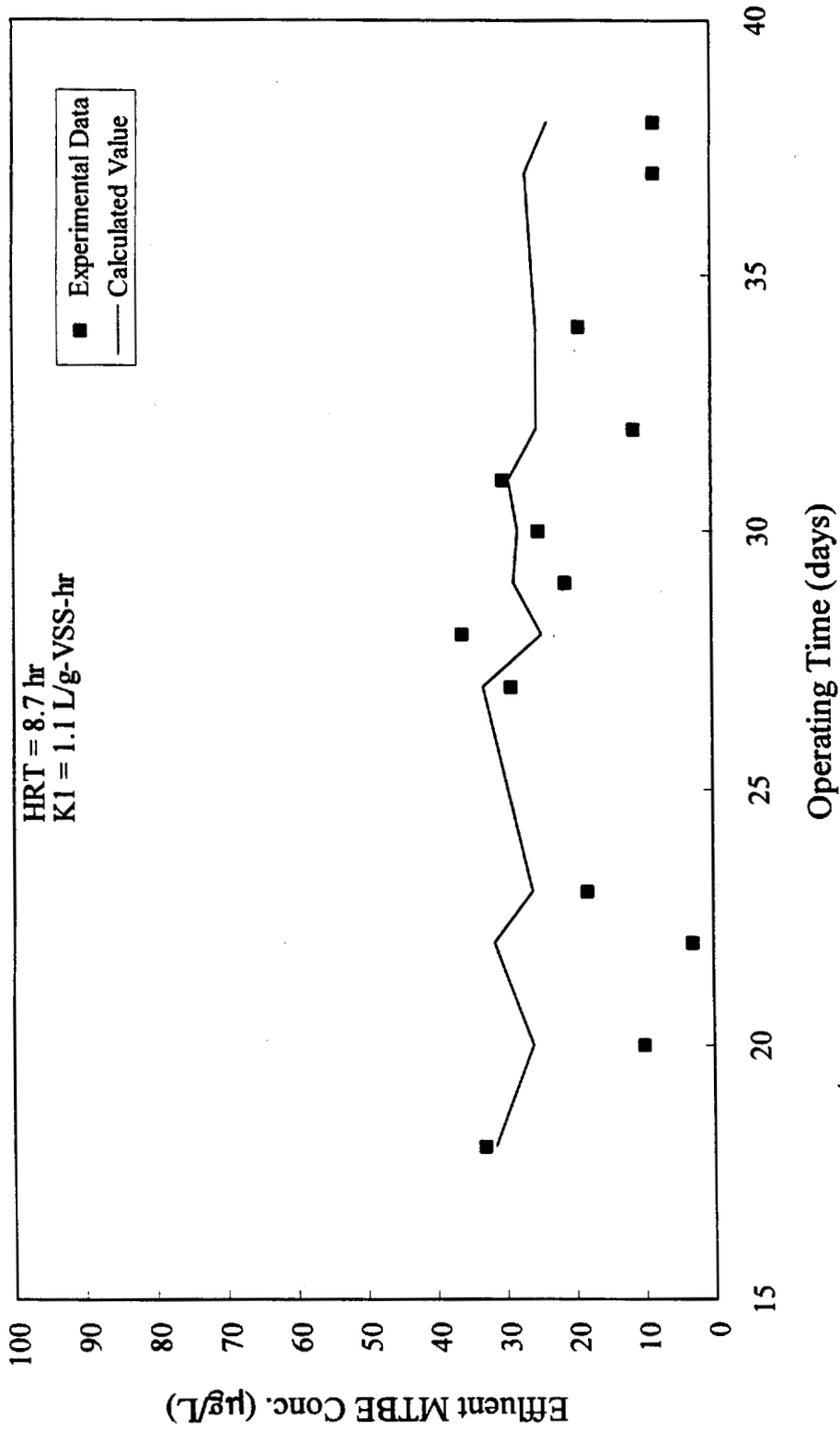


Figure 3-20. Comparison of the effluent MTBE concentration of the experimental data with that calculated by Equation (3-3) using the fitted  $K_1$  value for Run 2

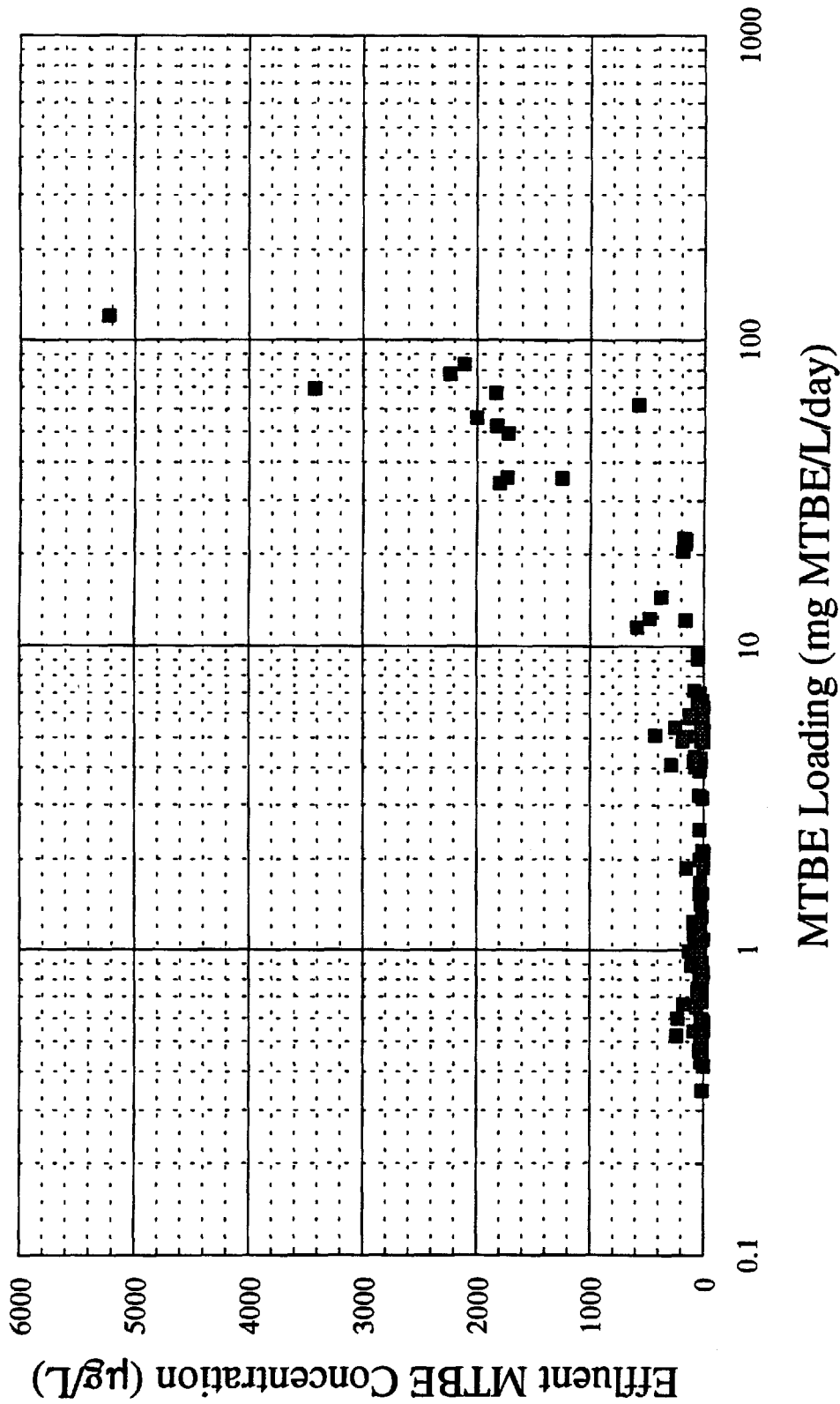


Figure 3-21. Relationship between the effluent MTBE concentration and its loading based on all the data obtained from this study

## Section 4

### MTBE DEGRADATION IN THE UV-H<sub>2</sub>O<sub>2</sub> PROCESS

#### A. Introduction

A plethora of studies have shown that the hydroxyl radical (HO•) can oxidize most organic substances. For example, the hydroxyl radical was found to be a key oxidant of hydrocarbons in the troposphere (Atkinson, 1986; Kenley *et al.*, 1978). It has also been used to oxidize various aromatic hydrocarbon contaminants in aqueous phase such as in ozonolysis (Hoigne and Bader, 1979). Because of its highly reactive nature, the hydroxyl radical can be a potential oxidant for refractory organic compounds which are not readily destroyed by other treatment processes. As discussed in the previous sections, although MTBE is demonstrated to be biodegradable, its biodegradation rate is significantly lower than that of benzene, toluene, and xylenes. The processes which generate highly reactive hydroxyl radicals may therefore provide a good alternative for treatment of MTBE.

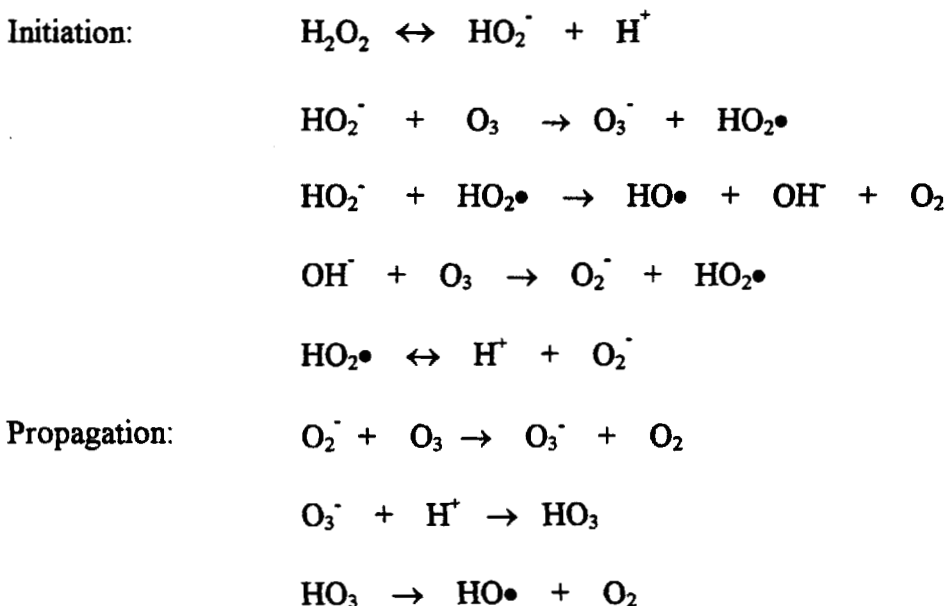
There are several processes that generate hydroxyl radicals as a means to remove organic contaminants in aqueous phase: reaction of ozone with hydrogen peroxide, hydroxide-catalyzed decomposition of ozone, photolysis of hydrogen peroxide by ultraviolet radiation, and the Fenton reaction. Among these processes, ozone-H<sub>2</sub>O<sub>2</sub> and hydroxide-ozone processes have been tested in either laboratory scale or pilot scale for the treatment of MTBE contaminated water (Tang and Wilcox, 1990). Therefore, this study only focused on evaluating the effectiveness of MTBE degradation in the UV-H<sub>2</sub>O<sub>2</sub> and Fenton reaction. In the following sections, the literature data and the basic mechanisms related to the generation and reaction of hydroxyl radicals are first reviewed. Data gathered from the field tests are then presented. Finally, the approach to design and implement the UV-H<sub>2</sub>O<sub>2</sub> process in the field is discussed.

## B. Literature Review

A hydroxyl radical can be generated by four different mechanisms: hydroxide catalyzed decomposition of ozone, reaction of ozone with hydrogen peroxide, photolysis of hydrogen peroxide, and ferrous iron catalyzed decomposition of hydrogen peroxide, also known as Fenton reaction. The mechanisms of hydroxyl radical generation are relevant to their effectiveness on the degradation of organic compounds. Generally speaking, UV irradiation is more effective in producing the hydroxyl radical than the other three mechanisms as will be seen from the reaction pathways reviewed below.

### *Hydroxyl Radical Generation via Reaction of Ozone with H<sub>2</sub>O<sub>2</sub> or with Hydroxide Ions*

Hydroxyl radicals can be generated by reacting ozone with H<sub>2</sub>O<sub>2</sub>. They can also be generated by hydroxide-catalyzed decomposition of ozone. The decomposition of ozone catalyzed by hydroxide ion and by hydrogen peroxide shares some common reactions. The following chain reactions have been proposed to explain the mechanism of the hydroxyl radical production via ozone-peroxide reaction or hydroxide catalyzed ozone decomposition (Stachelin and Hoigne, 1982).

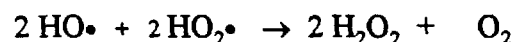
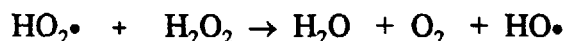


The net equation for hydroxyl radical formation is:



### *Photolysis of H<sub>2</sub>O<sub>2</sub>*

Both the O-O and O-H bonds of the H<sub>2</sub>O<sub>2</sub> molecule absorb UV light. H<sub>2</sub>O<sub>2</sub> exhibits continuous absorption of UV radiation with decreasing wavelength. Therefore, H<sub>2</sub>O<sub>2</sub> can dissociate by absorbing UV light. Under acidic and neutral conditions, the primary photolysis of H<sub>2</sub>O<sub>2</sub> by UV light at 254 nm produces hydroxyl radicals (i.e., 2 moles of hydroxyl radical generated per mole of H<sub>2</sub>O<sub>2</sub> photolyzed). The molar absorption coefficient of H<sub>2</sub>O<sub>2</sub> is 18.6 L/mol-cm. The hydroxyl radical may then react with H<sub>2</sub>O<sub>2</sub> to generate HO<sub>2</sub>• and O<sub>2</sub>, resulting in further decomposition of H<sub>2</sub>O<sub>2</sub> (Ogata *et al.*, 1983).

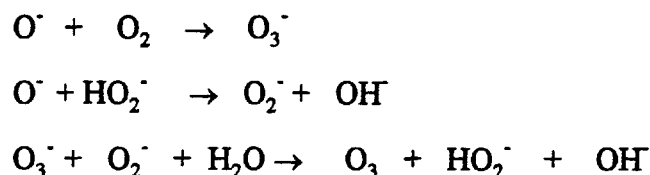


The photolysis of H<sub>2</sub>O<sub>2</sub> eventually leads to the formation of oxygen and water.



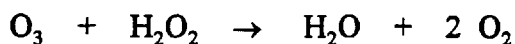
Nicole *et al.* (1990) showed that if the irradiation reactor had a non-reflecting wall or high values of internal optical density, the photolysis rate of  $\text{H}_2\text{O}_2$  obeys the zero order kinetics with respect to  $\text{H}_2\text{O}_2$  concentration; the rate of  $\text{H}_2\text{O}_2$  photolysis, however, can be described by an apparent first order kinetics with respect to  $\text{H}_2\text{O}_2$  concentration in the case of low values of optical density.

Under alkaline conditions, however, ozone is generated in the photolysis of  $\text{H}_2\text{O}_2$  via a transient ozonide.



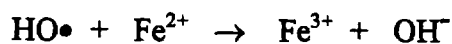
where  $\text{O}^\cdot$  and  $\text{HO}_2^\cdot$  are the basic forms of the hydroxyl radical,  $\text{HO}^\cdot$ , and  $\text{H}_2\text{O}_2$ , respectively.

The ozone generated will decompose to water and oxygen upon reaction with excess  $\text{H}_2\text{O}_2$ .

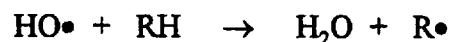


### ***Fenton's Reactions***

Fenton (1894) was the first to report that ferrous salts promoted the oxidation of organic compounds by  $\text{H}_2\text{O}_2$ . Such a combination of  $\text{H}_2\text{O}_2$  with a ferrous salt, now known as "Fenton's reagent," has since been demonstrated to be an effective oxidant for a wide variety of organic compounds. Past studies have shown that Fenton's reaction, i.e., the iron-catalyzed decomposition of  $\text{H}_2\text{O}_2$ , proceeds via a free radical chain process with hydroxyl radical as one of the intermediates. The chain reactions can be described by the following steps:



In the presence of organic compounds, the hydroxyl radicals react with the organic substrates to produce organic free radicals, which can undergo further degradation, dimerization, oxidation by  $\text{Fe}^{+3}$ , or reduction by  $\text{Fe}^{2+}$ .



As seen from the above equations,  $\text{Fe}^{2+}$  is rapidly consumed by  $\text{H}_2\text{O}_2$ , but can be regenerated from  $\text{Fe}^{3+}$  to allow the chain reactions to continue without continuous supply of  $\text{Fe}^{2+}$ . Since  $\text{Fe}^{3+}$  can form iron hydroxide precipitates under neutral to alkaline conditions, removing iron from the solution and thus prohibiting regeneration of  $\text{Fe}^{2+}$ , the Fenton reaction is often carried out under acidic conditions, or by using iron chelated to ligands to maintain Fe ions in soluble form. The ligands commonly used to complex  $\text{Fe}^{3+}$  include oxalate and citrate. Zepp *et al.* (1992) showed that the  $\text{Fe}^{3+}$  complexed by the ligands can be reverted to  $\text{Fe}^{2+}$  by photo-reduction at wavelength of 436 nm. This suggests that Fenton reaction can be used to destroy organic compounds under non-acidic conditions with the appropriate choice of ligands and sunlight irradiation.

### *Degradation Pathways of MTBE and Aromatics*

The degradation of organic compounds by the hydroxyl free radicals proceeds via two major pathways: hydrogen atom abstraction from the C-H bonds and addition of free radicals to  $\pi$  bonds. For MTBE, hydrogen abstraction is the major reaction mechanism. The hydroxyl free radical can abstract a hydrogen atom from the methyl group of either the methoxy group or the tertiary butyl group. The organic free radicals thus formed are further subjected to addition of peroxy free radicals or oxygen molecules, resulting in the generation of either tertiary butyl formate (TBF) or 2-methoxy 2-methyl propanal (MMP), as shown in Figure 4-1. These two intermediate products can be further degraded to formaldehyde, acetone, and  $\text{CO}_2$ .

The pathways were proposed by Japar *et al.* (1990) for OH-initiated atmospheric oxidation of MTBE. The same mechanisms are equally valid in the aqueous phase. Indeed, one of the by-products, tertiary butyl formate, was identified by mass spectroscopy in the effluent of the UV- $\text{H}_2\text{O}_2$  process for treatment of MTBE contaminated water (Bear *et al.*, 1989).

The degradation mechanisms of aromatic compounds by hydroxyl free radical attack can be illustrated by toluene degradation (Figure 4-2). Both the hydrogen abstraction and free radical addition mechanisms are responsible for the breakdown or transformation of toluene molecules. Hydrogen abstraction from the methyl group of toluene leads to the formation of benzaldehyde, while addition of the hydroxyl free radical to the benzene ring leads to the formation of phenol, diphenyl, and various smaller aldehydes or ketones from the scission of the benzene ring (Walling and Johnson, 1975)

### ***Kinetics of Hydroxyl Free Radical Reactions***

Hydroxyl free radical has a very high oxidative potential, only second to fluorine among all oxidants. Therefore, it is highly reactive towards many compounds. Table 4-1 summarizes the second order reaction rate constants for the reactions of the hydroxyl radical with some organic and inorganic solutes commonly found in water treatment processes. As seen in the table, the rate constants of the reaction between the hydroxyl free radical and the aromatic compounds are very high. Among the inorganic ions, carbonate and ferrous iron are slightly less reactive with the hydroxyl radical than the aromatic compounds. However, if the wastewater to be treated contains high alkalinity and iron concentrations, they will compete with the organic contaminants for the hydroxyl radical, hence reducing the degradation effectiveness of organic contaminants. The reaction rate constant between MTBE and the hydroxyl radical was determined using the relative rate method (Tang and Wilcox, 1990). In the relative rate method, MTBE and benzene reacted with hydroxyl radicals generated from ozonation of  $H_2O_2$  solution in a completely mixed reactor. Since the reaction rate constant of benzene is known, the reaction rate of MTBE can be determined based on the extent of MTBE degradation relative to that of benzene. The second-order reaction rate constant of MTBE was determined to be 0.15 of the reaction rate constant of benzene (Table 4-2).

### **C. Experimental Setup**

#### ***The Pilot Scale UV- $H_2O_2$ Process Unit***

Figure 4-3 shows the process diagram of the pilot UV- $H_2O_2$  process unit. Wastewater (primarily contaminated groundwater) was first pumped into a 200-gallon mixing tank to mix with 35%  $H_2O_2$  solution to oxidize ferrous iron to ferric iron. The peroxide was dosed to give the desired concentration for the UV- $H_2O_2$  reaction. Such a peroxide concentration was more than sufficient to completely oxidize the ferrous iron in the incoming wastewater. Anionic polymeric flocculant (acrylamide/acrylate aqueous

solution) was also dosed into the mixing tank to flocculate ferric hydroxide particles to enhance the downstream iron removal. Sodium hydroxide and sulfuric acid were used in conjunction with a pH controller to maintain a desired pH in the feed wastewater. The pH in the wastewater fed to the UV reactor was maintained at 7.0 except for the tests where pH effects were evaluated. MTBE and toluene were sometimes added in the mixing tank to study the effects of MTBE and other organic concentrations on the MTBE removal by the UV-H<sub>2</sub>O<sub>2</sub> process.

As mentioned earlier, ferrous iron would compete with organic compounds for hydroxyl radicals. In addition, once the iron is oxidized, it forms iron hydroxide flocs that can foul the UV lamp quartz and absorb and scatter UV light. The presence of iron in the feed water would therefore reduce the degradation efficiency of the UV-H<sub>2</sub>O<sub>2</sub> process under neutral or alkaline pH conditions. Consequently, a sand filter was installed in this process to remove flocculated iron hydroxide from the feed water. The sand filter was 24 inches in diameter and 54 inches in height. Sand was used as the sole medium for the sand filter. The actual height of sand was approximately 30 inches. The sand filter was not sized for continuous operation. It was backwashed daily. The iron concentration in the sand filter effluent was generally less than 0.5 mg/L.

The sand filter effluent was then pumped into the photoreactor unit. Figure 4-4 displays the simplified schematic diagram of the photoreactor unit. The photoreactor unit consisted of three UV chambers connected in series. Each UV chamber had a working volume of 10 gallons, and was equipped with a 10 kilowatt UV lamp. Each UV chamber also had its own sampling port for withdrawing the effluent sample, thus allowing the degradation efficiency of each chamber to be evaluated separately. The treated effluent of the UV photoreactor was pumped through an activated carbon bed to remove any residual organics in the treated water.

**Fouling of the Quartz Sleeve of the UV Lamps** The UV photoreactor system was operated in the daytime only. After completion of the daily experimental runs, the system

was cleaned with utility water and drained. The residual heat from the UV lamps dried the UV chambers in the night. Due to the high dissolved solids and calcium contents in the utility water, mineral salt residues were thus left coated on the quartz surface of the UV lamps. After approximately 3 weeks of operation, it was noticed from the data that the degradation efficiency of the UV-H<sub>2</sub>O<sub>2</sub> unit had deteriorated. A portion of the data reported in this study was collected when the degradation efficiency of the photoreactor unit had deteriorated due to fouling on the quartz sleeves. These data are reported with a note indicating the fouling conditions. It should be recognized that the fouling does not affect the validity of the data and the conclusion derived from them since the tests were conducted to compare the effects of a given process variable by maintaining all other operating conditions the same. The UV chambers were subsequently washed with 1% H<sub>2</sub>SO<sub>4</sub> solution for an hour, and then rinsed with utility water. After the cleaning process, the UV photoreactor regained its degradation effectiveness. Thereafter, the clean water was left in the chambers after the cleaning process to prevent mineral coating on the quartz sheaths of the UV lamps.

**Analytical Methods** The organic concentrations were determined using purge and trap gas chromatography. The quantification limits for BTEX, MTBE, and DIPE were 1 µg/L. H<sub>2</sub>O<sub>2</sub> and iron concentrations were determined based on calorimetric methods using CHEMetrics® kits.

#### **D. Results and Discussion**

The major process variables that impact the MTBE degradation efficiency of the UV-H<sub>2</sub>O<sub>2</sub> process include UV irradiation intensity, H<sub>2</sub>O<sub>2</sub> dosage, MTBE concentration, concentration of other organic compounds, alkalinity, iron concentration, pH, and hydraulic retention time. The UV irradiation intensity will be fixed once the equipment is selected. The wastewater used for this study contained very high alkalinity, up to 400 mg/L. Alkalinity had adverse effects on the UV-H<sub>2</sub>O<sub>2</sub> process. However, the high alkalinity in the wastewater might be desirable from the viewpoint that the results and the

related conclusions derived from the study would tend to be conservative. In addition, lowering the alkalinity requires subjecting the wastewater to a softening process or to pH adjustment accompanied by stripping of  $\text{CO}_2$ . Either process would significantly change the feed wastewater characteristics. Therefore, no efforts were made to study the effects of the UV irradiation intensity and alkalinity. However, the effects of the other process variables mentioned above on the MTBE degradation effectiveness of the UV- $\text{H}_2\text{O}_2$  process were evaluated.

In the following sections, the results of the effects of each process variable on the degradation efficiency of organics are discussed in a qualitative manner. Because of the complexity of the hydroxyl radical reactions in this process, definite, quantitative relations among the degradation effectiveness and the process variables have been difficult to obtain. However, some quantitative information from the pilot study data is presented in the last section.

### *Direct Photolysis of Organic Contaminants*

The spectral energy of UV irradiation is in the range of 400 to 600 kJ/mole, while the bond energy levels of the aliphatic and aromatic C-H bonds are in the range of 360 to 450 kJ/mole. Therefore, the organic contaminants in the aqueous phase may undergo direct photolysis upon UV irradiation. The contribution of direct photolysis (i.e., irradiation with UV alone without the assistance of  $\text{H}_2\text{O}_2$ ) to the degradation of organic contaminants in the UV- $\text{H}_2\text{O}_2$  process should be understood first before the degradation effectiveness of the process can be properly assessed. One test run was thus conducted to assess the decomposition of the hydrocarbons and ethers in the wastewater subject to UV irradiation without  $\text{H}_2\text{O}_2$  in the test equipment. The test results are summarized in Table 4-3. It appears that the substituted benzenes, including toluene, p,m,o-xylenes, and ethyl benzene, were photolyzed at faster rates than benzene, MTBE, and DIPE. These results are consistent with the observations that benzene was more photo-stable than aliphatic hydrocarbons at the wavelength of 254 nm, and that bond rupture in the alkyl group of

alkyl benzene occurred even at 254 nm wavelength. Rupture of the ether bond in aliphatic ethers requires short wavelength irradiation, < 200 nm (Wells, 1972). The test equipment was low in the irradiation wavelength below 200 nm. Therefore, the lack of degradation of MTBE and DIPE by direct photolysis can be expected.

### *Photolysis of H<sub>2</sub>O<sub>2</sub>*

The photolysis of H<sub>2</sub>O<sub>2</sub> by UV irradiation produces hydroxyl radicals as the initial chain reaction product, and eventually leads to the formation of oxygen and water. The sequences of the photolysis reactions have been described previously. According to Nicole *et al.* we attempted to extract *al.* (1990), the kinetics of H<sub>2</sub>O<sub>2</sub> photodegradation follows a first order reaction with respect to H<sub>2</sub>O<sub>2</sub> concentration under the conditions of low (1) optical density and (2) reflection on the internal wall of the photochemical reactor. These two conditions apply to the test equipment and the characteristics of the wastewater tested in this study. The kinetic expression for the photodegradation of H<sub>2</sub>O<sub>2</sub> according to Nicole *et al.* (1990) is:

$$-\frac{d[\text{H}_2\text{O}_2]}{dt} = \frac{2.3\varepsilon d\Phi}{V} rP_0[\text{H}_2\text{O}_2] \quad (4-1)$$

where  $\varepsilon$  = molar extinction coefficient of compound at the wavelength  $\lambda$  (L mol<sup>-1</sup> cm<sup>-1</sup>)  
 $\Phi$  = quantum yield for photolysis of compound at the wavelength  $\lambda$   
 $d$  = optical path length of light (cm)  
 $r$  = reflection coefficient (values varied with material of construction of the wall of the photoreactor)  
 $P_0$  = incident photonic flux (Einstein s<sup>-1</sup>)  
 $V$  = volume of irradiated solution

For a given photoreactor and UV lamp, the coefficients  $\varepsilon$ ,  $\Phi$ ,  $r$ ,  $P_0$ , and  $d$  are fixed.

Therefore, Equation (4-1) can be expressed as

$$-\frac{d[\text{H}_2\text{O}_2]}{dt} = k_{\text{H}_2\text{O}_2}[\text{H}_2\text{O}_2] \quad (4-2)$$

The flow pattern of liquid through the photoreactor in this study can be approximated as plug flow. Therefore, the kinetic constant,  $k_{\text{photo}}$ , of  $\text{H}_2\text{O}_2$  photolysis could be determined by the following equation:

$$[\text{H}_2\text{O}_2]_{\text{eff}} = [\text{H}_2\text{O}_2]_{\text{inf}} \exp(-k_{\text{H}_2\text{O}_2} \tau) \quad (4-3)$$

where  $\tau$  is the hydraulic retention time of the photoreactor. Figure 4-5 shows the result of one  $\text{H}_2\text{O}_2$  photodegradation test in which water containing only  $\text{H}_2\text{O}_2$  was subject to UV irradiation in the photoreactor under neutral conditions. The value of  $k_{\text{photo}}$  was determined to be  $0.39 \text{ min}^{-1}$ . The values of  $k_{\text{photo}}$  extracted from the  $\text{H}_2\text{O}_2$  degradation data collected during this study in the presence of organic contaminants varied from  $0.21$  to  $0.62 \text{ min}^{-1}$  with the average of  $0.38 \text{ min}^{-1}$  (Figure 4-6), which is in good agreement with the  $0.39 \text{ min}^{-1}$  determined from the  $\text{H}_2\text{O}_2$  solution. Therefore, once the value of  $k_{\text{photo}}$  is determined from a  $\text{H}_2\text{O}_2$  solution for a UV lamp, it can be used to predict the consumption of  $\text{H}_2\text{O}_2$  under other test conditions. Note that the  $k_{\text{photo}}$  was the apparent disappearance rate constant of  $\text{H}_2\text{O}_2$  concentration. It may reflect directly the kinetics of hydroxyl radical production.

### *Effects of $\text{H}_2\text{O}_2$*

Increasing  $\text{H}_2\text{O}_2$  dosage increases the generation of hydroxyl radicals, and therefore enhances the degradation of organic contaminants in the wastewater. Two tests were conducted to evaluate the effects of  $\text{H}_2\text{O}_2$ : The first test did not inject MTBE into the feed wastewater, while the feed wastewater in the 2nd test was dosed with about  $2 \text{ mg/L}$  MTBE. The results are tabulated in Tables 4-4 and 4-5. It is obvious from these results that the higher the  $\text{H}_2\text{O}_2$  dosage, the higher the degradation efficiency for all the organic compounds in both tests. Low  $\text{H}_2\text{O}_2$  dosage has an obvious impact on the degradation of MTBE and DIPE as evidenced in the test with a lower influent MTBE concentration: MTBE removal increased from 40% to 94% as the initial  $\text{H}_2\text{O}_2$  concentration was

increased from 24 to 110 mg/L. (Table 4-4). A similar effect was observed for DIPE also. The degradation rates of BTEX by hydroxyl radicals are significantly higher than those of the ethers. Thus, the removal of BTEX was less sensitive to the initial H<sub>2</sub>O<sub>2</sub> concentration.

In the test with a higher influent MTBE concentration, the effects of H<sub>2</sub>O<sub>2</sub> dosage on the degradation of MTBE and DIPE were less significant than those observed in the first test (Table 4-5). The photodegradation of H<sub>2</sub>O<sub>2</sub> in the test with the lower influent MTBE concentration was low compared with that in the test with the higher influent MTBE concentration. Consequently, the results of the former showed significantly lower degradation efficiency for every compound despite a lower organic loading. The pH and the iron concentration in both tests were almost identical, and the two tests were conducted only 16 hours apart. The test dosed with 2 mg/L MTBE had a higher level of other organic contaminants, particularly toluene. This indicates that the characteristics of the groundwater might have fluctuated between these two tests. It is not known whether the changes in the groundwater characteristics might have contributed to the deterioration in the degradation efficiency in the first test.

### *Effects of Other Organic Compounds on MTBE Degradation*

Because of their very high reactivity and low selectivity, the hydroxyl radicals, once generated, rapidly react with other compounds or with each other. So in these reactors the concentration of free radicals is very low. For the target organic compounds to be effectively degraded, they have to compete with each other for the trace-level, short-life hydroxyl radicals. Therefore, the degradation efficiency of a specific compound in the UV-H<sub>2</sub>O<sub>2</sub> process depends not only on its reaction rate constant with the hydroxyl radical, but also on the number of molecular species existing in the system, their concentrations, and their reaction rates with the hydroxyl radicals.

Quantification of the effects of other organic compounds on the degradation efficiency of the target compound is only possible when the fate of the hydroxyl radicals and the kinetic constants of all the reactions are known. Since very little such information is available, two tests were conducted to shed some light on these interaction effects.

In these two tests, the concentration of toluene varied. The results are tabulated in Tables 4-6 and 4-7. The results of Table 4-6 were obtained when the UV quartz sheath was fouled as evidenced from the low photolysis efficiency of  $\text{H}_2\text{O}_2$ . Both results showed similar trends: As the concentration of toluene increased, the degradation of MTBE, DIPE and benzene were more significantly deteriorated. The extent of deterioration in the degradation efficiency of these three compounds did not appear to correlate with their reaction rate constant with hydroxyl radicals, or with their concentration. Interestingly, the degradation of p,m-xylene, o-xylene, and ethyl benzene was not affected, even though their concentrations were significantly different. These results suggest that the degradation of organic contaminants in the UV- $\text{H}_2\text{O}_2$  process cannot be fully explained or quantified simply based on the initial reaction constants of these compounds with hydroxyl radicals.

### ***Effects of pH***

$\text{H}_2\text{O}_2$  is photolyzed almost completely to hydroxyl radical under acidic, neutral and slightly alkaline conditions (Ogata *et al.*, 1983). Above pH 9, however, ozone may be generated from photolysis of  $\text{H}_2\text{O}_2$  (Landi and Heidt, 1969). Therefore, photolysis of  $\text{H}_2\text{O}_2$  is not very sensitive to pH between pH 3 and 9. However, lowering pH shifts the equilibrium between  $\text{HCO}_3^-$  and  $\text{CO}_3^{2-}$ , i.e., converting more  $\text{CO}_3^{2-}$  to  $\text{HCO}_3^-$ . Both  $\text{HCO}_3^-$  and  $\text{CO}_3^{2-}$  are scavengers for hydroxyl radicals. The reaction rate of hydroxyl radical with  $\text{CO}_3^{2-}$  is at least one order of magnitude higher than that of hydroxyl radical with  $\text{HCO}_3^-$ . Therefore, lowering the pH can significantly enhance the degradation efficiency of organic compounds in the UV- $\text{H}_2\text{O}_2$  process by reducing the scavenge function from  $\text{CO}_3^{2-}$ , particularly for wastewater with an alkalinity of approximately 400 mg/L, such as used in

this study. In addition to reduction of  $\text{CO}_3^{2-}$ - $\text{HCO}_3^-$  scavengers, potential contribution from Fenton's reaction to the degradation of organic compounds can be significant at low pH with the presence of both soluble iron and  $\text{H}_2\text{O}_2$  as discussed in the previous section.

Table 4-8 summarizes the results of the pH effects on the degradation of organic compounds in the UV- $\text{H}_2\text{O}_2$  process. Four pH conditions, pH 3.5, 5.5, 7.0, and 9.5, were evaluated in the test. A pH controller was used to control the desirable pH values in the mixing tank using either  $\text{H}_2\text{SO}_4$  or  $\text{NaOH}$ . It should be noted that this set of tests was conducted during the time when the UV quartz sheath had been fouled as was found out later from the low  $\text{H}_2\text{O}_2$  photolysis efficiency (to be discussed below). The degradation rates of the organic compounds had therefore deteriorated at the time of the test. However, these results are still valid for evaluating the relative effects of pH.

As shown in Table 4-8, while the injection rate of  $\text{H}_2\text{O}_2$  into the mixing tank was maintained the same for these four test conditions, the concentration of  $\text{H}_2\text{O}_2$  was significantly lower at pH 9.5 than under neutral and acidic conditions. It seems that the decomposition of  $\text{H}_2\text{O}_2$  was accelerated at higher pH. The rate of  $\text{H}_2\text{O}_2$  photolysis in the UV photoreactor, on the other hand, appeared to be slightly slower at pH 9.5 as compared with that at neutral or acidic conditions: the pseudo first order rate constants of  $\text{H}_2\text{O}_2$  photolysis were calculated to be 0.064, 0.104, 0.078, 0.106  $\text{min}^{-1}$ , respectively. These rate constants were significantly lower than those reported in the "Photolysis of  $\text{H}_2\text{O}_2$ " section, indicating the fouling of the UV quartz sheath. As a matter of fact, the UV quartz sheath was cleaned after these tests. As the pH was lowered, the oxidation and subsequent flocculation and removal of Fe by sand filter was somewhat retarded. The soluble iron concentrations were < 0.5, 1, 2.4, and 5 mg/L at pH 9.5, 7.0, 5.5, and 3.5, respectively. The higher soluble Fe concentration at low pH, however, would promote Fenton's reaction, thus benefiting the overall removal of the organics.

The degradation of all the organic compounds in the UV- $\text{H}_2\text{O}_2$  process increased with decreasing pH, with the pH effects most obvious for MTBE and DIPE. Figures 4-7 and

4-8 plot the fraction of MTBE and toluene removal against the hydraulic retention time in the photoreactor in the semi-logarithmic scale. The slopes of the lines in these two figures represent the pseudo first order reaction rate constants of MTBE and toluene degradation. It is seen that the MTBE and toluene degradation rates increased slightly with decreasing pH between pH 9.5 and 5.5, which could be attributed to the reduction of  $\text{CO}_3^{-2}$  concentration with pH. The degradation rates of MTBE and toluene increased significantly as the pH was lowered to pH 3.5. The disproportionately higher degradation rates at pH 3.5 are believed to be assisted by Fenton's reaction in addition to the elimination of  $\text{CO}_3^{-2}$ - $\text{HCO}_3^-$  scavengers. The contribution of Fenton's reaction to the degradation of organic compounds is evidenced from the significant reduction in all the organic compounds even in the mixing tank before UV irradiation.

### *Effects of Iron and Low pH*

To further assess the impact of iron on the degradation of organic compounds at low pH, three additional tests were conducted. The test conditions are: (1) pH 7.0 with sand filter in operation; (2) pH 3.5 with sand filter in operation; and (3) pH 3.5 without passing the wastewater through the sand filter. The sand filter removed a portion of the soluble iron, probably via surface adsorption and surface catalyzed oxidation, such that the iron concentration into the photoreactor under test condition (2) was slightly lower than that under the test condition (3). In all three tests, the wastewater was dosed with MTBE and toluene to make their concentration in the feed approximately 2.5 mg/L and 10 mg/L, respectively. The test results are summarized in Table 4-9.

Due to the very high toluene concentration dosed into the mixing tank, the hydroxyl radicals generated from the Fenton reaction appeared to be mostly consumed by toluene as evidenced from the significant reduction of toluene concentration in the mixing tank between pH 7 and pH 3.5 conditions. Xylenes and ethylbenzene were also reduced by the Fenton reaction in the mixing tank, while the reduction in MTBE, DIPE and benzene were not significant. As seen from Table 4-9, there was slight enhancement, though not very

significant, in the degradation rates for all organic compounds at higher soluble iron concentration. This improvement is more clearly seen from Figure 4-9 as the curve representing the conditions of 6 mg/L Fe and pH 3.5 had a steeper slope than that representing pH 3.5 and 3 mg/L Fe.

### ***Effects of Iron Hydroxide Particulate***

The presence of iron hydroxide solids in the wastewater can retard the penetration of UV light through the photoreactor. The effects of iron hydroxide solids on the degradation efficiency of the UV-H<sub>2</sub>O<sub>2</sub> process were also evaluated in this study. In this set of tests, iron from the groundwater was oxidized and flocculated into iron hydroxide flocs in the mixing tank. The wastewater was then either passed through the sand filter to remove the iron hydroxide flocs or directly fed to the UV photoreactor. The results were summarized in Table 4-10. As expected, the presence of 7 mg/L of iron hydroxide particulate significantly deteriorated the degradation effectiveness of the UV-H<sub>2</sub>O<sub>2</sub> process, particularly for MTBE and DIPE. Oxidation of iron followed by flocculation and filtration are therefore necessary pretreatment steps for the effective usage of the UV-H<sub>2</sub>O<sub>2</sub> process if it is to be operated under neutral or alkaline conditions. Note that these two tests were carried out during the time when the UV quartz sheath was fouled, and therefore achieved smaller overall degradation efficiency.

### ***Total Organic Carbon Reduction in the UV-H<sub>2</sub>O<sub>2</sub> Process***

In some of the tests, the total organic carbon (TOC) in the influent and the effluent was monitored. These results together with the TOC of VOC data in the influent and effluent are shown in Table 4-11. The "TOC of VOC" is the TOC content of the total volatile organic compounds calculated by summing the concentrations of BTEX, MTBE, and DIPE. As displayed in the table, the reduction in TOC was in most cases smaller than the reduction of TOC resulting from removal of BTEX, MTBE, and DIPE. The results

indicate that the UV-H<sub>2</sub>O<sub>2</sub> process only partially oxidizes BTEX, MTBE, and DIPE to some intermediates, probably aldehydes and ketones, and not to CO<sub>2</sub>. The effects of the by-products from the UV-H<sub>2</sub>O<sub>2</sub> process on the aquatic toxicity are unknown and should be carefully examined before selecting this process for treatment.

### *Degradation Capability of the UV-H<sub>2</sub>O<sub>2</sub> Pilot Unit*

Figure 4-10 plotted the effluent MTBE concentration against the MTBE loading to the UV-H<sub>2</sub>O<sub>2</sub> pilot unit. The hydraulic retention time for all the data shown in this figure ranged from 3 to 6 minutes. The data collected under the UV lamp quartz sheath fouling conditions and under pH test conditions are excluded. In most cases, an effluent MTBE concentration below 100 µg/L could be achieved. As mentioned before, the degradation of MTBE and other organics was significantly impacted when high toluene concentration, greater than 10 mg/L, was dosed in the feed. The figure showed that an effluent MTBE concentration of less than 100 µg/L was achievable in the pilot UV-H<sub>2</sub>O<sub>2</sub> unit under an MTBE loading of 2000 to 4300 mg/L/day, depending on the concentration of other organic compounds.

### *Photoreactor Sizing*

Theoretically, a reactor model can be constructed to predict the performance of the UV-H<sub>2</sub>O<sub>2</sub> process if the following information is known: the kinetics of H<sub>2</sub>O<sub>2</sub> decomposition and of the subsequent hydroxyl radical generation related to the UV lamp used, the kinetics of the reaction of the hydroxyl radicals with the target species and with the reaction intermediates, and the kinetics of the reaction between the hydroxyl radical and the impurities in the wastewater. For the treatment of wastewater involving multiple organic contaminants and complex chain reactions, only partial kinetic information is available. Therefore, the construction of a complete reactor model for the UV-H<sub>2</sub>O<sub>2</sub> process has been very difficult.

Lacking a comprehensive reactor model, sizing of the photoreactor for a specific wastewater has been conventionally approached by sending samples of wastewater to the vendors for test, and extrapolating the test data for design. One of the rational engineering design bases used by the vendors for the photoreactor sizing was the specific energy requirement for 90% degradation,  $E_{90}$ .  $E_{90}$  is the energy input for a specific UV lamp required to reduce the concentration of the target compound by one order of magnitude per unit volume of the wastewater (i.e., kWh/1000 gal/log [ $C_{init}/C_{final}$ ]), where  $C_{init}$  and  $C_{final}$  are the initial and final concentrations of the specific compound subjected to the UV- $H_2O_2$  degradation).  $E_{90}$  can be easily calculated based on the following equations:

$$\text{For batch process:} \quad E_{90} = \frac{P \cdot t_r \cdot 1000}{V \cdot \log(C_{init} / C_{final})} \quad (4-4)$$

$$\text{For continuous process:} \quad E_{90} = \frac{P \cdot 1000}{Q \cdot \log(C_{init} / C_{final})} \quad (4-5)$$

where  $P$  = power of the UV lamp in kW  
 $t_r$  = reaction time, hr  
 $V$  = volume of liquid processed in the batch  
 $Q$  = flow rate, gal/hr

Thus, the value of  $E_{90}$  is determined for each compound of interest in the wastewater sample. The total energy required to achieve the desirable removal for each compound can then be determined based on its  $E_{90}$  value, its initial and target treated concentration, and the wastewater flow rate. The photoreactor lamp and the size of the reactor are then determined based on the compound which demands the highest energy input per unit hydraulic retention time to achieve the desired removal. A safety factor is usually incorporated in the final design.

Due to the complex chain reactions between the hydroxyl radicals and various organic and inorganic compounds, the degradation of a specific compound by the UV-peroxide

process is strongly affected by the chemical characteristics of the wastewater. In addition, different UV lamps from different vendors may have different energy output at different wavelengths, resulting in different efficiency of  $\text{H}_2\text{O}_2$  photolysis. Therefore, the  $E_{90}$  value for a specific compound will vary with the composition of the wastewater and the UV lamp used. In the following section, the  $E_{90}$  value extracted from the data obtained from this study was compiled to provide a general picture of how the  $E_{90}$  values for the ethers and BTEX are affected by the wastewater composition. Note that the test data under the UV lamp quartz sheath fouling conditions have been excluded from this analysis. Significantly higher  $E_{90}$  values will result if the UV lamp quartz sheath is dirty or the turbidity or opaqueness of the wastewater is high. The data obtained under low or high pH were not used in the  $E_{90}$  calculation either. These  $E_{90}$  values compiled below may potentially be used in the first pass screening process for treatment process selection.

The  $E_{90}$  values for MTBE under different test conditions were plotted against the total VOC concentration and against the molar ratio of total VOC to MTBE in the feed (Figures 4-11 and 4-12). The total VOC is the sum of benzene, toluene, xylenes, ethyl benzene, MTBE and DIPE. Under conditions where no one single compound dominated in its concentration in the feed, the  $E_{90}$  for MTBE varied from 20 to 80 kWh/1000 gal and was averaged at approximately 40 kWh/1000 gal. In a series of tests in which toluene concentration in the influent was significantly higher than the rest of the organic contaminants, the  $E_{90}$  for MTBE was drastically increased. As shown in both Figures 4-11 and 4-12, although the  $E_{90}$  for MTBE fluctuated with test conditions, there were no obvious effects of the total organic concentration and the molecular ratio of other organic compounds to MTBE on  $E_{90}$ . Similar phenomena were observed for DIPE and BTEX. Examples of  $E_{90}$  for toluene and DIPE were given in Figures 4-13 to 4-16. Similar plots for  $E_{90}$  for benzene, xylenes, and ethyl benzene are included in the Appendix.

Significantly higher values of  $E_{90}$  for compounds including toluene were also obtained under the high influent toluene concentration test conditions. Examination of the photolysis of  $\text{H}_2\text{O}_2$  under these test conditions showed that the decomposition rate of

H<sub>2</sub>O<sub>2</sub> was not affected. Therefore, the higher E<sub>90</sub> values could not be due to deficiency in hydroxyl radicals. It is speculated that some of the intermediates from the reaction of toluene and hydroxyl radical might act as hydroxyl radical scavengers so that the degradation of all the organic compounds was strongly retarded.

Table 4-12 summarizes the range and average of E<sub>90</sub> for MTBE, DIPE and BTEX obtained in this study. As previously discussed, the reaction between hydroxyl radicals and organic contaminants is complex. The E<sub>90</sub> values therefore vary significantly with test conditions, wastewater characteristics, and the UV lamp used, as evidenced from the variation E<sub>90</sub> shown in the table. The E<sub>90</sub> information should be used with caution.

#### ***Example of Using the E<sub>90</sub> Information for Sizing the UV Photoreactor***

As previously discussed, the complexity of the hydroxyl radical chain reactions and the variation in the UV lamp characteristics make the prediction of the performance of the UV-H<sub>2</sub>O<sub>2</sub> process very difficult. Therefore, if one decides to choose this process to decontaminate wastewater, a pilot test of the performance of the equipment is highly recommended. At least, samples should be taken and submitted to the vendor for batch testing. The batch test tends to give better degradation results than the continuous process, probably due to more uniform exposure of the wastewater to the UV irradiation. Therefore, a larger safety factor should be considered. The following example shows how the E<sub>90</sub> values can be used for the first pass screening of the size of the photoreactor (including the power of the UV lamp).

**Example:** One marketing terminal in X company is required to treat its wastewater before discharge. The wastewater contains 10 mg/L MTBE, 30 mg/L toluene, and 5 mg/L benzene. The discharge limits are 100 µg/L MTBE and 1 µg/L for both benzene and toluene. What sizes of the UV reactor and lamp should be used to treat the water to meet the discharge limit?

Assume the UV reactor will be supplied by the same vendor from this study. Based on Table 4-12, the average  $E_{90}$  for MTBE, benzene, and toluene are: 36, 27, and 20 kWh/1000 gal, respectively.

Based on Equation (4-2), the total energy input required to degrade the organic compounds to discharge limits is:

For MTBE:

$$P = [36 \cdot 1800 \cdot \log(10000/100)]/1000 = 129 \text{ kW}$$

For benzene:

$$P = [27 \cdot 1800 \cdot \log(5000/1)]/1000 = 179 \text{ kW}$$

For toluene:

$$P = [20 \cdot 1800 \cdot \log(10000/1)]/1000 = 144 \text{ kW}$$

Therefore, the total energy input from the UV lamps should be more than 180 kW multiplied by a safety factor. Equation 4-1 does not provide any guidance on selecting the hydraulic retention time. In general, a hydraulic retention time of 5 to 10 minutes should be appropriate for BTEX and MTBE.

### ***Optimum H<sub>2</sub>O<sub>2</sub> Dosage***

It was shown previously that the higher the hydrogen peroxide dosage, the more the organic compounds are degraded. However, at higher H<sub>2</sub>O<sub>2</sub> dosages, not all H<sub>2</sub>O<sub>2</sub> is decomposed, and it has been reported that residual H<sub>2</sub>O<sub>2</sub> can cause aquatic toxicity. In many cases, the residual H<sub>2</sub>O<sub>2</sub> concentration has to be removed using either activated carbon or reductants such as bisulfite. Consequently, indiscriminant use of high dosage of H<sub>2</sub>O<sub>2</sub> not only is expensive but also demands more operating supervision. On the other hand, due to the lack of selectivity of the hydroxyl radicals, generation of excess hydroxyl radicals is necessary in order for the target species, which react more slowly with the hydroxyl radicals, to be degraded to the desired level. Therefore, the optimum H<sub>2</sub>O<sub>2</sub>

dosage is the minimum  $\text{H}_2\text{O}_2$  concentration at which the target compounds can be removed to the desired level. Such an optimum  $\text{H}_2\text{O}_2$  concentration will vary with the composition of the contaminants, the concentration of hydroxyl radical scavengers present in the wastewater, the UV lamp, and the liquid hydraulic retention time in the photoreactor. Lacking a validated model for the UV- $\text{H}_2\text{O}_2$  process, the optimum  $\text{H}_2\text{O}_2$  dosage could not be predicted. Alternatively, the relationship between the  $\text{H}_2\text{O}_2$  dosage and the performance of the UV- $\text{H}_2\text{O}_2$  process on the degradation of MTBE and BTEX was extracted from the field test.

Figures 4-17 to 4-19 plot the effluent concentration of MTBE, benzene, and toluene against the molar ratio of  $\text{H}_2\text{O}_2$  to total VOC. The total VOC is the sum of MTBE, DIPE, benzene, toluene, xylenes, and ethylbenzene. As seen from Figure 4-17, for a  $[\text{H}_2\text{O}_2]/[\text{VOC}]$  molar ratio greater than 20, an effluent MTBE concentration of less than 100  $\mu\text{g}/\text{L}$  was achieved in most cases. At a molar ratio of  $[\text{H}_2\text{O}_2]/[\text{VOC}]$  greater than 20, the effluent concentrations of benzene and toluene were less than 10  $\mu\text{g}/\text{L}$  (Figures 4-18 and 4-19). It appears that for this specific UV equipment, a  $[\text{H}_2\text{O}_2]/[\text{VOC}]$  molar ratio of 20 to 40 would be adequate for achieving the desirable degradation of MTBE and BTEX. Note that during the whole field test, an effluent concentration of less than 1  $\mu\text{g}/\text{L}$  benzene was not consistently achieved in this UV- $\text{H}_2\text{O}_2$  process. This is probably due to the fact that as the contaminant concentration was reduced to a very low level (1-10  $\mu\text{g}/\text{L}$ ) during the UV- $\text{H}_2\text{O}_2$  process, its further reduction might be retarded due to the competition from other organic species and hydroxyl radical scavengers for the hydroxyl radicals. As a result, a carbon bed polishing unit might be needed to ensure a consistent compliance with less than 1  $\mu\text{g}/\text{L}$  of benzene in the effluent. Alternatively, using a larger safety factor in sizing the photoreactor is recommended if no polishing unit is to be installed.

As discussed in the section of "Photolysis of  $\text{H}_2\text{O}_2$ ," the photolysis rate (or consumption rate) of  $\text{H}_2\text{O}_2$  for a specific UV reactor was insensitive to the organic contaminants at low concentrations. Therefore, once the dosage or concentration of  $\text{H}_2\text{O}_2$  is determined from

the above approach, Equation (4-3) with the pertinent  $k_{H_2O_2}$  can be used to calculate the consumption and residual concentration of  $H_2O_2$ .

## E. Conclusions

1. The UV- $H_2O_2$  process was demonstrated to be capable of effectively degrading MTBE and other gasoline hydrocarbons under high MTBE and organic loading rates. Using a photoreactor equipped with a 30 kW UV lamp, less than 100  $\mu\text{g/L}$  MTBE in the effluent could be achieved for treating a wastewater with a MTBE loading up to 4300 mg/L/day. The hydraulic retention time under these conditions ranged from 3 to 6 minutes.
2. There is little reduction in the total organic carbon through the UV- $H_2O_2$  process. The by-products are likely to be aldehydes and ketones. The aquatic toxicity issue of the treated effluent from the UV- $H_2O_2$  process was not addressed in this study, but should be carefully examined when choosing this technology.
3. Iron present in the wastewater would deteriorate the degradation efficiency of the UV- $H_2O_2$  process under neutral and alkaline pH conditions because ferrous iron competes with organic compounds for hydroxyl radicals and ferric iron hydroxide flocs might foul the UV lamp quartz sheath and block UV light. Therefore, the UV- $H_2O_2$  process should incorporate an iron removal pretreatment step. However, if the pH was lowered to 3.5, presence of iron would increase hydroxyl radical generation through Fenton's reaction, and significantly increase the overall degradation efficiency of the UV- $H_2O_2$  process.
4. The degradation of organic contaminants in the UV- $H_2O_2$  process involves complex chain reactions, of which most of the kinetic information is not known. Prediction of the reaction results will be difficult, and laboratory and/or pilot testing is strongly recommended before selection of the process and sizing of the equipment. This study provided some engineering design data such as  $E_{90}$  and  $H_2O_2$  consumption under different operating conditions which may be used in the first pass screen process for process selection.

Table 4-1. The Kinetic Constants for the Reaction of Hydroxyl Radicals with Organic and Inorganic Solutes in Aqueous Solutions (From: F. Rose and A. Rose, 1977)

Reaction	pH	k (M <sup>-1</sup> s <sup>-1</sup> )
•OH + OH → H <sub>2</sub> O <sub>2</sub>	7	4 - 5.5x10 <sup>9</sup>
	0.4	6 x 10 <sup>9</sup>
	3	6 x 10 <sup>9</sup>
	3.7	5.2 x 10 <sup>9</sup>
•OH + HO <sub>2</sub> → H <sub>2</sub> O + O <sub>2</sub>	7	3 x 10 <sup>9</sup>
	3	1.5 x 10 <sup>10</sup>
	0.8	1.4 x 10 <sup>10</sup>
	0.46 - 6.75	7.1 x 10 <sup>9</sup>
•OH + HCO <sub>3</sub> <sup>-</sup> → H <sub>2</sub> O + CO <sub>3</sub> <sup>-</sup> or HCO <sub>3</sub> + OH <sup>-</sup>	6.5	1 x 10 <sup>7</sup>
	8.4	1.5 x 10 <sup>7</sup>
	---	3.6 - 7.9 x 10 <sup>7</sup>
•OH + CO <sub>3</sub> <sup>2-</sup> → OH <sup>-</sup> + CO <sub>3</sub> <sup>-</sup>	< 11.6	2 - 4.7 x 10 <sup>8</sup>
•OH + Fe <sup>2+</sup> → Fe <sup>3+</sup> + OH <sup>-</sup>	0.4	1.7 x 10 <sup>9</sup>
	0.8	1.2 x 10 <sup>9</sup>
	1	2.3 x 10 <sup>9</sup>
	2	5 x 10 <sup>9</sup>
	3.5	5 x 10 <sup>9</sup>
	4.5	3.4 x 10 <sup>9</sup>
•OH + H <sub>2</sub> O <sub>2</sub> → HO <sub>2</sub> + H <sub>2</sub> O	3	1.2 x 10 <sup>7</sup>
	6	4.5 x 10 <sup>7</sup>
	7	1.7 - 2.6 x 10 <sup>7</sup>
	8.4	6.5 x 10 <sup>7</sup>

Table 4-1. The Kinetic Constants for the Reaction of Hydroxyl Radicals with Organic and Inorganic Solutes in Aqueous Solutions (From: F. Rose and A. Rose, 1977) (Continued)

Reaction	pH	k (M <sup>-1</sup> s <sup>-1</sup> )
$\bullet\text{OH} + \text{H}_2\text{PO}_4^- \rightarrow \text{H}_2\text{PO}_4 + \text{OH}^-$	7 3.85 - 4.0	< 1.2 x 10 <sup>7</sup> 2.2 x 10 <sup>7</sup>
$\bullet\text{OH} + \text{HPO}_4^{2-} \rightarrow ?$	--- 9.0 - 12.3	< 5 x 10 <sup>6</sup> 7.9 x 10 <sup>5</sup>
$\bullet\text{OH} + \text{HSO}_4^- \rightarrow \text{SO}_4^- + \text{H}_2\text{O}$	7	0.69 - 1.6 x 10 <sup>6</sup>
$\bullet\text{OH} + \text{C}_6\text{H}_6 \rightarrow \text{Product}$ (Benzene)	1 2 3 6 - 7 9 10.5	0.74 - 2.3 x 10 <sup>9</sup> 5.4 x 10 <sup>9</sup> 3.3 - 6.3 x 10 <sup>9</sup> 5 x 10 <sup>9</sup> 3.2 x 10 <sup>9</sup> 6.8 x 10 <sup>9</sup>
$\bullet\text{OH} + \text{C}_6\text{H}_5\text{CH}_3 \rightarrow \text{product}$ (Toluene)	3 7	3.0 x 10 <sup>9</sup> 6.8 x 10 <sup>9</sup>
$\bullet\text{OH} + \text{o-xylene} \rightarrow \text{product}$	7	6.7 x 10 <sup>9</sup>
$\bullet\text{OH} + \text{m-xylene} \rightarrow \text{product}$	7	7.5 x 10 <sup>9</sup>
$\bullet\text{OH} + \text{p-xylene} \rightarrow \text{product}$	7	7.0 x 10 <sup>9</sup>

Table 4-2. Reaction Rate Constants of MTBE, Toluene, and m-Xylene Determined by the Relative Rate Constant Method (Tang and Wilcox, 1990)

Benzene		MTBE		$K_m/K_b$
Influent	Effluent	Influent	Effluent	
0.846	0.171	0.513	0.316	<b>0.158</b>
0.995	0.063	0.534	0.16	<b>0.157</b>
3.521	1.572	2.133	1.811	<b>0.143</b>
4.213	1.162	2.264	1.657	<b>0.139</b>
Benzene		Toluene		$K_t/K_b$
Influent	Effluent	Influent	Effluent	
0.431	0.059	0.396	0.058	<b>0.924</b>
1.254	0.327	1.15	0.284	<b>1.019</b>
2.693	1.459	2.469	1.304	<b>1.03</b>
Benzene		m-Xylene		$K_x/K_b$
Influent	Effluent	Influent	Effluent	
0.382	0.03	0.209	0.015	<b>1.098</b>
1.121	0.206	0.611	0.111	<b>1.01</b>
2.32	0.635	1.264	0.352	<b>0.976</b>

**Table 4-3. Photodegradation of Organic Compounds by UV Irradiation in the Test Photoreactor**

	MTBE		Benzene		Toluene		p,m-Xylene	
	Conc. (µg/L)	Removal	Conc. (µg/L)	Removal	Conc. (µg/L)	Removal	Conc. (µg/L)	Removal
Influent	3710	0.00%	400	0.00%	4890	0.00%	980	0.00%
Lamp-1 Effluent	3680	0.81%	300	25.00%	2530	48.26%	370	62.24%
Lamp-2 Effluent	3590	3.23%	300	25.00%	2010	58.90%	210	78.57%
Lamp-3 Effluent	3370	9.16%	270	32.50%	1150	76.48%	86	91.22%

	o-Xylene		E-Benzene		DIPE	
	Conc. (µg/L)	Removal	Conc. (µg/L)	Removal	Conc. (µg/L)	Removal
Influent	350	0.00%	220	0.00%	400	0.00%
Lamp-1 Effluent	150	57.14%	110	50.00%	300	25.00%
Lamp-2 Effluent	86	75.43%	80	63.64%	300	25.00%
Lamp-3 Effluent	37	89.43%	43	80.45%	270	32.50%

Table 4-4. Effects of H<sub>2</sub>O<sub>2</sub> Concentration on the Degradation of Organic Compounds in the UV-H<sub>2</sub>O<sub>2</sub> Process - Low Influent MTBE Concentration

Inf. H <sub>2</sub> O <sub>2</sub> (mg/L)	MTBE (µg/L)			DIPE (µg/L)		
	24	40	116	24	40	116
Influent	200	240	210	290	310	300
Lamp-1	130	140	74	220	190	90
Lamp-2	140	99	36	210	96	20
Lamp-3	120	63	12	150	46	4
Overall Removal	40.00%	73.75%	94.29%	48.28%	85.16%	98.67%

Inf. H <sub>2</sub> O <sub>2</sub> (mg/L)	Benzene (µg/L)			Toluene (µg/L)		
	24	40	116	24	40	116
Influent	550	610	590	1710	1710	1750
Lamp-1	350	190	78	940	460	190
Lamp-2	230	51	10	550	100	15
Lamp-3	110	15	4	230	21	2
Overall Removal	80.00%	97.54%	99.32%	86.55%	98.77%	99.89%

Inf. H <sub>2</sub> O <sub>2</sub> (mg/L)	p,m-Xylene (µg/L)			o-Xylene (µg/L)		
	24	40	116	24	40	116
Influent	260	270	280	95	98	100
Lamp-1	131	23	30	47	47	13
Lamp-2	61	11	3	25	4	1
Lamp-3	23	3	1	10	1	2
Overall Removal	91.15%	98.89%	99.64%	89.47%	98.98%	98.00%

Inf. H <sub>2</sub> O <sub>2</sub> (mg/L)	E-Benzene (µg/L)			H <sub>2</sub> O <sub>2</sub> (mg/L)		
	24	40	116	24	40	116
Influent	84	87	90	24	40	116
Lamp-1	47	62	10	16	22	76
Lamp-2	2	5	< 1	12	12	60
Lamp-3	11	1	< 1	8	10	42
Overall Removal	86.90%	98.85%	99.44%	66.67%	75.00%	63.79%

Table 4-5. Effects of H<sub>2</sub>O<sub>2</sub> Concentration on the Degradation of Organic Compounds in the UV-H<sub>2</sub>O<sub>2</sub> Process - Higher Influent MTBE Concentration

Inf. H <sub>2</sub> O <sub>2</sub> (mg/L)	MTBE (µg/L)			DIPE (µg/L)		
	35	78	90	35	78	90
Influent	1820	1980	1940	320	330	340
Lamp-1	910	1070	740	140	140	79
Lamp-2	560	620	230	49	59	14
Lamp-3	220	250	47	10	13	1
Overall Removal	87.91%	87.37%	97.58%	96.88%	96.06%	99.71%

Inf. H <sub>2</sub> O <sub>2</sub> (mg/L)	Benzene (µg/L)			Toluene (µg/L)		
	35	78	90	35	78	90
Influent	750	680	740	2770	2310	2490
Lamp-1	150	150	71	450	430	200
Lamp-2	23	38	9	50	85	10
Lamp-3	5	8	2	4	7	< 1
Overall Removal	99.33%	98.82%	99.73%	99.86%	99.70%	99.98%

Inf. H <sub>2</sub> O <sub>2</sub> (mg/L)	p,m-Xylene (µg/L)			o-Xylene (µg/L)		
	35	78	90	35	78	90
Influent	410	360	380	150	140	160
Lamp-1	56	58	26	22	22	10
Lamp-2	6	11	2	3	5	< 1
Lamp-3	< 1	2	< 1	< 1	< 1	< 1
Overall Removal	99.88%	99.44%	99.87%	99.67%	99.64%	99.69%

Inf. H <sub>2</sub> O <sub>2</sub> (mg/L)	E-Benzene (µg/L)			H <sub>2</sub> O <sub>2</sub> (mg/L)		
	35	78	90	35	78	90
Influent	130	110	120	35	78	90
Lamp-1	20	21	10	21	55	43
Lamp-2	2	4	< 1	10	40	21
Lamp-3	< 1	< 1	< 1	6	21	12
Overall Removal	99.62%	99.55%	99.58%	82.86%	73.08%	99.44%

Table 4-6. Effects of Influent Toluene Concentration on the Degradation of MTBE and Other Volatile Organic Compounds in the UV-H<sub>2</sub>O<sub>2</sub> Process - Test #1

	MTBE (µg/L)			Toluene (µg/L)		
	Run-1	Run-2	Run-3	Run-1	Run-2	Run-3
<b>Influent</b>	3220	4490	3880	7100	4660	1920
<b>Lamp-1</b>	1720	2340	1960	1030	360	170
<b>Lamp-2</b>	970	1280	1060	110	39	22
<b>Lamp-3</b>	700	560	470	25	3	1
<b>Removal</b>	78.26%	87.53%	87.89%	99.65%	99.94%	99.95%
	Benzene (µg/L)			DIPE (µg/L)		
	Run-1	Run-2	Run-3	Run-1	Run-2	Run-3
<b>Influent</b>	370	320	290	370	320	290
<b>Lamp-1</b>	140	89	84	140	89	84
<b>Lamp-2</b>	55	28	24	55	28	24
<b>Lamp-3</b>	24	13	7	27	13	7
<b>Removal</b>	93.51%	95.94%	97.59%	92.70%	95.94%	97.59%
	p,m-Xylene (µg/L)			o-Xylene (µg/L)		
	Run-1	Run-2	Run-3	Run-1	Run-2	Run-3
<b>Influent</b>	260	300	290	90	110	110
<b>Lamp-1</b>	33	17	25	13	5	6
<b>Lamp-2</b>	< 1	2	2	2	< 1	< 1
<b>Lamp-3</b>	< 1	< 1	< 1	< 1	< 1	< 1
<b>Removal</b>	99.81%	99.83%	99.83%	99.44%	99.55%	99.55%
	E-Benzene (µg/L)			H <sub>2</sub> O <sub>2</sub> (mg/L)		
	Run-1	Run-2	Run-3	Run-1	Run-2	Run-3
<b>Influent</b>	93	110	100	125	127	130
<b>Lamp-1</b>	14	4	6	110	117	117
<b>Lamp-2</b>	< 1	< 1	< 1	100	102	103
<b>Lamp-3</b>	< 1	< 1	< 1	87	89	88
<b>Removal</b>	99.46%	99.55%	99.50%	30.40%	29.92%	32.31%

Table 4-7. Effects of Influent Toluene Concentration on the Degradation of MTBE and Other Volatile Organic Compounds in the UV-H<sub>2</sub>O<sub>2</sub> Process - Test #2

	MTBE (µg/L)			Toluene (µg/L)		
	Run-1	Run-2	Run-3	Run-1	Run-2	Run-3
Influent	2590	2370	2910	18200	15034	5120
Lamp-1	1890	1900	1740	14060	6240	950
Lamp-2	1640	1590	650	7250	2660	170
Lamp-3	1340	1170	150	2990	620	5
Removal	48.26%	50.63%	94.85%	83.57%	95.88%	99.90%

	Benzene (µg/L)			DIPE (µg/L)		
	Run-1	Run-2	Run-3	Run-1	Run-2	Run-3
Influent	340	350	290	340	350	290
Lamp-1	260	250	130	260	250	130
Lamp-2	200	180	27	200	180	27
Lamp-3	140	87	3	140	87	3
Removal	58.82%	75.14%	98.97%	58.82%	75.14%	98.97%

	p,m-Xylene (µg/L)			o-Xylene (µg/L)		
	Run-1	Run-2	Run-3	Run-1	Run-2	Run-3
Influent	790	890	820	280	340	320
Lamp-1	220	330	120	88	120	49
Lamp-2	66	120	13	27	55	7
Lamp-3	30	24	< 1	13	12	< 1
Removal	96.20%	97.30%	99.94%	95.36%	96.47%	99.84%

	E-Benzene (µg/L)			H <sub>2</sub> O <sub>2</sub> (mg/L)		
	Run-1	Run-2	Run-3	Run-1	Run-2	Run-3
Influent	200	220	170	90	110	88
Lamp-1	61	92	29	60	80	67
Lamp-2	21	40	4	40	66	45
Lamp-3	9	9	< 1	20	35	21
Removal	95.50%	95.91%	99.71%	77.78%	68.18%	76.14%

Table 4-8. Effects of pH on the Degradation of Organic Compounds in the UV-H<sub>2</sub>O<sub>2</sub> Process

	MTBE (µg/L)				DIPE (µg/L)			
	pH 9.5	pH 7.0	pH 5.5	pH 3.5	pH 9.5	pH 7.0	pH 5.5	pH 3.5
<b>Influent</b>	2730	2416	2310	1550	320	270	280	140
<b>Lamp-1</b>	2250	1700	1900	510	210	220	200	23
<b>Lamp-2</b>	1770	1490	1410	220	160	130	110	4
<b>Lamp-3</b>	1830	1100	850	99	140	80	46	1
<b>Removal</b>	32.97%	54.47%	63.20%	93.61%	56.25%	70.37%	83.57%	99.29%

	Benzene (µg/L)				Toluene (µg/L)			
	pH 9.5	pH 7.0	pH 5.5	pH 3.5	pH 9.5	pH 7.0	pH 5.5	pH 3.5
<b>Influent</b>	320	620	530	140	1270	1170	1090	240
<b>Lamp-1</b>	210	330	240	11	460	520	440	3
<b>Lamp-2</b>	160	98	73	7	240	120	110	< 1
<b>Lamp-3</b>	140	43	20	5	130	41	17	< 1
<b>Removal</b>	56.25%	93.06%	96.23%	96.43%	89.76%	96.50%	98.44%	> 99.79%

	p,m-Xylene (µg/L)				o-Xylene (µg/L)			
	pH 9.5	pH 7.0	pH 5.5	pH 3.5	pH 9.5	pH 7.0	pH 5.5	pH 3.5
<b>Influent</b>	200	150	170	23	74	58	62	12
<b>Lamp-1</b>	66	43	54	< 1	26	23	23	< 1
<b>Lamp-2</b>	30	3	6	< 1	12	3	3	< 1
<b>Lamp-3</b>	16	< 1	< 1	< 1	5	< 1	< 1	< 1
<b>Removal</b>	92.00%	99.67%	> 99.71%	> 97.83%	93.24%	> 99.14%	> 99.19%	> 95.83%

	E-Benzene (µg/L)				H <sub>2</sub> O <sub>2</sub> (mg/L)			
	pH 9.5	pH 7.0	pH 5.5	pH 3.5	pH 9.5	pH 7.0	pH 5.5	pH 3.5
<b>Influent</b>	80	72	69	14	73	123	100	110
<b>Lamp-1</b>	29	29	28	< 1	68	111	92	96
<b>Lamp-2</b>	15	4	4	< 1	64	97	83	87
<b>Lamp-3</b>	7	1	< 1	< 1	56	81	74	73
<b>Removal</b>	91.25%	98.61%	> 99.28%	> 96.43%	23.29%	34.15%	26.00%	33.64%

Table 4-9. Effects of pH and Soluble Iron Concentrations on the Degradation of Organic Compounds in the UV-H<sub>2</sub>O<sub>2</sub> Process

	MTBE (µg/L)			DIPE (µg/L)		
	pH 7.0 Fe=0 mg/L	pH 3.5		pH 7.0 Fe=0 mg/L	pH 3.5	
		Fe=3 mg/L	Fe=6 mg/L		Fe=3 mg/L	Fe=6 mg/L
<b>Influent</b>	2200	2690	2280	280	220	240
<b>Lamp-1</b>	1930	590	510	270	19	15
<b>Lamp-2</b>	1170	210	130	130	4	2
<b>Lamp-3</b>	750	69	14	50	< 1	< 1

	Benzene (µg/L)			Toluene (µg/L)		
	pH 7.0 Fe=0 mg/L	pH 3.5		pH 7.0 Fe=0 mg/L	pH 3.5	
		Fe=3 mg/L	Fe=6 mg/L		Fe=3 mg/L	Fe=6 mg/L
<b>Influent</b>	280	220	240	10500	1560	1710
<b>Lamp-1</b>	270	19	15	5840	11	8
<b>Lamp-2</b>	130	4	2	1670	7	< 1
<b>Lamp-3</b>	50	< 1	< 1	240	< 1	< 1

	p,m-Xylene (µg/L)			o-Xylene (µg/L)		
	pH 7.0 Fe=0 mg/L	pH 3.5		pH 7.0 Fe=0 mg/L	pH 3.5	
		Fe=3 mg/L	Fe=6 mg/L		Fe=3 mg/L	Fe=6 mg/L
<b>Influent</b>	820	300	320	300	140	130
<b>Lamp-1</b>	460	2	2	250	< 1	< 1
<b>Lamp-2</b>	110	< 1	1	43	< 1	1
<b>Lamp-3</b>	14	< 1	2	7	< 1	4

	E-Benzene (µg/L)			H <sub>2</sub> O <sub>2</sub> (mg/L)		
	pH 7.0 Fe=0 mg/L	pH 3.5		pH 7.0 Fe=0 mg/L	pH 3.5	
		Fe=3 mg/L	Fe=6 mg/L		Fe=3 mg/L	Fe=6 mg/L
<b>Influent</b>	190	68	79	130	130	136
<b>Lamp-1</b>	120	< 1	< 1	60	63	77
<b>Lamp-2</b>	31	< 1	< 1	40	35	46
<b>Lamp-3</b>	5	< 1	< 1	13	14	25

Table 4-10. Effects of Iron Hydroxide Floccs on the Degradation of Organic Compounds in the UV-H<sub>2</sub>O<sub>2</sub> Process

	MTBE (µg/L)		DIPE (µg/L)	
	Fe=0 mg/L	Fe=7 mg/L	Fe=0 mg/L	Fe=7 mg/L
Influent	1950	1340	340	360
Lamp-1	1080	1130	180	260
Lamp-2	670	910	80	190
Lamp-3	268	700	16	120
Removal	86.26%	47.76%	95.29%	66.67%
	Benzene (µg/L)		Toluene (µg/L)	
	Fe=0 mg/L	Fe=7 mg/L	Fe=0 mg/L	Fe=7 mg/L
Influent	790	1010	3510	4240
Lamp-1	240	580	900	2210
Lamp-2	56	360	170	1330
Lamp-3	10	170	9	520
Removal	98.73%	83.17%	99.74%	87.74%
	p,m-Xylene (µg/L)		o-Xylene (µg/L)	
	Fe=0 mg/L	Fe=7 mg/L	Fe=0 mg/L	Fe=7 mg/L
Influent	520	690	190	260
Lamp-1	120	360	47	140
Lamp-2	9	210	8	75
Lamp-3	1	71	< 1	31
Removal	99.81%	89.71%	99.74%	88.08%
	Ethylbenzene (µg/L)		H <sub>2</sub> O <sub>2</sub> (µg/L)	
	Fe=0 mg/L	Fe=7 mg/L	Fe=0 mg/L	Fe=7 mg/L
Influent	140	190	48	55
Lamp-1	39	110	46	48
Lamp-2	8	63	32	36
Lamp-3	< 1	25	20	30
Removal	> 99.64%	86.84%	58.33%	45.45%

Table 4-11. Total Organic Carbon Reduction in the UV-H<sub>2</sub>O<sub>2</sub> Process

Run Conditions	Flow Rate (gpm)	TOC (mg/L)			TOC of VOC (mg/L)		
		Inf	Eff	Rmvd	Inf	Eff	Rmvd
Preliminary Test, GW, H <sub>2</sub> O <sub>2</sub>	10	12	16	-4	3.355	0.004	3
Preliminary Test, GW, H <sub>2</sub> O <sub>2</sub>	10	22	19	3	2.706	0.012	3
Preliminary Test, GW, H <sub>2</sub> O <sub>2</sub>	10	27	26	1	2.665	0.013	3
HRT, 10 gpm, 10 ppm M	10	15	12	3	5.853	0.103	6
HRT, 5 gpm, 10 ppm M	5	17	9	8	4.302	0.014	4
HRT, 10 gpm, 10 ppm M	10	21	18	3	5.295	0.591	5
HRT, 10 gpm, 20 ppm M	10	22	19	3	9.020	2.087	7
HRT, 10 gpm, 20 ppm M	10	24	21	3	9.883	2.405	7
Performance Test after Acid Wash	6	19	17	2	5.899	0.004	6
Performance Test after Acid Wash	6	18	14	4	5.568	0.033	6
Performance Test after Acid Wash	6	16	9	7	9.184	0.007	9
Tol + MTBE ~ 12 mg/L	6	23	13	10	11.403	0.016	11
Effect of Toluene	6	25	22	3	17.208	1.545	16
Effect of Toluene	6	36	33	3	20.087	4.015	16
Effect of Toluene	6	15	15	0	8.306	0.113	8
Effect of pH and Iron	6	24	25	-1	12.715	0.835	12
Effect of pH and Iron	6	17	11	6	4.071	0.050	4
Effect of pH and Iron	6	20	13	7	3.981	0.017	4
Base Run, Without H <sub>2</sub> O <sub>2</sub>	6	20	17	3	9.036	3.934	5

Table 4-12. The Range and Average of E<sub>90</sub> for MTBE, DIPE, and BTEX

Components	E <sub>90</sub> (kWh/1000 gal/90% compound degradation)		
	Low	High	Average
MTBE	20	79	36
DIPE	7	62	31
Benzene	5	41	27
Toluene	6	38	20
o-Xylene	11	45	26
p,m-Xylene	6	60	20
Ethyl Benzene	11	51	23

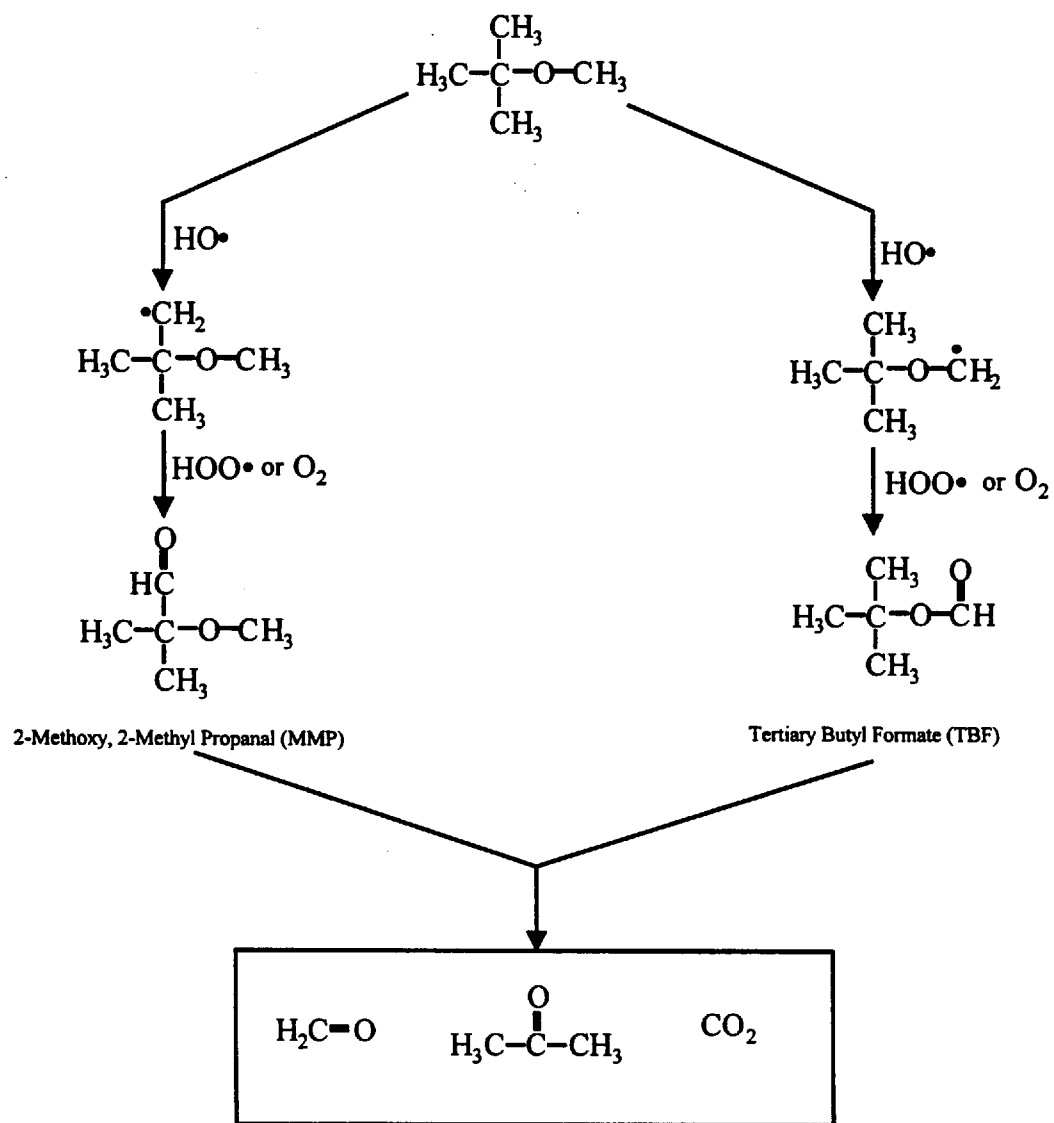


Figure 4-1. Hypothetical pathways of MTBE degradation by hydroxyl free radical chain reactions

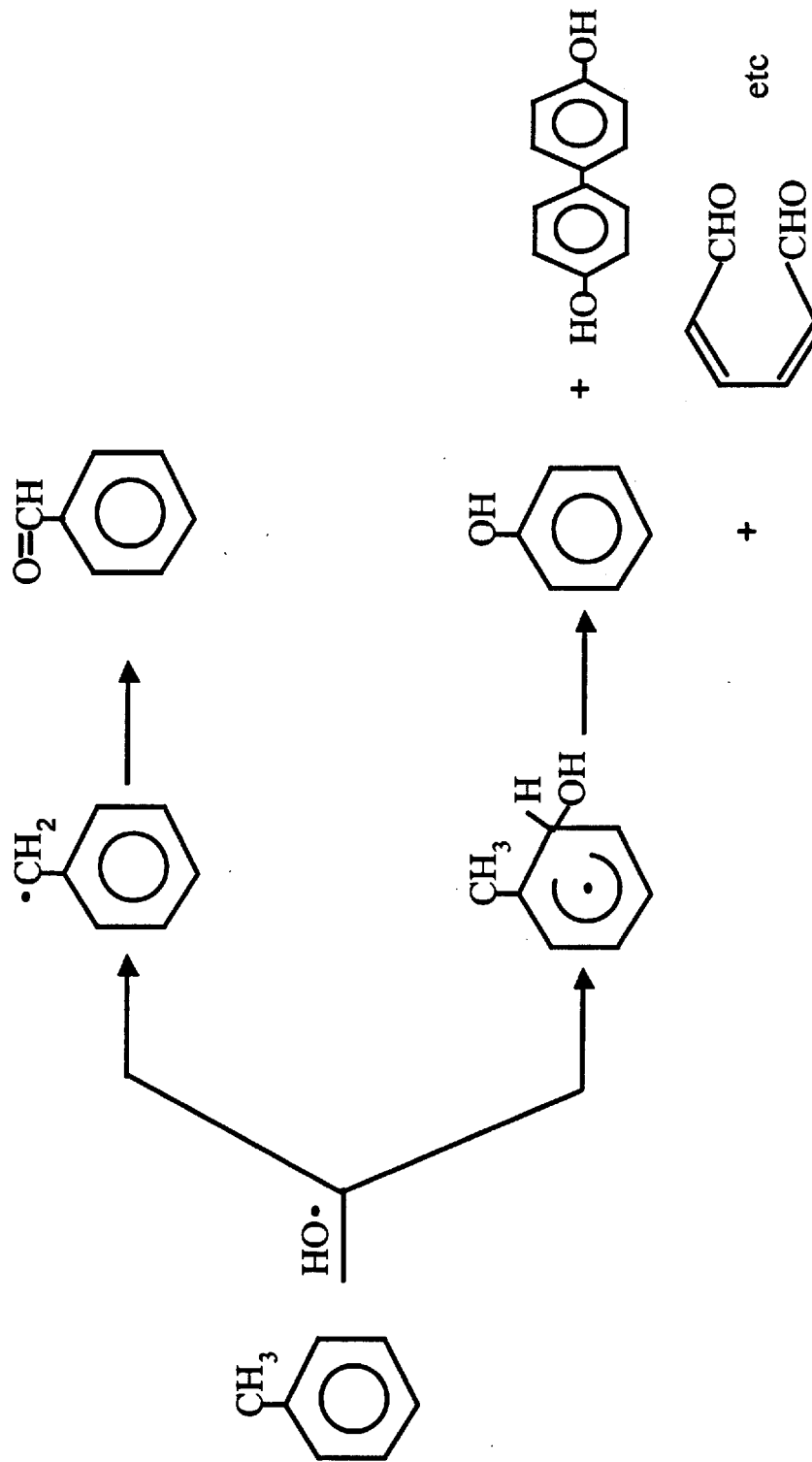


Figure 4-2. Hypothetical pathways of toluene degradation by hydroxyl free radical attack

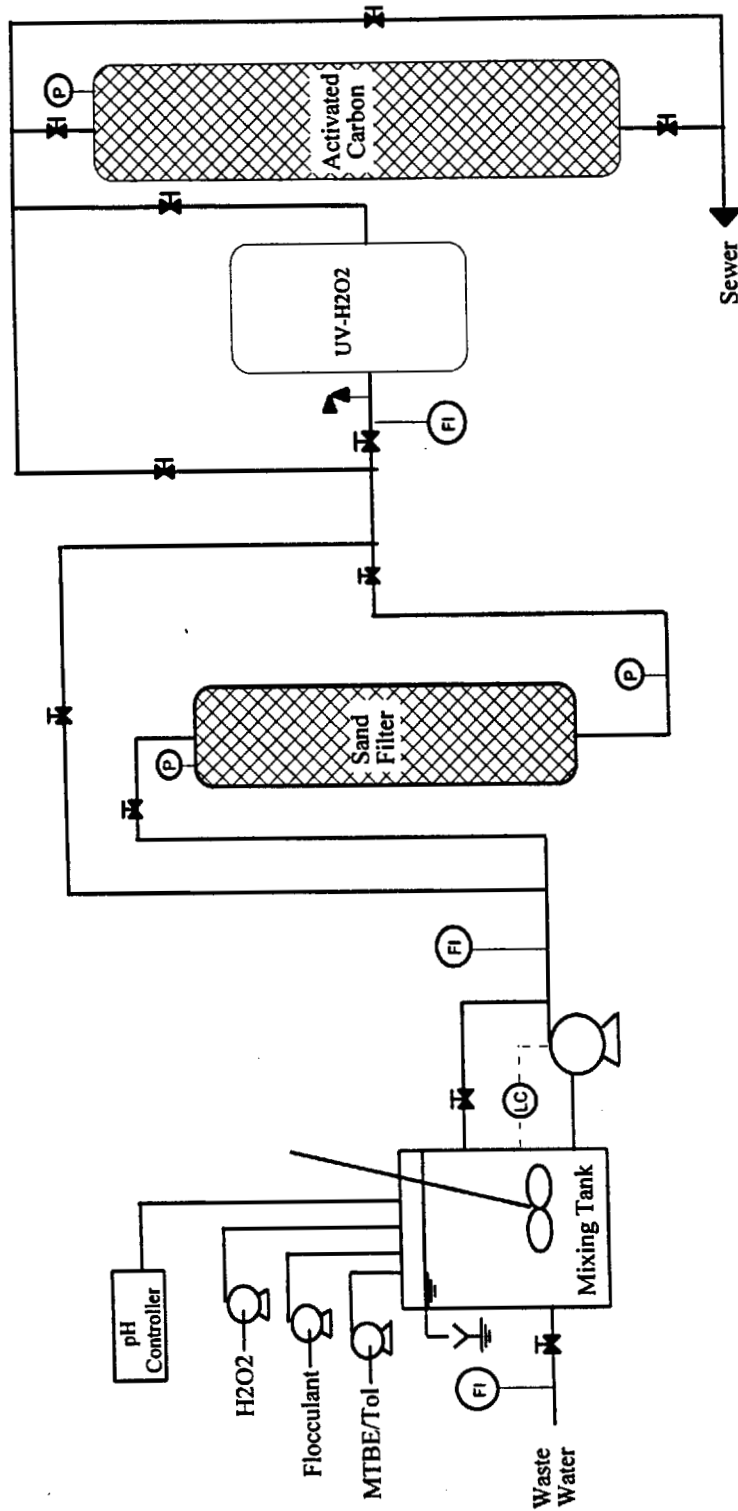


Figure 4-3. Flow diagram for the UV-H<sub>2</sub>O<sub>2</sub> groundwater treatment process

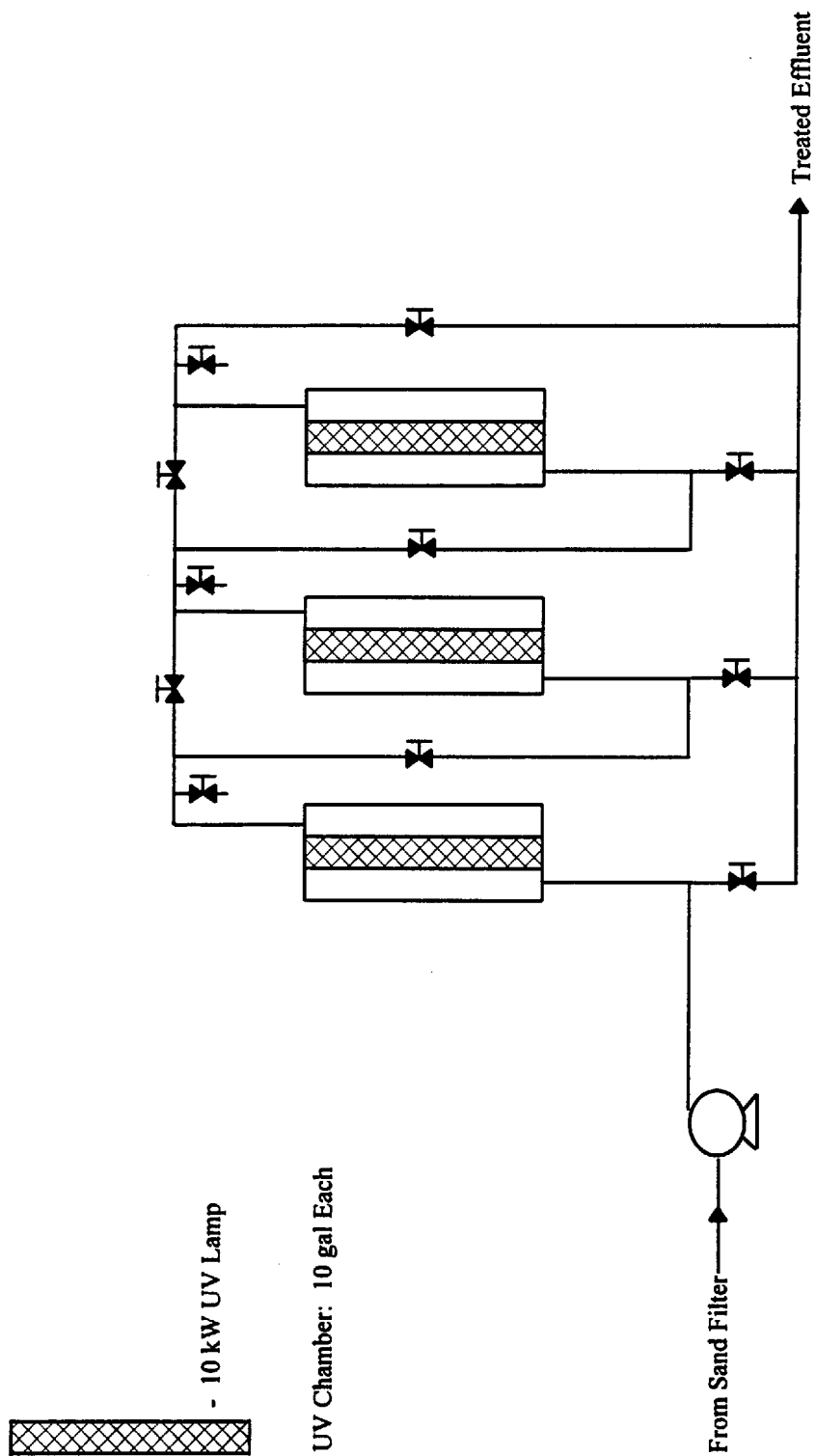


Figure 4-4. Flow diagram for the UV-H<sub>2</sub>O<sub>2</sub> equipment

Photolysis of H<sub>2</sub>O<sub>2</sub> by UV in the Test Equipment

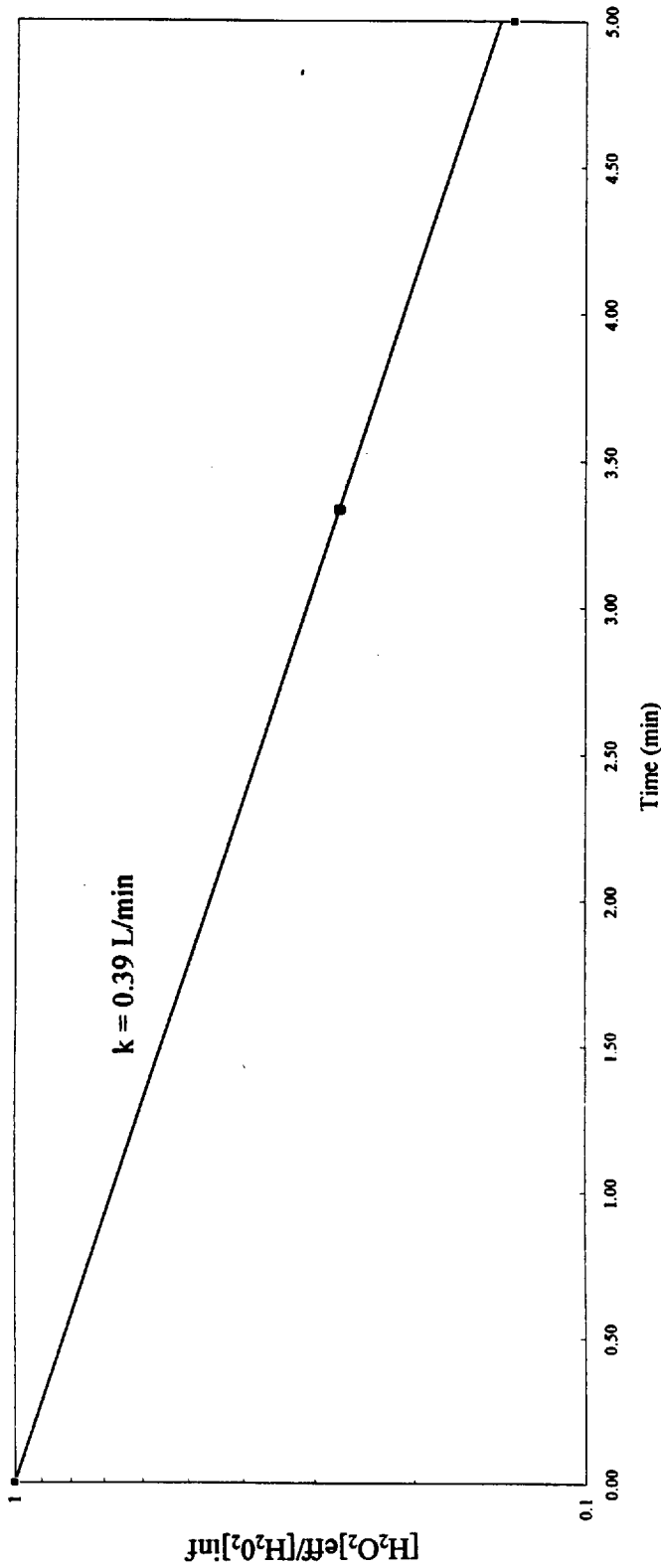


Figure 4-5. Photolysis of H<sub>2</sub>O<sub>2</sub> by UV in the test photoreactor

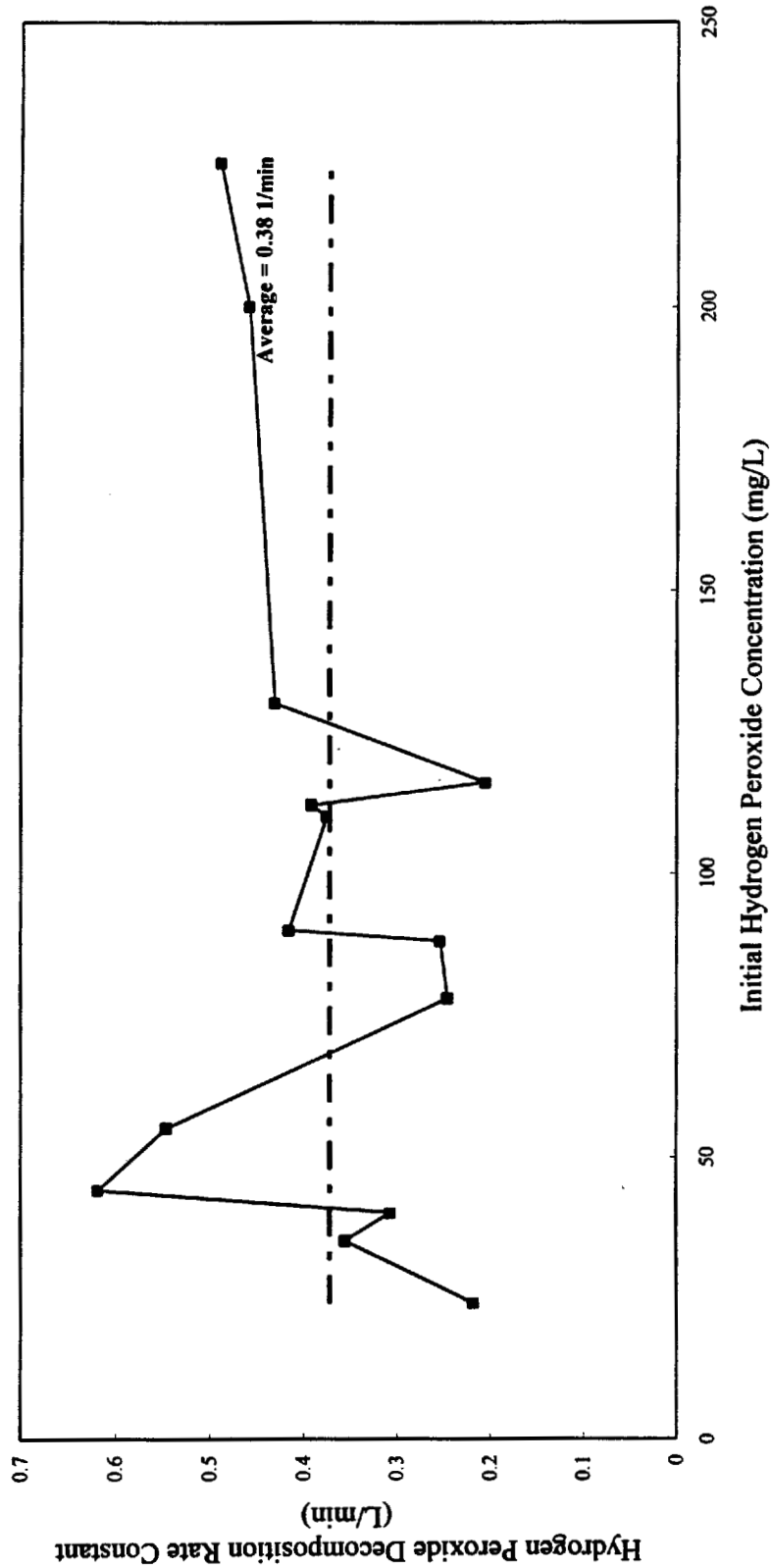


Figure 4-6. Rate constant of H<sub>2</sub>O<sub>2</sub> photodegradation by UV irradiation in the presence of organic contaminants

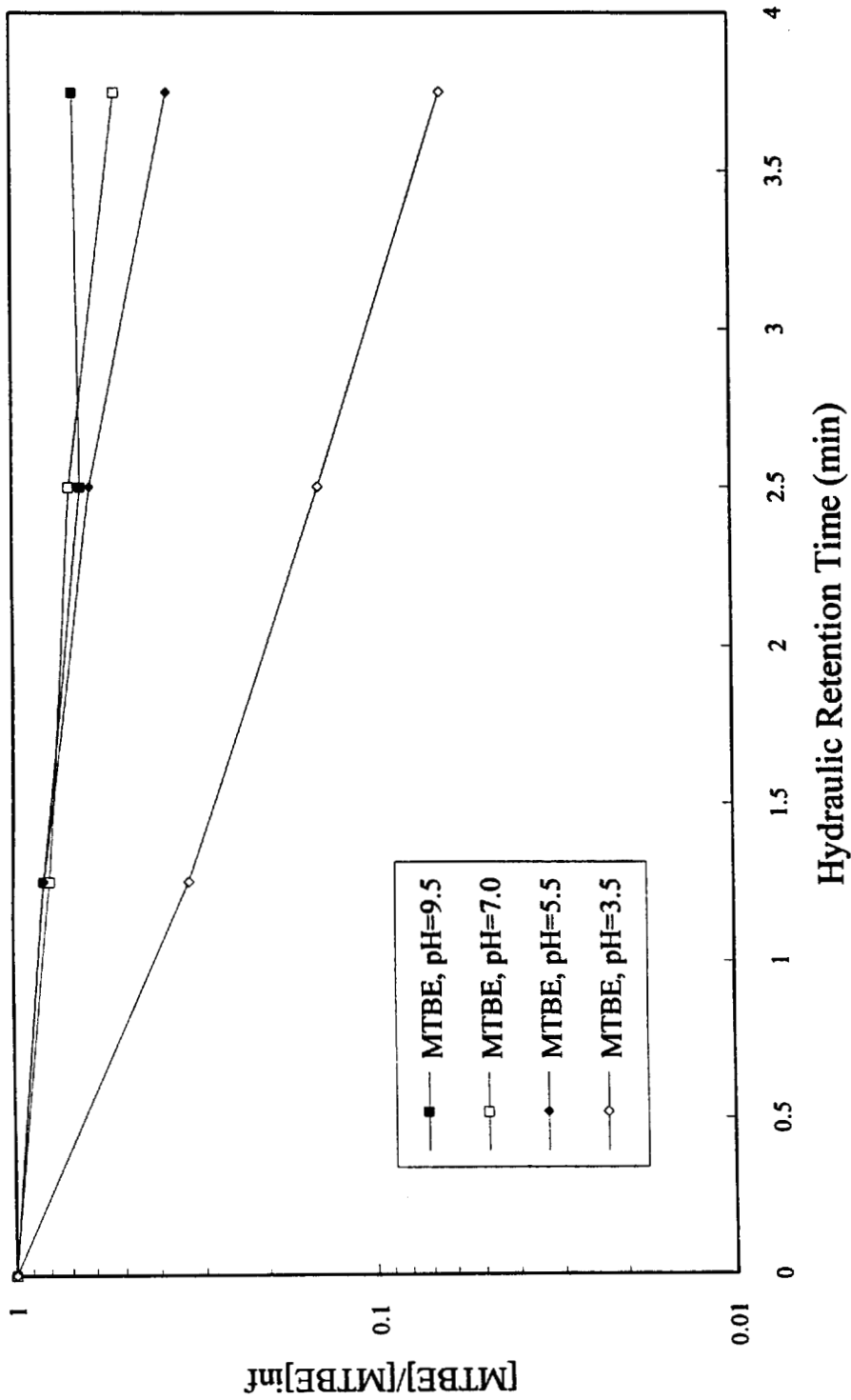


Figure 4-7. Degradation of MTBE by the UV-H<sub>2</sub>O<sub>2</sub> process under different pH conditions

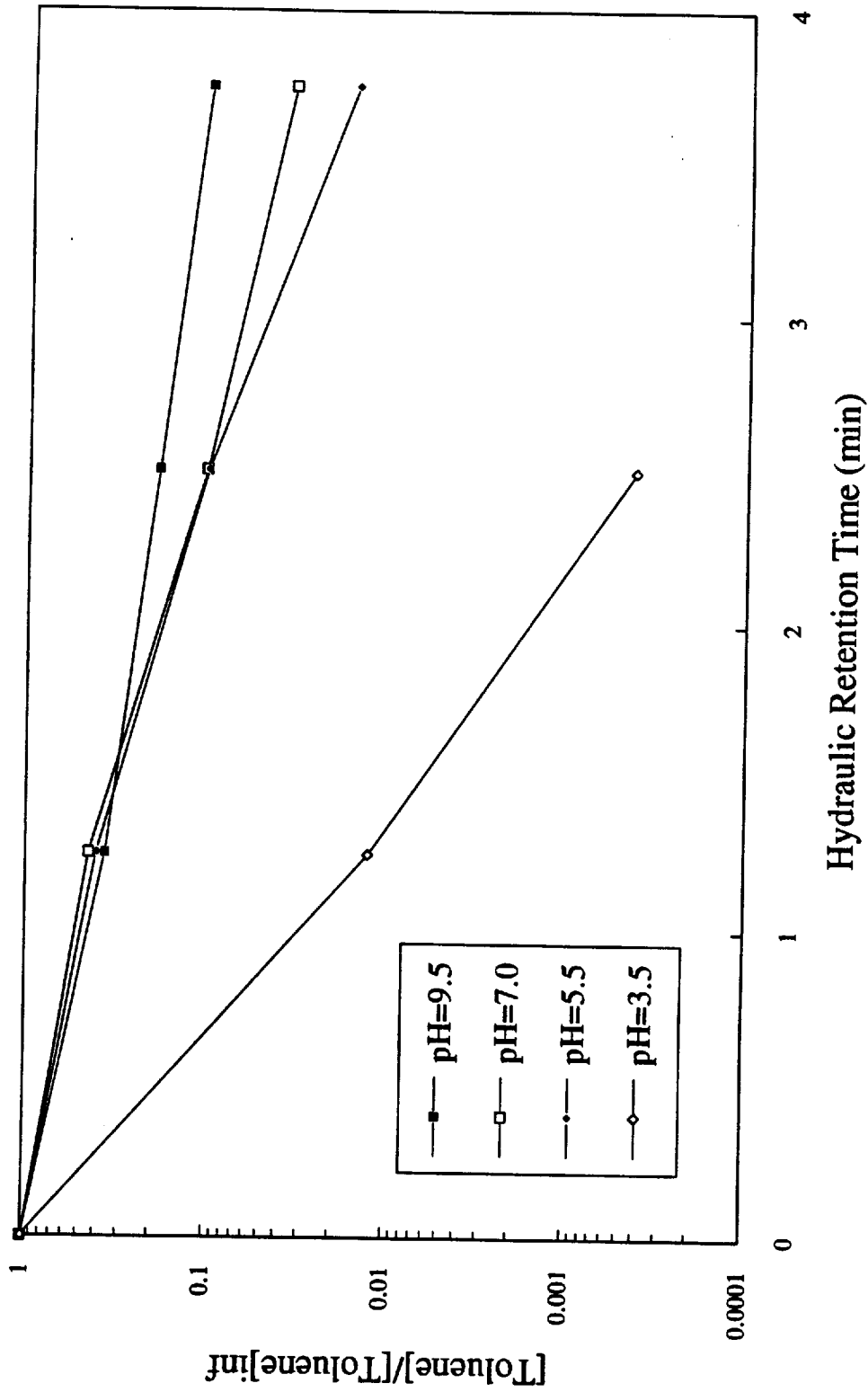


Figure 4-8. Degradation of toluene by the UV-H<sub>2</sub>O<sub>2</sub> process under different pH conditions

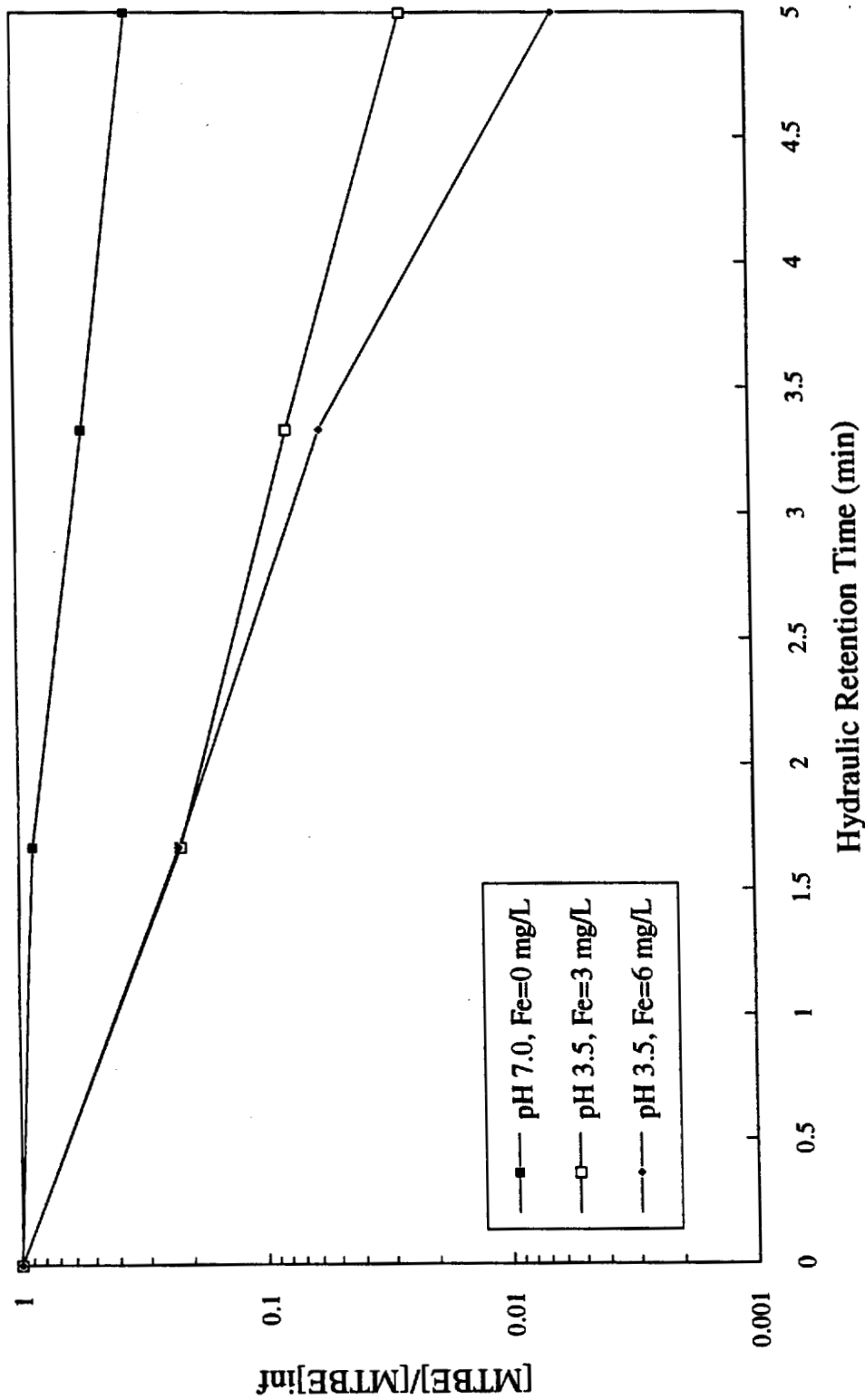


Figure 4-9. Effects of pH and soluble iron concentration on MTBE degradation in the UV-H<sub>2</sub>O<sub>2</sub> process

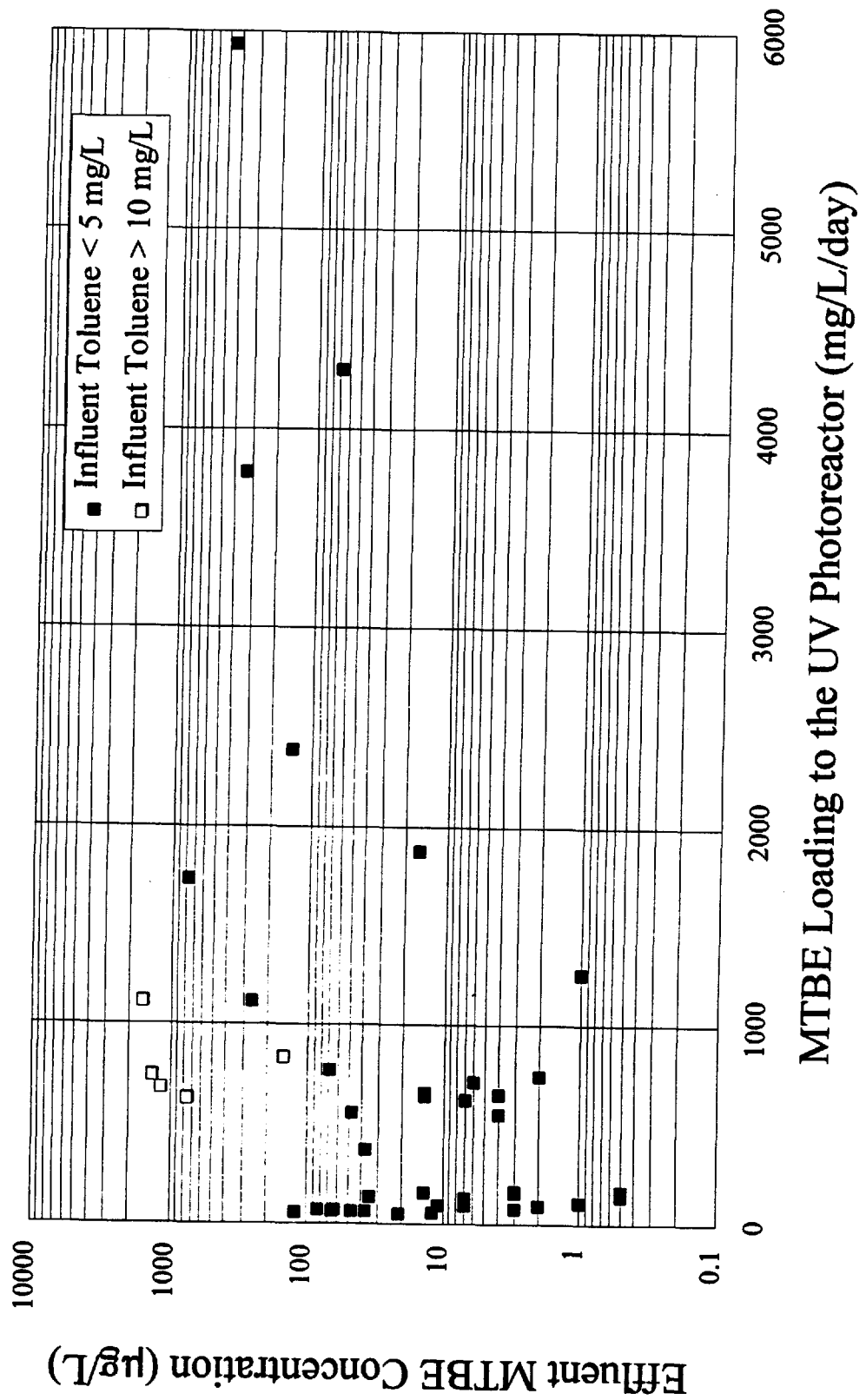


Figure 4-10. Summary of the effluent MTBE concentration in the pilot UV-H<sub>2</sub>O<sub>2</sub> unit under different MTBE loading conditions

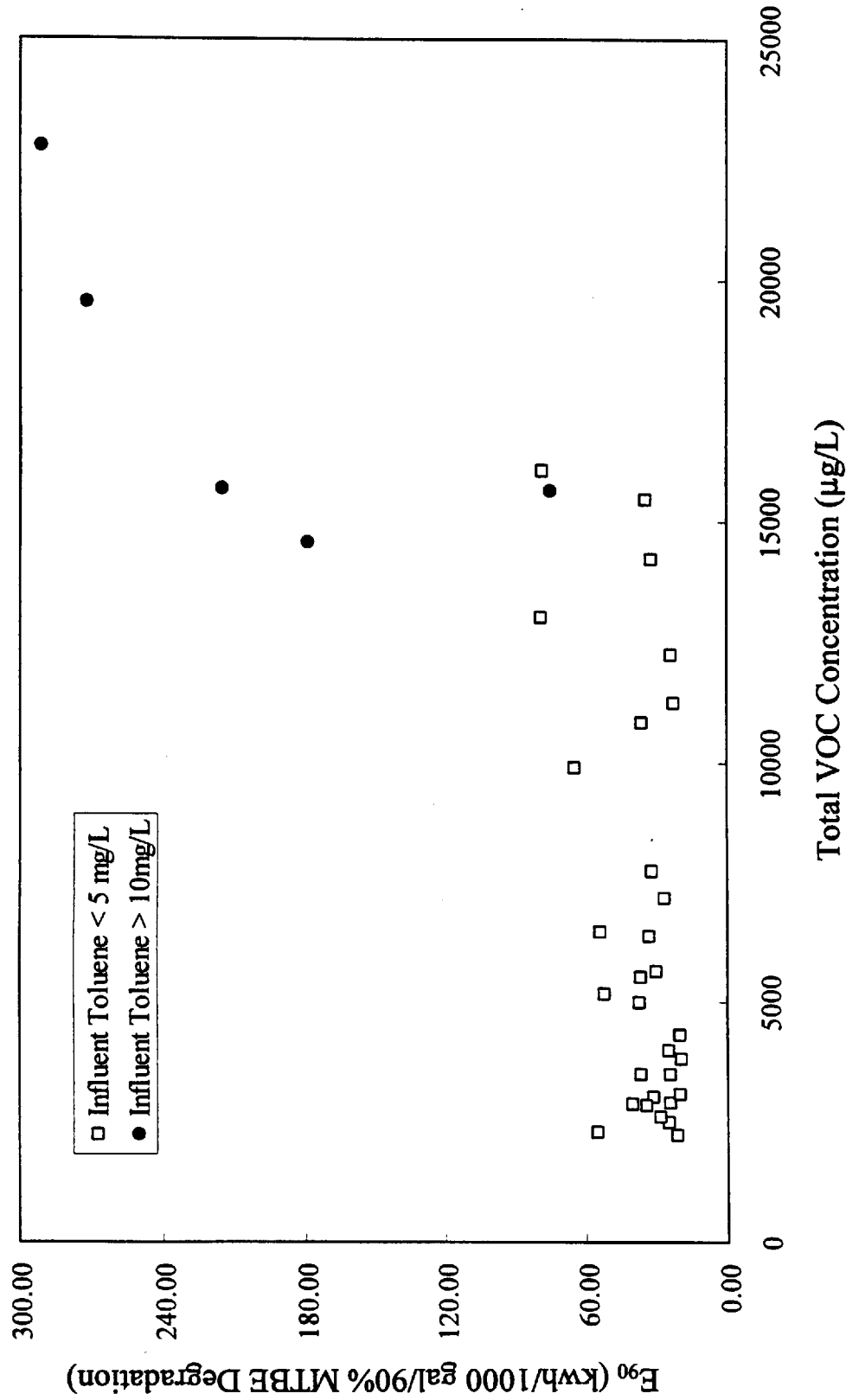


Figure 4-11. Summary of the effects of total VOC concentration in the feed on the E<sub>90</sub> for MTBE

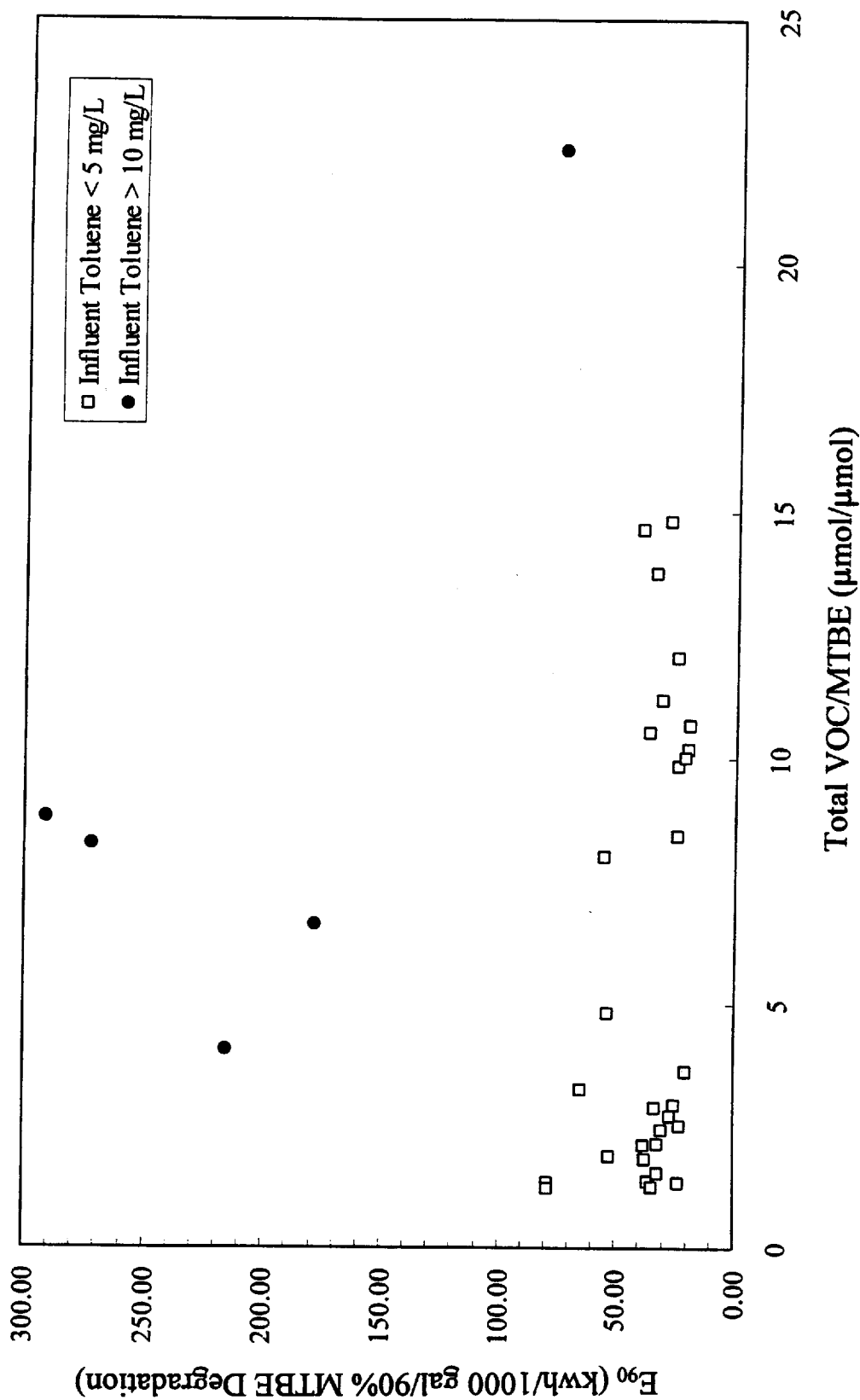


Figure 4-12. The effects of molar ratio of total VOC to MTBE in the feed on the E<sub>90</sub> of MTBE

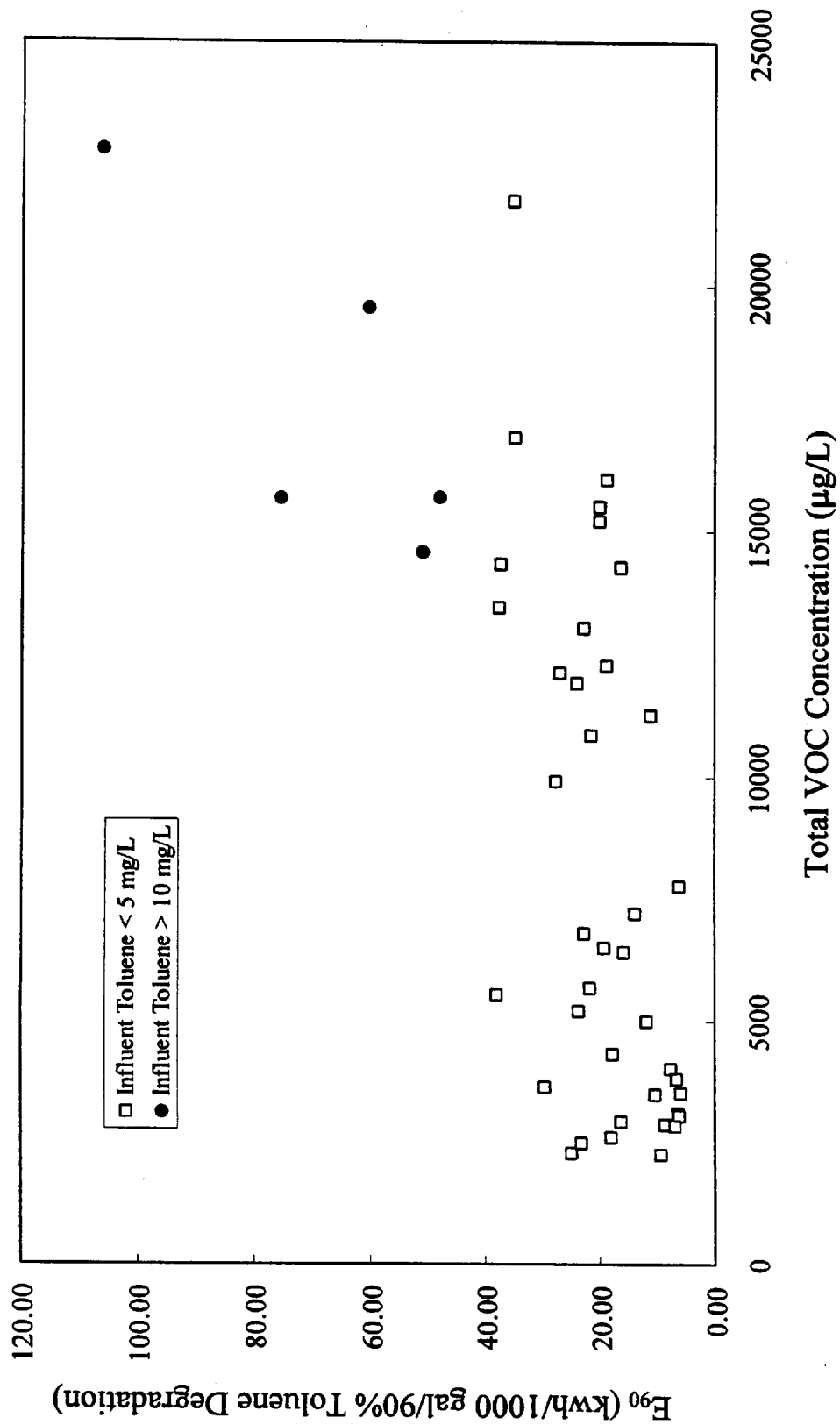


Figure 4-13. The effects of total VOC concentration in the feed on the E<sub>90</sub> of toluene

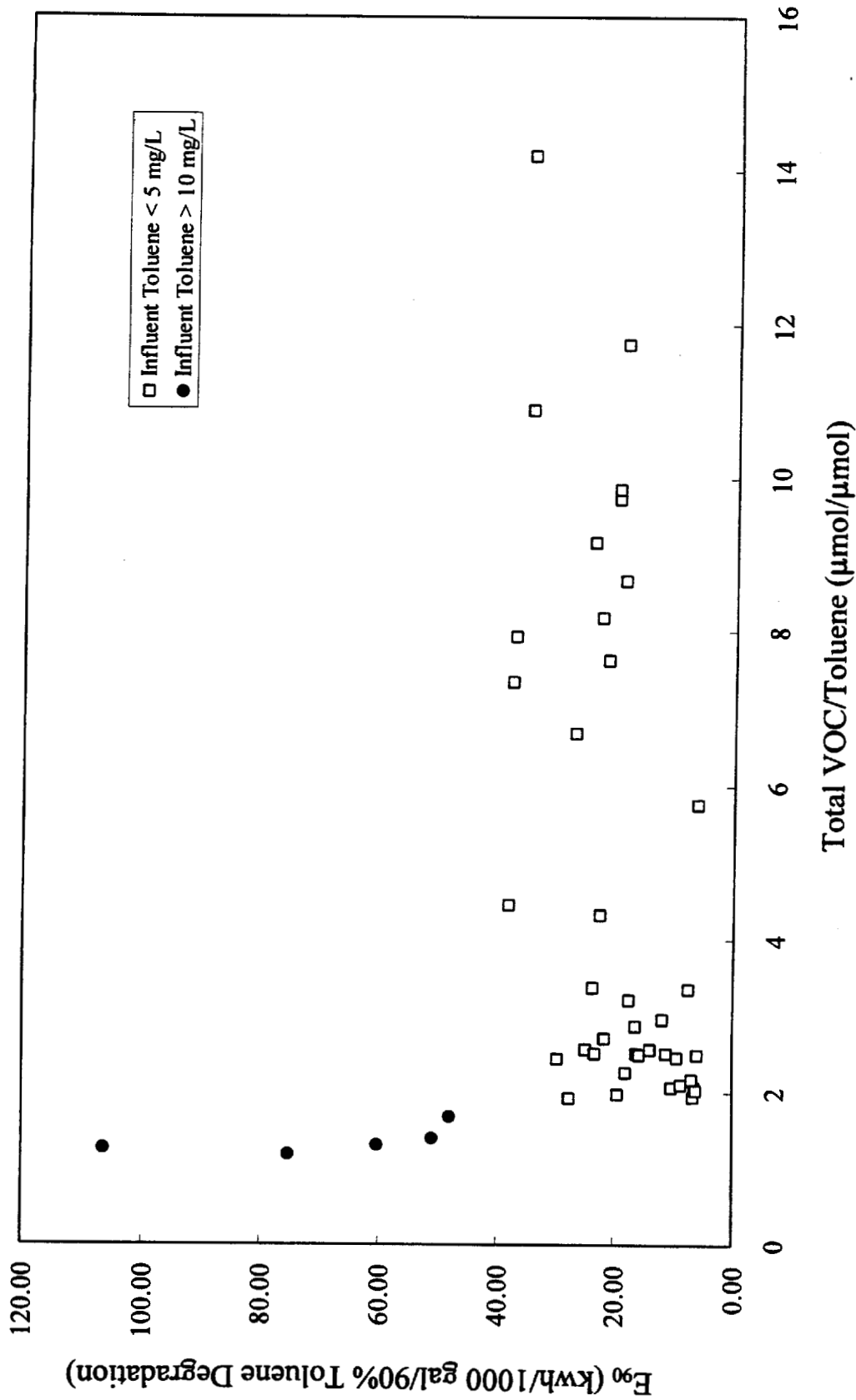


Figure 4-14. The effects of molar ratio of total VOC to toluene in the feed on the  $E_{90}$  of toluene

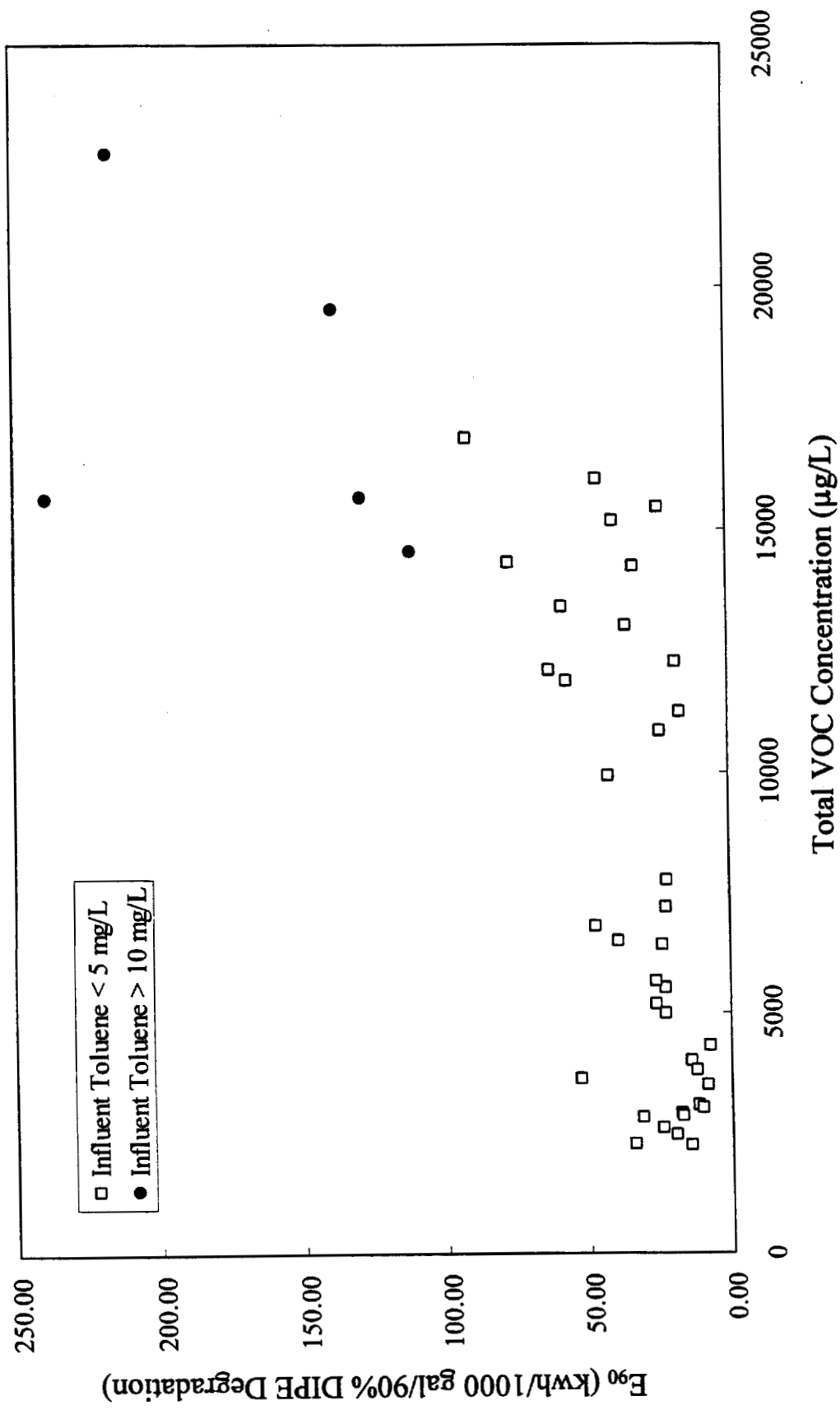


Figure 4-15. The effects of total VOC concentration in the feed on the E<sub>90</sub> for DIPE

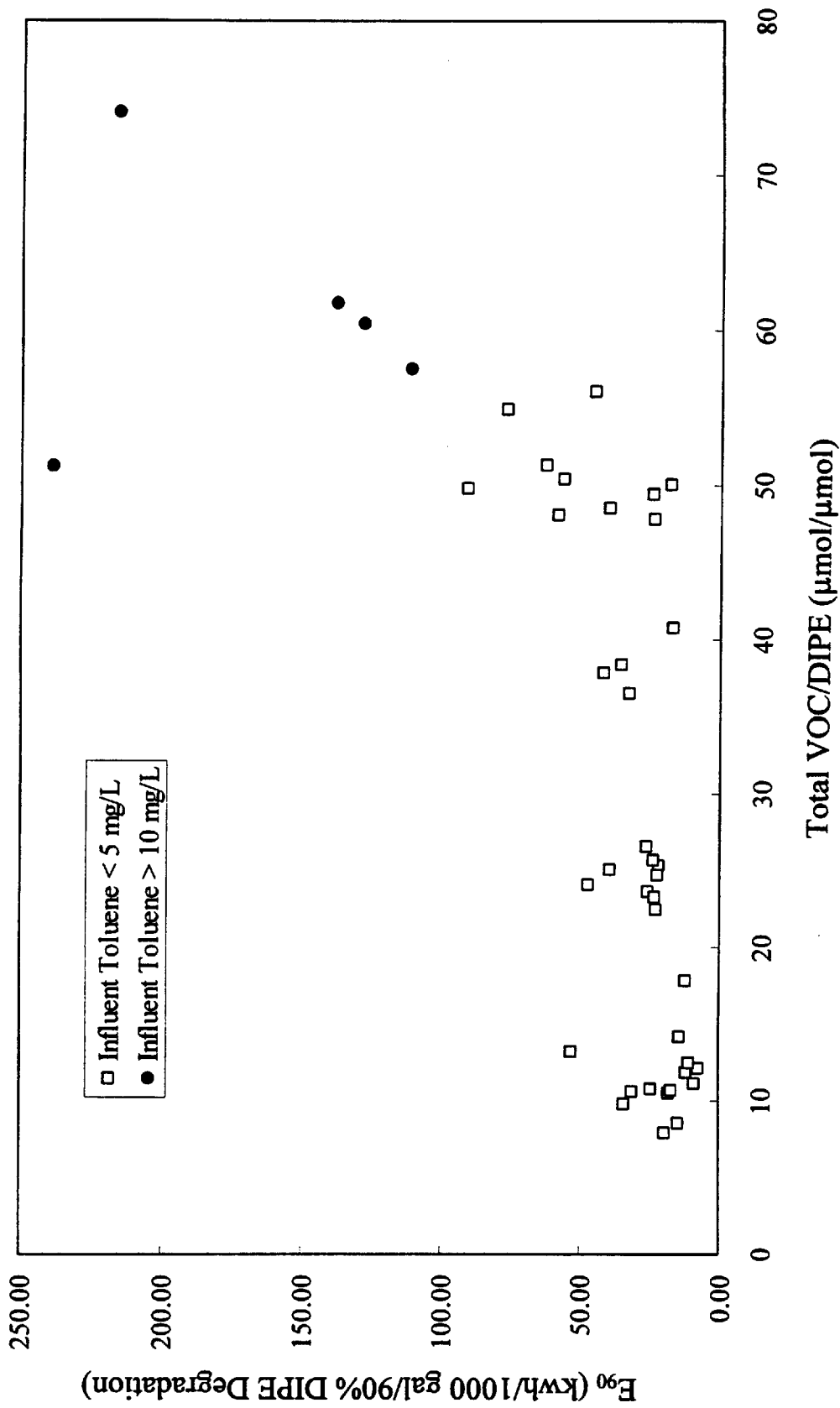


Figure 4-16. The effects of molar ratio of total VOC to DIPE in the feed on the  $E_{90}$  of DIPE

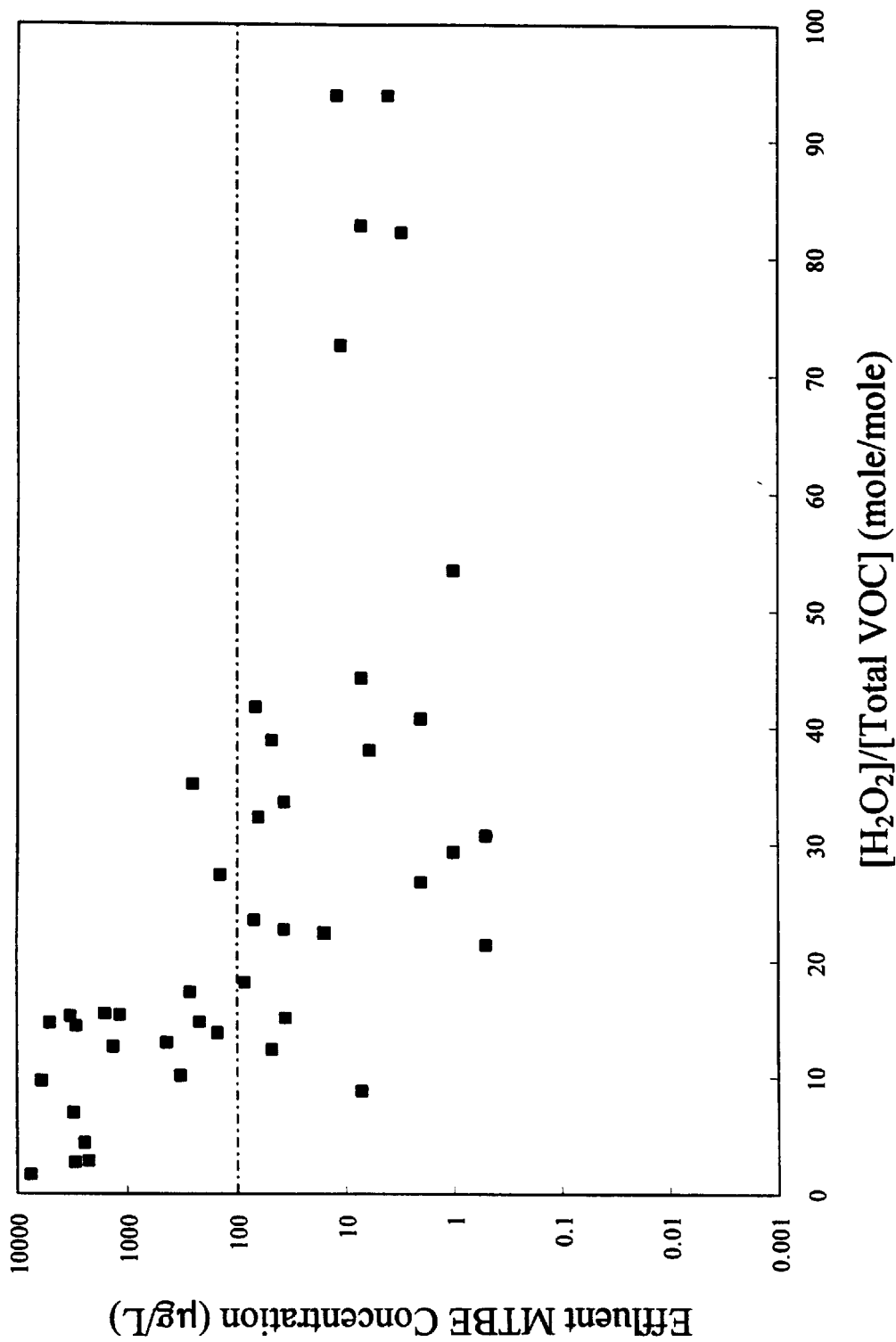


Figure 4-17. Effluent MTBE concentration and the molar ratio of H<sub>2</sub>O<sub>2</sub> to total VOC

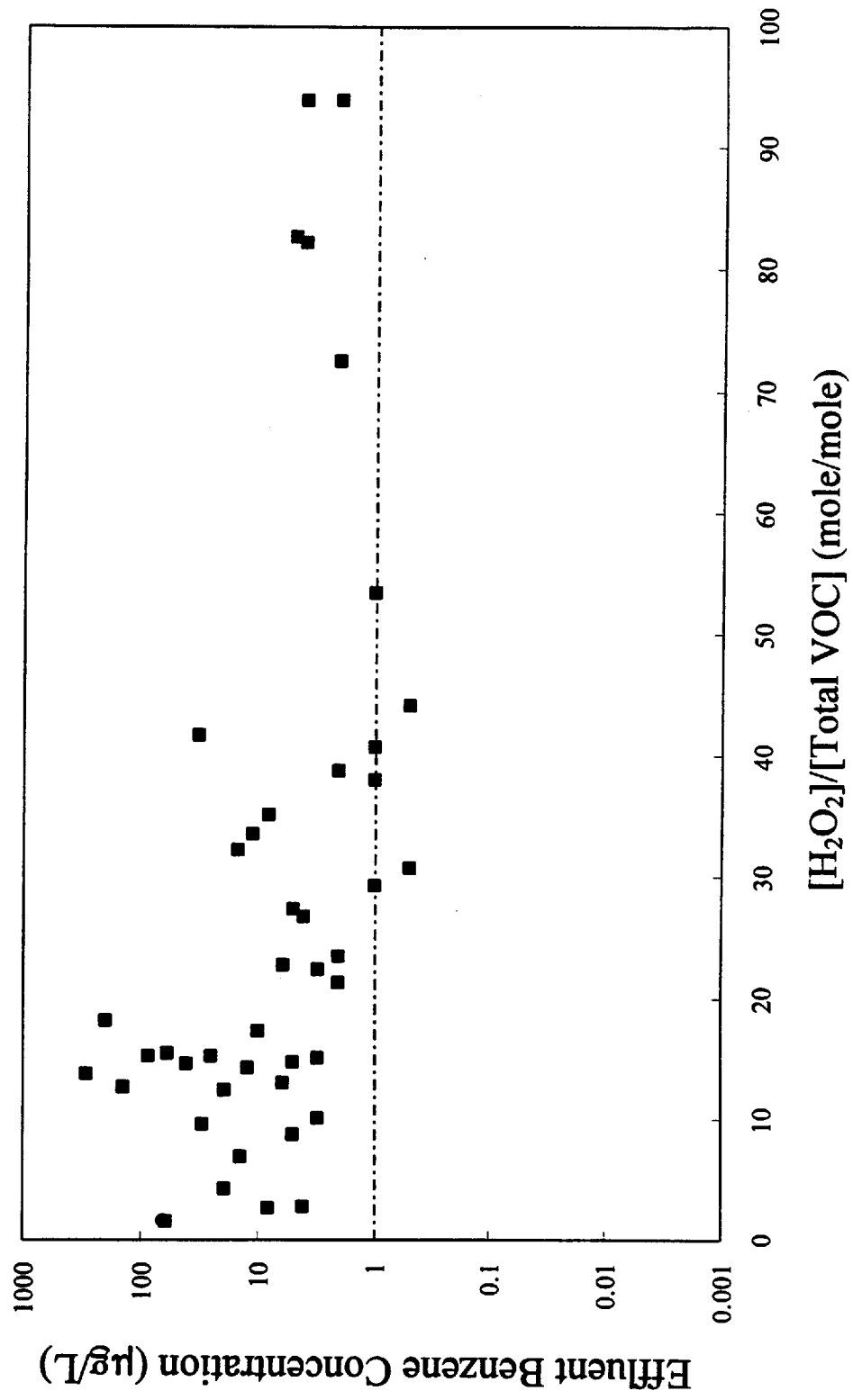


Figure 4-18. Effluent benzene concentration and the molar ratio of H<sub>2</sub>O<sub>2</sub> to total VOC

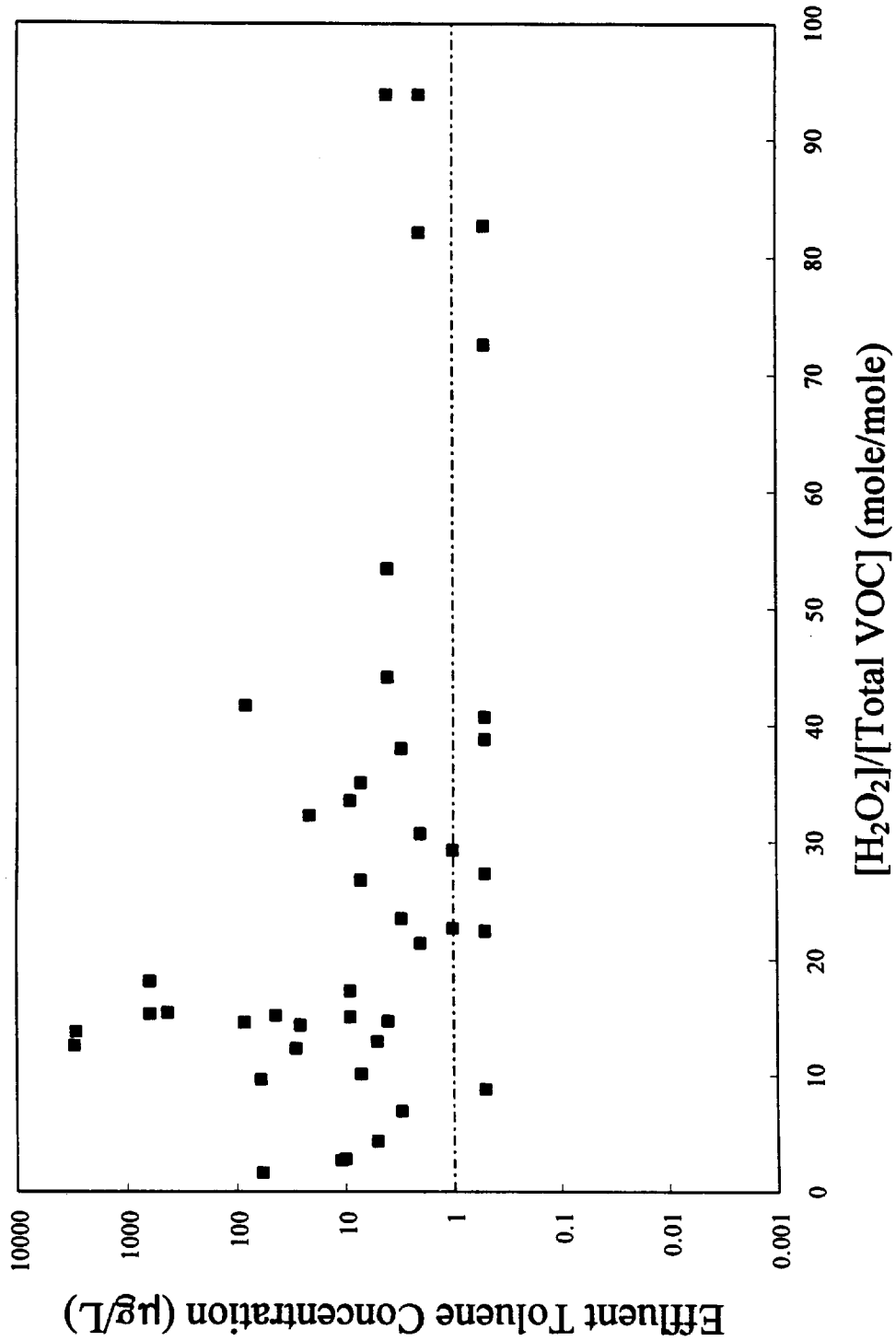


Figure 4-19. Effluent toluene concentration and the molar ratio of H<sub>2</sub>O<sub>2</sub> to total VOC

## REFERENCES

Atkinson, R. 1986. Kinetics and Mechanisms of the Gas-Phase Reactions of the Hydroxyl Radical with Organic Compounds under Atmospheric Conditions. *Chem. Rev.* 86:69-201.

Bear, G. R., I. Dzidic, W. T. Tang, S. C. Wallace, K. K. Angel, M. D. Balicki, J. J. Gentempo. 1989. Identification of MTBE and DIPE Oxidation Byproducts. Research Summary, Shell Development Company, Houston, Texas.

Fenton, H. J. H. 1894. Oxidation of Tartaric Acid in Presence of Iron. *J. Chem. Soc.* 65:899-910.

Hoigne, J, and H. Bader. 1979. Ozonation of Water: Oxidation-Competition Values of Different Types of Waters Used in Switzerland. *Ozone: Sci. Eng.* 1:357-372.

IT Corporation. 1991. Cost-Effective, Alternative Treatment Technologies for Reducing the Concentrations of Methyl Tertiary Butyl Ether and Methanol in Groundwater. API Publication #4497, American Petroleum Institute. Washington, D. C.

Japar, S. M., T. J. Wallington, J. F. O. Richert, and J. C. Ball. 1990. The Atmospheric Chemistry of Oxygenated Fuel Additives: t-Butyl Alcohol, Dimethyl Ether, and Methyl t-Butyl Ether. *International J. Chem. Kinetics.* (22) 1257-1269.

Kenley, R. A., J. E. Davenport, and D. G. Hendry. 1978. Hydroxyl Radical Reactions in the Gas Phase. Products and Pathways for the Reaction of OH with Toluene. *J. Phys. Chem.* 82:1095-1096.

Landi, V. R. and L. J. Heidt. 1969. Flash Photolysis Study of the Mechanism of Ozonide Ion Decay in Basic Aqueous Hydrogen Peroxide. *J. Phys. Chem.* 73:2361-2367.

Nicole, I., J. De Laat, M. Dore, J. P. Duguet et C. Bonnel. 1990. Utilization of U.V. Radiation in Water Treatment: Measurement of Photonic Flux by Hydrogen Peroxide Actinometry. *Water Research*. (24) 157-168.

Ogata, Y., K. Tomizawa, and K. Furuta. 1983. Photochemistry and Radiation Chemistry of Peroxides. In *The Chemistry of Peroxides*. Ed. Saul Patai. John Wiley & Sons. New York.

Ross, F., and a. B. Ross. 1977. Selective Specific Rates of Reactions of Transients from Water in Aqueous Solutions. III. Hydroxyl Radical and Perhydroxyl Radical and Their Radical Ions. U. S. National Standard Reference Data Service, National Bureau of Standards. Washington, D. C.

Salanitro, J. P., L. A. Diaz, M. P. Williams, and H. L. Wisniewski. 1994. Isolation of a Bacterial Culture That Degrades Methyl t-Butyl Ether. *Applied and Environmental Microbiology*. 60(7):2593-2596.

Standard Methods for the Examination of Water and Wastewater. 1985. 16th Edition. American Public Health Association. Washington, D. C.

Staelin, J. and J. Hoigne. 1982. Decomposition of Ozone in Water: Rate of Initiation by Hydroxide Ions and Hydrogen Peroxide. *Environ. Sci. Technol.* 16:676-681.

Sun, P. T. and J. P. Salanitro. 1994. Aerobic Biodegradation of MTBE - A Microbial Physiological and Kinetics Evaluation. Petroleum Environmental Research Forum Project 90-10.

Tang, W. T. and M. E. Wilcox. 1990. Stoichiometry and Kinetics of Benzene, Toluene, Xylene, and MTBE Degradation by H<sub>2</sub>O<sub>2</sub> and ozone. Research Summary, Shell Development Company. Houston, Texas.

Tang, W. T. and M. E. Wilcox. 1993. MTBE Biodegradation in Laboratory Scale Fluidized Bed Biological Reactors. Unpublished Results. Shell Development Company. Houston. Texas.

U.S. Environmental Protection Agency. 1982. Methods for Organic Chemical Analysis of Municipal and Industrial Wastewater, James Longbottom and James Lichtenberg, eds, EPA 600/4-82-057, July 1982.

Young, D. C., J. F. Hall, and B. V. Klock 1993. Evaluation of Technologies for the Treatment of Petroleum Product Marketing Terminal Wastewater. API Publication #4581, American Petroleum Institute. Washington, D. C.

Walling, C. 1975. Fenton's Reagent Revisited. *Acc. Chem. Res.* 8:125-131.

Walling, C., and R. A. Johnson. 1975. Fenton's Reagent. V. Hydroxylation and Side-Chain Cleavage of Aromatics. *J. Amer. Chem. Soc.* (97) 363-367.

Wells, C. H. J. 1972. Introduction to Molecular Photochemistry. Chapman and Hall Ltd. London, England.

Zepp, R. G., B. C. Faust, and J. Hoigne. 1992. Hydroxyl Radical Formation in Aqueous Reaction (pH 3-8) of Iron(II) with Hydrogen Peroxide: The Photo-Fenton Reaction. *Environ. Sci. Technol.* 26:313-319.

## APPENDICES

**Section 2 Appendices**

**FLUIDIZED BED BIOLOGICAL PROCESS**

Table A2-1. Monitoring data for the fluidized bed biological process

Date	Influent		Effluent		Influent		Effluent		Influent		Fluidization	Bed
	pH	pH	TEMP C	Temp C	DO PPM	DO PPM	Flow GPM	Flow GPM	Flow GPM	Flow GPM	Flow GPM	Height FT
2/2/94	6.56	6.78	14.6	13.5	7.8	4	0.9	31				7.5
2/3/94	6.6	6.74	14.7	14.6	6.2	4	0.9	31.8				7.5
2/4/94	6.8	6.59	15	14.6	6.6	3.9	1.1	31.8				7.5
2/5/94	6.7	6.66	14.8	14.7	6.5	4.1	1	30.5				7.5
2/6/94	6.49	6.69	15.2	15.4	6.2	3.9	1	30.6				7.5
2/7/94	6.77	6.85	15.4	15.7	5.5	4.1	0.9	30.6				
2/8/94	6.58	6.77	14.2	14.3	6.1	4.2	0.9	30.6				
2/9/94	6.78	6.78	13.4	11.8	6.8	4	0.9	31.9				7.5
2/10/94	6.66	6.88	13.8	9	6.6	3.7	1.3	31				
2/11/94	6.89	7.01	14.6	13.5	6.7	3.5	1.3	30.9				
2/12/94	6.78	6.78	15.2	14.8	6.4	3.9	1.4	30.3				7.5
2/13/94	6.78	6.78	12.9	13.4	6.6	4	1.3	30.3				7.5
2/14/94	6.57	6.67	13.4	13.2	5.9	4.1	1.3	30.3				
2/15/94	6.78	6.48	15.9	14.4	6.5	4	1.2	30.7				
2/16/94	6.78	6.5	14.6	14.6	6.4	4	0.9	30.1				7.5
2/17/94	6.77	6.54	14.8	14.7	6.4	4	0.9	30.1				
2/18/94	n/a	6.56	n/a	15.6	n/a	4	0.9	26.8				
2/19/94	n/a	6.48	n/a	17.1	n/a	3.4	0	26.8				
2/20/94	n/a	6.49	n/a	18.1	n/a	4	0	27.9				7.75
2/21/94	n/a	6.55	n/a	17.2	n/a	4	0	26.5				
2/22/94	n/a	6.61	n/a	14.5	n/a	4	0	29				
2/23/94	6.71	6.58	14.8	14.6	6	4	0.8	30.1				
2/24/94	6.66	6.65	15.1	14.8	6	4	0.9	30.1				7.75
2/25/94	6.68	6.56	14.5	14.7	6.4	4	0.9	30.1				
3/2/94	6.7	6.65	14.7	15.6	6.7	3.4	0.9	30.1				7.75
3/3/94	6.66	6.64	14.8	15.4	6.8	4.1	0.9	30.1				
3/4/94	6.68	6.62	14.3	15.6	6.8	3.6	1.1	30.1				7.75
3/5/94	6.73	6.6	14.8	16.7	7.3	3.3	1.1	30.1				
3/6/94	n/a	6.78	n/a	18	n/a	4	0	17.8				6.75
3/7/94	n/a	6.88	n/a	16.8	n/a	4.3	0	18.9				
3/8/94	6.71	6.81	16.8	17.1	6.8	3.7	1.4	25.6				7.3
3/9/94	6.77	6.74	14.8	16.7	7.2	4.1	1.2	29.2				
3/10/94	6.76	6.68	14.8	15	6.9	3.5	1.2	29.2				7.75
3/11/94	6.78	6.9	14.8	14.3	6.7	3.7	1.2	29.2				
3/12/94	6.8	7.01	14.5	13.9	6.6	4.1	1.2	29.2				
3/13/94	6.8	6.87	14.9	13.8	6.9	3.7	1.2	29.4				7.75
3/14/94	6.8	6.77	14.6	16.2	7.3	3.9	1.2	29.6				
3/15/94	6.8	6.81	14.5	16.5	7	3.7	1.1	29.4				8
3/16/94	6.78	6.71	14.2	14.2	7.1	3.8	1.1	29.2				
3/17/94	6.8	6.77	14.9	11.9	6.3	3.9	1	30.1				8
3/18/94	6.81	6.54	14.9	12.9	7.1	3.9	1.1	30				

A-1

Table A2-1. Monitoring data for the fluidized bed biological process (Continued)

Date	Influent Effluent		TEMP		DO		Influent	Fluidization	Bed
	pH	pH	C	C	PPM	PPM	Flow GPM	Flow GPM	Height FT
3/19/94	6.82	6.78	14.5	12.3	6.4	3.7	1	30	8
3/20/94	n/a	n/a	n/a	n/a	n/a	n/a	n/a	n/a	n/a
3/21/94	6.9	6.65	13.5	15.8	7	3.9	1	30	
3/22/94	6.82	6.78	14.6	16.1	7.1	3.8	1	30	
3/23/94	6.79	6.88	14.3	15.6	6.6	4.1	1.1	30	8
3/24/94	6.78	6.9	14.5	16.7	6.8	3.3	1.1	30	
3/25/94	6.78	6.89	14.6	16.4	7.4	3.8	1	30	8
3/26/94	6.74	6.89	14.6	15.6	7.2	3.9	1.2	30	
3/27/94	6.89	6.88	14.6	15.8	7.1	4.1	1	30	
3/28/94	6.88	6.79	14.5	16.1	7	3.8	1.2	30	
3/29/94	6.68	6.69	14.8	15.6	6.8	3.7	1	30	8
3/30/94	n/a	n/a	n/a	n/a	7	3.8	1.4	30	
3/31/94	n/a	n/a	n/a	n/a	6.9	4	1.2	30	
4/1/94	7.03	6.82	15.8	16.8	5.9	4.1	1.1	30	
4/2/94	No Influent flow								
4/3/94	No Influent flow								
4/4/94	No Influent flow								
4/7/94	6.78	7.11	14.5	17.6		4	1.4	30	
4/8/94	6.68	7.01	14.7	13.8	7.5	3.8	1.5	30	8.25
4/9/94	6.78	6.89	14.8	15.6	7.4	3.7	1	30.1	
4/10/94	6.89	6.71	14.6	15.4	6.8	3.9	0.9	30.1	8.5
4/11/94	6.89	6.65	14.8	15.5	7.2	3.8	0.9	30.1	
4/12/94	6.88	6.69	14.9	15.8	6.5	4.1	1	30.1	
4/13/94	6.89	7.01	13.8	17.6	6.7	3.8	1	30	
4/14/94	No influent flow; pipe damaged								
4/15/94	6.87	7.12	14.7	19.5	6.8	4	1.1	30	
4/16/94	6.88	7.23	14.7	20.4	6.8	4	1	30	
4/17/94	6.85	7.43	14.7	22.5	6.7	3.4	1.2	30	
4/18/94	6.78	7.45	14.4	20	7.2	4	1.1	30	
4/19/94	6.87	7.23	14.8	20.5	6.9	3.7	1	30	8.5
4/20/94	6.89	7.21	14.5	19.6	6.8	3.5	1	30	
4/21/94	6.92	7.14	14.6	18.9	6.4	4	1.1	30	
4/22/94	6.91	7.01	14.8	17.6	6.5	3.8	1.1	29.5	8.7
4/23/94	6.99	7.11	14.3	19.9	6.7	4	1	30	
4/24/94	6.98	7.09	14.4	23.2	6.7	3.9	1	30	
4/25/94	6.99	6.69	14.5	20.6	6.6	3.7	1	30	
4/26/94	7.01	6.96	14.5	18.6	6.5	4	2	30	
4/27/94	6.98	6.89	14.4	21.2	8	3.8	2	30.8	
4/28/94	6.97	6.74	14.4	17.1	8.2	3.8	2.2	30.7	
4/29/94	6.92	6.66	14.5	15.7	8.4	3.9	2	30.8	
4/30/94	7.06	6.75	14.5	16.4	8	4.1	2	30.2	

Table A2-1. Monitoring data for the fluidized bed biological process (Continued)

Date	Influent		Effluent		Influent		Effluent		Influent		Fluidization	Bed
	pH	pH	TEMP C	Temp C	DO PPM	DO PPM	Flow GPM	Flow GPM	Flow GPM	Flow GPM	Flow GPM	Height FT
5/1/94	7.1	6.77	14.7	16.5	8.2	3.9	2.1	30.2				
5/2/94	7.08	7.01	14.6	16.4	8.7	4.2	1.8	30.5				
5/3/94	7.01	6.68	14.5	16.8	8.1	3.9	2	30				9
5/4/94	6.89	6.69	14.6	17.5	8	3.8	2.1	30				
5/5/94	6.99	6.66	14.7	17.8	7.8	4	2	30.1				
5/6/94	6.87	6.78	14.8	17.6	8.1	3.8	2	30				9
5/7/94	6.89	6.8	14.5	17.9	8.1	3.6	2	30				
5/8/94	6.91	6.8	14.4	17.6	8.2	4	2	30				
5/9/94	6.91	6.8	14.1	17.6	8.5	4.1	2	30				
5/10/94	6.88	6.8	14.1	17.5	8.3	4	2	30				
5/11/94	6.87	6.8	14.4	17.8	8.4	3.9	2	30				
5/12/94	6.89	6.77	14.5	17.7	7.8	3.6	2	30				
5/13/94	6.89	6.78	13.7	17.6	7.9	3.6	3.5	30				9.25
5/15/94	6.89	6.77	14.3	18.2	8.5	4	3.5	30				
5/16/94	6.92	6.89	14.3	17.9	8.7	4	3.5	30				
5/17/94	6.89	6.81	14.1	16.8	9.2	3.7	3.5	30				
5/18/94	6.92	6.79	14.4	16.4	9.3	3.2	3.5	30				
5/19/94	6.89	6.88	14.4	16.4	10.1	3.6	3.5	30				
5/20/94	6.91	6.75	14.5	15.5	9.3	4	3.5	30				9.5
5/21/94	6.89	6.81	14.5	16.1	9.5	4	3.3	30				
5/22/94	6.81	6.82	14.3	15.9	10.3	3.8	3.4	30				
5/23/94	8.89	6.79	14.1	15.9	10.3	4	3.6	30				
5/24/94	6.88	6.82	14.2	16.1	10.9	3.8	3.5	30				9.75
5/25/94	6.89	6.89	14.1	16.5	10.8	3.9	3.5	30				
5/26/94	6.87	6.93	14.5	16.7	11.2	4	3.5	30				
5/27/94	6.88	6.92	14.3	17.2	10.5	3.8	3.5	30				
5/30/94	6.88	6.97	14.1	16.8	12.3	4	3.5	30				
5/31/94	6.89	7.09	14.3	16.7	13.4	3.7	3.5	30				9.8
6/1/94	6.89	7.03	14.3	17.8	14.2	3.8	3.4	30				
6/2/94	6.91	7.02	14.5	16.5	12.3	3.8	3.5	30				
6/3/94	6.89	6.94	14.1	16.7	13.2	3.7	3.5	30				9.8
6/4/94	6.89	7.04	14.3	16.8	11.9	3.8	3.5	30				
6/5/94	6.92	7.02	14.2	17	10.9	3.9	3.5	30				9.8
6/6/94	6.89	7.1	14.3	16.6	11.5	3.8	3.5	30				
6/7/94	6.91	6.99	14.2	18.9	12.3	3.8	3.5	30				
6/8/94	6.98	6.98	14.5	16.5	11.4	3.8	3.5	30				10
6/9/94	6.89	6.89	14.3	17.8	12.2	4	3.5	30				
6/10/94	6.92	6.89	14.3	17.4	10.5	3.9	3.5	30				
6/11/94	6.89	6.78	14.2	17.7	11.4	3.7	3.5	30				10
6/12/94	6.91	6.87	14.3	17.6	12.1	3.6	3.5	30				
6/13/94	7.01	6.79	14.2	17.6	14.4	4.2	3.5	30				10
6/14/94	7.01	6.89	14.4	18.1	14.1	4.1	3.4	30				9.75

Table A2-1. Monitoring data for the fluidized bed biological process (Continued)

Date	Influent Effluent		Influent	Effluent	Influent	Effluent	Influent	Fluidization	Bed
	pH	pH	TEMP C	Temp C	DO PPM	DO PPM	Flow GPM	Flow GPM	Height FT
6/15/94	7.08	6.72	14.3	18.6	12.6	3.8	3.4	30	
6/16/94	7.09	6.66	14.3	17.8	12.2	3.7	3.5	30	
6/17/94	7.01	7.02	14.2	17.6	11.8	4.2	3.6	30	10
6/18/94	6.98	6.98	14.3	17.8	11.1	3.8	3.4	30	
6/19/94	7.01	6.89	13.9	17.8	11.1	4	3.5	30	10
6/20/94	7.01	6.89	14.3	17.9	9.9	3.9	3.5	30	
6/21/94	6.95	6.88	14.8	17.8	10.6	3.9	3.5	30	10.25
6/22/94	6.98	6.94	14.5	17.6	12.2	3.9	3.5	30	
6/23/94	6.89	7.02	14.4	18	10.8	4	3.7	30	
6/24/94	7.01	7.11	14.6	17.6	9.8	3.7	3.6	30	10.25
6/25/94	6.99	7.05	14.5	17.7	11.2	3.6	3.5	30	
6/26/94	7.02	7.03	14.5	16.9	10.8	4	3.5	30	10.25
6/27/94	7.11	6.89	14.3	17.5	11.3	3.5	3.5	30	
6/28/94	7.02	6.88	14.4	17.2	10.9	3.7	3.4	30	
6/29/94	6.93	6.92	14.2	17.8	11.4	3.8	3.5	30	9.5
6/30/94	6.78	6.63	14.5	17.1	10.6	4	3.3	32	
7/5/94	6.88	6.93	14.2	17.6	10.6	3.4	3.5	30	
7/6/94	7.02	6.94	14.4	17.6	11	3.4	3.4	30	9.5
7/7/94	6.96	6.9	14.5	17.8	11.2	4	3.5	30	
7/8/94	6.89	6.78	14.1	18	11.5	3.8	3.5	32	
7/9/94	6.93	6.87	14.1	18.7	12.1	4	3.5	31	10
7/10/94	6.93	6.9	14.3	18.7	12.4	4.2	3.5	31	
7/11/94	7.02	6.89	14.2	18.8	12.3	3.7	3.6	30	
7/12/94	7.01	6.89	14.4	17.9	10.9	3.2	3.4	31	10
7/13/94	7.1	6.89	14.2	18.7	11.4	4	3.5	30	
7/14/94	6.9	6.9	14.3	17.8	12.1	4.1	3.5	31	10
7/15/94	7.01	6.95	14.2	17.6	12.2	3.7	3.6	30.9	10
7/16/94	6.93	6.78	14.9	18.6	12.5	4	3.5	30	
7/17/94	6.89	6.89	14.9	18.6	12.4	4	3.5	30.9	
7/18/94	6.93	7.2	14.8	18.9	11.2	3.8	3.4	30.9	10.25
7/19/94	6.89	7.01	15	17.9	11.5	3.6	3.6	30.9	
7/20/94	6.93	6.89	14.9	17.9	13.2	3.6	3.6	30.9	
7/21/94	6.89	6.88	14.8	18.6	12.5	3.3	3.4	30.9	10.3
7/24/94	7.01	6.89	14.7	17.8	10.4	4	3.6	29.9	10.25
7/25/94	6.92	6.9	15	18	12.1	4	3.6	30	
7/26/94	7.02	6.9	15	18.6	12.4	4	3.6	30	
7/27/94	7.03	6.78	14.7	18.7	13.4	4	3.5	30	10.25
7/28/94	6.9	6.92	15.1	18.9	13.4	3.6	3.6	30	
7/29/94	6.93	6.89	14.8	18.7	12.1	3.7	3.5	30	
7/31/94	7.05	6.97	14.6	16.8	11.5	3.8	3.6	30	
8/1/94	7.05	6.89	14.6	17.5	11.6	3.9	3.7	30	10.25
8/2/94	6.89	6.88	14.8	17.3	11.4	3.6	3.5	30	

Table A2-1. Monitoring data for the fluidized bed biological process (Continued)

Date	Influent		Effluent		Influent		Effluent		Influent		Fluidization	Bed
	pH	pH	TEMP C	Temp C	DO PPM	DO PPM	Flow GPM	Flow GPM	Flow GPM	Flow GPM	GPM	Height FT
8/3/94	6.91	6.95	14.8	18.3	12.4	3.8	3.5	30				
8/4/94	7.01	6.89	14.4	17.8	14.3	3.8	3.5	30				
8/5/94	6.93	6.89	14.6	18.7	14.4	3.7	3.5	30				10.5
8/6/94	6.89	6.89	14.8	18.9	14.5	3.6	3.5	30				
8/7/94	6.95	6.93	14.5	19.1	14.5	4	3.5	30				
8/8/94	6.94	6.95	14.7	17.9	14.7	3.5	3.5	30				
8/9/94	7.03	7.04	14.6	18.9	17.6	3.5	3.5	30				
8/10/94	7.05	7.04	14.8	18.5	16.8	3.6	3.5	30				10
8/11/94	7.02	6.89	15.1	18.5	17.8	3.6	3.5	30				

Table A2-2. Monitoring data of the fluidized bed biological process - COD, NH<sub>3</sub>, NO<sub>3</sub>, and PO<sub>4</sub> data

Date	Influent COD-t (mg/L)	Effluent COD-t (mg/L)	Influent COD-s (mg/L)	Effluent COD-s (mg/L)	Effluent NH3 (mg/L)	Effluent NO3 (mg/L)	Effluent PO4 (mg/L)
2/2/94	66	35	45	32	< 0.5	< 0.1	< 0.5
2/3/94	55	31	48	25	< 0.5	< 0.1	< 0.5
2/4/94	65	38	59	35	n/a	n/a	n/a
2/6/94	63	49	58	30	< 0.5	< 0.1	< 0.5
2/7/94	58	30	52	24	< 0.5	< 0.1	< 0.5
2/8/94	59	33	55	26	< 0.5	< 0.1	< 0.5
2/9/94	49	34	42	27	< 0.5	< 0.1	< 0.5
2/10/94	48	33	44	26	< 0.5	< 0.1	< 0.5
2/16/94	45	n/a	38	n/a	n/a	n/a	n/a
2/17/94	43	n/a	38	n/a	n/a	n/a	n/a
2/18/94	n/a	n/a	n/a	n/a	n/a	n/a	n/a
2/19/94	n/a	n/a	n/a	n/a	n/a	n/a	n/a
2/20/94	n/a	38	n/a	27	< 0.5	< 0.1	< 0.5
2/21/94	n/a	36	n/a	26	< 0.5	< 0.1	< 0.5
2/22/94	n/a	34	n/a	26	< 0.5	< 0.1	< 0.5
2/23/94	20.98	34	45	26	< 0.5	< 0.1	< 0.5
2/24/94	21.21	32	43	24	n/a	n/a	n/a
3/2/94	33	21	28	19	< 0.5	< 0.1	< 0.5
3/3/94	32	22	28	19	< 0.5	< 0.1	< 0.5
3/4/94	32	22	29	20	< 0.5	< 0.1	< 0.5
3/5/94	33	23	30	21	< 0.5	< 0.1	< 0.5
3/6/94	n/a	39	n/a	36	< 0.5	< 0.1	< 0.5
3/7/94	n/a	23	n/a	29	< 0.5	< 0.1	< 0.5
3/8/94	38	15	36	8	< 0.5	< 0.1	< 0.5
3/9/94	52	39	47	29	< 0.5	< 0.1	4
3/10/94	38	23	32	21	< 0.5	< 0.1	4
3/11/94	38	22	36	19	1.2	< 0.1	4
3/12/94	n/a	n/a	n/a	n/a	1.4	0.2	4
3/13/94	n/a	n/a	n/a	n/a	1.3	0.2	3
3/14/94	43	17	38	12	1.2	< 0.1	2
3/15/94	39	19	36	16	0.8	0.2	3
3/16/94	40	18	32	17	1.2	0.2	2
3/17/94	35	21	32	21	1.3	< 0.1	2
3/18/94	34	17	32	15	1.3	< 0.1	2
3/19/94	33	19	31	14	1.3	< 0.1	2
3/20/94	32	18	30	13	2	< 0.1	2
3/21/94	34	19	29	14	1	< 0.1	2.4
3/22/94	45	21	28	15	1	< 0.1	2.6
3/23/94	33	12	26	11	1	< 0.1	2.3
3/24/94	32	15	25	13	0.9	0.5	2

Table A2-2. Monitoring data of the fluidized bed biological process - COD, NH<sub>3</sub>, NO<sub>3</sub>, and PO<sub>4</sub> data (Continued)

Date	Influent COD-t (mg/L)	Effluent COD-t (mg/L)	Influent COD-s (mg/L)	Effluent COD-s (mg/L)	Effluent NH3 (mg/L)	Effluent NO3 (mg/L)	Effluent PO4 (mg/L)
3/25/94	34	16	26	12	0.8	< 0.1	2.1
3/26/94	32	15	27	11	1.2	< 0.1	2.1
3/27/94	31	14	28	12	1	< 0.1	2.2
3/28/94	36	16	32	6	1	0.4	2.6
3/29/94	35	19	28	14	1	0.4	2
3/30/94	45	19	41	14	0	0.1	2
4/1/94	44	12	59	9	0	0.5	n/a
4/8/94	n/a	n/a	n/a	n/a	2	0.2	2
4/9/94	n/a	n/a	n/a	n/a	2.5	0.2	2.6
4/10/94	n/a	n/a	n/a	n/a	4.1	0.2	3.6
4/11/94	43	28	32	26	3.7	0.2	3.6
4/12/94	n/a	n/a	n/a	n/a	3.5	0.3	3.6
4/15/94	33	28	30	25	4.6	0.4	5
4/16/94	n/a	n/a	n/a	n/a	4.6	0.5	4
4/17/94	n/a	n/a	n/a	n/a	4.7	0.6	5
4/18/94	45	25	34	22	5.8	0.8	5
4/19/94	44	22	35	21	6.8	2	4
4/20/94	42	21	35	21	6.3	5	4
4/21/94	41	16	31	14	5.4	7	4.6
4/22/94	n/a	n/a	n/a	n/a	4.8	7	4.6
4/24/94	39	21	39	21	4.6	6	3
4/25/94	38	26	36	19	4.2	15	4
4/26/94	42	18	34	16	0	18	2
4/28/94	n/a	n/a	n/a	n/a	6	1	n/a
4/29/94	n/a	n/a	n/a	n/a	6.5	4	n/a
4/30/94	n/a	n/a	n/a	n/a	20	3	n/a
5/1/94	n/a	n/a	n/a	n/a	7.5	3	3.5
5/2/94	33	14	32	13	6.6	6	3
5/3/94	34	14	31	14	4	3	3
5/4/94	32	16	29	14	5.3	4	3
5/5/94	35	13	32	12	4.5	3	3
5/6/94	29	15	27	10	3.6	1	2.6
5/8/94	35	18	30	16	0	3	0.5
5/9/94	37	21	29	18	3	6	3.4
5/10/94	36	19	32	19	4	6	4
5/11/94	38	19	32	17	10	7	3.5
5/12/94	38	21	31	18	9	4	3
5/13/94	n/a	n/a	n/a	n/a	7	5	4.5
5/15/94	n/a	n/a	n/a	n/a	4	5	3

Table A2-2. Monitoring data of the fluidized bed biological process - COD, NH<sub>3</sub>, NO<sub>3</sub>, and PO<sub>4</sub> data (Continued)

Date	Influent COD-t (mg/L)	Effluent COD-t (mg/L)	Influent COD-s (mg/L)	Effluent COD-s (mg/L)	Effluent NH3 (mg/L)	Effluent NO3 (mg/L)	Effluent PO4 (mg/L)
5/16/94	33	16	28	15	5	6	4
5/17/94	46	21	40	19	4.5	5.2	4.5
5/18/94	45	24	42	17	5.2	5.3	4.7
5/19/94	53	23	44	18	5.6	5.6	6.7
5/20/94	51	22	43	18	5.4	7.8	6.2
5/21/94	n/a	n/a	n/a	n/a	4.3	4.5	3.6
5/22/94	n/a	n/a	n/a	n/a	3.2	6.7	3.4
5/23/94	32	12	29	11	5.4	7.6	3.4
5/24/94	33	14	31	13	4.3	5.6	2.5
5/25/94	31	15	29	13	5	6	3
5/26/94	33	14	32	15	4.4	6	2.5
5/27/94	31	14	29	14	3.6	7	3
5/31/94	43	16	38	14	4.5	5	3
6/1/94	42	15	39	14	5	5	3
6/2/94	42	14	36	12	4.6	5	3
6/3/94	44	14	38	13	5	5	3
6/5/94	n/a	n/a	n/a	n/a	3.4	3	2.6
6/6/94	76	36	72	27	4	6	2.4
6/7/94	74	34	72	34	4.3	6	3
6/8/94	67	35	62	35	4	6	3
6/9/94	66	39	63	24	4.3	5	3
6/10/94	68	27	56	20	4	6	3
6/11/94	n/a	n/a	n/a	n/a	4.5	4	3
6/12/94	n/a	n/a	n/a	n/a	4	5	4
6/13/94	49	42	48	21	2	6	3
6/14/94	55	31	50	26	3	4	4
6/15/94	52	28	48	24	3	4	5
6/16/94	66	27	58	24	3	10	4
6/17/94	72	26	58	21	2	28	5
6/18/94	n/a	n/a	n/a	n/a	0	25	5
6/19/94	n/a	n/a	n/a	n/a	0	25	5
6/20/94	67	25	56	21	0	30	5
6/21/94	66	24	55	21	0	24	5
6/22/94	65	26	54	21	0	24	5
6/23/94	46	22	56	21	0	15	5
6/24/94	68	32	55	21	3	12	5
6/25/94	n/a	n/a	n/a	n/a	3	6	5
6/26/94	n/a	n/a	n/a	n/a	0.4	16	5
6/27/94	56	29	45	24	0	7	3

Table A2-2. Monitoring data of the fluidized bed biological process - COD, NH<sub>3</sub>, NO<sub>3</sub>, and PO<sub>4</sub> data (Continued)

Date	Influent COD-t (mg/L)	Effluent COD-t (mg/L)	Influent COD-s (mg/L)	Effluent COD-s (mg/L)	Effluent NH3 (mg/L)	Effluent NO3 (mg/L)	Effluent PO4 (mg/L)
6/28/94	55	28	47	22	0	7	3
6/29/94	57	26	44	21	0	9	3
6/30/94	49	26	42	29	0.2	1	0.5
7/5/94	n/a	n/a	n/a	n/a	0	3	2
7/6/94	52	26	45	22	0	4	2
7/7/94	n/a	n/a	n/a	n/a	0	1	2
7/8/94	n/a	n/a	n/a	n/a	2.4	3	3
7/9/94	n/a	n/a	n/a	n/a	3.3	5	3
7/10/94	n/a	n/a	n/a	n/a	4	5	3
7/11/94	44	13	38	8	2	5	3
7/12/94	45	13	34	7	3	5	3
7/13/94	70	35	61	25	4	7	5
7/14/94	67	45	66	24	4	9	4
7/15/94	66	23	54	61	2	10	3.4
7/16/94	65	25	56	26	3	8	3
7/17/94	45	22	37	27	2	6	4
7/18/94	47	23	38	30	5	5	2
7/19/94	54	28	53	21	5	7	7
7/20/94	55	27	52	25	3	0	6
7/21/94	51	26	48	21	6	8	3
7/25/94	47	31	44	28	5	21	5
7/26/94	49	31	35	24	3	12	4
7/27/94	56	35	43	25	2	7	3
7/29/94	n/a	n/a	n/a	n/a	2	6	3.4
7/31/94	n/a	n/a	n/a	n/a	0	0	3
8/1/94	n/a	n/a	n/a	n/a	0	4	4
8/2/94	55	32	50	26	0	4	4
8/3/94	n/a	n/a	n/a	n/a	0	7	3
8/4/94	n/a	n/a	n/a	n/a	0	7	6
8/5/94	56	26	50	19	0	9	4
8/6/94	n/a	n/a	n/a	n/a	n/a	n/a	n/a
8/7/94	n/a	n/a	n/a	n/a	n/a	n/a	n/a
8/8/94	67	33	65	28	1.5	5	4
8/9/94	n/a	n/a	n/a	n/a	n/a	n/a	n/a
8/10/94	66	32	58	29	2	3.5	4

Table A2-2. Monitoring data of the fluidized bed biological process - Total Fe, Soluble Fe, and Suspended Solids

Date	Influent Fe-t (mg/L)	Effluent Fe-t (mg/L)	Influent Fe-s (mg/L)	Effluent Fe-s (mg/L)	Effluent TSS (mg/L)	Effluent VSS (mg/L)
2/2/94	8.6	1	6.8	0.7	n/a	n/a
2/3/94	8.8	1.2	7	0.8	n/a	n/a
2/4/94	9	n/a	7.9	n/a	n/a	n/a
2/6/94	8.7	0.8	6.6	0.3	n/a	n/a
2/7/94	8.7	0.8	6.7	0.4	n/a	n/a
2/8/94	8.5	0.85	6.8	0.4	n/a	n/a
2/9/94	8.6	1	6	0.6	n/a	n/a
2/10/94	8.6	0.9	6	0.5	n/a	n/a
2/16/94	8.9	n/a	7	n/a	n/a	n/a
2/17/94	8.6	n/a	6.7	n/a	n/a	n/a
2/18/94	n/a	n/a	n/a	n/a	n/a	n/a
2/19/94	n/a	n/a	n/a	n/a	n/a	n/a
2/20/94	n/a	1	n/a	0.2	n/a	n/a
2/21/94	n/a	1	n/a	0.2	n/a	n/a
2/22/94	n/a	0.4	n/a	0.1	n/a	n/a
2/23/94	9.1	0.4	6.8	0.1	n/a	n/a
2/24/94	8.7	n/a	6.6	n/a	n/a	n/a
3/2/94	8	2.1	6.7	0.2	n/a	n/a
3/3/94	8	1	6.7	0.2	n/a	n/a
3/4/94	8.1	1.1	6.6	0.2	n/a	n/a
3/5/94	7.8	1.1	6.9	0.2	n/a	n/a
3/6/94	n/a	1.1	n/a	0.2	n/a	n/a
3/7/94	n/a	2.6	n/a	0.2	n/a	n/a
3/8/94	7.8	2.3	5.9	0.3	n/a	n/a
3/9/94	8	2	5.8	0.2	n/a	n/a
3/10/94	7.9	1.5	5.8	0.2	n/a	n/a
3/11/94	8.2	1	6	0.1	n/a	n/a
3/12/94	8.1	1	6	0.1	n/a	n/a
3/13/94	8.1	1.5	5.8	0.2	n/a	n/a
3/14/94	8.1	1.1	6.2	0.2	n/a	n/a
3/15/94	6.9	1	5.9	0.2	n/a	n/a
3/16/94	6.9	1.1	5.4	0.3	n/a	n/a
3/17/94	7.2	1.2	6.4	0.4	n/a	n/a
3/18/94	7.2	1.4	6.6	0.6	n/a	n/a
3/19/94	7.8	1.5	6.9	1	n/a	n/a
3/20/94	7.2	2	6.8	n/a	n/a	n/a
3/21/94	7.3	2.1	6.9	1.1	n/a	n/a
3/22/94	6.9	1.8	6.4	1.5	n/a	n/a
3/23/94	7.2	1.9	6.5	1.2	n/a	n/a
3/24/94	7.2	2.2	6.6	1.5	n/a	n/a

Table A2-2. Monitoring data of the fluidized bed biological process - Total Fe, Soluble Fe, and Suspended Solids (Continued)

Date	Influent Fe-t (mg/L)	Effluent Fe-t (mg/L)	Influent Fe-s (mg/L)	Effluent Fe-s (mg/L)	Effluent TSS (mg/L)	Effluent VSS (mg/L)
3/25/94	7.5	2.5	6.7	1.2	n/a	n/a
3/26/94	7.1	2.1	6.7	1.3	n/a	n/a
3/27/94	7	2	6.8	1.4	n/a	n/a
3/28/94	7.4	1.8	6.5	1.2	n/a	n/a
3/29/94	7.2	2.1	6.4	1.5	n/a	n/a
3/30/94	7.2	1	6.6	0.6	n/a	n/a
4/1/94	7.5	1	7	0.5	n/a	n/a
4/8/94	7.6	0.5	6.9	0.3	n/a	n/a
4/9/94	7.4	1.5	6.9	0.5	n/a	n/a
4/10/94	7.3	2.1	6.8	0.5	n/a	n/a
4/11/94	7.2	2.1	6.8	0.6	n/a	n/a
4/12/94	7.2	2	6.8	0.7	n/a	n/a
4/15/94	7.8	1.5	6.9	1	n/a	n/a
4/16/94	7.8	1.5	6.9	1	n/a	n/a
4/17/94	7.6	1.6	6.8	1	n/a	n/a
4/18/94	7.6	1.7	6.9	1	n/a	n/a
4/19/94	7.6	1.4	6.9	1	n/a	n/a
4/20/94	7.8	1.6	6.8	1	n/a	n/a
4/21/94	7.8	2	7	0.8	n/a	n/a
4/22/94	8	1.2	7.6	0.6	n/a	n/a
4/24/94	8.1	1.3	7.7	0.8	n/a	n/a
4/25/94	7.7	1.4	7.5	0.8	n/a	n/a
4/26/94	7.6	2	7.4	1.3	n/a	n/a
4/28/94	7.6	1.8	7.4	0.6	n/a	n/a
4/29/94	7.8	1.6	7.4	0.6	n/a	n/a
4/30/94	7.6	1.2	7.4	0.6	n/a	n/a
5/1/94	7.4	1.2	7.2	0.6	n/a	n/a
5/2/94	7.7	1.6	7.5	0.8	0	0
5/3/94	7.8	1.3	7.7	0.8	0	0
5/4/94	7.8	1.4	7.7	0.8	1	0
5/5/94	8	1.4	7.6	0.6	0	0
5/6/94	8.2	1.4	7.7	0.8	2	0
5/8/94	8.3	1.8	7.5	0.9	n/a	n/a
5/9/94	8.1	1.7	7.6	0.9	n/a	n/a
5/10/94	7.9	1.9	7.4	1.1	n/a	n/a
5/11/94	7.8	1.9	7.5	1.3	n/a	n/a
5/12/94	7.9	1.7	7.6	1.3	n/a	n/a
5/13/94	8.1	2.1	7.5	1.5	0	0
5/15/94	8.1	1.7	7.6	1.6	n/a	n/a

Table A2-2. Monitoring data of the fluidized bed biological process - Total Fe, Soluble Fe, and Suspended Solids (Continued)

Date	Influent Fe-t (mg/L)	Effluent Fe-t (mg/L)	Influent Fe-s (mg/L)	Effluent Fe-s (mg/L)	Effluent TSS (mg/L)	Effluent VSS (mg/L)
5/16/94	8.3	2.1	7.7	1.4	n/a	n/a
5/17/94	8.4	1.7	7.9	1.6	n/a	n/a
5/18/94	8.4	2.8	7.8	1.4	4	2
5/19/94	8.5	2.2	7.6	1.2	n/a	n/a
5/20/94	8.1	1.7	7.5	1.3	3	1
5/21/94	8	1.5	7.6	1.5	n/a	n/a
5/22/94	7.9	1.9	7.8	1.6	n/a	n/a
5/23/94	8.2	2	7.6	1.5	8	2
5/24/94	8.3	1.6	7.7	1.6	8	2
5/25/94	8.1	1.8	7.8	1.5	8	2
5/26/94	7.9	1.7	7.7	1.5	8	2
5/27/94	7.9	1.8	7.7	1.4	11	3
5/31/94	8.2	2	7.8	1.7	11	1
6/1/94	8.1	2.1	7.7	1.6	8	2
6/2/94	8	1.8	7.8	1.6	8	2
6/3/94	7.9	1.8	7.7	1.6	8	2
6/5/94	7.8	1.8	7.6	1.6	8	2
6/6/94	8.1	1.8	7.7	1.4	10	3
6/7/94	8	2.2	7.8	1.3	7	2
6/8/94	7.9	2.3	7.8	1.2	8	1
6/9/94	7.9	2.6	7.8	1.3	6	1
6/10/94	8	2.2	7.8	1.3	8	2
6/11/94	8.2	2.3	7.6	1.5	9	1
6/12/94	8.1	2.6	7.9	1.3	10	2
6/13/94	8.2	3.1	7.9	1	9	2
6/14/94	8.3	2.6	7.9	1.3	35	15
6/15/94	8.4	2.4	8	1	8	4
6/16/94	8.1	2.3	7.7	1.2	6	2
6/17/94	8	2.6	7.8	1	7	2
6/18/94	8	2.1	7.8	1.7	8	1
6/19/94	8.4	2.1	7.6	1.7	7	2
6/20/94	8.5	2.4	7.6	1.6	6	1
6/21/94	8.7	2	7.6	1.7	6	2
6/22/94	7.9	2.1	7.5	1.5	7	1
6/23/94	7.8	2.5	7.5	1.5	8	2
6/24/94	7.7	2.2	7.4	1.5	7	2
6/25/94	7.8	2.1	7.4	1.5	6	2
6/26/94	7.8	2.5	7.8	2	7	1
6/27/94	8	5.8	7.7	1.4	33	14
6/28/94	8	6.8	7.8	1.4	45	19

Table A2-2. Monitoring data of the fluidized bed biological process - Total Fe, Soluble Fe, and Suspended Solids (Continued)

Date	Influent Fe-t (mg/L)	Effluent Fe-t (mg/L)	Influent Fe-s (mg/L)	Effluent Fe-s (mg/L)	Effluent TSS (mg/L)	Effluent VSS (mg/L)
6/29/94	7.9	8.6	7.9	1.7	77	43
6/30/94	7.8	1.2	7	0.6	n/a	n/a
7/5/94	8	4	7.9	2.6	n/a	n/a
7/6/94	7.9	3.5	7.9	2.6	n/a	n/a
7/7/94	7.9	3.4	7.9	2.6	n/a	n/a
7/8/94	8	3.6	7.7	2.3	n/a	n/a
7/9/94	8.2	3.4	7.8	2.3	n/a	n/a
7/10/94	8.2	4.3	7.8	2.4	6	4
7/11/94	7.8	4	7.8	2.5	5	2
7/12/94	7.9	3.4	7.6	2	4	1
7/13/94	8.2	4.2	7.7	2.1	3	1
7/14/94	8	4.2	7.9	2.1	3	1
7/15/94	7.6	3.5	7.4	2.7	4	2
7/16/94	8	1.9	7.5	1.8	6	2
7/17/94	8	2.7	7.3	1.7	4	2
7/18/94	7.6	2.8	7.7	2.1	6	2
7/19/94	7.5	2.6	7.4	2.2	8	2
7/20/94	7.7	3.2	6.9	1.8	8	4
7/21/94	7.8	3.4	6.9	1.7	10	6
7/25/94	7.9	2.1	7.5	1.4	21	9
7/26/94	7.9	2.6	7.2	1.5	15	10
7/27/94	8.2	2.6	7.7	2.2	21	9
7/29/94	8.1	3	7.8	2.8	32	8
7/31/94	7.9	3.4	7.9	2.6	23	11
8/1/94	7.5	4.3	7.3	3.5	9	4
8/2/94	7.6	4.3	7	3.7	11	2
8/3/94	7.7	3.3	7.7	3.3	12	2
8/4/94	7.8	3.2	7.7	3.2	6	2
8/5/94	7.8	4.5	7.7	3.3	7	2
8/6/94	n/a	n/a	n/a	n/a	11	6
8/7/94	n/a	n/a	n/a	n/a	14	6
8/8/94	7.7	3.3	7.5	2.9	14	6
8/9/94	n/a	n/a	n/a	n/a	11	6
8/10/94	7.8	3.7	7.6	3	10	7

**Section 3 Appendices**

**THE ACTIVATED SLUDGE PROCESS**

Table A3-1. Performance data of the activated sludge system for MTBE biodegradation - Run 1

Time (day)	MTBE		DIPE		Benzene		Toluene		E-Benzene		Xylenes	
	INF	EFF	INF	EFF	INF	EFF	INF	EFF	INF	EFF	INF	EFF
	(µg/L)	(µg/L)	(µg/L)	(µg/L)	(µg/L)	(µg/L)	(µg/L)	(µg/L)	(µg/L)	(µg/L)	(µg/L)	(µg/L)
0	250	11	400	12	770	<1	1800	<1	110	<1	400	<1
1	300	4	430	7	810	<1	2400	<1	91	<1	580	<1
2	340	38	380	25	870	<1	1900	9	100	<1	420	19
3	360	11	420	8	830	<1	1800	3	100	<1	380	<1
4	370	8	460	<1	910	3	1900	<1	120	<1	400	<1
5	360	13	460	2	890	2	2100	<1	120	<1	450	<1
6	400	16	440	3	910	<1	2000	<1	110	<1	410	<1
7	330	11	380	8	840	<1	1900	<1	100	<1	390	<1
8	360	24	460	43	950	<1	1900	<1	120	<1	400	<1
9	380	18	420	16	870	<1	1700	<1	110	<1	340	<1
10	380	14	470	8	960	2	1700	<1	120	<1	366	<1
12	330	13	450	#N/A	920	<1	1900	<1	120	<1	378	<1
13	600	13	410	14	830	<1	2000	<1	100	<1	430	<1
14	610	6	410	<1	820	<1	2000	<1	110	<1	450	<1
15	540	9	410	4	780	<1	1600	<1	100	<1	347	<1
16	390	4	410	2	860	<1	1700	<1	110	<1	342	<1
17	420	2	460	<1	880	<1	1700	<1	110	<1	344	<1
18	430	9	470	7	950	<1	3100	<1	100	<1	640	<1
19	400	20	460	10	910	<1	2700	<1	95	<1	570	<1
20	390	84	390	18	850	<1	2960	<1	61	<1	680	<1
21	420	17	490	12	880	<1	1900	<1	110	<1	380	<1
22	430	27	480	32	930	<1	1800	<1	110	<1	370	<1
23	310	22	390	29	#N/A	<1	#N/A	<1	#N/A	<1	#N/A	<1
29	500	22	450	21	960	18	2800	27	120	2	450	10
30	480	170	450	190	860	210	1700	350	110	23	380	112
31	430	220	490	330	870	8	1700	4	90	<1	370	<1
32	380	240	380	380	780	<1	1400	2	110	<1	300	<1
33	470	61	460	56	930	<1	2000	<1	23	<1	410	<1
34	540	53	480	<1	960	<1	2200	<1	120	<1	680	<1
37	540	28	480	<1	940	<1	1800	<1	120	<1	620	<1
38	560	18	500	<1	970	<1	2000	<1	130	<1	640	<1
39	580	26	460	<1	950	<1	2000	<1	120	<1	620	<1
40	550	17	440	<1	880	<1	1800	<1	110	<1	540	<1
41	490	7	480	<1	830	<1	1600	<1	100	<1	349	<1
42	320	7	410	3	940	<1	1600	<1	130	<1	419	<1
43	#N/A	6	#N/A	2	#N/A	<1	#N/A	<1	130	<1	#N/A	<1
44	380	7	490	5	1000	<1	1900	<1	#N/A	<1	400	<1

Table A3-2. Performance data of the activated sludge system for MTBE biodegradation  
- Run 2

Time (day)	MTBE		DIPE		Benzene		Toluene		E-Benzene		Xylenes	
	INF	EFF	INF	EFF	INF	EFF	INF	EFF	INF	EFF	INF	EFF
	(µ/L)	(µ/L)	(µg/L)	(µg/L)	(µg/L)	(µg/L)	(µg/L)	(µg/L)	(µg/L)	(µg/L)	(µg/L)	(µg/L)
0	340	79	410	140	850	<1	1600	<1	100	<1	325	<1
1	360	69	420	130	870	<1	1500	<1	100	<1	314	<1
2	330	62	370	110	760	<1	1300	<1	90	<1	272	<1
3	320	94	480	190	690	<1	1500	<1	100	<1	197	<1
5	420	84	490	170	880	<1	1700	3	110	<1	366	<1
6	410	92	470	150	930	<1	1700	4	120	<1	379	<1
7	410	66	450	120	880	<1	1600	2	110	<1	351	<1
8	450	90	490	150	980	<1	1800	2	120	<1	390	<1
9	430	67	470	120	960	<1	1700	<1	110	<1	365	<1
10	440	21	500	59	900	<1	1600	<1	120	<1	330	<1
11	390	34	430	75	850	<1	1600	<1	120	<1	329	<1
12	400	59	450	120	830	<1	1250	<1	10	<1	340	<1
13	390	80	440	140	770	<1	1600	<1	90	<1	330	<1
14	360	130	370	150	850	12	2000	25	110	<1	410	<1
15	260	44	310	60	680	<1	2000	<1	100	<1	420	<1
16	290	42	340	46	770	<1	2400	<1	120	<1	500	<1
18	390	33	350	23	990	<1	6100	<1	140	<1	660	<1
20	320	10	380	4	810	<1	3200	<1	160	<1	1330	<1
22	390	3	370	<1	880	<1	4700	<1	220	<1	1110	<1
23	320	18	320	8	600	<1	2600	<1	13	<1	630	<1
27	407	29	411	7	1230	<1	5208	<1	243	<1	1223	<1
28	302	36	478	9	809	<1	4016	<1	182	<1	931	<1
29	353	21	374	6	1055	<1	4459	<1	218	<1	1080	<1
30	346	25	357	7	948	<1	4652	<1	227	<1	1123	<1
31	360	30	310	4	710	<1	4000	3	210	<1	1030	<1
32	310	11	300	4	690	<1	3930	2	200	<1	1000	<1
34	310	19	290	20	590	<1	2340	<1	130	<1	670	<1
37	330	8	320	6	720	<1	3350	<1	180	<1	900	<1
38	290	8	310	3	610	<1	2970	<1	160	<1	800	<1
39	290	#N/A	310	2	590	#N/A	3060	<1	150	<1	810	<1

Table A3-3. Performance data of the activated sludge system for MTBE biodegradation  
- Run 3

Time (day)	MTBE		DIPE		Benzene		Toluene		E-Benzene		Xylenes	
	INF (µg/L)	EFF (µg/L)										
0	1210	150	320	8	720	<1	1310	<1	88	<1	329	<1
1	1430	130	350	9	740	<1	1380	<1	92	<1	324	<1
3	1310	21	300	2	750	<1	1290	<1	90	<1	310	<1
4	970	74	350	9	770	<1	1320	<1	87	<1	101	<1
5	1000	30	290	4	770	<1	1390	<1	93	<1	322	<1
6	1350	11	420	3	760	<1	1310	<1	100	<1	319	<1
8	#N/A	4	#N/A	4	#N/A	<1	#N/A	<1	#N/A	<1	#N/A	<1
9	1280	31	330	4	749	<1	1470	<1	97	<1	323	<1
10	1340	20	330	3	780	<1	1670	<1	110	<1	353	<1
11	1530	18	360	2	760	<1	1580	<1	99	<1	335	<1
12	#N/A	3	#N/A	2	#N/A	<1	#N/A	<1	#N/A	<1	#N/A	<1
13	1400	13	370	3	810	<1	1670	<1	100	<1	354	<1
14	1590	13	360	2	700	<1	1390	<1	93	<1	311	<1
16	1170	190	460	2	780	<1	1520	<1	99	<1	327	<1
17	1240	5	380	2	710	<1	1390	<1	91	<1	312	<1
18	1270	3	460	2	810	<1	1620	<1	110	<1	351	<1
19	1270	4	410	<1	790	<1	1520	<1	110	<1	350	<1
20	1160	3	380	<1	580	<1	590	<1	10	<1	317	<1
21	1180	4	420	<1	750	<1	1500	<1	98	<1	327	<1
22	1290	250	380	35	690	<1	1860	<1	120	<1	410	<1
23	1240	15	390	2	710	<1	1760	<1	110	<1	378	<1
24	1310	8	370	<1	690	<1	1530	<1	100	<1	329	<1
27	1500	3	330	<1	450	<1	1440	<1	99	<1	177	<1
28	1230	430	400	93	800	160	1320	310	93	<1	338	0
29	450	145	400	47	740	4	1470	7	110	<1	315	<1
30	480	34	390	14	830	<1	1600	<1	120	<1	356	<1
31	510	17	420	5	790	<1	1510	<1	110	<1	325	<1
32	830	#N/A	420	#N/A	760	#N/A	1430	#N/A	110	#N/A	324	#N/A
33	780	38	410	7	760	<1	2050	<1	110	<1	421	<1
34	600	32	350	8	870	<1	2260	<1	130	<1	490	<1
35	310	7	330	7	830	<1	2500	<1	120	<1	520	<1
36	2260	56	360	5	800	<1	2120	<1	100	<1	440	<1
38	370	17	440	9	870	<1	1620	<1	120	<1	380	<1
39	370	38	390	9	870	<1	1640	<1	120	<1	398	<1
40	2770	590	330	17	780	<1	1500	<1	110	<1	350	<1
41	2950	480	390	20	840	<1	1570	<1	110	<1	368	<1
42	3460	370	410	14	810	<1	1790	<1	110	<1	388	<1
43	2920	160	410	7	750	<1	1830	<1	110	<1	390	<1
47	400	28	360	9	790	<1	1820	<1	110	<1	390	<1
48	340	28	400	5	760	<1	1500	<1	110	<1	350	<1
49	1030	30	360	5	800	<1	1670	<1	110	<1	390	<1
50	980	38	350	10	900	<1	2180	<1	140	<1	530	<1
54	1710	89	400	12	820	<1	1830	<1	120	<1	410	<1

Table A3-4. Performance data of the activated sludge system for MTBE biodegradation  
- Run 4

Time (day)	MTBE		DIPE		Benzene		Toluene		E-Benzene		Xylenes	
	INF (µg/L)	EFF (µg/L)										
0	1090	45	400	11	810	<1	1790	<1	120	<1	410	<1
1	790	55	390	14	830	<1	1810	<1	120	<1	390	<1
2	380	18	390	14	720	<1	1500	<1	99	<1	330	<1
3	840	35	370	12	830	<1	2090	<1	120	<1	460	<1
4	640	31	410	13	790	<1	1880	<1	120	<1	440	<1
6	2450	184	350	14	770	2	2140	<1	120	<1	490	<1
8	7410	570	400	17	810	<1	1970	<1	130	<1	450	<1
14	14500	5220	380	110	690	<1	1230	<1	78	<1	327	<1
15	8080	1840	370	48	760	<1	1370	<1	100	<1	345	<1
16	9270	2240	440	47	770	<1	1380	<1	100	<1	343	<1
17	8290	#N/A	430	#N/A	760	#N/A	1330	#N/A	97	#N/A	322	#N/A
20	10080	2110	540	44	980	<1	1740	<1	130	<1	430	<1
21	#N/A	2450	#N/A	50	#N/A	<1	#N/A	<1	#N/A	<1	#N/A	<1
22	#N/A	3870	#N/A	85	#N/A	<1	#N/A	<1	#N/A	<1	#N/A	<1
23	#N/A	3890	#N/A	86	#N/A	<1	#N/A	<1	#N/A	<1	#N/A	<1
24	8380	3430	420	59	700	2	1400	2	90	<1	346	<1
26	7850	5910	180	190	290	<1	510	<1	31	<1	152	<1

Table A3-5. Monitoring data of the activated sludge system for MTBE biodegradation - Run 1

Time (days)	pH		Temp		DO		Sludge		COD		Total Fe	
	INF	EFF	INF	EFF	Aeratr	Clarifier	Recycle	Waste	INF	EFF	INF	EFF
			(C)	(C)	(mg/L)	(mg/L)	(gpm)	(mL)	(mg/L)	(mg/L)	(mg/L)	(mg/L)
0	6.77	7.56	14.8	17.8	9.2	5.6	0.2		47	9	7.9	2.3
1	6.76	7.7	14.8	17.5	9	4.9	0.2		32	7	8.2	1
2	6.88	7.72	14.8	17.5	9	5.6	0.2		36	8	8.1	1
3	6.8	7.75	14.5	17.2	8.9	5.4	0.2					
4	6.9	8.01	15.2	18.7	9	5.1	0.2				8.2	0.4
5	6.79	8.41	15.3	19	11.6	4.8	0.2		37	8	7.6	1.9
6	6.81	7.6	14.9	15.2	9.1	6.6	0.2		35	9	6.5	2.1
7	6.69	7.2	14.8	19.1	9	6.4	0.2		33	14	6.5	1.6
8	6.81	7.64	14.5	16.4	9	5.2	0.2		32	8	6.6	1.4
9	7.01	7.43	14.9	17.6	8.9	4.6	0.2		30	8	7.2	1.6
10	6.89	7.29	14.5	15.4	9.5	4.5	0.2				7.6	2
12	6.9	5.98	13.5	18.6	8.7	2.3	0.2		29	8	7.3	2.4
13	6.82	6.3	14.6	18.3	8.8	2.6	0.2		28	9	6.9	2
14	6.79	6.4	14.3	18.2	8.5	3.4	0.2		25	8	7.2	2.1
15	6.78	6.87	14.5	18.3	8.4	3.5	0.2		24	6	7.2	2.1
16	6.78	6.9	14.6	18.5	8.6	3.3	0.2		23	7	7.7	2.2
17	6.74	7.01	14.6	16.2	8.3	3.6	0.2		23	8	7.2	2.6
18	6.89	6.79	14.6	17.3	8.4	2.4	0.2		22	8	7.2	2.4
19	6.88	6.81	14.5	18.9	8.6	3.1	0.2		32	8	7.2	2.1
20	6.68	6.81	14.8	14.9	8.2	1.9	0.2		28	8	7.2	2.6
21			14.4	16.8	8.9	2.7	0.2		21	10	7.1	2.1
22			14.7	18.4	9.2	6	0.2				6.6	1.8
23	7.04	7.15	14.7	18.6	8.7	4.2	0.2		51	36	7.6	1.8
29	6.7	7.22	14.5	15.4	6.4	1.4	0.2					
30	6.68	6.89	14.7	14.7	2.5	0.8	0.2		33	12	7.2	1.6
31	6.78	6.76	14.8	17.1	3.4	0.8	0.2	1000			7.4	1.7
32	6.89	6.76	14.6	17.1	3.5	0.7	0.2				7.3	1.7
33	6.89	6.89	14.8	17.1	3.6	0.7	0.2	1000	32	10	7.2	2.1
34	6.88	6.56	14.9	17.1	3.5	0.5	0.2	1000			7.2	1.7
35	6.89	6.4	14.5	16.1	3.8	0.8	0.2		31	15		
37	6.87	7.3	14.7	15.7	8.4	4.5	0.2		30	19	7.8	2
38	6.88	7.12	14.3	16.4	7.6	4.4	0.2				7.8	2.4
39	6.85	7.3	13.9	16.1	6.7	4.3	0.2				7.7	2.5
40	7.01	7.33	14.7	16.1	6.5	4.1	0.2	1000	32	23	7.7	2
41	7.01	7.05	14.5	15.7	6.5	4.4	0.2	1000	35	21	8.1	2.5
42	6.99	7.12	14.5	15.5	5.6	4.4	0.2	1000	35	21	7.8	2.6
43	6.92	6.99	14.5	15.4	5.4	4.1	0.2	1000	31	16	7.8	2.4
44	7.01	6.96	14.6	15.1	6.3	2.1	0.2	1000			8	2.4

Table A3-6. Monitoring data of the activated sludge system for MTBE biodegradation  
- Run 2

Time (days)	pH		Temp		DO		Sludge		COD		Total Fe	
	INF	EFF	INF	EFF	Aerativ	Clarifier	Recycle	Waste	INF	EFF	INF	EFF
			(C)	(C)	(mg/L)	(mg/L)	(gpm)	(mL)	(mg/L)	(mg/L)	(mg/L)	(mg/L)
0	7.01	7.14	14.3	16.7	7	3.4	0.2	1000			7.8	2.1
1	7.1	7.34	14.3	16.8	6.7	4.5	0.2	1000			7.8	2.1
2	7.1	7.56	14.5	16.9	6.9	4.5	0.2	1000	41	20	7.8	2.1
3	7.03	7.53	14.6	16.2	5.6	3.2	0.2	1000	31	18	7.9	2.4
4	7.01	7.01	14.5	17.1	7.2	3.2	0.2	1000				
5	6.87	7.12	14.4	17	9.1	4.1	0.2	1000			7.8	3.8
6	6.89	7.41	14.4	16.6	8.2	4.8	0.2	1000			7.4	2
7	6.89	7.44	14.5	17.2	8.2	6.6	0.2	1000			7.8	2
8	7.01	7.51	14.3	18.9	8.9	6.2	0.2				7.6	1.8
9	6.98	7.45	14.6	17.6	8.8	6	0.2	1000	27	11	7.7	2
10	6.89	7.46	14.5	15.8	8.5	5.4	0.2	1000	25	12	7.8	2
11	6.88	7.46	14.6	15.8	8.3	5.1	0.2	1000	25	15	7.8	2.1
12	6.87	7.57	14.6	15.9	8.6	5.1	0.2	1000	26	12	8	1.8
13	6.89	7.34	14.7	16.3	8.8	5.1	0.2	1000	24	12	8.2	1.6
14	6.89	7.43	14.5	16.8	8.2	4.9	0.2	1000			8.2	2.1
15	6.91	7.44	14.4	16.4	6.6	4.8	0.2	1000			8.4	2
16	6.91	7.35	14.1	16.3	7.6	5.4	0.2	1000	31	10	7.8	1.9
17	6.88	7.45	14.1	16.6	7.5	5.2	0.2	1000	30	9	8	1.9
18	6.87	7.43	14.4	16.3	8.2	4.3	0.2	1000	34	10	7.8	2.1
19	6.89	7.45	14.5	16.7	8.4	5	0.2	1000	30	10	7.9	2.1
20	6.89	7.4	14.3	16.4	8.4	4.6	0.2	1000				
22	6.95	7.12	14.1	17.4	6.8	4.7	0.2	1000			7.8	2.2
23	7.01	7.34	14.2	17.6	7.4	4.3	0.2	1000	32	10	8.5	2.3
24	6.89	7.32	14.2	17.3	8.2	4.6	0.2	1000	43	13	8.5	2.3
25	6.89	7.06	14.5	17.6	8.5	5.6	0.2	0	41	14	8.4	2.1
26	6.93	7.44	14.5	17.7	8.7	4.8	0.2	0	40	14	8.3	2.1
27	6.95	7.21	14.5	17.5	8.5	4.7	0.2	0	38	12	8.2	2
28	6.95	7.17	14.7	18	8.3	4	0.2	0			8.5	2.2
29	6.98	7.13	14.6	16.7	8.5	4.3	0.2	0			8.1	2.4
30	6.95	7.23	14.4	18.2	8.6	4.6	0.2	0	34	11	8	2.5
31	7.03	7.26	14.5	17.6	8.5	4.5	0.2	0	31	12	7.9	2
32	7.01	7.33	14.7	17.5	8.4	4.6	0.2	0	29	12	8.2	2.2
33	7.01	7.17	14.6	18.4	8.3	4.5	0.2	0	33	10	8.3	2.1
34	6.92	7.24	14.5	17.5	8	4.3	0.2	0	29	11	8.1	1.9
37	6.89	7.22	14.2	17	8.3	4.7	0.2	0				
38	6.87	7.21	14.2	17.4	8.3	4.6	0.2	0	35	13	8.1	2.1

Table A3-7. Monitoring data of the activated sludge system for MTBE biodegradation  
- Run 3

Time (days)	pH		Temp		DO		Sludge	Sludge	COD		Total Fe	
	INF	EFF	INF	EFF	Aerati r	Clarifier	Recycle	Waste	INF	EFF	INF	EFF
			(C)	(C)	(mg/L)	(mg/L)	(gpm)	(mL)	(mg/L)	(mg/L)	(mg/L)	(mg/L)
0	7.08	7.47	14.6	17.8	8.9	4	0.25	1100	62	14	8.2	2.2
1	7.01	6.98	14.2	19	8.7	3.5	0.25	660	64	12	7.8	2.5
2	7.01	6.84	14.3	17.7	8.6	4	0.25	660	62	15	7.9	2
3	7.03	6.44	14.4	17.9	8.1	3.3	0.25	660			7.6	2.6
4	7.04	6.89	14.6	17.9	8	4.3	0.25	500			7.9	2.4
5	7.01	7.06	14.4	18.6	8	4.4	0.25	500	38	17	8.1	2.2
6	6.93	6.62	15	21.2	7.6	4	0.25	250	37	19	8.3	3
7	7.04	7.01	14.6	20.6	8.6	4.3	0.25	250	40	21	8.4	2.4
8	7.01	7.4	14.4	21.3	8.4	4.4	0.25	250	57	15	7.9	2.6
9	7.03	7.11	14.6	20.2	8.6	4.6	0.25	250	58	19	8.2	2.9
10	7.01	7.25	14.7	19.8	8	4.2	0.25	550			8	3.5
11	7.02	7.15	14.7	19.9	7.3	4.3	0.25	550			8.1	3
12	7.02	7.13	14.8	22.8	7.6	4.3	0.25	1000	56	15	8.5	2.6
13	7.03	6.89	15	21.3	7.7	4.2	0.25	800	57	15	8.5	2.1
14	6.98	7.05	14.3	20.2	7.6	4.3	0.25	800	56	15	8	3.2
15	7.02	7.06	14.7	19.8	8.2	4	0.25	800	55	15	7.7	3
16	7.11	7.22	14.7	19.8	7.6	3.8	0.25	800	56	15	7.9	3
17	7.05	7.3	14.8	20.2	6.9	3.4	0.25	800			7.8	3.2
18	7.04	7.12	14.8	20.4	6.9	3.5	0.25	800			7.8	3.2
19	7.11	7.15	14.7	19.9	7.7	2.7	0.25	660	48	11	7.8	3
20	7.02	7.5	14.8	19.8	7.4	3.6	0.25	660	51	12	7.8	2.7
21	6.98	7.21	14.6	21.2	7.4	4.2	0.25	660	56	14	7.9	2.5
27	6.89	6.97	15.2	23.2	6.5	3.2	0.25	1500			8.2	4.4
28	6.93	7.03	15.1	23.4	5.4	3.4	0.25	1500	42	12	8	4.7

Table A3-8. Monitoring data of the activated sludge system for MTBE biodegradation  
- Run 4

Time (days)	pH		Temp		DO		Sludge Recycle (gpm)	Sludge Waste (mL)	COD		Total Fe	
	INF	EFF	INF	EFF	Aeratr	Clarifier			INF	EFF	INF	EFF
			(C)	(C)	(mg/L)	(mg/L)			(mg/L)	(mg/L)	(mg/L)	(mg/L)
0	6.93	5.94	14.6	22.1	6.7	3.7	0.25	1250	54	21	7.7	3.3
1	7.07	7.2	14.6	18	8.2	5.3	0.25	1250			7.8	3.2
2	7.02	7.18	14.5	18.1	8.1	5.2	0.25	1150			7.8	4.5
3	7.01	7.06	14.5	18.4	7.6	4.2	0.25	1140	45	18	8	6.5
4	6.98	7.3	15.1	18.4	7.4	4.2	0.25	1100				
5	6.79	7.31	14.5	18.3	6.7	4.4	0.25	1100				
6	6.89	7.09	14.8	18.5	6.9	4.5	0.25	1100	50	28	7.7	5.6
7	6.99	7.15	14.6	19.3	6.9	3.9	0.25	1100				
8	7.01	7.24	14.5	19.7	6.5	3.7	0.25	1140	61	26	7.8	4.5
9	7.03	7.45	13.7	20.8	7.4	4.3	0.25	1210				
14	6.89	7.34	14.5	22.3	8.8	4.5	0.5	1100				
15	6.9	7.23	15	23.2	8.8	4.6	0.5	1100				
16	6.9	7.43	15	23.2	8.7	4.6	0.5	1000				
20	6.89	7.21	15.4	21.1	8.7	6	0.5	1100				
21	6.89	7.21	15.5	23.2	9.8	6	0.5	1100				
22	6.9	7.32	14.2	21.2	9.8	5.6	0.5	1100				
23	6.92	7.32	14.3	17.6	10.2	5.6	0.5	1100				
24	6.97	7.45	15.3	16.6	8.9	5.7	0.5	1100				
25	6.8	7.23	14.3	17.1	8.8	5.5	0.5					

**Section 4 Appendices**

**THE UV-H<sub>2</sub>O<sub>2</sub> PROCESS**

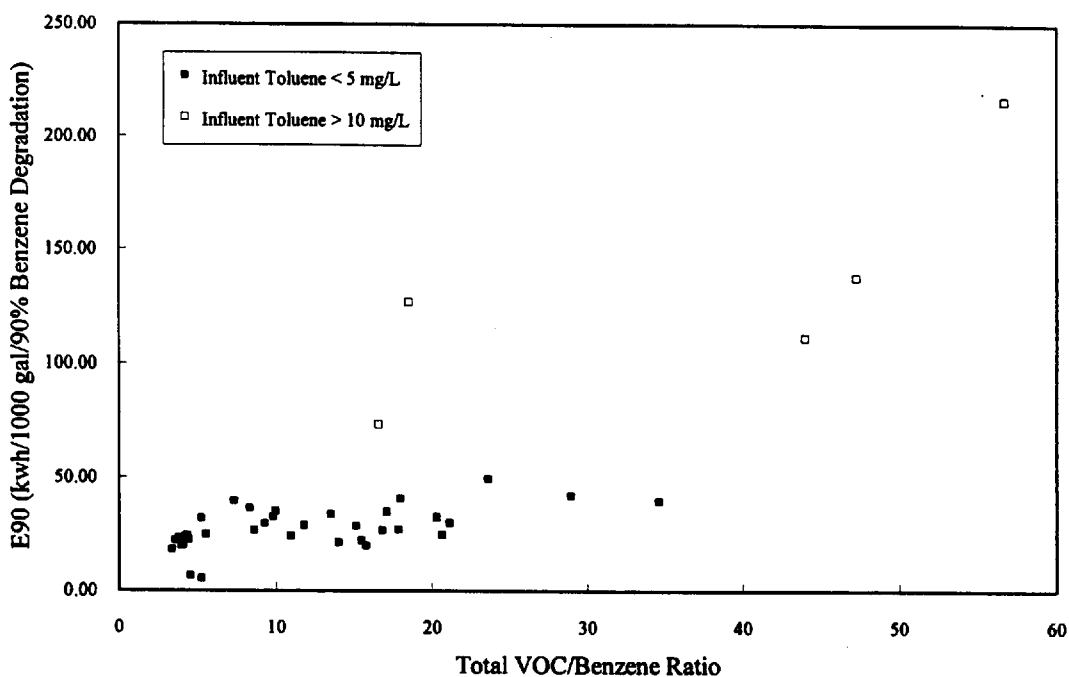


Figure A4-1. The effects of molar ratio of total VOC to benzene in the feed on the E<sub>90</sub> of benzene

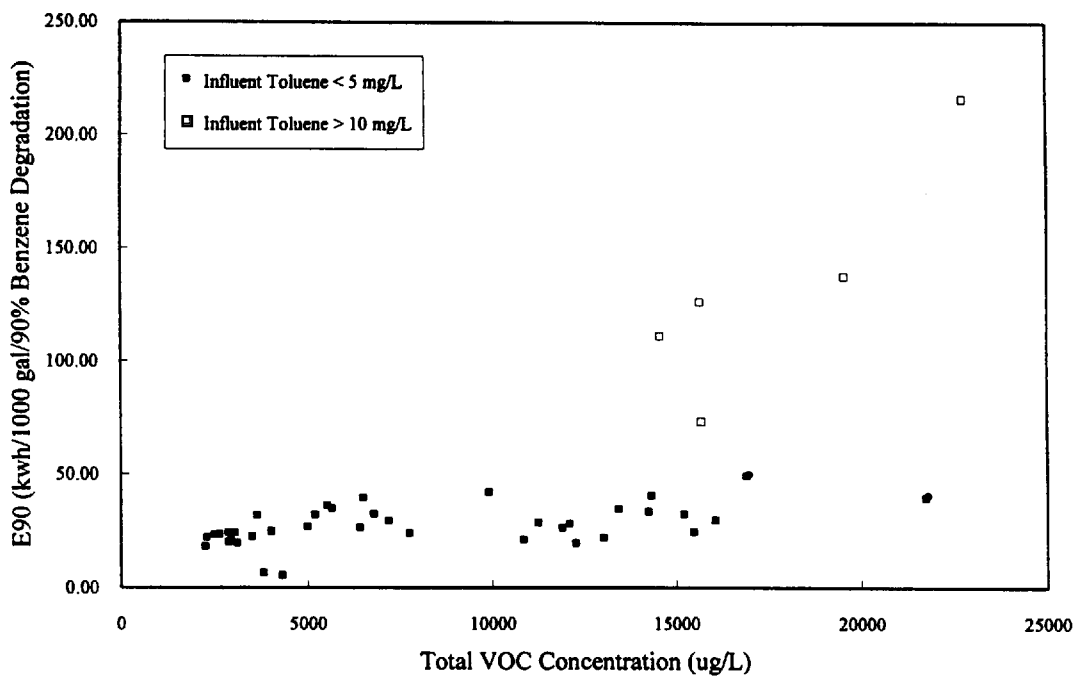


Figure A4-2. The effects of total VOC concentration in the feed on the E<sub>90</sub> for benzene

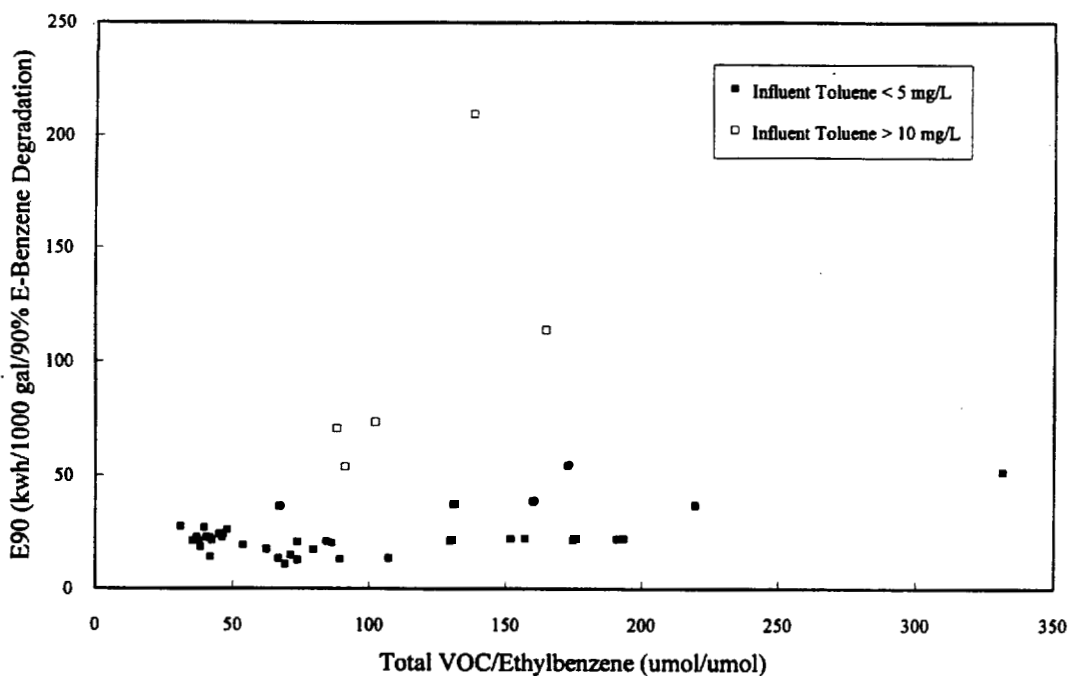


Figure A4-3. The effects of molar ratio of total VOC to ethyl benzene in the feed on the E<sub>90</sub> of ethyl benzene

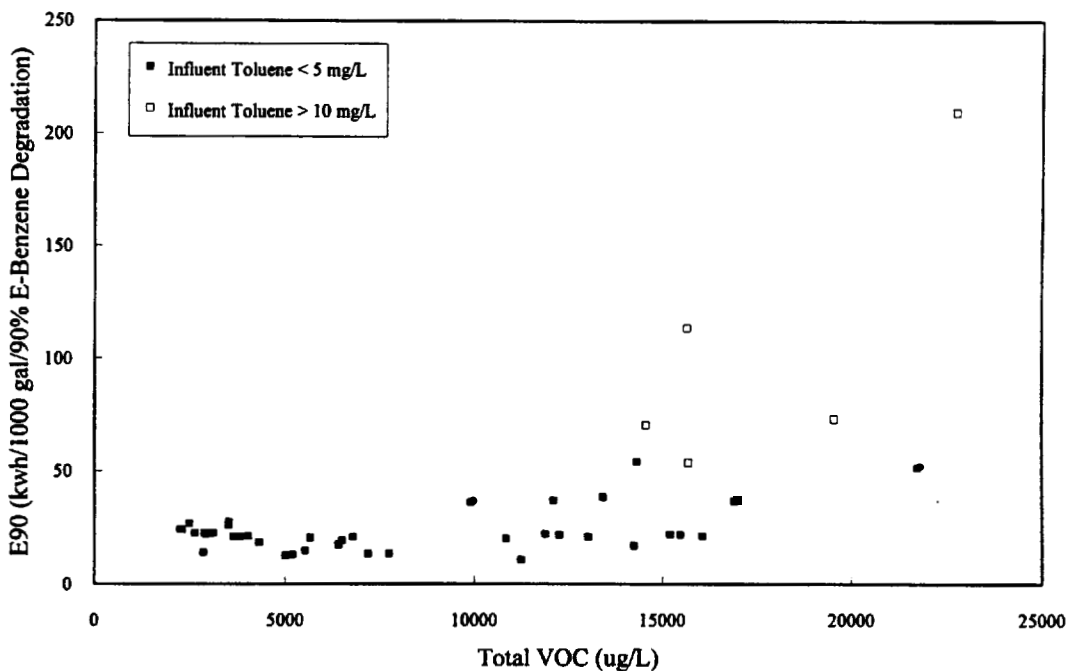


Figure A4-4. The effects of total VOC concentration in the feed on the E<sub>90</sub> for ethyl benzene

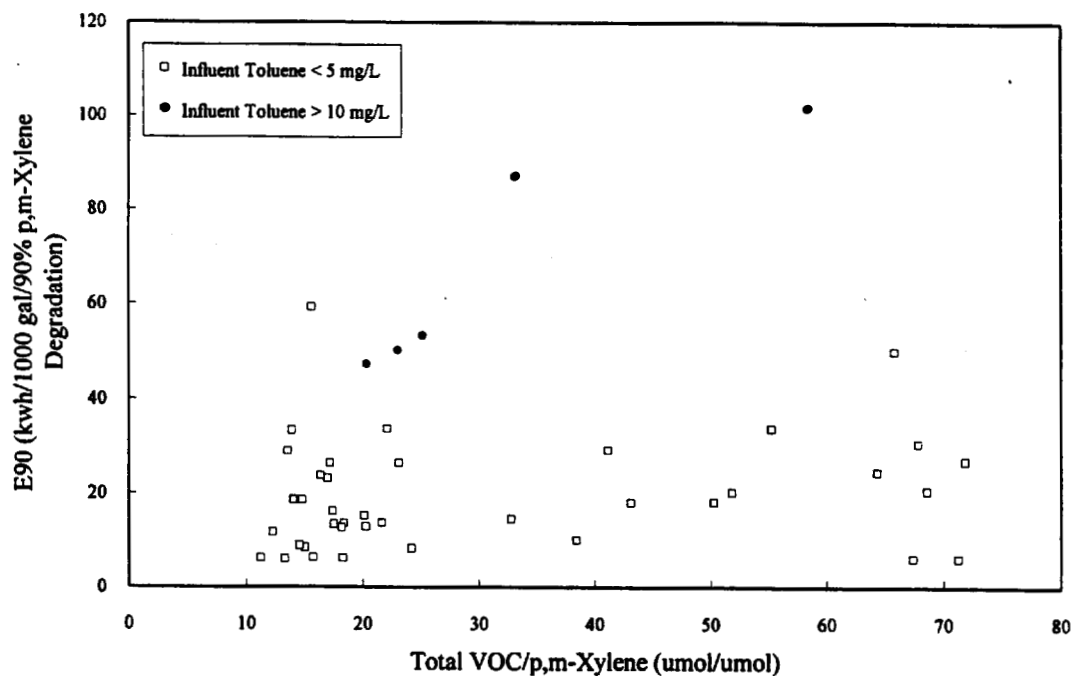


Figure A4-5. The effects of molar ratio of total VOC to p,m-xylene in the feed on the E<sub>90</sub> of p,m-xylene

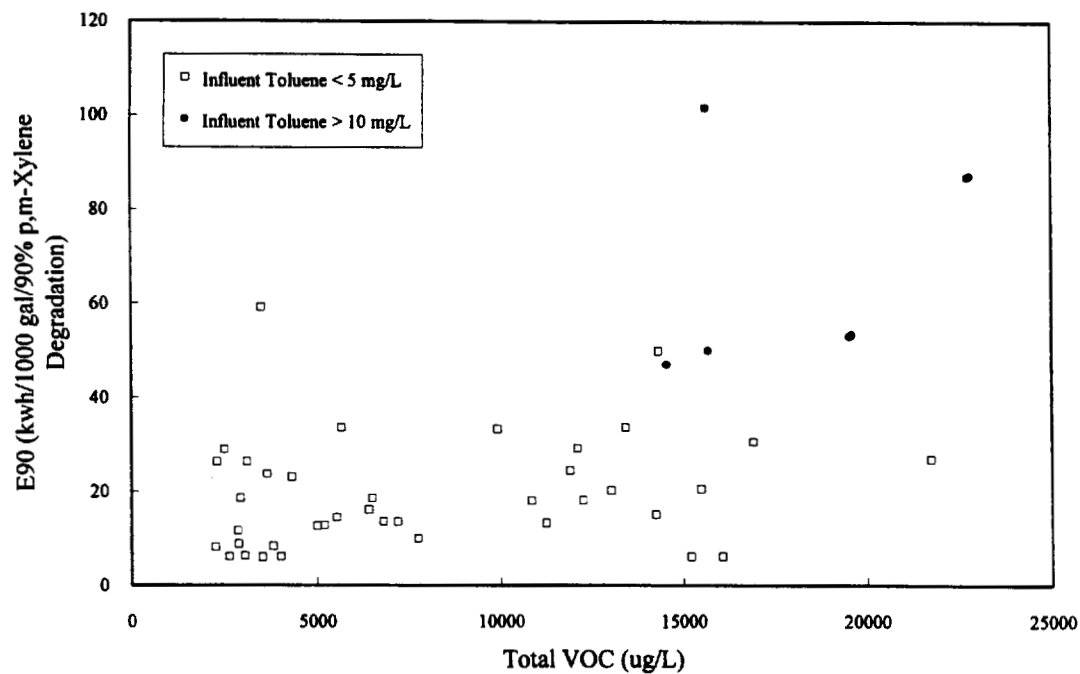


Figure A4-6. The effects of total VOC concentration in the feed on the E<sub>90</sub> for p,m-xylene

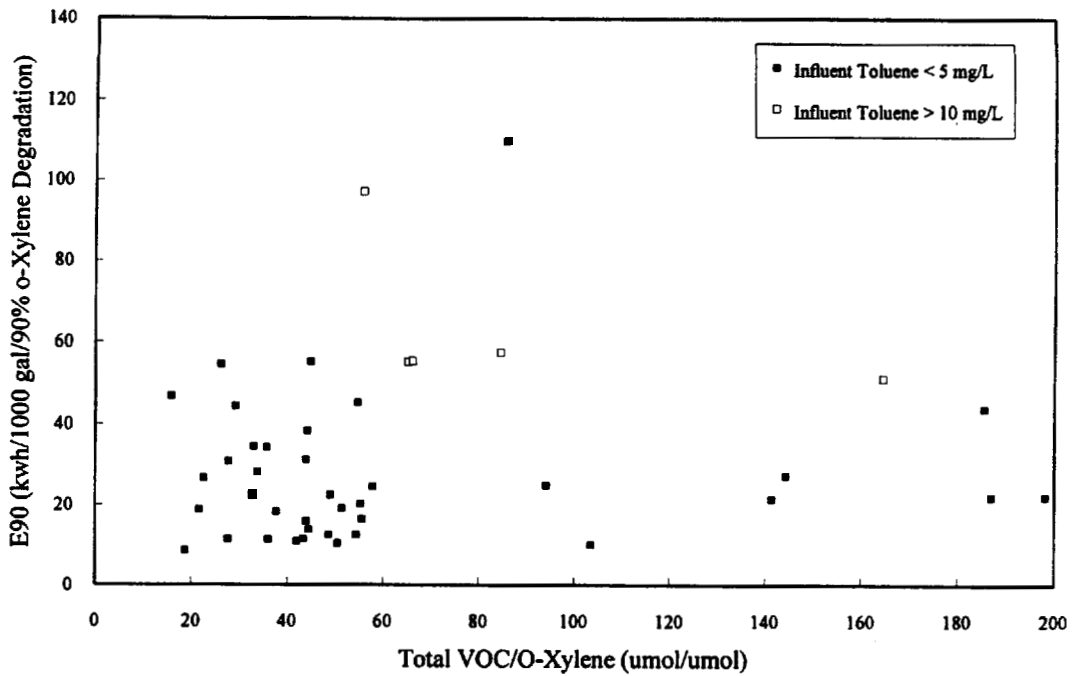


Figure A4-7. The effects of molar ratio of total VOC to o-xylene in the feed on the E<sub>90</sub> of o-xylene

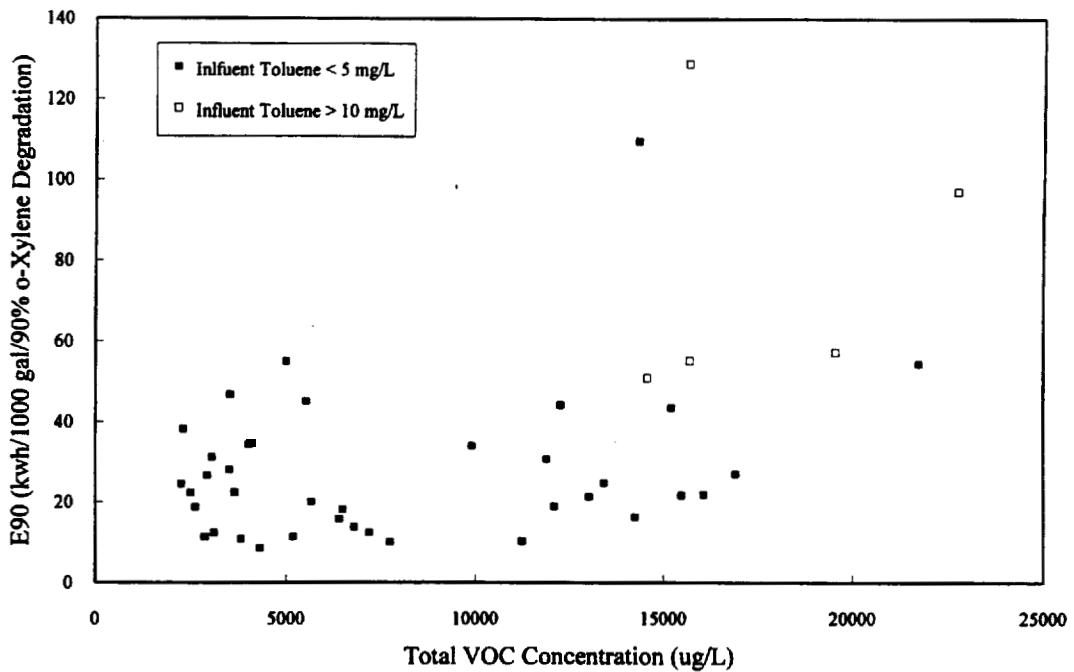


Figure A4-8. The effects of total VOC concentration in the feed on the E<sub>90</sub> for o-xylene

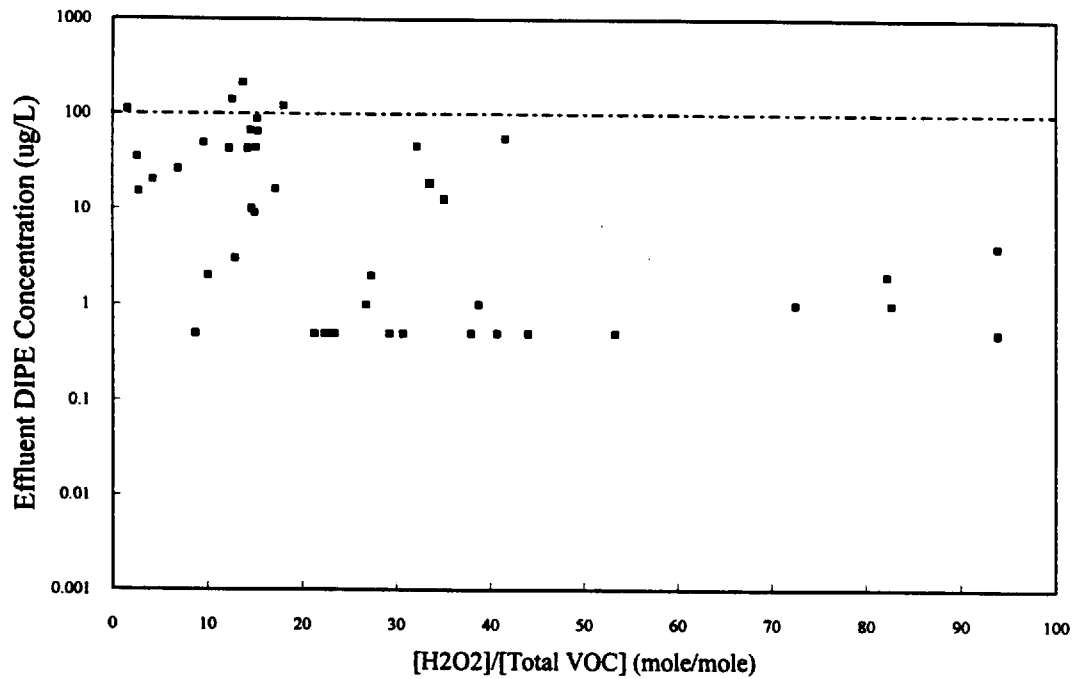


Figure A4-9. Relation between the effluent DIPE and the molar ratio of [H<sub>2</sub>O<sub>2</sub>]/[Total VOC]

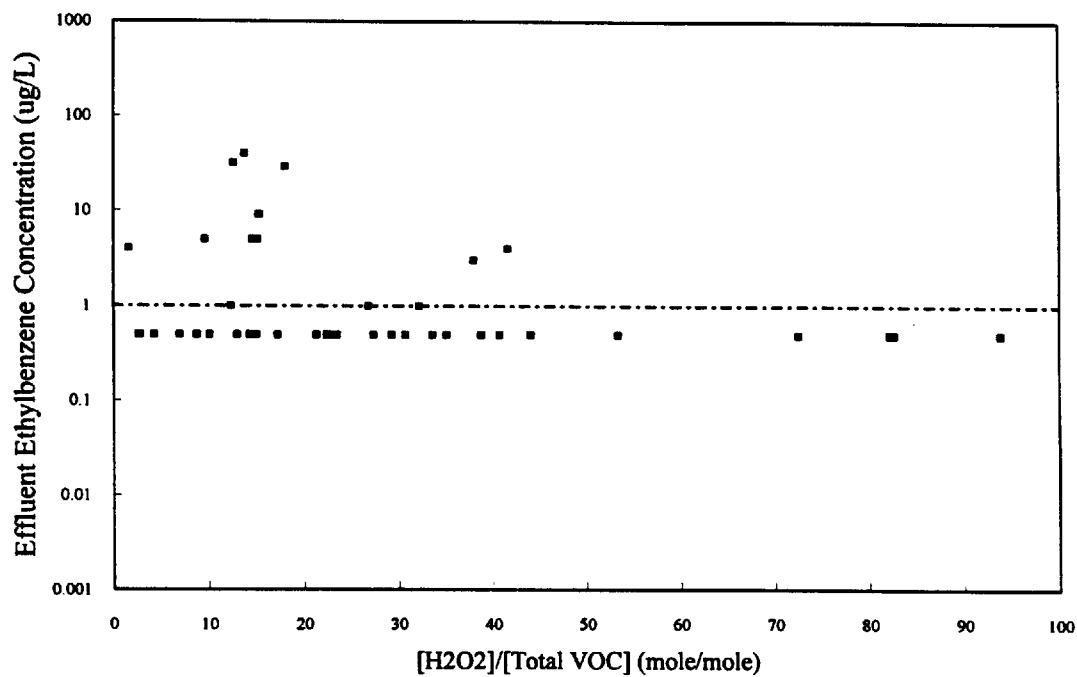


Figure A4-10. Relation between the effluent ethylbenzene and the molar ratio of [H<sub>2</sub>O<sub>2</sub>]/[Total VOC]

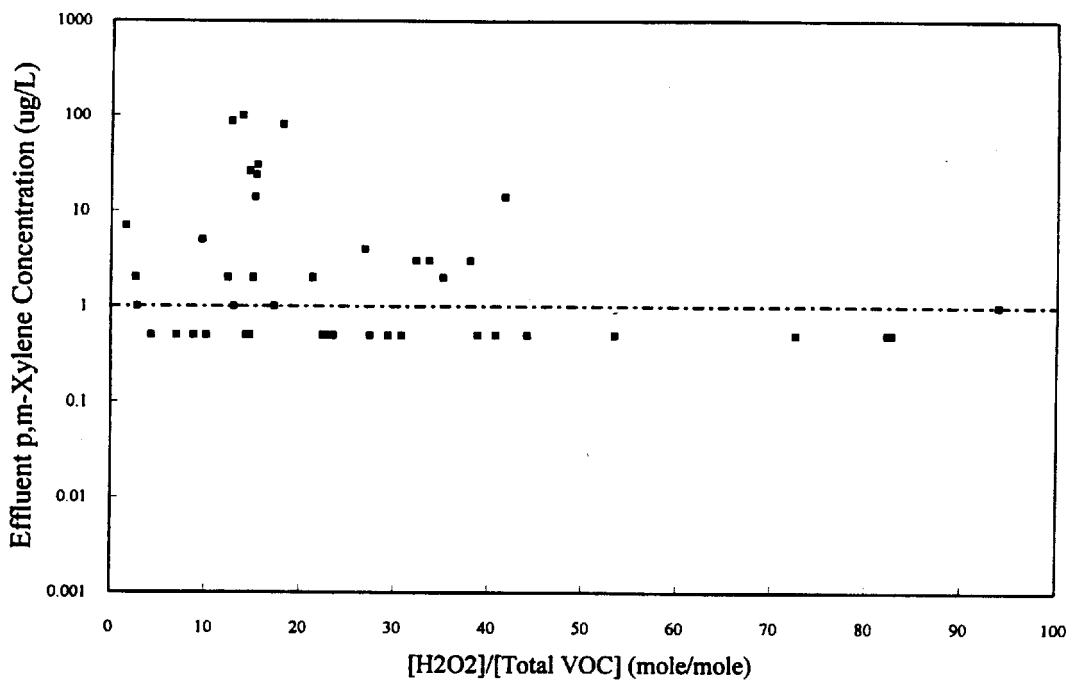


Figure A4-11. Relation between the effluent p,m-xylene and the molar ratio of [H<sub>2</sub>O<sub>2</sub>]/[Total VOC]

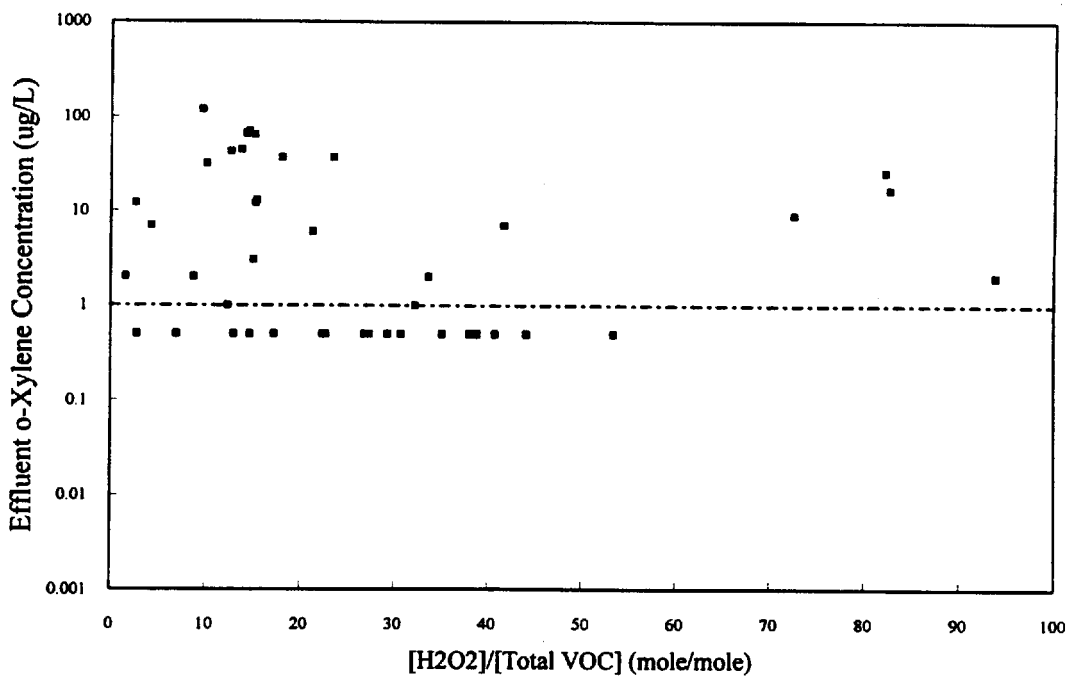


Figure A4-12. Relation between the effluent o-xylene and the molar ratio of [H<sub>2</sub>O<sub>2</sub>]/[Total VOC]



**American  
Petroleum  
Institute**

1220 L Street, Northwest  
Washington, D.C. 20005  
202-682-8000  
<http://www.api.org>

**ORDER NO. I46550**